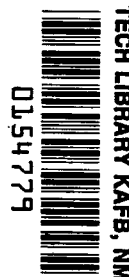


NASA TECHNICAL NOTE



NASA TN D-2645

NASA TN D-2645



A STUDY OF THE DYNAMIC MODEL TECHNIQUE IN THE ANALYSIS OF HUMAN TOLERANCE TO ACCELERATION

Prepared under Contract No. NASr-37 *by*
STANLEY AVIATION CORPORATION
Denver, Colo.

for



A STUDY OF THE DYNAMIC MODEL TECHNIQUE
IN THE ANALYSIS OF HUMAN TOLERANCE
TO ACCELERATION

Distribution of this report is provided in the interest of information exchange. Responsibility for the contents resides in the author or organization that prepared it.

Prepared under Contract No. NASr-37 by
STANLEY AVIATION CORPORATION
Denver, Colo.

for

NATIONAL AERONAUTICS AND SPACE ADMINISTRATION

For sale by the Office of Technical Services, Department of Commerce,
Washington, D.C. 20230 -- Price \$6.00



FOREWORD

The work described in this report was performed under a contract (Number NASr-37) granted to Stanley Aviation Corporation in April 1961 by the National Aeronautics and Space Administration. Quarterly status reports have been issued in July 1961 (Stanley Report No. 776) and October 1961 (Stanley Report No. 787) and this document represents the Final Report on a research study to investigate human tolerance to short duration acceleration using the dynamic model technique.

Stanley Aviation Corporation wishes to thank Mr. G. J. Pesman and Mr. H. F. Scherer of the National Aeronautics and Space Administration (Manned Spacecraft Center) for their valuable assistance during this program. Also, the cooperation of the following agencies who supplied important experimental data is acknowledged; Holloman Air Force Base, Naval Air Material Center, Federal Aviation Agency, Aeromedical Laboratory of the Wright Air Development Division, Aviation Crash Injury Research of Cornell University.

TABLE OF CONTENTS

	<u>Page</u>
FOREWORD	iii
SUMMARY	ix
SYMBOLS	xiii
1.0 INTRODUCTION	1
1.1 The Problem	3
1.2 Historical Background	5
1.3 Choice of a Dynamic Model	7
2.0 EXISTING DATA	9
2.1 Experimental Background	9
2.2 Present Tolerance Limits	10
3.0 GENERAL PRINCIPLES OF THE DYNAMIC MODEL	13
3.1 Physical Interpretation of the Model	13
3.2 The Influence of Damping	16
3.3 Multi-Degree of Freedom Systems	18
3.4 Correlation with Experimental Data	19
4.0 LINEAR SYSTEMS	21
4.1 Characteristics of Single Degree of Freedom System	22
4.1.1 Continuous Step Inputs	22
4.1.2 Other Continuous Input Functions	25
4.1.3 Rectangular Inputs	26
4.1.4 Impulsive Inputs	27
4.1.5 Sinusoidal Inputs	30
4.2 Restraint Effects	31
4.2.1 Seat Cushion Effects	31
4.2.2 Rebound	34
4.3 The Importance of Rise Time	35
4.4 Application to Escape Systems	38
4.5 The Two Degree of Freedom Model	39
4.6 The Three Degree of Freedom Model	43
5.0 NON-LINEAR SYSTEMS	48

TABLE OF CONTENTS (Cont'd)

	<u>Title</u>	<u>Page</u>
6.0	DIGITAL COMPUTER STUDIES	50
7.0	ANALOG COMPUTER STUDIES	51
8.0	ANALYSIS OF EXPERIMENTAL DATA	53
8.1	Availability of Data	53
8.2	Spinal Headward Data	55
8.3	Transverse Backward Data	59
8.4	Transverse Forward Data	61
8.5	Multi-Directional Accelerations	62
9.0	TENTATIVE TOLERANCE CRITERIA	63
10.0	THE NEED FOR FURTHER WORK	66
11.0	CONCLUSIONS	67
	REFERENCES	69

LIST OF TABLES

<u>Table No.</u>	<u>Title</u>	
1	SOURCES OF EXPERIMENTAL DATA	72
2	NOTATION USED IN EXPERIMENTAL ANALYSIS	74

LIST OF FIGURES

<u>Figure No.</u>	<u>Title</u>	
1	DEFINITION OF ACCELERATION REGIMES	75
2	SUMMARY OF HEADWARD ACCELERATION DATA	76
3	SUMMARY OF BACKWARD ACCELERATION DATA	77
4	ALLOWABLE SHORT DURATION ACCELERATIONS (HIAD)	78
5	DYNAMIC MODELS OF A HUMAN SUBJECTED TO ACCELERATION	79
6	DYNAMIC RESPONSE OF A SINGLE SPRING-MASS SYSTEM	80
7	INFLUENCE OF INITIAL DEFLECTION ON RESPONSE OF SINGLE DEGREE OF FREEDOM SYSTEM	81
8	INFLUENCE OF DAMPING ON RESPONSE OF SINGLE DEGREE OF FREEDOM SYSTEM FOR STEP INPUT	82
9	RESPONSE OF SINGLE DEGREE OF FREEDOM SYSTEM FOR VARIOUS INPUT DURATIONS	83

TABLE OF CONTENTS (Cont'd)

<u>Figure No.</u>	<u>Title</u>	<u>Page</u>
10	INFLUENCE OF DAMPING ON TOLERANCE CRITERIA FOR IMPULSIVE INPUTS	84
11	INFLUENCE OF DAMPING ON TOLERANCE CURVE	85
12	RESPONSE OF SINGLE DEGREE OF FREEDOM SYSTEM TO SINUSOIDAL INPUT	86
13	INFLUENCE OF CUSHION ON TOLERANCE LIMITS	87
14	TOLERANCE CURVES PREDICTED BY TWO DEGREE OF FREEDOM SYSTEM	88
15	DEFLECTIONS AND FREQUENCIES FOR VARIOUS MASS RATIOS ASSOCIATED WITH THE TWO DEGREE OF FREEDOM SYSTEM	89
16	TOLERANCE CURVES PREDICTED BY THREE DEGREE OF FREEDOM SYSTEM	90
17	TOLERANCE TO SINUSOIDAL INPUT ACCELERATIONS: COMPARISON OF THREE DEGREE OF FREEDOM SYSTEM RESULTS WITH EXPERIMENT	91
18	TYPICAL DIGITAL COMPUTER ANALYSIS	92
19	ANALOG COMPUTER - SIMPLIFIED FLOW DIAGRAM	93
20	ANALOG COMPUTER - EXPERIMENTAL ARRANGEMENT	94
21	TYPICAL ANALOG COMPUTER ANALYSIS	95
22	RISE TIME EFFECTS (ANALOG COMPUTER)	96
23	ANALYSIS OF EXPERIMENTAL HEADWARD ACCELERATION DATA	97
24	DEFINITION OF EQUIVALENT RECTANGULAR INPUT	98
25	ANALYSIS OF EXPERIMENTAL BACKWARD ACCELERATION DATA	99
26	ANALYSIS OF EXPERIMENTAL FORWARD ACCELERATION DATA	100
27	TOLERANCE TO SHORT DURATION ACCELERATIONS AS A FUNCTION OF VELOCITY CHANGE AND AVERAGE ACCELERATION	101

LIST OF APPENDICES

	<u>Title</u>	
APPENDIX A	NOTE ON MATHEMATICAL METHODS AND ANALYTICAL TECHNIQUES	A.1

TABLE OF CONTENTS (Cont'd)

	<u>Title</u>	<u>Page</u>
APPENDIX B	GENERAL THEORY OF A LINEAR, UNDAMPED, SINGLE DEGREE OF FREEDOM MODEL	B.1
APPENDIX C	THEORY OF A NON-LINEAR, UNDAMPED, SINGLE DEGREE OF FREEDOM SYSTEM, SUBJECTED TO A STEP INPUT	C.1
APPENDIX D	THE SINGLE DEGREE OF FREEDOM SYSTEM SUBJECTED TO AN IMPULSIVE INPUT	D.1
APPENDIX E	THE INFLUENCE OF DAMPING ON A LINEAR SINGLE DEGREE OF FREEDOM SYSTEM	E.1
APPENDIX F	EJECTION OF ESCAPE CAPSULE OR SEAT	F.1
APPENDIX G	THE EFFECT OF A LINEAR CUSHION ON TOLERANCE LIMITS - EQUIVALENT SYSTEMS	G.1
APPENDIX H	REBOUND IN A LINEAR SYSTEM	H.1
APPENDIX I	THE INFLUENCE OF RISE TIME	I.1
APPENDIX J	THE TWO DEGREE OF FREEDOM SYSTEM	J.1
APPENDIX K	THE THREE DEGREE OF FREEDOM SYSTEM	K.1
APPENDIX L	SUMMARY OF RELEVANT HOLLOMAN A.F.B. AND STANLEY AVIATION TEST RESULTS	L.1

SUMMARY

This report is concerned with the study of human tolerance to abrupt accelerations where the duration times are less than one tenth of a second.

A dynamic model analogous to the human body, consisting of a spring-mass system, is used in the analysis. When an acceleration is applied to the base of the spring, the response of the system is similar to the dynamic response of the human body under the influence of the same acceleration. If the input acceleration-time history is assumed to have a simple form, such as that represented by a step, rectangular or ramp function, the solution of the motion of the model in terms of the spring deflection and mass acceleration is relatively simple. The basic mathematics involved in obtaining this dynamic response is developed in the Appendices for a variety of simple input forms. The tolerance criterion adopted consists of setting a limit on the mass acceleration attained by the mass, so that the peak mass acceleration achieved under given input conditions is an important parameter. A linear, undamped, single degree of freedom system is used as the basic model, but the influence of damping and non-linearity of the spring on tolerance limits is also considered. The output of the model, in terms of the mass acceleration, depends on the input duration and damping, but can be as much as twice the value of the input acceleration. In the impact region, velocity change is an important criterion.

A physical interpretation of the motion of the mass is given and the response characteristics of the system for step, rectangular, ramp, parabolic and sinusoidal inputs are described. The model is used in a qualitative study of restraint and seat cushion effects, and for the case of an occupant in an escape capsule or seat. The influence

of rate of onset on dynamic response is considered and the influence of rise time and spring frequency on tolerance levels is deduced.

The theory of two and three degree of freedom systems is developed in an attempt to obtain a better representation of the human body. These preliminary investigations show that such models can be used, but, further information on the mechanical properties of the body are desirable. On present evidence, it is considered that the single degree of freedom system represents a useful working model, and over-complication at this stage will not provide better analysis techniques.

The equations of motion governing the motion of the spring-mass system contain certain coefficients that must be evaluated by correlation with experimental data. All the available test results have been reviewed, but end point information is very limited; and only tentative conclusions could be drawn. Values of equivalent frequency and allowable mass acceleration have been deduced for the headward, forward and backward acceleration directions. In the data analyses, an equivalent rectangular input was used for defining the input acceleration and duration time, in an attempt to remove inconsistencies in the choice of these values.

When complex acceleration inputs have to be studied, as is usual in a practical case, analytical solutions of the equations of motion are not possible and numerical methods must be used. A digital computer (IBM 1620) has been programmed for this purpose and an electronic analog developed that can be used for rapid analyses. The method of applying these techniques is described.

The primary use of the dynamic model is for the analysis of arbitrary inputs to predict if a given acceleration time history

will prove harmful to a human, or not. Depending on the direction of the applied acceleration, a frequency is assigned to the spring-mass system and the output (mass acceleration) of the model is determined for the given input. Comparing the maximum mass acceleration with the relevant allowable value enables the expected tolerance level to be determined.

SYMBOLS

The notation presented here refers to the main text only. Because of the large amount of mathematics involved, some duplication of symbols used in the text and Appendices has proved necessary. For the symbols used in the Appendices, reference should be made to the list of symbols preceding each Appendix.

A	amplification factor for sinusoidal input
A_j	output amplitude (three degree of freedom, $j = 1, 2, 3$)
c	damping coefficient ($c = \frac{K}{m}$)
E_c	energy absorption capacity of cushion
F	force
g	acceleration due to gravity
G_c	gravitationally normalized input acceleration $\left(\frac{\ddot{y}_c}{g}\right)$
G_p	gravitationally normalized mass acceleration $\left(\frac{\ddot{y}_p}{g}\right)$
G'	gravitationally normalized steady applied acceleration
k	spring stiffness
K	damping constant
m_j	mass associated with three degree of freedom system ($j = 1, 2, 3$)
m_p, m_q	mass associated with one or two degree of freedom system
m_c	mass of escape system or seat
R_j	ratio of output to input accelerations for three degree of freedom system ($j = 1, 2, 3$)
t	time
t_r	rise time
Δt	input duration time
Δt_c	limiting duration time for impulsive theory

v	velocity or velocity change	
Δv_B	bottoming velocity change	
\ddot{y}_B	acceleration required to bottom cushion ($=\omega^2\delta_B$)	
\ddot{y}_o	input acceleration applied to system, relative to fixed datum	
\ddot{y}_p	acceleration of mass m_p relative to fixed datum	
$\ddot{\bar{y}}$	apparent acceleration of mass due to force developed in its own spring-damper relative to fixed datum (multi-degree of freedom system)	
\ddot{y}_{co}	amplitude of sinusoidal input acceleration	
α	step input function (acceleration)	
β	slope of ramp input function (rate of onset of acceleration)	
γ	constant in parabolic input function	
δ	deflection of spring	
$\dot{\delta}$	rate of change of deflection of spring (velocity)	
$\ddot{\delta}$	rate of change of velocity of spring (acceleration)	
δ_B	deflection of spring at bottoming	
δ_s	initial deflection of spring	
ζ_n	"frequency" ($=\omega_n^2 = \frac{k_n}{m_p}$)	
μ_j	real part of output amplitude	} three degree of freedom model
ν_j	imaginary part of output amplitude	
ϕ	phase angle	
ω	spring frequency ($\omega^2 = \frac{k}{m_p}$)	
ω_o	damped frequency of system ($\omega_o^2 = \omega^2 - c^2$)	
Ω	frequency of sinusoidal input	
Ω_i	coupled frequency ($i = 1,2,3$)	

1.0 INTRODUCTION

The importance of the problem of human reaction to applied accelerations has been recognized for many years, but recent advances in the aerospace sciences have underlined the fact that adequate knowledge in this area is still lacking. It is well known that much higher accelerations can be sustained if the duration time is short, than if the acceleration is applied over a long period. Abruptly applied accelerations are encountered by humans in many situations such as automobile and aircraft crashes, ejection from high speed aircraft, re-entry, surface impact on landing and during accelerating rocket flight. Man's tolerance to short duration accelerations must be known with some degree of accuracy before safe advances can be made in these areas. Although a considerable amount of experimental information has been obtained to date, the way in which it has been gathered and presented does not allow adequate predictions to be made about future projects from the available data.

The solution of the problem is not simple and will require a high degree of cooperation between the various groups of diverse talents and experiences working in the human factors field. In this respect, it is important that the knowledge gained by each group is transmitted in such a way that its significance is not overlooked because of misunderstanding or lack of familiarity with the particular branch of science or engineering concerned. The purpose of this report is to present the results of a study that essentially emphasises the analytical approach to the subject. The investigation is mainly theoretical, but the experimental results of others play an important part in the development of the theory. The mathematics involved might appear trivial to the dynamicist but, at the same time, might present a barrier to the non-mathematically minded biologist. This barrier must not prove insurmountable, since the engineering

approach presents one aspect of the problem which can have important implications in other fields. For this reason, an attempt has been made in the present report to explain the basic engineering approach to the subject and point out the physical implications of the mathematical results.

In justifying a mathematical approach to the problem of human tolerance to abrupt accelerations it should be pointed out that no branch of science is complete or exact until an acceptable theory has been developed and checked by correlation with experiment. The postulating of a dynamic model is one attempt to produce a workable analogy, and by analyzing the motion of a spring-mass system under the influence of an applied acceleration, and attempting to relate the results to the observed response of a human under similar conditions, it is hoped that the model can be used to predict whether or not a given acceleration-time history will prove harmful. At least, the information gained will make a valuable addition to the gathering stock-pile of knowledge in the acceleration stress field and contribute to an overall understanding of the problem.

The investigations described in this report are confined to a study of the dynamics of human tolerance to short duration accelerations where the injurious effects are mainly of a structural nature, rather than hydraulic effects associated with longer duration accelerations which have been extensively studied in the centrifuge. Short duration is taken here to include the impulse (or impact) region which refers to accelerations of duration 0 to approximately 0.01 sec. and the plateau region, which extends the regime to approximately 0.1 sec. The term plateau region is derived from the general shape of the tolerance curve which appears to level off for durations of approximately 0.01 sec. to

0.1 sec., as indicated in Figure 1. The form of the tolerance curve will be discussed in more detail in Section 2.2.

1.1 The Problem

When a human is subjected to an abrupt acceleration of sufficient magnitude, injuries that are mainly of a mechanical nature can result. These depend to some extent on the direction of application of the acceleration but can consist of bone fracture, internal organ rupture and bruises. Cardiovascular shock and debilitation can also result and head injuries from impact blows and neck snap can occur, although for the purpose of this study, perfect head restraint is assumed. The medical and biomechanical aspects are of extreme importance but, in the semi-empirical analysis used here, it is sufficient to determine an acceleration level that will cause any injury that is liable to seriously impair the subject's functional ability. This criterion has been taken as the definition of an end point for the analysis of experimental results and when physiological effects giving rise to discomfort are noticeable but do not impair the subject's functional ability, the condition is termed near-end point.

Very simply stated, the problem is to determine a means of predicting whether or not a particular acceleration input to a vehicle will prove injurious to the occupant. In the past, experimental methods have been used where volunteers have been subjected to high accelerations in an attempt to determine tolerance limits for the human body. These tests have supplied valuable information, but are often difficult to interpret and the results cannot easily be applied to other cases where the conditions might be radically different from those pertaining to the test. From the point of view

of vehicle design, the lack of reliable information imposes performance penalties on the vehicle since, when human life is involved, it is natural to take a very conservative view of the available allowables. Further, expensive development testing is necessary to evaluate the vehicle from the human factors standpoint.

Experiment has shown that the accelerations measured on the human body can, under some conditions, greatly exceed the vehicle accelerations. Although the occupant's response cannot be measured with any degree of accuracy, since it is difficult to obtain a rigid mount for the measuring instrument and it is certain that different parts of the body experience different accelerations, the qualitative results provide an important clue to one way in which the problem can be tackled. The response of the occupant must be related in some way to the vehicle acceleration, which is the most convenient parameter for reference purposes. This can be done by postulating an analogous spring-mass system to represent the man and studying the motion of the mass when an acceleration is supplied to the base of the spring.

This concept of a dynamic model representing a human under the influence of a short duration acceleration is developed in this report and its application to various aspects of the problem discussed. In particular, an analytical method is developed that can be used to determine whether or not an arbitrary acceleration-time history is tolerable to man. The mathematics involved in studying the dynamics of the model have been separated from the main text and reported in Appendix form, but constant reference is made to the mathematical analyses and the implications of the results.

1.2 Historical Background

A complete review of the work done in the field of acceleration stress is out of place here and will not be attempted. Even investigations covering the short duration regime have produced a tremendous amount of work and fairly comprehensive bibliographies exist, (see, for instance, Refs. 1 and 2). Only work relevant to the present project will be mentioned in an attempt to approach the problem with the correct perspective.

The first systematic study of the problem was undertaken in Germany during World War II, when the dangers associated with the ejection seat were recognized. The work of Wiesehofer (Ref. 3) and Richter (Ref. 4) had shown that vehicle, or input, accelerations up to about 20 G could be withstood. Examination of the breaking loads of various vertebrae (reported by Ruff and Geertz in Refs. 5 and 6) led to what was probably the first tolerance curve for headward accelerations, indicating a plateau limit of 20 G. Geertz studied the dynamics of ejection by considering two masses coupled together by an elastic spring and noted the importance of overshoot.

At the close of the war, British workers carried out tests using vertical catapults which culminated in the design of the Martin-Baker seat (Ref. 7) which develops approximately 20 G's over 0.1 sec. The work of Latham (Ref. 8) is particularly noteworthy as he studied the response of a man-seat system experimentally and theoretically using spring-mass systems and an analog computer, and suggested optimum cushion characteristics for use with ejection seats. A summary of German and early British work on this topic is contained in Reference 9.

In the U.S.A., ejection seat design was pioneered by various government establishments. Kroeger (Ref. 10) studied the interaction of a man and his ejection seat with a view to reducing the overshoot acceleration attained by the man. Watts, Mendelson and Kornfield (Ref. 11) observed experimentally the influence of rate of increase of acceleration on the overshoot experienced by various parts of the body. More recently the work of Hess (Ref. 12), Kornhauser (Ref. 13) and Brock (Ref. 14) has utilized the dynamic model concept to study the influence of rapidly applied accelerations on man and animals. The effect of restraint elasticity on a subject's response has also been investigated (Ref. 15) and the vibration studies of von Gierke and Coermann (e.g. see Refs. 16 and 17) have illustrated the existence of resonance phenomena in the human body, and contributed greatly to an understanding of the physical processes involved.

More direct experimental measurements have utilized the rocket sled in which animals and humans have been exposed to accelerations approaching, and in excess of, end point magnitudes. The work of Stapp (Refs. 18 and 19) and Beeding (Ref. 20) in this area is particularly well known. In the impact regime, simple drop tests have given useful data on man's tolerance to impulsively applied forces. Many people have engaged in this type of work and the results of Holcomb (Ref. 21) and Swearingen (Ref. 22) are of particular interest.

At Stanley Aviation, experimental work associated with the B-58 escape capsule development program indicated that the dynamic response of the human was extremely important and accelerations measured on test subjects indicated that accelerations far in excess of the normally accepted tolerance levels could be withstood if the application time was extremely

short. Theoretical studies by Payne (Refs. 23 and 24) showed that a simple mechanical model of the human body, consisting of an elastic spring-mass system, could be used as a basis for a theory to explain and correlate experimental data, and his work laid the foundations of the present study. A brief summary of the dynamic model technique and its application to the analysis of human tolerance to acceleration was given in Ref. 25.

1.3 Choice of a Dynamic Model

Medical research has shown that when the human body is subjected to impulsive or steady state forces, deformation and displacement of the structural components and organs occur which result from forces generated within the body. The transmission, amplification and attenuation of these internal forces must result from basic processes that can be explained by the laws of physics, but the effects, and therefore an understanding of the effects, are masked by the complexity of the human body, the limitations on the type of experiment that can be performed, and the complicated subjective response of the subject.

Taking a broad view, the human body consists of a bony structural skeleton, held together by tough fibers, which provides mechanical support and a lever system on which the muscles act. The slightly curved vertebrae or spinal column is the basic structural component and consists of a number of vertebrae acting as load carrying elements and separated by supporting tissues which act as shock absorbers and connecting links. The rib cage and abdominal cavity contain the visceral organs (heart, lungs, liver, etc.) which are fairly massive components, suspended freely by connective tissues from a muscle and bone support. The basic constituents such as bone

tissue, ligaments and muscle exhibit properties familiar to the engineer, such as elasticity, compressibility, shearing and tensile strength. In addition, when the body is exposed to comparatively low frequency vibrations, resonances occur within the body which can be observed directly and by the low tolerance level of the subject to a particular frequency of vibration.

It appears likely, then, that the motions induced in the body by rapidly applied accelerations can be explained by considering the elements of the body as mechanical systems exhibiting elastic properties. At the same time, because of the complexity of the body structure, a complete description of body response in terms of integrated mechanical models is not possible at this stage. However, a start has to be made somewhere and it is logical to investigate the motions of a simple spring-mass system which is known to exhibit dynamic response characteristics similar to the human body. For instance, a man subjected to a headward acceleration along the spinal axis (which is known to frequently produce spinal fractures) can be represented by a single spring-mass system where the spring has stiffness characteristics similar to the spine and the mass approximates that of the man. The motion of the spring-mass system for a given input acceleration can be mathematically predicted with accuracy, and if reasonable correlation can be obtained between the theory and experimental observations made with a man, the model can be used as a basis for predicting human tolerance to arbitrary acceleration inputs. An improved model would include mechanical components (dampers) to simulate the damping effect of the human body. A further refinement can be obtained by employing multiple spring-mass systems to represent various parts of the body.

The mechanical model consisting of one or more spring-mass systems can therefore be regarded as an approximate analog of the human body for studying response to short duration accelerations, but it is in no way a true representation, and regarding it as such may be misleading. It will only predict gross effects and relies on the establishment of certain criteria obtained from experimental data before it can be used. Even so, it should prove a powerful tool in the analysis of acceleration-time histories and the evaluation of techniques for increasing human tolerance levels. The actual model used is not so important as the fact that certain equations can be deduced which explain the existing experimental data and lend themselves to the prediction of future events.

2.0 Existing Data

2.1 Experimental Background

A variety of experimental facilities have been used in an attempt to establish the acceleration levels to which man can be subjected before some form of physical injury results. These include rocket sleds, catapults, shake tables and drop test facilities. When human subjects are used the tolerance level is governed by the reaction of the test subject to a variety of conditions and it is possible that the actual upper limit may be considerably higher than that determined from voluntary exposure. The severe injury threshold has been investigated with the use of animals, but some caution should be used in applying these results to humans because of physiological and psychological differences. The analysis of accidents has given some information on the human injury threshold, but the conditions governing these cases are far from controlled.

The main difficulties in interpreting experimental data are; correct interpretation of the results of measuring instruments, the effect of seat and harness configuration, lack of standard acceleration input patterns, orientation of the subject, differences in response of individual subjects and the often unreproducible nature of the experiments. Qualitatively, experiment has shown that the major factors influencing human tolerance to short duration accelerations are:

- (a) direction of application of input
- (b) magnitude of the input acceleration
- (c) duration of the input
- (d) rate of application of the acceleration ("rate of onset")
- (e) orientation of the body

These pioneer experiments, often carried out at great risk to the volunteers, have produced tentative values for human tolerance levels, but prediction of tolerance is still an art rather than a science.

The useful application of a dynamic model depends on experimental data and all the known results have been consulted in the course of the present investigation. Wherever possible, data referring only to properly restrained subjects in rigid seats and subjected to acceleration forces near the major directional axes has been used. The work of Stapp and his successors at Holloman A.F.B. has constituted the main source of information, but the cooperation of all persons and agencies engaged in this field is acknowledged.

2.2 Present Tolerance Limits

In 1959, Eiband (Ref. 2), realizing the need for a critical survey of the status of experimental data, made a comprehensive survey of the existing literature. He

approximated the form of the input acceleration to a trapezoidal pulse (see inset of Fig. 2) and used the plateau duration and magnitude as the two significant variables. Plotting vehicle (input) acceleration in G's against duration time he produced suggested tolerance curves based on the more reliable experimental data. Two of these curves, referring to accelerations applied in the headward and backward directions, are reproduced in Figures 2 and 3. These curves found a ready application amongst designers and have proved invaluable, but still suffer from certain drawbacks. Inspection will show that there is a considerable unknown area between the region of voluntary human exposure and the known region of injury. In the headward case, this unknown area covers over 20 G in the ordinate, which includes the region of most interest today. In addition, the boundaries are not particularly well defined and a few more reliable points might well change the general shape of the curves, particularly in the impulse region. The method of analysis of the results was in no way rigid as the deduction of a plateau level and duration time from a complex acceleration trace is no easy task and various combinations of the two parameters are equally correct. The five hog points shown in Fig. 2 were apparently obtained from a single experiment which is not particularly valid, since the experiment represented an end point. The reverse argument is also true since it is difficult to fit criteria based on a trapezoidal input to the complex acceleration-time histories encountered in practice.

Included in Figure 2 is a tolerance curve based on German data relating to compressive strength tests performed on the human spine (Ref. 5). This information was used by Ruff to calculate the static load necessary to cause rupture and used to define the "plateau" region of the tolerance curve. In the impulse region, dynamic considerations led to the linear tolerance

line similar in shape to that suggested by Eiband. The Ruff curve estimates tolerance limits at approximately half the input values resulting from Eiband's work.

The general form of these curves merits some comment. It can be seen that for duration times up to 0.01 sec. the tolerance level drops off linearly (log - log scale) as the duration time increases. This can be explained in terms of dynamic response, since the acceleration achieved by the man takes a finite time to develop. When full overshoot is attained (at about 0.01 sec.) any further increase in the duration time does not increase the man's response for a given input level, until the "long" duration regime is approached when hydraulic effects become noticeable and reduce the tolerance level still further.

The curves published in the Handbook of Instructions for Aircraft Designers (H.I.A.D.) contain the human tolerance limits that usually have to be met by present day aircraft designs. This publication (Ref. 26) and its derivatives (e.g. Ref. 27) have been the subject of considerable discussion on the validity of these curves (see for instance Ref. 28) of which the one pertaining to headward and backward accelerations is shown in Figure 4. It certainly appears that the H.I.A.D. curves should refer to the vehicle rather than the man, since they do not take into account the man's dynamic overshoot. Inconsistencies in the definition of time when referred to rate of onset and duration time are also apparent, and the interpretation of allowables in the short duration time region containing the rate of onset curves is impossible. Further, although "rate of onset" is important, it will be shown later that it is not a limiting criterion.

This discussion of the existing information shows that the presently accepted human tolerance levels to short duration accelerations leave much to be desired, and one merit of the analytical approach is that it forms the basis of a more consistent definition of tolerance levels and lends itself to the study of any type of acceleration input. The method of applying the dynamic model to this end will be described later.

3.0 General Principles of the Dynamic Model

3.1 Physical Interpretation of the Model

The dynamic model proposed as a basis for an analytical study of the tolerance of the human body to short duration accelerations is a spring-mass system composed, in its simplest form, of a mass m_p (the equivalent mass of the man) attached to a spiral spring considered to have zero mass. This basic model is illustrated in Figure 5(a). The spring exhibits elastic properties in that it tends to return to an equilibrium point when a displacement is introduced into the system. When a displacement is induced, the restoring force developed in the spring is proportional to the displacement or deflection and the factor of proportionality is called the spring constant (k). Thus the restoring force F for a given deflection δ can be written

$$F = k \delta$$

If, after displacement, the spring is allowed to move freely, it will oscillate about the equilibrium point with a certain fixed amplitude (maximum deflection), exhibiting harmonic, sinusoidal motion. The number of complete oscillations or vibrations per second is the frequency (ω) which is related to the spring stiffness and mass by the expression

$$\omega = \sqrt{\frac{k}{m_p}}$$

As a result of its motion, the system possesses an internal velocity which is the rate of change of deflection with time ($d\delta/dt$) and referred to as the spring velocity in this report, and an acceleration or rate of change of velocity with time ($d^2\delta/dt^2$) which is always towards the equilibrium point. The spring velocity and acceleration can be interpreted as the velocity and acceleration of the mass with respect to the base of the spring. The usual sign convention is that the deflection is positive in compression and negative in extension.

When an acceleration input is applied to the base of the spring, the system moves in such a way that the mass acceleration relative to some fixed axes is the resultant of the input acceleration and the acceleration resulting from the spring deflecting. The complete motion of the mass is best illustrated by a specific example.

In Appendix B the equations governing the motion of a single spring system subjected to a step input acceleration are developed, for the case of a linear spring (force directly proportional to the deflection). Solution of the equation of motion leads to the following expressions for the deflection, velocity and acceleration of the spring (Equations B.7, B.8, B.9 respectively).

$$\text{deflection} \quad \delta = \frac{\alpha}{\omega^2} (1 - \cos \omega t)$$

$$\text{velocity} \quad \frac{d\delta}{dt} = \dot{\delta} = \frac{\alpha}{\omega} \sin \omega t$$

$$\text{acceleration} \quad \frac{d^2\delta}{dt^2} = \ddot{\delta} = \alpha \cos \omega t$$

where α is the step input acceleration and t represents time.

These expressions are plotted in Figure 6.(a) to (c) and can be interpreted as follows. The deflection of the spring (defined as the difference between the unloaded and loaded length) is zero at time zero and again at a time represented by $\omega t = 2\pi$ and is never negative for this type of input. The maximum value of $2\alpha/\omega^2$ is reached when $\omega t = \pi$. The spring velocity is essentially a sine wave of amplitude α/ω having a zero value initially and at maximum deflection. The spring acceleration starts off equal to the input acceleration (but in the opposite sense) and is directed towards the spring base. It then decreases to zero at the point in time when the system is in equilibrium (force developed in the spring equals the input force) and the velocity is a maximum, reverses its direction and peaks at $\omega t = \pi$ and is then in the same direction as the input acceleration. It then decreases to zero again when the velocity builds up to a maximum in the negative direction.

The resultant mass acceleration (\ddot{y}_p) contains the two components - spring acceleration and input acceleration - and from Equation B.10 is given by

$$\ddot{y}_p = \alpha(1 - \cos \omega t)$$

The spring acceleration is in the same direction as the input for $\pi/2 < \omega t < 3\pi/2$ so in this region the resultant mass acceleration is greater than the input, a condition known as overshoot. In fact the peak value of the resultant mass acceleration, which occurs when $\omega t = \pi$, is twice the input acceleration, which is the 100% overshoot case. The motion of the spring continues with time in this manner, and the mass acceleration experiences a succession of maxima at $\omega t = \pi, 3\pi, 5\pi$ etc. until the input is removed.

At the onset of the applied acceleration the spring stores up potential energy until it carries a load equal to the increase in "weight" of the mass. At this stage the mass still has

kinetic energy and the spring continues to compress until this is destroyed, at which point the spring deflection and mass acceleration attain maximum values (spring fully compressed) and all the internal energy is in the form of potential energy of the spring.

The maximum mass acceleration (from Equation B.2) is given by

$$\ddot{y}_p = \omega^2 \delta_{\max}$$

when there is no damping present, so the maximum mass acceleration, or the maximum spring deflection is indicative of the peak response of the system. Since the spring-mass system is analagous to the human body, a correct choice of spring frequency (ω) corresponding to the relevant part of the body under investigation enables the mass acceleration or spring deflection to be calculated (for a given acceleration input), which can be taken as a measure of the dynamic response of the man. If criteria can be developed for the values of \ddot{y}_p and/or δ that correspond to some end point in the man, the model can then be used to predict tolerance limits. The necessary correlation can be obtained from a study of the available experimental data.

3.2 The Influence of Damping

Resistance to motion is always present in any system and the effect is normally referred to as damping. When the motion is vibrational by nature, as in the case of a spring-mass system, the presence of damping successively reduces the amplitude of the vibration until the motion is completely eliminated. Typical commonplace examples of damped motion are the diminishing amplitude of a pendulum swinging in air due to the air resistance and the decay of electrical vibrations in an oscillatory circuit resulting from the resistance to electron motion. Whenever resistance to motion is present, energy is dissipated (usually in the form of heat) and the system gradually runs down.

In the human body, vibrations set up in the various elements will be damped by the surrounding matter and a mechanical analog of the body should allow for these effects. The mechanical resistance of the body causes viscous damping, which is akin to that obtained with a fluid dash pot, which can be regarded as consisting of a loosely fitting piston moving into an oil-filled cylinder. The dash pot mechanism is included in the spring-mass system to represent all the damping present as shown in Figure 5.(b). The mechanical influence of the dash pot is to produce a resistive force which is proportional to the velocity of the mass, so that

$$F = K \dot{\delta}$$

where $\dot{\delta}$ is the mass velocity resulting from the spring motion (spring velocity) and K is called the damping constant. The damping coefficient (C) is the quantity normally used and this is related to the damping constant (K) by the expression

$$C = \frac{K}{m_p}$$

As explained in Appendix E, three damping regimes exist. These are critical damping ($C = \omega$), dead beat ($C > \omega$) and sub-critical damping ($C < \omega$). The latter case is of importance in the human body where the damping is small but not negligible.

When damping is included in the spring-mass system, its main influence on the output is to reduce the vibrational amplitude and the mass acceleration so that, generally, damping is beneficial. Tolerance criteria can again be applied to the model, but some ambiguity is introduced into the definition of tolerance. The mechanical quantity corresponding to the observed physiological effect can be represented by the mass acceleration, which is a measure of the total force transmitted through the system, or the strain (proportional to deflection)

resulting from the force developed in the spring alone. At this stage, it appears that the criterion adopted depends on the part of the body concerned; thus, the latter criterion is more reconcilable with the physiological facts for massive organs with elastic attachments, but the former might be more applicable to the spinal mode where crushing forces on the individual elements are important.

A more detailed discussion of the influence of damping will be found in Section 4.

3.3 Multi-Degree of Freedom Systems

In dynamics, a system in which the motion is specified by only one coordinate is said to have one degree of freedom. The single mass system described above fulfils this condition, since the motion of the mass relative to the spring base can be described by one coordinate. Generally, the number of degrees of freedom is the same as the number of masses contained in the system, so the models shown in Figure 5.(c) and (d) are termed two and three-degree of freedom systems respectively.

When the human body is subjected to an acceleration input, more than one part of the body can be set in vibration. The particular mode excited depends on its frequency and the duration of the input. Thus, low frequency modes are slow to excite and require comparatively long input durations before they produce any noticeable effects. Shake table tests, where human subjects have been exposed to sinusoidal inputs of various frequencies and amplitudes, have shown that the human body exhibits two distinct low frequency modes in addition to the much higher frequency spinal mode.

Although a dynamic model cannot give an exact representation of the body, it should at least contain elements representing the major vibrational modes. For the sitting man it seems

likely that three mechanical systems are sufficient to explain the important features of response to short duration inputs, if the arms and head are assumed perfectly restrained. There is, then, a need for refining the basic dynamic model by including more degrees of freedom. The theory of a two-degree of freedom model is developed in Appendix J and that for a three-degree of freedom model in Appendix K. The mathematics is naturally more complicated, but the objects are the same in that the deflections developed in each spring and the dynamic response of the mass associated with each system must be evaluated. Using multi-degree of freedom models it will be possible to investigate the response of various parts of the body simultaneously and to study the influence of interactions between the modes. The model is quite general in that values of mass and spring frequency may be assigned to fit a particular problem. In this way, the spinal column may be considered as a number of spring-mass systems in series which can be built up to include the results of experimental measurements made on vertebrae. This application has been attempted with the two-degree of freedom model with some degree of success, but it might well be that over complication leads to less instructive results.

3.4 Correlation with Experimental Data

The equation of motion of a single degree of freedom model with a linear spring and no damping is derived in Appendix B (B.5) and can be written

$$\ddot{y}_c = \omega^2 \delta + \ddot{\delta}$$

For the general case of an arbitrary acceleration input this equation can be solved in a step-by-step fashion to give the variation of the spring deflection with time. The spring deflection can then be related to the resultant mass acceleration, since $\ddot{y}_p = \omega^2 \delta$, so that a time history of the output

acceleration can be obtained corresponding to the response of the man. It is now necessary to establish a maximum value of the mass acceleration that can be tolerated before an end point is reached. This can be done by analyzing the input acceleration traces of the available experimental data, obtaining the relevant mass accelerations and correlating these with the medical histories of the test subjects.

A more direct approach is available if the results of Eiband (Ref. 2) are used as a starting point. The data plotted in Figure 2 indicates that, in the "plateau" region, the upper tolerance level based on the vehicle acceleration is about 40 G. Since the results quoted by Eiband are limited to tests that used rigid seats and good restraint, the vehicle acceleration can be taken as the input acceleration to the model. It will be shown later that the "plateau" region corresponds to duration times that allow 100% overshoot in the output of the dynamic model used for headward accelerations. This means that the output is exactly twice the input, and using the input of 40 G taken from Eiband's curves, this implies a criterion of 80 G on the mass acceleration before an end point is reached.

The frequency of vibration of the particular part of the body under consideration must also be known. In some cases this can be measured directly from vibration tests but, for the headward case mentioned above, no such results are available. However, a value of the spring frequency relevant to the dynamic model when used to analyze spinal inputs can be obtained indirectly by applying the results of the mathematical analysis to Eiband's results in the impulse region. Impulsive inputs are considered in Appendix D and Equation D.23 gives the maximum mass acceleration (G_p) attained for an impulsive input of G_c lasting for a time Δt , viz. $G_p(\max) = G_c \omega \Delta t$. This equation holds for $\Delta t < \frac{2}{\omega}$. Taking logarithms of each

side gives the relationship

$$\log G_c = \log \frac{G_p(\max)}{\omega} - \log \Delta t$$

which represents the equation of a straight line of slope -1, and implies that, if $\log G_c$ were plotted against $\log \Delta t$, a series of straight lines of slope -1 would be obtained, their position relative to the time axis being governed by the value of $\log \frac{G_p(\max)}{\omega}$. Eiband presented his results in just

this way, and it is found that his points, based on hog data do fall approximately on a straight line. Accepting a value of 80 for $G_p(\max)$, and fitting the above equation to Eiband's results gives a value of $\omega = 280$ rad/sec. (approx.) or roughly 44 cycles per second.

Bearing in mind the accuracy of the Eiband curve, it is possible, therefore, to evaluate the coefficients appearing in the equation of motion and to deduce a criterion for the maximum allowable response of the spring-mass system. One of the objects of this research program was to collect the available experimental data in an attempt to define the dynamic model more exactly and test its usefulness as a method of analyzing the tolerability of arbitrary acceleration inputs.

4.0 Linear Systems

The response of a spring-mass system to a given input depends on the way in which the restoring force develops in the spring with change in deflection. If equal increments of deflection produce equal increments of force, the spring is said to possess linear characteristics and a plot of force against deflection produces a straight line (see Figure B.1(b)). The force-deflection relationship for a linear spring is,

$$F = k \delta$$

where k is the spring stiffness, or, in acceleration units,

$$\frac{F}{m_p} = \frac{k}{m_p} \delta = \omega^2 \delta$$

where ω is the spring frequency. It is known that certain parts of the human body exhibit non-linear characteristics at the higher input amplitudes, but an approximation to a linear system can often be made. Considerable progress can be made on the assumption of a linear spring system and the mathematics is simplified considerably.

4.1 Characteristics of Single Degree of Freedom System

The response of a single degree of freedom model will be investigated analytically using various types of input accelerations. The equation of motion for an undamped system was quoted earlier as

$$\ddot{y}_c = \omega^2 \delta + \ddot{\delta}$$

This is an ordinary second order differential equation describing the variation of the deflection (δ) with time. The input (\ddot{y}_c) can have any arbitrary variation with time, but a closed form solution of the equation of motion is possible only if the input-time relationship can be represented in some simple mathematical form. The response of the dynamic model to a number of simple acceleration inputs is examined below. This simple approach gives important qualitative results and can often be used as an approximation of a practical case.

4.1.1 Continuous Step Input

If the applied acceleration jumps instantaneously to some finite value (α) at $t = 0$ and remains at that value indefinitely, the input can be represented by

$$\ddot{y}_c = \alpha$$

and is termed a step input. This case is analyzed in Appendix B and the relevant equations for zero damping are

Equation of motion (Equation R.6)

$$\ddot{\delta} + \omega^2 \delta = \alpha$$

Spring deflection (Equation B.7)

$$\delta = \frac{\alpha}{\omega^2} (1 - \cos \omega t)$$

Resultant mass acceleration (Equation B.10)

$$\ddot{y}_p = \alpha (1 - \cos \omega t)$$

where \ddot{y}_p represents the resultant mass acceleration.

Maximum mass acceleration (Equation B.16)

$$\ddot{y}_p(\max) = 2\alpha$$

The resultant mass acceleration is analagous to the response of a human when subjected to similar input conditions, and is illustrated in Figure 7. (see also Fig. B.2) in non-dimensional form. It can be seen that the output is less than the input for values of $\omega t < \pi/2$, is equal to it when $\omega t = \pi/2$, and for values of ωt between $\pi/2$ and $3\pi/2$, the output is always greater than the input. In the latter case the output acceleration is said to overshoot the input acceleration. When $\omega t = \pi$, the mass acceleration is exactly twice the input which represents 100% overshoot. The output reduces to zero at a time represented by $\omega t = 2\pi$ and thereafter the pattern is repeated in a cyclic manner. When some initial deflection is present in the spring the mass acceleration is given by B.11 as

$$\ddot{y}_p = \alpha (1 - \cos \omega t) + \omega^2 \delta_s \cos \omega t$$

In deriving this equation it was assumed that the influence causing the initial deflection made no force contribution to the motion of the mass. It can be seen from Figure 7 that such a disturbance increases the mass acceleration for $\omega t < \pi/2$ and $5\pi/2 > \omega t > 3\pi/2$ etc, but in the region where the mass acceleration is a maximum, the value is actually reduced and the peak mass acceleration is given by

$$\ddot{y}_p(\max) = 2\alpha - \omega^2 \delta_s$$

The explanation of this reduction is that, when an initial deflection is present, the compression δ_s is attained without a velocity being introduced into the system, so that less kinetic energy is available and the maximum deflection and mass acceleration are reduced.

If the disturbing force acts throughout the acceleration cycle, (contributing an acceleration G') the peak mass acceleration is given by

$$\ddot{y}_p(\max) = 2(\alpha + G') - \omega^2 \delta_s = 2\alpha + G'$$

so that, in this case, the peak mass acceleration is increased by the value of the steady G' field.

Thus, preloading in a direction opposite to that of the input acceleration can alleviate the peak body response if the loading force is removed when the input reaches the same value, which would occur if an inelastic restraint was employed. In practice, of course, this improvement is difficult to achieve due to such effects as curvature of the spinal column, rebound, and the presence of multi-directional accelerations.

When damping is included in the system the equation of motion contains an additional term due to the force exerted on the mass by the damper, as explained in Appendix E, from which the following have been extracted.

Equation of motion (Equation E.3)

$$\ddot{\delta} + 2c\dot{\delta} + \omega^2\delta = \alpha$$

where C is the damping coefficient

Resultant mass acceleration (Equation E.9)

$$y_p = \alpha \left\{ 1 - e^{-ct} (\cos \omega_0 t - \frac{c}{\omega_0} \sin \omega_0 t) \right\}$$

where $\omega_0^2 = \omega^2 - c^2$ and ω_0 is the damped frequency

Maximum mass acceleration (Equation E.11)

$$\ddot{y}_p(\max) = \alpha (1 + e^{-ct})$$

where $t = \frac{1}{\omega_0} \tan^{-1} \left(-\frac{2c\omega_0}{\omega_0^2 - c^2} \right)$ and the angle is in the second quadrant

Spring deflection (Equation E.5)

$$\delta = \frac{\alpha}{\omega^2} \left\{ 1 - e^{-ct} \left(\frac{c}{\omega_0} \sin \omega_0 t + \cos \omega_0 t \right) \right\}$$

These equations refer to the sub-critically damped case where $\omega^2 > c^2$. The presence of damping terms modifies the output of the single degree of freedom model, as shown in Figure E.2, where it can be seen that maximum value of the mass acceleration is reduced, but it is achieved earlier. Figure 8 compares the response of a damped system based on the total force acting on the mass (proportional to mass acceleration) and on the spring strain (proportional to deflection) given by $F = k \delta$ so that

$$\frac{F}{m_p} = \frac{k\delta}{m_p} = \omega^2 \delta = \alpha \left\{ 1 - e^{-ct} \left(\frac{c}{\omega_0} \sin \omega_0 t + \cos \omega_0 t \right) \right\}$$

which has a maximum when $\omega_0 t = \pi$.

Up to maximum compression, for a given damping ratio c/ω , (where $c/\omega = 1$ represents critical damping), the acceleration based on the force developed in the spring is always lower than that based on total force and so represents a more optimistic tolerance criterion. Thus a study of the response of the damped system to a continuous step input indicates that a tolerance curve based on input accelerations will be less severe in the plateau region (full overshoot always attained) than the undamped case, and that allowables based on total force will be lower than those using spring force as a criterion.

4.1.2 Other Continuous Input Functions

The other simple input forms treated in Appendix B are; the linear ramp represented by $\ddot{y}_c = \beta t$ where β is the slope of the function, and the parabolic input represented by $\ddot{y}_c = \gamma t^2$. These are mainly of academic interest in themselves, since an input acceleration will not go on increasing indefinitely, but

the solutions can be useful if the input approximates to either form during the onset phase. In this case, the response to either the ramp or parabolic function can be used for the starting conditions to be used in the second phase. An input function taking the form of a ramp followed by a constant function is quite common in practice, however, a direct solution exists for this type of input as shown in Section 4.3.

The expressions for the appropriate mass accelerations are

Linear ramp (Equation B.13)

$$\ddot{y}_p = \beta \left(t - \frac{\sin \omega t}{\omega} \right)$$

Parabolic (Equation B.15)

$$\ddot{y}_p = \gamma t^2 - \frac{2\gamma}{\omega^2} (1 - \cos \omega t)$$

4.1.3. Rectangular Input

In practice, the input acceleration is applied for a short time (Δt) only, and the mass continues to move after the removal of the applied acceleration, just as a car continues to move after the accelerating force has been removed. The peak mass acceleration is usually attained at some time greater than Δt , so the solutions of the equations of motion for $t > \Delta t$ are important. This case can be treated by considering an input that rises instantaneously to some value α , remains constant for a time Δt and then becomes zero.

The response of an undamped single degree of freedom system to a rectangular input is treated in Appendix B, where it is shown that the resultant mass acceleration is given by (B.18)

$$\ddot{y}_p = \alpha (2 - 2 \cos \omega \Delta t)^{1/2} \sin(\omega t + \phi)$$

where ϕ is a phase angle given by $\tan^{-1} \left(\frac{1 - \cos \omega \Delta t}{\sin \omega \Delta t} \right)$ and time is measured from $t = \Delta t$.

The peak mass acceleration is shown to be (B.19)

$$\ddot{y}_p(\max) = \alpha (2 - 2 \cos \omega \Delta t)^{1/2}$$

This expression shows that the maximum mass acceleration depends on the frequency of the system and the input duration time, for a given value of α . This dependency is shown in Figure B.5 of Appendix B, and Figure 9 illustrates the typical response of the system for various input duration times. The output can be less than, equal to, or greater than the input acceleration, depending on the input duration. Hence, for small input durations the response of the model is low and quite high input accelerations can be tolerated. For the condition

$$\frac{y_p(\max)}{\alpha} = (2 - 2 \cos \omega \Delta t)^{1/2} < 1 \quad \text{i.e. } \omega \Delta t < \pi/3$$

the peak output acceleration is always less than the input, and the tolerable input accelerations are always greater than the critical value assigned to the mass acceleration. The condition of 100% overshoot is given by

$$2 - 2 \cos \omega \Delta t = 4$$

$$\text{i.e. } \omega \Delta t = \pi$$

so that for duration times greater than $\Delta t = \pi/\omega$ the tolerance level is independent of the pulse duration.

4.1.4. Impulsive Inputs

If the input duration time is extremely small, the motion of the system is of an impulsive nature and may be assessed in terms of velocity change since

$$\frac{\text{impulse}}{\text{mass}} = \frac{\text{force} \times \text{time}}{\text{mass}} = \text{velocity change}$$

In this report the impulse region covers duration times that are so short that full overshoot in the output response is not achieved. The impulse region is also referred to as impact and the short duration input acceleration are sometimes called "spike" inputs, although the latter term strictly refers to triangular shaped inputs.

The single degree of freedom system with no damping is analyzed in Appendix D for the general case of a non-linear spring. If n is put equal to unity, the equations are applicable to the linear system discussed here. The peak mass acceleration, from Equation D.21, can be represented by

$$\ddot{y}_p(\max) = \omega v$$

and depends only on the frequency of the system and the velocity change introduced by the impulse, so that input acceleration and duration times need not necessarily be considered as tolerance parameters. However, these terms can be introduced by writing the above equation in the form (Equation D.23)

$$\ddot{y}_p(\max) = \omega \dot{y}_c \Delta t$$

which is the relationship used in fitting the theory to experimental data, as explained in Section 3.4. For a given frequency, it is the area represented by $\dot{y}_c \Delta t$ that is important. Equation D.22 of Appendix D gives the duration limit over which the impulse theory is valid as

$$\Delta t_c = \frac{2}{\omega}$$

When damping is present in the system, the peak mass acceleration derived in Appendix E (Equation E.19) is

$$\ddot{y}_p(\max) = \omega v e^{-c t}$$

where the damping influence is contained in the e^{-ct} term, and the time at which the maximum occurs is described by

$$t = \frac{1}{\omega_0} \left\{ \tan^{-1}\left(\frac{\omega_0}{c}\right) - 2 \tan^{-1}\left(-\frac{\omega_0}{c}\right) \right\}$$

from Equation E.18 where $\tan^{-1}(\omega_0/c)$ and $\tan^{-1}(-\omega_0/c)$ are in the third and second quadrants respectively.

If the force developed in the spring is used tolerance criterion, the relevant acceleration is $\omega^2 \delta_{max}$ given by Equation E.16

$$\omega^2 \delta_{max} = \omega v e^{-ct}$$

where t is now $\frac{1}{\omega_0} \tan^{-1}(\omega_0/c)$. The two criteria are compared in Figure 10 for various damping values.

Using the deductions of Section 4.1.1 and the results quoted above, allows the influence of damping on the general form of the tolerance curve (based on total force) to be determined. Figure 11 shows how the position of the tolerance curve is affected by the choice of certain damping ratios. It can be seen that, for damping ratios associated with the human body (15 to 20%), the tolerance curve is moved up about 20% in the plateau region (~ 8 G). In the impulse region the tolerance line moves up with increasing damping until the value $c/\omega = 0.27$ is reached (see also Figure 10), and then back to the undamped line at $c/\omega = 0.5$. This is due to the fact that for c/ω values up to 0.5 the maximum output occurs after $t = 0$ (see discussion following Equation E.19) and some energy is dissipated. For $c/\omega > 0.5$ the tolerance curve moves down, since the force is transmitted through the damper immediately. Using spring strain as a criterion, the tolerance curve would become less stringent as the damping increased throughout the whole region. This is because the peak spring force is always reduced when damping is present.

4.1.5 Sinusoidal Inputs

If the applied acceleration fluctuates in a sinusoidal fashion it can be represented by the expression

$$\ddot{y}_c = \ddot{y}_{co} \sin \Omega t$$

where \ddot{y}_{co} is the amplitude and Ω the frequency of the motion. A continuous vibration of this form normally involves duration times outside the range of the model considered here, but in some cases a particular acceleration can be approximated by the initial cycle or cycles of a sine wave.

The solution of the equation of motion is developed in Appendix E. The expression for δ (see Equation E.28) has two distinct parts, one representing an oscillation of frequency (ω_0) dependent on the parameters of the spring-mass system, and the other describing a motion of frequency (Ω), the forcing function. The former, known as the transient solution, is given by

$$\delta = \frac{\ddot{y}_{co} \Omega e^{-ct}}{(\omega_0^2 - \Omega^2)^2 + 4c\Omega^2} \left\{ \frac{(\Omega^2 - \omega_0^2)}{\omega_0} \sin \omega_0 t + \frac{2c\omega_0}{\omega_0} \sin(\omega_0 t + \phi) \right\}$$

where $\phi = \tan^{-1} \frac{\omega_0}{c}$ and $\omega_0^2 = \omega^2 - c^2$ The part that oscillates with the applied frequency is called the steady state solution and is represented by

$$\delta = \frac{\ddot{y}_{co}}{(\omega^2 - \Omega^2)^2 + 4c\Omega^2} \left\{ (\omega^2 - \Omega^2) \sin \Omega t - 2c\Omega \cos \Omega t \right\}$$

The output of the system is the resultant of these two terms as shown in Figure 12. As time increases, the transient term is gradually damped out due to the influence of the e^{-ct} term, the rate of attenuation depending on the damping constant of the system.

The steady state solution was used in Appendix E to obtain the amplification factor (A) which indicates the amount of overshoot in the output acceleration. This is given by

$$A = \frac{1}{\{(\omega^2 - \Omega^2)^2 + 4c\Omega^2\}^{1/2}}$$

This expression has a maximum when $\Omega^2 = \omega^2 - 2c^2$ i.e.,

$$A = \frac{1}{2c\omega_0}$$

which represents the case of resonance. When no damping is present, resonance occurs when $\Omega = \omega$ and the amplification can be infinite. Under these conditions very high output amplitudes result for small input amplitudes, but the presence of even a small amount of damping modifies the picture considerably.

4.2 Restraint Effects

During the analysis of the experimental data it became apparent that the results depended to a large extent on the type of restraint used in the particular experiment. The importance of good restraint has long been recognized in the design of harness systems and practical experience counts for a great deal in this field. Although outside the terms of the present study, it was decided to make a brief investigation of the influence of restraint on the output of the dynamic model. Although the results are of a qualitative nature they illustrate the usefulness of the model and provide pointers for future work.

4.2.1. Seat Cushion Effects

The single degree of freedom system is modified to include an elastic cushion by placing a spring in series with the one

representing the human body, as shown in Figure G.1 of Appendix G. If damping is ignored the model can be represented by a simple equivalent spring system where the equivalent frequency ω is related to the two component spring frequencies ω_1 (man) and ω_2 (cushion) by the following expression (Equation G.4)

$$\omega^2 = \frac{\omega_1^2 \omega_2^2}{\omega_1^2 + \omega_2^2}$$

The cushion spring effectively reduces the overall frequency of the system which implies that the response will be slower and, for a given input duration in the impulse region, of smaller magnitude (decreasing ω moves the tolerance curve up). This is true if the cushion does not bottom as shown by Equation G.9 which gives the ratio

$$\frac{\ddot{y}_p \text{ max (with cushion)}}{\ddot{y}_p \text{ max (no cushion)}} = \frac{1}{\left(1 + \frac{\omega_1^2}{\omega_2^2}\right)^{1/2}}$$

The maximum mass acceleration of the system is always reduced by using a cushion, and the reduction is greater for small values of ω (i.e. a soft cushion) which is illustrated graphically in Figure G.2. For long duration times the full 100% overshoot is always attained and the cushion has no effect on the output of the system or the tolerance curve.

If the cushion bottoms during the motion the mathematical analysis proceeds as explained in Appendix G. The cushion spring has to be restrained at some deflection given by δ_{2B} (deflection at bottoming) and thereafter the input is transferred directly to the body spring. At the instant of bottoming any kinetic energy of the cushion spring is transferred to the body spring, only the potential energy being retained.

In the impulse region, it can be shown (Equation G.11) that the peak mass acceleration after bottoming is

$$\ddot{y}_p(\text{max}) = \omega_1 \left(\Delta v^2 - \frac{2E_1}{m_p} \right)^{1/2}$$

where Δv is the velocity change introduced by the impulse and E_c is the energy absorption capacity of the cushion, i.e. the potential energy $(\frac{1}{2} k_2 \delta_{2B}^2)$ stored in the cushion spring at bottoming. Comparing this equation with that representing the output of the single (body) spring system (Equation D.21)

$$\ddot{y}_p(\max) = \omega_1 \Delta v$$

it can be seen that the output is again reduced due to attenuation in the cushion. The bottoming velocity can be written

$$\Delta v_B = \left\{ \frac{2 E_c}{m_p} \frac{\left(1 + \frac{\omega_1^2}{\omega_2^2}\right)}{\frac{\omega_1^2}{\omega_2^2}} \right\}^{1/2}$$

which is small for a weak cushion spring (ω_2 and k_2 small) and for large values of the body spring (ω_1 and k_1 large). The beneficial influence of the cushion in the impulse region, even when bottoming occurs, can be seen from Equation G.15

$$\frac{\ddot{y}_p \text{ max (with cushion)}}{\ddot{y}_p \text{ max (no cushion)}} = \left(1 - \frac{2 E_c}{m_p \Delta v^2}\right)^{1/2}$$

So, for a given velocity change, the attenuation of the impulse depends on the energy absorption capacity of the cushion and is independent of stiffness ratio.

When relatively long duration inputs are considered a bottoming cushion can have very severe effects on human tolerance. The solution developed in Appendix G gives the maximum mass acceleration after bottoming as

$$\ddot{y}_p(\max) = \alpha + \left\{ \alpha^2 + 2\alpha \ddot{y}_B - \ddot{y}_B^2 \left(1 + \frac{\omega_1^2}{\omega_2^2} - \frac{\omega_1^4}{\omega_2^4}\right) \right\}^{1/2}$$

This shows that for the condition

$$\frac{2\alpha}{\ddot{y}_B} > 1 + \frac{\omega_1^2}{\omega_2^2} - \frac{\omega_1^4}{\omega_2^4}$$

which is true for all finite values of the frequency ratio, the overshoot can exceed 100% which represents a much more severe acceleration imposed on the human than when no cushion is present. Thus, large bottoming velocities are dangerous and if bottoming must occur it should happen as early as possible.

Summarizing, for impulsive inputs a cushion is always beneficial and increases the tolerance level; for longer duration inputs, the cushion has no influence unless it bottoms, in which case considerable magnification of the output can occur. These conclusions are presented, in graphical form, in Figure 13 and Figure G.4 of Appendix G.

4.2.2. Rebound

The phenomenon termed rebound can occur when the acceleration applied to the occupant of a seat is suddenly removed and the occupant is thrown into his harness system. The undamped linear single degree of freedom model can be used to analyze this problem as explained in Appendix H. The body spring goes in to compression in the usual way when the acceleration is applied to the seat pan and when the input is removed after a time Δt , the spring returns to its original position, but with a certain velocity. At this stage, the body spring becomes inoperative and the restraint spring starts to compress, decelerating the mass. From Equation H.11 the maximum deceleration is given by

$$y_p(\max) = -\alpha \omega_2 \Delta t$$

where ω_2 is the restraint frequency and α is the initial step input. This expression is similar to that derived for the impulsive input (Equation D.23 of Appendix D) but

ω_2 is now the important parameter. The ratio of the peak mass accelerations imposed during the impact phase and rebound respectively can be formed, viz.

$$\frac{\ddot{y}_p \text{ max (rebound)}}{\ddot{y}_p \text{ max (input)}} = \frac{\omega_2}{\omega_1}$$

where ω_1 is the frequency of the body spring. The expression for the mass acceleration in rebound can be maximized for a particular input duration and "start of rebound" time to give

$$\ddot{y}_p(\text{max}) = -2\alpha \frac{\omega_2}{\omega_1}$$

Regarding ω_2 and ω_1 as the equivalent man-harness and man-cushion frequencies respectively, it follows that considerable amplification of the input acceleration is possible, if the equivalent restraint system is stiffer than the equivalent cushion system.

4.3 The Importance of Rise Time

An expression that often appears in the literature on acceleration stress is "rate of onset of acceleration" which is usually quoted in units of G per sec. Rate of onset has frequently been used as a critical parameter in determining human tolerance to abrupt accelerations and in some cases test subjects have reported being able to sense different onset rates. The dynamic model is based on the concept that the acceleration response of the subject is the important criterion and, in this context, the maximum input acceleration and duration time are the important parameters. If the input acceleration is less than half the allowable mass acceleration, the peak mass acceleration will never exceed the critical value regardless of the rate of onset (e.g. a step input where the rate of onset is infinite). When the input acceleration is greater than half the allowable mass acceleration, the overshoot is influenced by the rate of onset, but it is more explicit to refer to the time taken to reach a certain plateau or peak value, i.e. the rise time t_r , since the frequency of

the system (cycles per second) is also involved. The definition of rise time will be clarified by reference to Figures I.1(a) and (b). Rate of onset, in itself, does not mean very much unless the peak input acceleration is also specified, then - rate of onset x rise time = peak input acceleration.

The simple case of an input consisting of a linear ramp function followed by a constant is studied in Appendix I. For zero damping, the model response is given by Equation I.5.

$$\ddot{y}_p = \beta t_r - \frac{2\beta}{\omega} \left\{ \cos \omega \left(t - \frac{t_r}{2} \right) \sin \frac{\omega t_r}{2} \right\}$$

where β is the slope of the ramp function, i.e. the rate of onset of acceleration.

When the ramp input is operative, i.e. before the acceleration levels off, the mass acceleration is given by Equation B.13 as

$$\ddot{y}_p = \beta t \left(t - \frac{\sin \omega t}{\omega} \right)$$

This function exhibits no maxima, only points of inflection and the acceleration output has the form shown in Figure B.2 of Appendix B. The fluctuations of the output about the input are governed by the values of ω and β , overshoot is still present in the output, but is combined with an increasing input to give the effect shown in the figure. The important quantity is the degree of overshoot obtained when the input acceleration has levelled off and remained constant for a long time. This can be represented by Equation I.8 which gives

$$\frac{\ddot{y}_p^{(max)}}{\beta t_r} = 1 - (-)^n \frac{\sin \frac{\omega t_r}{2}}{\frac{\omega t_r}{2}}$$

where n is an integer and βt_r is the plateau value of the input. The integer n enters the expression since $\sin \frac{\omega t_r}{2}$ may be positive or negative, depending on the quadrant containing the angle $\omega t_r/2$. It is shown in Appendix I that for $n = 1$,

$$0 \leq \omega t_r \leq 2\pi$$

and for $n = 2$

$$2\pi \leq \omega t_r \leq 4\pi$$

and so on. The above expression is plotted against ωt_r in Figure I.2 and the curve exhibits a series of humps. For very small values of ωt_r (representing a short rise time or a low frequency system) the overshoot is 100%; as ωt_r increases, the degree of overshoot decreases eventually reaching zero when the output equals the input. When ωt_r is increased further, some overshoot is again obtained, the pattern repeating itself, but with rapidly decreasing amplitude.

For a given system having a certain frequency ω , the rise time of the input is, therefore, an important parameter if the input exceeds half the tolerable output. For a given rise time, a low frequency system will exhibit greater overshoot than a high frequency system. These theoretical deductions have been further illustrated in the analog computer studies reported in Section 7.0.

The theory indicates that, if the rise time is long enough, very large input acceleration can be tolerated. However, it must be remembered that the present model is limited to structural effects and a large rise time means a long total duration, which involves other tolerance criteria.

4.4 Application to Escape Systems

The limiting acceleration-time history that is permissible, from human tolerance considerations, during the ejection phase of an escape capsule or seat has been the subject of considerable experimental research, and the dynamic model will have important applications in this area.

Basically, the approach is similar to that described in the general applications described so far, but the model now consists of two masses coupled together by a spring representing the occupant and his cushion (Figure F.1). The theory is developed in Appendix F for impulsive and continuous inputs. Equation F.8 gives the peak acceleration experienced by the man for the zero damping case as

$$\ddot{y}_p(\max) = \frac{2F}{m_c + m_p}$$

where F is the applied force (constant), m_c is the seat, or capsule mass, and m_p represents the occupant's mass. Now $\frac{F}{m_c + m_p}$ is the acceleration obtained for the system as a whole, so the acceleration history calculated by regarding the escape system and occupant as a rigid body can be used in assessing the occupant's tolerance to the input.

During the acceleration phase, the occupant provides a downward force on the escape device, modifying its acceleration and it is shown in Appendix F that the ratio of the peak accelerations of man and escape device is given by

$$\frac{\ddot{y}_p(\max) \text{ occupant}}{\ddot{y}_c(\max) \text{ escape device}} = 2 \left(1 - \frac{m_p}{m_p + m_c} \right)$$

Thus, the lighter the seat or capsule compared to the occupant, the lower the relative accelerations, but the peak occupant

output is always twice the value calculated for the combined masses. When an impulsive input is considered, the system can again be treated as a rigid body.

4.5 The Two Degree of Freedom Model

The single degree of freedom system does not predict the decrease in tolerable accelerations in the higher duration time region (from .07 sec. to 1 sec.). The quite rapid drop in the tolerance curve suggests that a second lower frequency mode exists, and this has in fact been verified by shake table tests (Ref. 16). The predominant mode indicated by these tests has a frequency of 5 cps. With two distinct modes present, it seemed likely that a two degree of freedom model, such as that illustrated in Figure 5(c), could be used to investigate the dynamics of the body under the influence of short duration accelerations. Since data on the dynamic properties of various parts of the body is sparse, the application of the model was limited to the following two cases:

1. The upper spring-mass system representing the visceral mode of 5 cps, and the lower system the spinal mode at 44 cps.
2. The upper spring-mass system representing the thoracic vertebrae, and the lower system the lumbar vertebrae, (the data given in Ref. 5 being used for this application).

The mathematical analysis of the model is given in considerable detail in Appendix J so that only the important results need be quoted here. The solution of the equations of motion were developed for the zero damping case in order to reduce the algebra involved so that the influence of the important parameters could be more readily seen. The

solution for a step input is of particular interest, since it yields all the important information about the response of the model. Equations J.35 and J.36 give the deflections

$$\delta_p = \frac{\ddot{y}_c \omega_p^2}{\Omega_1^2 - \Omega_2^2} \left\{ -\frac{1 - \cos \Omega_1 t}{\Omega_1^2} + \frac{1 - \cos \Omega_2 t}{\Omega_2^2} \right\}$$

$$\delta_q = \frac{\ddot{y}_c}{\Omega_1^2 - \Omega_2^2} \left\{ \frac{\omega_q^2 - \Omega_1^2}{\Omega_1^2} (1 - \cos \Omega_1 t) + \frac{\Omega_1^2 - \omega_q^2}{\Omega_2^2} (1 - \cos \Omega_2 t) \right\}$$

where δ_p , and δ_q are the deflections in the upper and lower spring and ω_p and ω_q are the uncoupled frequencies of the upper and lower system respectively. Ω_1 and Ω_2 are the coupled frequencies and are given in Equation J.29 and J.30 by the expressions

$$\Omega_1 = \frac{1}{2} \left\{ \omega_p^2 + \omega_q^2 + \omega_{pq}^2 - [(\omega_p^2 + \omega_q^2 + \omega_{pq}^2)^2 - 4\omega_p^2 \omega_q^2]^{1/2} \right\}$$

$$\Omega_2 = \frac{1}{2} \left\{ \omega_p^2 + \omega_q^2 + \omega_{pq}^2 + [(\omega_p^2 + \omega_q^2 + \omega_{pq}^2)^2 - 4\omega_p^2 \omega_q^2]^{1/2} \right\}$$

where $\omega_{pq}^2 = \frac{m_p}{m_q} \omega_p^2$ and m_p and m_q are the masses associated with each spring.

Since damping has been omitted, it is permissible to express the tolerance criterion as a limit on deflection in either or both springs.

Time histories of the deflections were obtained for a range of values of the parameters m_p/m_q , ω_p and ω_q with the aid of a digital computer and maximum values of $\omega_p^2 \delta_p / \ddot{y}_c$ and $\omega_q^2 \delta_q / \ddot{y}_c$ (the overshoot factors) were obtained from the results. The two applications are discussed separately.

1. Model Representing the Visceral and Spinal Modes

The spring q is taken as analagous to the spinal mode and the low frequency visceral mode is represented by the

spring p. For short duration inputs to the base of the system the displacement of the mass m_q is quite small and so the deflection in the spring p is small, giving rise to insignificant forces acting in opposite directions on the masses m_p and m_q respectively. Hence, the force acting on the mass m_q is virtually that of the single degree of freedom system. As the input duration time increases, so the displacement of the mass q increases, which in turn increases the deflection and the force in the spring p. This force is reacted back through the mass q to the spring q, such that a larger force must be applied to the base of the system for a given constant input acceleration. The build up of forces within the system is revealed as deflections of the spring q. A limit on this deflection is used as the main tolerance criterion, which may be related to the limit on acceleration used previously (80 G) by application of the relationship $\ddot{y}_q = \omega_q^2 \delta_q$. Values of \ddot{y}_q (max) were obtained for four ratios of m_p to m_q since the exact ratio is not known with any degree of accuracy. Several maxima were obtained in the output for each mass ratio and these values were used to construct the curves shown in Figure 14. The first maximum occurred at approximately $t = 0.0114$ sec. and was the same for each mass ratio and equal to that for the single degree of freedom spinal model. Hence, for times less than $t = 0.0114$, the normal spinal headward tolerance curve is applicable.

The ratio of m_p to m_q is quite important in that as m_p/m_q increases, so the tolerable acceleration decreases. Neglecting damping, the mass ratio giving the best fit to the presently available data is $\frac{m_p}{m_q} = 1.0$. However, for

duration times of the order of .05 sec. or greater, damping is important and with, say, 15% critical damping in the spinal mode, and some 30% critical damping in the visceral mode, then the curves corresponding to values of $\frac{m_p}{m_q} = 1.5$ or 2 would probably give a better fit to the experimental results.

Although these results diminish the duration of the plateau region considerably, they are instructive in that they give a probable explanation of the reduction in tolerable G's for duration times of the order of .08 sec.

2. Application to the Upper and Lower Spine

The stiffness and mass data relating to the human spine given by Ruff (Ref. 5) were used to estimate the frequency ratio (ω_p/ω_q) and mass ratio (m_p/m_q) for the two degree of system representing the spine as two springs and associated masses in series. Values of 0.67 for the frequency ratio and 2.5 for the mass ratio were obtained. The frequency ratio was assumed to be exact, but various massratios in the region of 2.5 were assumed in view of possible errors in Ruff's value. Using various values of ω_p (thereby fixing ω_q) and of mass ratio, the digital computer was used to find maximum values of $\frac{\delta_p}{\ddot{y}_c}$ and $\frac{\delta_q}{\ddot{y}_c}$.

For input values of 30, 35 and 40 G (corresponding to the known tolerance levels in the plateau region) values of δ_p and δ_q were then obtained and plotted against frequency for each value of mass ratio. Tolerance criteria of $\delta_p = 0.02$ ft. and $\delta_q = 0.033$ ft. were taken from Ruff's experiments on spinal breaking loads, and it was assumed that the two parts of the spine failed simultaneously, as indicated by Ruff's work. For the three mass ratios used, this procedure yielded three pairs

of frequencies (and three pairs of frequency ratios ($\frac{\omega_p}{\omega_q}$)) for each value of input acceleration. These frequency ratios were then examined to determine which gave the best agreement with Ruff's figure of 0.67. It was found that, for all acceleration inputs, the frequency ratio corresponding to a mass ratio of three gave the best agreement, and these results are shown in Figure 15. The absolute values of frequency obtained were then used to calculate the coupled frequencies Ω_1 , corresponding to input accelerations of 30, 35 and 40 G, yielding values of 280, 300 and 335 rad/sec., respectively. The coupled frequency (Ω_1) should be the same as the frequency deduced for the single degree of freedom model. However, experimental results indicate that the tolerable input (plateau region) is about 40 G, and the spinal frequency is approximately 225 rad/sec.

The results of this analysis are not very encouraging, but do point the way for more detailed future investigations. The work of Coermarnat W.A.D.D. might well provide more detailed information on the mechanical characteristics of the body that could be used in this type of analysis.

4.6 The Three Degree of Freedom Model

In the analysis of the two degree of freedom model, the concept of a normal (or resonant) mode was introduced. The two degree of freedom model was described uniquely by two such modes. The three degree of freedom system may be described by three normal modes and, in general, the number of normal modes required for a full description of the unidirectional motion of a system is the number of degrees of freedom it possesses. This in turn is (generally) the number of attached (but not rigidly attached) masses comprising the system. In Appendix F a system of two

masses joined by a spring is analyzed. The frequency (ω) of oscillation of such a system is given by

$$\omega = \left\{ \frac{k}{\frac{m_c m_p}{m_c + m_p}} \right\}^{1/2}$$

where m_c and m_p are the masses and k is the stiffness of the connecting spring. The effective mass of this simple system is $\frac{m_c m_p}{m_c + m_p}$ and is termed the inertia of the system.

Several masses, each connected to the adjacent mass by a spring and a damper will now be considered. For convenience of reference, the number of masses shall be $n + 1$, hence the springs and dampers number n of each. Such a system has n normal modes, since the first does not contribute to the number of degrees of freedom. For each normal mode there exists an equivalent mass or inertia, and the general motion of the system is a combination of these normal modes of vibration, as was illustrated in the solution obtained for the two degree of freedom model. Generally, it is found that a system can be described practically by a relatively small selection of these modes; often only one mode, (that with the lowest frequency, referred to as the first mode) will suffice. For example, the response of a conventional fixed wing airplane to aileron control, and the phenomenon of aileron reversal, can be explained adequately by restricting the deformation of the airplane to its first wing torsion mode. Naively, perhaps, the supposition is that the response of a complex structure, such as the human body, to a very abrupt acceleration (less than .05 sec.) can be represented adequately by the first spinal mode, and for longer duration accelerations by the introduction of the first and second visceral modes. Each mode is characterized by an inertia, a frequency and a damping constant. It is this characterization that allows the representation of the human body by a simple mass-spring system, or a combination of such systems.

The development of a three degree of freedom model representing the human body subject to spinal accelerations was considered sufficient to demonstrate the usefulness and limitations of this approach.

Shake table tests on human subjects have shown that two distinct low frequency modes are present in the human body. The frequencies of these modes are five and ten cycles per second respectively (these frequencies were suggested by Dr. Coermann of W.A.D.D., and are based on experimental evidence). Although Coermann measured total body modes, the spinal frequency is relatively high, and the two low frequencies may be regarded as the natural frequencies of the visceral masses. This assumption leads to the model shown in Figure 5 (d), which represents a mechanical analogy of the spine and visceral masses.

The analysis of such a model is dealt with in considerable detail in Appendix K. The deflection (δ_1) in the spinal spring is obtained for a general rectangular input, and for an impulsive input. A solution for a sinusoidal input is also developed, using the concept of complex numbers to reduce the algebra involved.

(a) Solution for a Rectangular Input Acceleration

The general solution for a rectangular input is given in Equations K.32 (a) and (b) with damping included in each mode. The solution for a step input, which is a special case of the rectangular input analysis, is useful since it includes all the maxima that can be obtained with various duration rectangular inputs and yields sufficient points to obtain an accurate graph of the tolerable accelerations.

The solution for the step input is represented by Equations K.32 (for δ_1) and K.37 (for $\dot{\delta}_1$) and the constants

contained in these equations are obtained from K.31 and K.37.

The criterion for injury is expressed as a limit on the force ($m\ddot{y}_1$) exerted by the spring and damper of constants k_1 and $2K_1$, respectively, on the mass m_1 , i.e.

$$m\ddot{y}_1 = k_1\delta_1 + 2K_1\dot{\delta}_1$$

This limit may be expressed in terms of the acceleration

$$\ddot{y}_1 = \omega_1^2\delta_1 + 2c_1\dot{\delta}_1$$

Time histories of \ddot{y}_1/y_c were obtained for several values of the damping coefficients c_1 with the aid of a digital computer, and the maximum values obtained by inspection. The values of tolerable input accelerations given in Fig. 16 were obtained by putting $\ddot{y}_1(\text{max}) = 80 \text{ G}$, and dividing this by each maxima of \ddot{y}_1/y_c in turn. The zero damping case does not differ significantly from the results plotted in Fig. 14 for the two degree of freedom model, and the conclusion is that the two degree of freedom system is sufficient for accelerations of less than say one second. The effect of damping is very pronounced for duration times where the low frequency modes are important. From the similarity of the undamped case to that of the two degree of freedom it is not unreasonable to suppose that damping will have a similar effect upon the tolerable accelerations predicted by the two degree of freedom model.

(b) Solution for a Sinusoidal Input Acceleration

The response of a spring mass system subjected to a sinusoidal input acceleration can be divided into two parts. (See Appendix E).

1. The transient response with a frequency dependent upon the parameters of the system.

2. The steady state response with the frequency of that of the input acceleration.

When tolerance to long duration inputs is considered, only the steady state response is important.

The equations governing the three degree of freedom model are developed in Appendix K. The application of this model to the human tolerance curve involves calculating the ratio R of the output to input amplitudes, given by (K.46).

$$R_j = \frac{(\mu_j^2 + \nu_j^2)^{1/2}}{\ddot{y}_{co}}$$

where \ddot{y}_{co} is the amplitude of the input acceleration and μ_j and ν_j are the real and imaginary parts respectively of the output amplitude A_j and are defined by Equation K.45.

The ratios R_1 , R_2 and R_3 , corresponding to the three modes of vibration, were calculated on the digital computer for various input frequencies (1 to 17 cps) and damping values of 15% critical in Mode 1 (spinal), 3% in Mode 2 (10 cps visceral), and 25, 30 and 35% in Mode 3 (5 cps visceral). These values of damping coefficients were suggested by a survey of experimental results.

The low frequency criteria were taken from the tolerance curve of Ref. 16 (Fig. 21), which is replotted in Fig. 17a. One method used the tolerable input corresponding to the first minimum (point A) to obtain a reference amplitude for both low frequency modes. In the second method, points A and B were used to define reference amplitudes for Modes 3 and 2 respectively. The tolerance level for the high frequency mode was established by assuming a critical allowable deflection (δ_c) that gave

the best fit with the curve of Ref. 16. The value of δ , so obtained (Fig. 17.b) was 0.01 ft., which is about 20% of the spinal breaking deflection for steady loading, but it must be remembered that the curves of Ref. 16 are based on voluntary tolerance (greater than 20 sec. duration).

The agreement obtained between the theory and the experimental results of Ref. 16 is not particularly good. However, the experimental results may be at fault, rather than the theory, and an evaluation of the usefulness of the three degree of freedom system should await further developments in both the theoretical and experimental fields.

5.0 Non-Linear Systems

It is known that certain parts of the body respond in a non-linear fashion in certain force ranges so that the analogous linear spring system represents an ideal case. In a non-linear system, equal increments of applied force do not produce equal increments of deflection and a force-deflection plot does not produce a straight line. Non-linearity in the human body shows up as increasing effective stiffness as the applied force increases. Mathematically, a non-linear spring can be represented in a variety of ways, but a good approximation is to represent the force-deflection characteristics by the relationship

$$F = k_n \delta^n$$

where n is an integer. The equation of motion now takes the form

$$\ddot{y}_c = \omega_n^2 \delta^n + \ddot{\delta}$$

The solution of this equation is developed in Appendix C for a step input and for an impulsive input in Appendix D. The peak mass acceleration for a step input is from Equation C.10

$$\ddot{y}_p(\max) = (n+1)\alpha$$

and for the impulsive case (Equation D.16)

$$\ddot{y}_p(\max) = \zeta_n \left(\frac{n+1}{2} \frac{v^2}{\zeta_n} \right)^{\frac{n}{n+1}}$$

where $\zeta_n = \omega_n^2$. Knowing the maximum allowable value of α in the plateau region from experiment and assuming a value of n , the step input formula gives a value for the allowable peak mass acceleration. Now the expression describing the impact case can be rearranged to give

$$\left\{ \ddot{y}_p(\max) \right\}^{\frac{n+1}{2n}} = \zeta_n^{\frac{1}{2n}} \left(\frac{n+1}{2} \right)^{\frac{1}{2}} \alpha \Delta t$$

which can be used to represent the tolerance curve in the impact region of Figure 2 for any value of n , since

$$\log \alpha = \frac{n+1}{2n} \log \frac{\ddot{y}_p(\max)}{\zeta_n^{\frac{1}{2n}} \left(\frac{n+1}{2} \right)^{\frac{1}{2}}} - \log \Delta t$$

A plot of $\log \alpha$ against $\log \Delta t$ would give a straight line of slope -1, the actual position of the line being controlled by the value of the remaining expression in the above equation. Using the allowable value of the mass acceleration $(n+1)\alpha$, where α is obtained from experiment (plateau region of Figure 2), results in certain values of ζ (or ω) corresponding to the chosen value of n . For headward accelerations, drop tests have shown that the critical impulsive velocity change is 11 ft/sec., and using the maximum permissible spine deflection of 0.05 ft., as deduced by Ruff (Ref. 5), values of the "equivalent linear spring frequency" can be deduced corresponding to various values of n . Such a value would correspond to a linear model that would predict the correct conditions at maximum deflection. In view of what has been said above, and the accuracy of the available experimental results, it is considered that a strictly linear model ($n = 1$) is adequate for the present studies.

6.0 Digital Computer Studies

The equation of motion for the undamped, linear single degree of freedom model is

$$\ddot{y}_c = \omega^2 \delta + \ddot{\delta}$$

where the input acceleration \ddot{y}_c can take any form, depending on the conditions of the case under consideration. For simple input forms that can be approximated by a concise mathematical formulae, the equation of motion can be solved by analytical methods, as demonstrated previously. When the input is of a complex nature - the case usually met in practise - the solution must be obtained by an iterative or step-by-step procedure. Such a procedure can be exceedingly tedious and time consuming if performed by hand, so one normally seeks the aid of an automatic digital computer.

The Stanley Aviation IBM 1620 computer has been programmed to solve the equation of motion of a linear single degree of freedom system for any arbitrary acceleration or force input. The program uses the Fortran system and is quite general in that the coefficients relevant to the particular problem can be used. The equation of motion is solved for the deflection (δ) which is then related to the mass acceleration (\ddot{y}_p) by the expression

$$\ddot{y}_c - \ddot{y}_p = \ddot{\delta}$$

The results are presented on a card output, in a form suitable for automatic plotting on a Benson-Lehner data plotter, and contain information on δ , $\dot{\delta}$, $\ddot{\delta}$ and \ddot{y}_p against time. The machine employs a time interval that is automatically adjusted to give the desired accuracy of $\pm 3\%$ in the result, which means that quite complex inputs can be handled.

The time involved in obtaining a solution using the computer varies from 15 to 30 minutes, depending on the complexity of the input acceleration-time history. The mass acceleration-time plot is studied to establish if the peak acceleration exceeds the allowable value for the particular direction of applied input.

A typical analysis is shown in Fig. 18. The example used is taken from the test program being carried out on the Daisy Track sled at Holloman A.F.B. The subject was a male bear (Run No. 390) fully restrained, and the acceleration was measured on a rigid portion of the sled and no cushion was present. The output shown in Fig. 18 represents the response of the equivalent spring-mass system, using a frequency of 278 rad/sec. (spinal mode). The high frequency peaks appearing in the input might be instrument "hash" and have very little effect on the output, which exceeded 80 G, the critical mass acceleration deduced from Eiband's work. The subject did in fact incur a spinal injury during the test.

The digital computer has also been used with the two and three degree of freedom models, but only for limited input forms.

7.0 Analog Computer Studies

A special purpose analog computer has been developed at Stanley Aviation to aid in the study of human tolerance to short duration accelerations. Although this computer was developed outside the N.A.S.A. research program, a brief description of the device is necessary, since it was used in the analysis of some of the experimental data.

The analog computer is capable of solving the equation governing the motion of a spring-mass system in a continuous fashion by operating on an applied voltage input that simulates

the applied acceleration. Using the D.C. operational amplifier as the basic component, the electronic network can be arranged to perform multiplication, summation and integration of the voltages in the circuit. Thus, mathematical operations can be performed on the voltage that are analogous to the operations necessary for the solution of the equation of motion of the mechanical model.

The basic principles of the analog circuit are illustrated by Fig. 19, where an electronic network is arranged to solve the equations pertaining to a single degree of freedom model with damping. Fig. 20 shows an experimental arrangement, where the input is read directly from a given trace, represented by a current carrying wire. A magnetic pick-up follows the trace and generates a voltage proportional to the magnitude of the acceleration. This voltage is fed into the analog circuit and the output voltage (equivalent to the mass acceleration) is presented on a cathode ray tube. The analog can work in real time or a "scaled time" depending on the time constants of the net work.

The influence of rise time on the response of the spring-mass system has been investigated using the analog. These tests were conducted in the course of a check out on the accuracy of the computer and should not be regarded as confirmation of the theory, since the computer only performs the operations suggested by the theory. In this respect it is only as good as the theory that governs the dynamic model. Some computer outputs are shown in Figs. 21 and 22. These are direct traces of pictures taken of the cathode ray tube during a test, using a polaroid camera, and show the input acceleration and the mass acceleration determined by the analog. The scale used for the output is half that used for the input so overshoot was attained in each case. Fig. 21(a) illustrates

the output obtained using a step input and zero damping; the error involved is about 3%. The results presented in Fig. 21(b) refer to another Daisy Track experiment (Run No.389). The input acceleration was applied in the headward direction and reached over 50 G. The bear subject received spinal injuries that would be expected from the peak mass response of over 80 G. Fig. 22(a) shows a typical trace obtained during the tests when the variation of rise time was investigated. A ramp input function followed by a constant value was used and the peak mass accelerations obtained gave good agreement with the theory, showing that the accuracy of the analog analysis is quite acceptable. (Fig. 22 (b)).

The main advantage of the analog technique is that the characteristics of the mechanical system can be varied at will by adjusting the equivalent parameters in the analog. Such important parameters as restraint and cushion characteristics and body position can be optimized without resorting to expensive and time-consuming test programs. With this in view, a more advanced computer, including cushion and restraint characteristics, is presently being developed by Stanley Aviation.

8.0 Analysis of Experimental Data

8.1 Availability of Data

One of the disappointing aspects of this program is the dearth of usable experimental information. Considerable evidence exists that vehicle accelerations of up to 30 G can be withstood for duration periods of up to 1/10th of a second in the spinal and transverse directions, but the vital areas of interest, including the plateau region covering a range of input values from 30 to 50 G, and the impulse region for input accelerations exceeding 50 G, have not been adequately explored.

This is understandable from the nature of the experiments and the need for using human subjects to get realistic data, and much of the information that does exist is based on animal test subjects chosen because some degree of similarity of body structure exists between the animal and man. Thus, bears, chimpanzees, and to a lesser extent hogs, have been used. Another disappointing feature of the experimental program is the lack of existing methodical documentation of tests that were carried out some years ago. In many instances, when information was requested on tests that were apparently of extreme interest, it was found that comprehensive records of the tests did not exist, or had been destroyed.

In early experiments, for instance the German work and tests carried out by the Naval Air Materials Laboratory, many of the injuries were sustained at relatively low G values due to inadequate restraint. The experimental programs were designed to meet the immediate needs that existed at the time, and there was very little standardization of input acceleration pattern, restraint system, seat and instrumentation. Thus, many of the results obtained are limited by the lack of reproducibility and the absence of strictly controlled conditions, and the information of interest in an evaluation of the dynamic model is masked by a variety of factors.

The problem of instrumentation is always present in human factors experiments and much of the early work presents conflicting results because of the inability to measure the relevant parameters with any degree of accuracy. Accelerometers are extremely sensitive to their immediate environment and good mounting and attachment are essential. In many cases, the instrument can record the peculiar response of the mount rather than the gross accelerations imposed on the vehicle and, in some experimental arrangements, resonance vibrations can be set up in the main structure (sometimes termed ringing) which

again gives an erroneous response. The response of an accelerometer of a certain natural frequency is analagous to that of the spring-mass model, so that overshoot can occur in a similar manner, depending on the duration and frequency of the applied acceleration. Rigid mountings are therefore essential to obtaining reliable readings. For this reason, accelerations measured on the human body during tests are highly suspect and should only be regarded as indicative of trends rather than the actual acceleration of the part of the body being investigated.

All the agencies known to be active in the field of experimental acceleration stress were contacted in an attempt to obtain as much experimental information as possible. The bulk of the usable results came from the work of Stapp carried out at Edwards A.F.B., with a rocket-sled, and that of Beeding at Holloman A.F.B., using the pneumatically propelled Daisy Track sled. A summary of the agencies contacted and the results obtained is given in Table 1. Because of the shortage of results, the analysis of experimental data was restricted to those relating to applied accelerations in the spinal headward, transverse backward, and transverse forward directions. Much of the experimental information used was taken from the literature which is referenced in this report, and the data used that is not readily available is summarized in Appendix L.

8.2 Spinal Headward Data

The logical starting point for the analysis of the headward acceleration is the data presented by Eiband (Ref. 2). As discussed in Section 2.2, Eiband's method of presentation of the results is highly subjective, since no firm criteria were used in assigning G levels and duration times. Eiband's actual results are plotted in Fig. 2, and again in Fig. 23, where the notation used indicates the source of the information, the

run identification number, and the type of analysis used. Thus, Eiband's original results have the letter E after the run number (see Table 2). These results were re-analyzed using exactly the same technique as that used by Eiband, eliminating some information that was considered unreliable, e.g. where more than one point on the graph had been deduced from a single end-point experiment. The analysis was performed as objectively as possible and the discrepancies between the results and the original deductions serve to illustrate the need for a more exact method of analysis of the results. Eiband's results have been supplemented by the additional data that was available, and can be identified by the symbol E'.

Considering the plateau region, although the information is limited, there is some evidence of the tolerance line lying just above the 40 G input acceleration level, and in view of the accuracy of the data, 40 G appears to be a reasonable value. Since this represents half the maximum response of the model, the allowable peak mass acceleration is taken as 80 G. The position of the tolerance curve in the impulse region controls the value of the ratio $G_p(\text{max})/\omega$ for the dynamic model. The slope of the line, from single degree of freedom theory is - 1, and fitting a line to the experimental data gives a value for ω . The value deduced for ω is then 278 rad/sec.

A method suggested for standardizing the analysis consists of comparing the dynamic model output obtained with a particular test, with that from a standard input. In the plateau region, an equivalent rectangular input, of duration Δt and input acceleration G_c , was deduced. To do this, the output of the undamped, linear, single degree of freedom model was obtained using the system characteristics deduced above. The equivalent rectangular input is then one which gives the same peak mass acceleration (assuming 100% overshoot) and the

same velocity change ($G_c \Delta t$). The input acceleration and duration time of the equivalent rectangular input are then used as the parameters for plotting on the tolerance curve.

In the impulse region, full overshoot is not attained and another criterion is necessary. The rise time is very short and the input was considered rectangular. Using the peak input acceleration from the experiment an equivalent rectangular input was constructed where the dynamic response was the same as that obtained from the experimental acceleration time history. The duration of the equivalent rectangular pulse was then taken as Δt for plotting purposes. Inconsistencies due to the finite rise time can be removed by comparing the experimental velocity change with that obtained from the equivalent rectangular input, and adjusting the value of G_c used until agreement is obtained between the two velocity changes. The results obtained from this analysis are plotted in Fig. 23 and denoted by the letter S. Fig. 24 illustrates the definitions used.

The general effect of this procedure is to move the experimental points to the right, implying that the effective input acceleration was of lower magnitude but lasted for a longer time than assumed in the original plot. Only one point (S50S) remains in the impulse region - meager evidence for fixing the position of the tolerance line. This run concerned a hog experiment that showed a severe end point and a two inch layer of styrafoam restraint was used that did not bottom out during the run. So even this point cannot be regarded as reliable. The procedure for finally fixing the position of the impulse tolerance line should now proceed by an iterative process - obtaining the new frequency and evaluating the equivalent rectangular input and so on - until agreement is obtained between the calculated and assumed frequency. However, in view of the unreliability of the experimental point,

this procedure was not adopted and evidence from another source was sought.

Simple drop tests, if properly controlled, can provide extremely valuable results in the impulse region, also accident data such as those reported in Ref. 29 can be consulted, but the latter rely on deduced information and the degree of injury usually greatly exceeds the tolerance level used here. Accident data are also difficult to analyze from the point of view of applied force direction. Experiments conducted by Swearingen and reported in Ref. 22 appear to give the most reliable impact region results. The safe limit suggested from a large number of drop tests carried out with human subjects, seated on rigid seats, corresponds to an impulsive velocity change of 11.35 ft. per sec. From Equation D.23 of Appendix D, this velocity change is given by $G_p(\max) = \omega \Delta v$, which gives a value of the frequency of the equivalent spinal spring of $\omega = 226$ rad/sec. Human drop tests carried out at Stanley Aviation have indicated that velocity changes up to 10 ft/sec. can easily be tolerated, whereas Stapp (Ref. 18) has claimed a velocity change of 17.25 ft/sec. had no serious effects on a hog subject (Run 49) but full information on this test is not available.

If the lower value of spinal frequency (226 rad/sec.) is accepted, the influence on the model output for impulsive inputs can be visualized, since the maximum accelerations produced for two different frequencies is in the ratio of those frequencies for a given duration time. A lower frequency value implies less overshoot and higher tolerable input accelerations. In the plateau region, a reduction in frequency means a raising of the tolerable input level due to the increase in overshoot when studying the experimental results which have a finite rise time.

The tolerance line for durations greater than those contained in the plateau region has been sketched in as shown on Fig. 23. The slope has been taken as -1 , since the two degree of freedom model has indicated that this is the right order and might even be greater, depending on the relevant mass ratio (see Section 4.5).

8.3 Transverse Backward Data

When the direction of the accelerating force is at right angles to the body and towards the rear of the body it is termed backward. This type of acceleration is encountered during deceleration when the occupant of the vehicle is in the forward facing position. It was found that more information existed on this direction than any other, but evidence was again sparse in the impulsive region. Fig. 25 summarizes the available, usable data on a plot presenting vehicle acceleration against duration time.

The original Eiband tolerance curve did not show a plateau because of the lack of data, but a reasonable value for the maximum input acceleration in this region appeared to be 40 G. Using this value, the information contained in point D.E and the expected slope of -1 , gives a value of 33 rad/sec. for the equivalent system frequency. However, using the point S26E, the frequency obtained is 134 rad/sec. Point D.E is based on accident (fall) evidence and should be well within the end point region, whereas S26E was obtained from Stapp's hog experiments where the acceleration values were taken from an instrument mounted on the seat bottom. The acceleration obtained does not agree with the measured velocity change, which appears to be fairly reliable, and is probably an over estimate. Thus, from a first evaluation of Eiband's results, it was decided to use $\omega = 134$ rad/sec. in obtaining the equivalent rectangular input. Kornhauser (Ref. 30) has

suggested a critical velocity change of 80 ft/sec. and assuming a $G_p(\text{max})$ of 80 gives a frequency of 32 rad/sec. This line is shown in Fig. 25 and coincides with that based on accident data, which is not surprising. However, the Kornhauser figure is based on survival data, which involves a more severe tolerance criterion than that used here.

As further data became available and was analyzed by the Eiband method (points E'), it was apparent that this method of analysis indicated a lowering of the tolerance level in the plateau region (approx. 35 G). One particular end point experiment from the Holloman data ($H675E'$) did not appear to fit into the general pattern and indicated a very low tolerance level. However, the subject used in this test had an abnormally long torso and a very tight shoulder strap arrangement had to be used. This pre-stressing of the spine in a direction at right angles to the acceleration appears to have lowered the tolerance limit, and this test should be discounted.

When the equivalent rectangular input analysis was applied to the data in an attempt to standardize the criterion and take account of the rise time effects, most of the points in the plateau region were moved to the right into the long duration regime as shown in Fig. 25. This meant that a new plateau tolerance level had to be determined, and this was deduced to be about 45 G. The impact points were also moved to the right and the points of S26S and S27S controlled the position of the tolerance line in the impulsive region. (Note S26S was calculated from acceleration data measured by the accelerometer placed on top of the seat, which correlates with the velocity change and corresponds to the lower point $S26E'$ in Fig. 25). The most reasonable value for ω was found to be approximately 95 rad/sec. Continuing the iterative process was considered to be unnecessary as the position change

introduced is not greater than the accuracy of the original experiments. The impact velocity change corresponding to $\omega = 95$ rad/sec. is 30.5 ft/sec. A tentative tolerance curve is shown by the full line in Fig. 25.

The tolerance lines of Fig. 25 are presented, in the manner used by Kornhauser (Ref. 30), in Fig. 27. The lines representing duration times in Ref. 30 were found to be in error and have been recalculated for use here. Good agreement between the two sets of results is evident, except in the impulse region (0 - 0.02 sec.) where Kornhauser accepted a greater permissible velocity change than that used in this report.

8.4 Transverse Forward Data

The available data from experiments performed with the acceleration vector in the transverse forward (or sternumward) direction is given in Fig. 26. Very little evidence exists, none of which is deemed as particularly reliable. Some tests at Holloman A.F.B. have been conducted with the subject in the rearward facing position (acceleration forward) but as comparatively low G values. Experiment H.335 is of particular interest since it represents a definite end point and even on the equivalent rectangular input analysis the point appears to indicate a much lower tolerance level than for other input directions. Other tests under similar conditions (e.g. Run 332, peak G's 37.5 and Run 337, peak G's 39.0) indicate near end point conditions, but unfortunately the acceleration traces for these runs are not available. An explanation for this low tolerance level might lie in the fact that the subjects were inclined at 10° to the direction of the acceleration, giving an upward component that might have a strong influence on the body organs. In experiment S39S, the subject (a chimpanzee) received no injuries but obviously suffered pain and hydraulic effects would be difficult to determine.

If it is assumed that the frequency involved is the same as that for the backward direction, the impulse region can be defined by the lines shown in Fig. 26, the position depending on the value of G_p (max) used. The equivalent input analysis (using $\omega = 134$ rad/sec.) was applied to the data and the end point experiment S38S was found to lie beyond all the tolerance lines and so does not help much in the final choice of line. If experiment H.335 can be ignored as a statistical fluctuation it appears likely that the tolerance limits are similar to those for the backward direction, but enough evidence does not exist to draw even tentative conclusions.

The Stanley "static" drop tests (Appendix L) in which the force was in the forward direction, showed that velocity changes of up to 28 ft/sec. did not produce any signs of an end point, which indicates equivalent spring frequencies of $\omega = 80.5$ ($G_p \text{ max} = 70$), $\omega = 92$ ($G_p \text{ max} = 80$) and $\omega = 103.5$ ($G_p \text{ max} = 90$) radians per second. Since no injuries were incurred, the allowable velocity change might be higher, which would reduce the frequencies quoted above. Due to the attenuation system extending the pulse duration in these tests, and the inaccuracies of the recording instruments, some difficulty is encountered in positioning them on the tolerance curve, but they appear to be on the border of the impulse and plateau regions and cannot be considered as concrete evidence.

8.5 Multi-Directional Accelerations

Although the study of the influence of multi-directional accelerations on the human body is not part of the program described here, a brief description of the experimental results obtained at Stanley Aviation is of interest.

A large number of drop tests were carried out in support of the B-58 escape capsule development program. These included capsule drops from moving trucks and experiments performed with a monorail facility that enabled a known vertical and horizontal velocity to be imparted to the capsule. A yielding metal attenuator was used to minimize the impact forces experienced by the occupant, and accelerometers were mounted on the seat to record acceleration inputs in the three major directions. The tests which are of particular interest in assessing tolerance levels are listed in Appendix L.

Because of the nature of the tests, the capsule occupant experienced high accelerations in the transverse, spinal and lateral directions. When each direction is considered separately the results obtained are shown in Figs. 23, 25 and 26, but this analysis is not considered valid in view of the multi-directional nature of the applied accelerations, and the points are included for their interest value only and have not been used in determining the tolerance lines. The effects of multi-directional inputs on human tolerance are of extreme importance, since these inputs are often encountered in practice. A research program is presently underway to determine tolerance criteria for this type of input based on the magnitude and direction of the resultant acceleration experienced by the capsule. The results of this study will be published at the completion of the program under Ref. 31.

9.0 Tentative Tolerance Criteria

Because of the sparse evidence available, it is impossible to give firm recommendations for the values of the coefficients to be used with the dynamic model. The equivalent rectangular input concept has been introduced in an attempt to standardize the presentation of experimental tolerance data and to take

account of the effects of different rise times encountered in the tests. This method of analysis is not ideal and can be criticized on various counts, but it represents an improvement on existing methods. The application of this analysis has transferred many of the experimental points to the longer duration region, resulting in less evidence in the important impulse and plateau regimes.

The analysis of spinal headward accelerations has shown that the maximum plateau input acceleration can be taken as 40 G with some degree of confidence. The selection of an equivalent spinal frequency is not so well defined and because of the shortage of results in the impulse region, the most reliable evidence can be taken from the critical velocity change deduced from Swearingen's drop tests which gives a value for ω of 225 rad/sec.

Most of the data analyzed concerned the transverse backward direction, although most of the experiments concerned relatively long durations. The plateau tolerance line falls at a value of 45 G for the input acceleration and the most sensible position for the impulse tolerance line corresponds to a frequency of 95 rad/sec., which is somewhat higher than the value suggested by the evidence from accident survival. The adoption of the more pessimistic tolerance line appears justified since it satisfies the few sled test points available and accident cases usually represent extreme end points.

No satisfactory conclusions could be made from the transverse forward data, but a frequency of 95 rad/sec., as for the backward case, is suggested. From a physiological stand point the plateau tolerance level might be lower than that for the backward direction because of the position of the spine relative to the internal organs. There is some experimental evidence to support this fact and until more relevant tests have been

conducted, it is suggested that the allowable peak input acceleration is taken as 35 G.

Tentative values suggested for use with the single degree of freedom, undamped dynamic model are, therefore, as follows:

Headward Direction

frequency 225 rad/sec.

maximum allowable mass acceleration 80 G

Backward Direction

frequency 95 rad/sec.

maximum allowable mass acceleration 90 G

Forward Direction

frequency 95 rad/sec.

maximum allowable mass acceleration 70 G

The impulse or impact regions based on these criteria represent duration times from zero up to 0.009 sec. (headward), and 0.02 sec. (backward and forward). The end of the plateau region corresponds to duration times of 0.09 sec. (headward), 0.06 sec. (backward), and approximately 0.08 sec. (forward).

It should be remembered that these values are applicable to the undamped model. Damping will introduce changes in the tolerance levels as explained earlier, but these are considered to be small enough to be ignored at this stage, in view of the accuracy of the available experimental data. Also, if the Eiband type analysis is being used, the tolerance areas defined by the points E' in Figures 23, 25, and 26 are applicable.

10.0 The Need for Further Work

Research requirements in the field of human tolerance to short duration accelerations are considerable and only suggestions arising from the particular aspect described in this report will be mentioned here. The following broad suggestions are made:

1. Experimental work should be planned with the complete acceleration-time spectrum in mind to insure adequate coverage of impulse, plateau and hydraulic regimes.
2. More attention should be paid to experimental detail of individual experiments from the point of view of planning input acceleration programs that are more amenable to simple analysis and to the measurement of relevant experimental quantities and cross checking results by alternate instrumentation.
3. Where possible, more than one test to be carried out under a given set of conditions - giving reproducibility of results.
4. Standard objective, medical examination procedures should be devised to estimate degree of tolerance in experimental work.
5. More cooperation between experimentalists, theoreticians and persons with applied experience in the field, in the planning of experiments.
6. The theoretical and practical investigation of the influence of restraint systems on human dynamic response should be a matter of priority and the optimization and standardization of restraint systems used in tests should be agreed to.

7. More experimental data in the impulse region is essential - this could be achieved by simple, controlled drop tests which are reasonably inexpensive and give reliable results.
8. Human tolerance levels applicable to multi-directional acceleration inputs should be investigated using theoretical and experimental techniques.
9. Analytical studies should continue with the aim of producing more comprehensive models and more reliable values for the appropriate coefficients.
10. Experimental methods for the direct measurement of physical and mechanical characteristics of the body under dynamic conditions should be extended, and the correlation of human and animal response should be investigated to ensure the correct interpretation of experimental results using animal subjects.

It is only fair to point out that some of these suggestions are already being complied with in the acceleration stress field, and what is hoped for here is, a more universal acceptance of an agreed policy in attacking the many problems that still exist.

11.0 Conclusions

The research program reported here has developed a single degree of freedom dynamic model, consisting of a spring-mass analog of the human body, that can be used to predict human tolerance to abrupt accelerations. Variations of the basic model can be used to predict the quantitative effects of restraint systems and seat cushions, but more work is required in this field. Two and three degree of freedom models can be used for a better representation of the human body, but the

full significance of this approach will depend on further research. There is still a lack of reliable experimental data, but coefficients that can be used with the undamped single degree of freedom model have been suggested for the headward, forward, and backward acceleration directions.

The analytical solutions developed for simple input forms can be used in limited applications and for quantitative studies, but digital or analog computers are required for the analysis of complex acceleration inputs.

The analytical approach to the problem of acceleration stress and consideration of the dynamic response of the human body when subjected to short duration accelerations can make significant contributions towards a solution of the many problems involved. It is emphasized that cooperation amongst the persons engaged in the study of various aspect of acceleration phenomena will provide the surest means of obtaining a complete understanding of the overall problem.

REFERENCES

<u>No.</u>	<u>Name</u>	<u>Title, etc.</u>
1	Clark C. C. and Faubert D.	"A Chronological Bibliography on the Biological Effects of Impact." The Martin Company (Baltimore), E.R. 11953. Sept. 1961.
2.	Eiband M. A.	"Human Tolerance to Rapidly Applied Acceleration - A Summary of the Literature" NASA Memo 5-19-59E. June 1959
3.	Wiesehofer H.	Deutsche Versuchsanstalt fur Luftfahrt Aldershof U.M. 1175. 1943 (Also Ref.9)
4.	Richter H.	Ernst Heinkel Flugzeugwerke Res.Rep.3009. 1940 (Also Ref.9)
5.	Ruff S.	"Brief Acceleration: Less Than One Second" German Aviation Medicine World War II, Vol.I P584 Dept, of the Air Force. April 1950
6.	Geertz A.	"Limits and Special Problems in the Use of Seat Catapults" Armed Services Technical In- formation Agency, A.T.I. 56946. Aug. 1946
7.	Martin J.	"Ejection from High Speed Aircraft" J. Roy. Aero Soc, Vol. LX P 659. Oct. 1956
8.	Latham F.	"A Study in Body Ballistics: Seat Ejection" Proc. Roy. Soc. (London) Series B, Vol. 147, P 121. 1957
9.	Lovelace W. R., Baltes E. J. and Wulff V. J.	"The Ejection Seat for Emergency Escape from High Speed Aircraft" Air Technical Services Command TSEAL 3-696-74C. Aug. 1945
10.	Kroeger W. J.	"Internal Vibration Excited in the Operation of Personnel Emergency Escape Catapults" Frankford Arsenal, Philadelphia, M.R. 340.1946
11.	Watts D. T. Mendelson E.S.and Kornfield A.T.	"Human Tolerance to Accelerations Applied from Seat to Head During Ejection Seat Tests" N.A.M.C. Philadelphia, Rep. TED NAM 256005 Jan. 1947
12.	Hess J. L.	"The Approximation of the Response of the Human Torso to Large Rapidly Applied Upward Accelerations by that of an Elastic Rod and Comparison with Ejection Seat Data" Douglas Aircraft Co. Inc. Rep.No. ES 26472. Nov.1956

<u>No.</u>	<u>Name</u>	<u>Title, etc.</u>
13.	Kornhauser M.	"Impact Protection for Human Structure" Proc. American Astronaut (Western Regional Meeting) Aug. 1958
14.	Brock F. J.	"Acceleration Shock Protection Experiments Using Live Pigs" McDonnell Aircraft Corp.
15.		"Dynamic Response of Restrained Subjects During Abrupt Acceleration" Northrop Corp. Rep.No. NAI-54-585. Sept. 1954
16.	Goldman D. E. and Von Gierke H.E.	"The Effects of Shock and Vibration on Man" N.M.R.I. Bethesda, L and R. Series No. 60-3 Jan. 1960
17.	Coermann R. R., Ziegenrucker G. H., Witter A. L. and Von Gierke H. E.	"The Passive Dynamic Mechanical Properties of the Human Thorax-Abdomen System and the Whole Body System" J. Aero Med., Vol. 31, No. 6, P 443. June 1960
18.	Stapp, J. P.	"Tolerance to Abrupt Deceleration" Collected Papers on Aviation Medicine Agardograph No.6 P.122. London 1955
19.	Stapp J. P.	"Human Exposures to Linear Deceleration" Part 2 W.A.D.C. AF Tech. Rep. No. 5915
20.	Beeding E. J. and Mosely J. D.	"Human Deceleration Tests" Holloman A.F.B. AFMDC Tech. Note 60-2. Jan. 1960
21.	Holcomb G. A.	"Human Experiments to Determine Human Tolerance to Landing Impact in Capsule Systems" Presented at Fifth Symposium on Ballistic Missiles and Space Technology, Los Angeles, Aug. 1960
22.	Swearingen J.J., McFadden E.B., Garner J. D. and Blethrow J. G.	"Human Voluntary Tolerance to Vertical Impact" Aerospace Medicine, Vol. 31 P.989. Dec. 1960
23.	Payne P. R.	"Preliminary Investigation of the Dynamics of a Man-Carrying Capsule Subjected to External Forces" Stanley Aviation Report No. 1189 July 1960
24.	Payne P. R.	"The Dynamics of Human Response to Acceleration" Presented at 32nd Annual Forum of the Aero-Space Medical Association, Chicago, April 1961

<u>No.</u>	<u>Name</u>	<u>Title, etc.</u>
25.	Shapland D. J.	"The Dynamic Model - An Engineering Approach to the Problem of Tolerance to Abrupt Accelerations" Presented at the Symposium on Acceleration Stress, San Antonio, Nov. 1961
26.		"Handbook of Instructions for Aircraft Designers" Vol. I ARCDM 80-1, April 1960
27.		"Capsule Escape System Specifications" General Dynamics (Convair) FZC-4-344 (G) Feb. 1961
28.	Holcomb G.A.	"Impact Studies of the United States Aerospace Industry" Presented at the Symposium on Acceleration Stress, San Antonio, Nov. 1961
29.	Hasbrook A. H.	"Human Factors - The Basis for Crash Safety Design" Aviation Crash Injury Research, Phoenix, AV-CIR-63-0-108, Sept. 1959
30.	Kornhauser M. and Gold A.	"Application of the Impact Sensitivity Method to Animate Structures" Presented at the Symposium on Acceleration Stress, San Antonio, Nov. 1961
31.	Holcomb G. A., Huheey M. and Skidmore R.	"Abrupt Impact Tests Using Biological Specimens to Determine the Landing Impact Tolerance of the B-58 Escape Capsule" Stanley Aviation Report No. 1302 (to be published)

Table 1. Sources of Experimental Data

Source	Information Supplied	Subject	End Point	Near End Point	Direction of Acceleration	Comments
Holloman A.F.B.	Daisy Track Runs 96 - 707	Human Human Bear	1 1 2	2	Forward Backward Headward	Data on some runs not available.
Stapp, Refs. 18, 19.	As published	Human Chimpanzee Hog	1 1 1 2 1 1 1	4 1 2	Backward Headward Backward Forward Headward Backward Forward	More end points reported, but data not used since full information not given in published work.
N.A.M.L. Philadelphia	Some 4,500 tests investigated	Human	2		Headward	Low input values (20 G). Neck injuries.
W.A.D.D. (Aeromed. Lab.)	Couch drop tests and shake tests	Human and Bear				Maximum 36.5 G Information on low frequency modes.
F.A.A. Oklahoma City	Drop tests	Human	1		Headward	Instrumentation suspect, velocity changes calculated. End points represent series of experiments.

Table 1. Sources of Experimental Data (contd.)

Source	Information Supplied	Subject	End Point	Near End Point	Direction of Acceleration	Comments
Geertz, Ref. 6	German ejection seat tests	Human			Headward	Early German work, no injuries with good restraint.
R.A.E. England						No information supplied
Stanley Aviation	Capsule drop tests	Human and Bear	2	2	Multi- directional	Multi-directional accelerations.

Table 2. NOTATION USED IN EXPERIMENTAL ANALYSIS *

Symbol	Subject	Initial Letters	Reference	Number	Final Letter	Type of Analysis
○	Bear	H	Holloman A.F.B.		E	Original Eiband Analysis
◻	Chimpanzee	S	Ref. 18			
		SA	Ref. 19	Refers to Test Number	E'	Eiband Type Analysis by Stanley Aviation
		G	Ref. 6			
△	Human	D	Ref. 29		S	Equivalent Rectangular Input Analysis
◇	Hog	ST	Stanley Aviation			

Full Shading e.g. ▲ - end point
 Half Shading e.g. ▴ - near end point
 No Shading e.g. △ - no injury

* Except Figures 2 and 3, where Eiband's original nomenclature has been used.

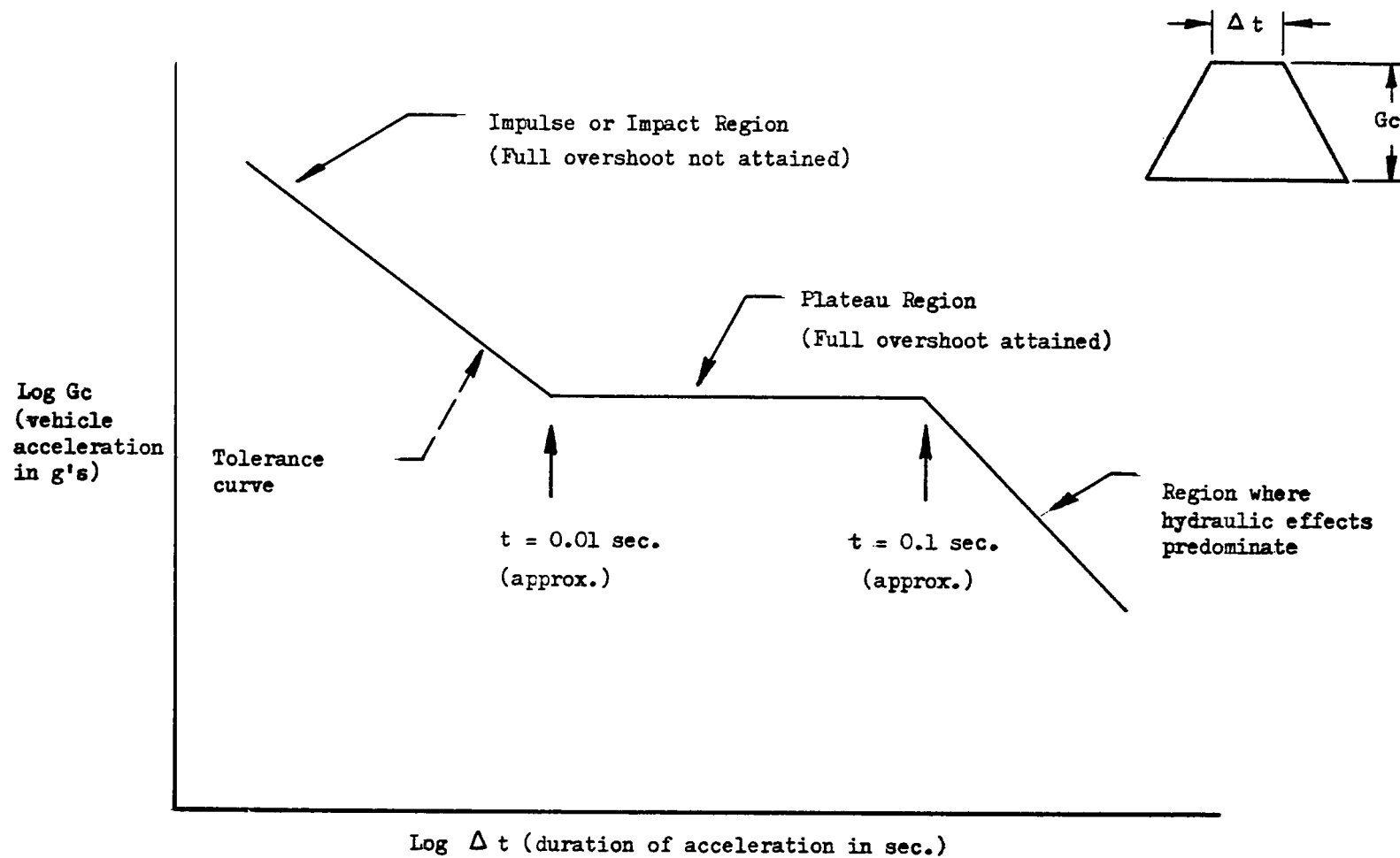


Fig. 1 Definition of Acceleration Regimes

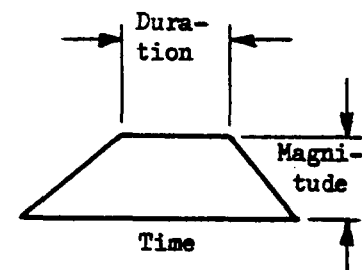
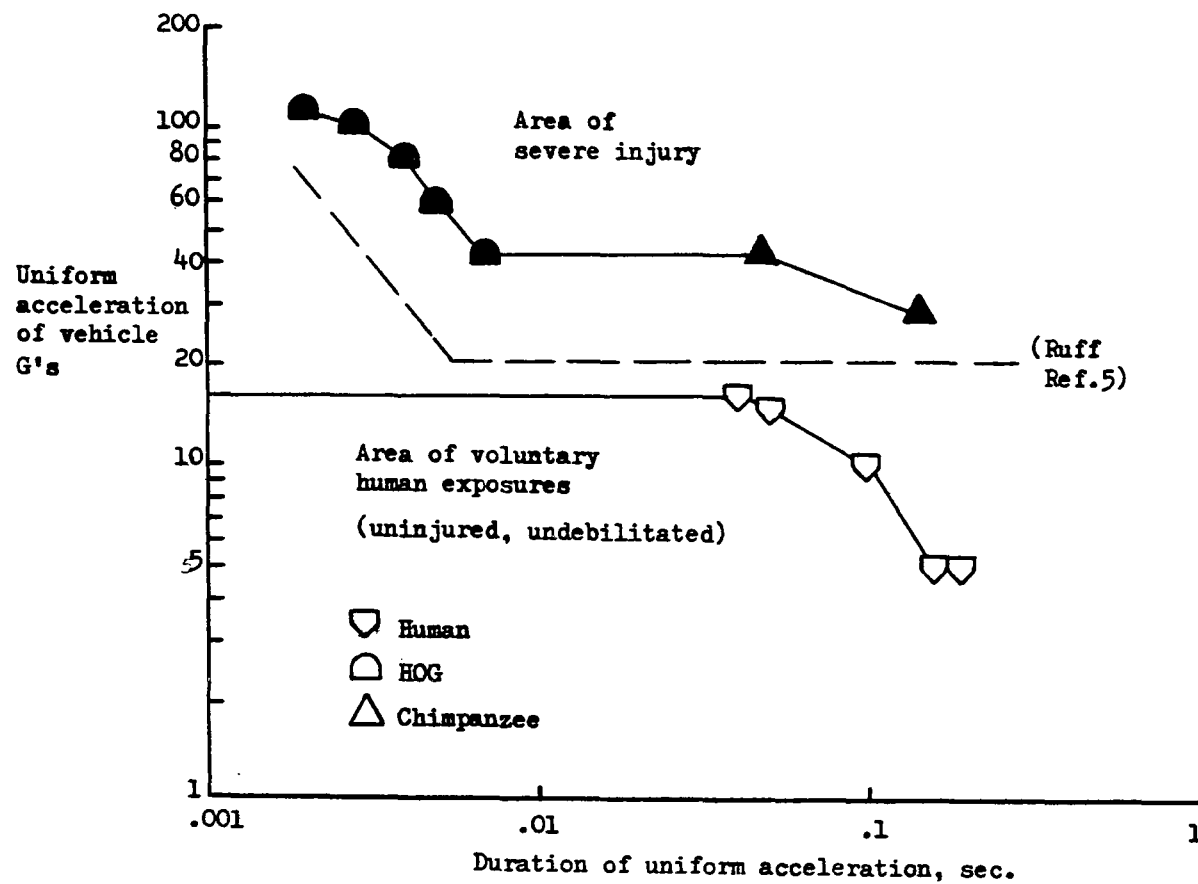


Fig. 2. Summary of Headward Acceleration Data (after Eiband, Ref. 2).

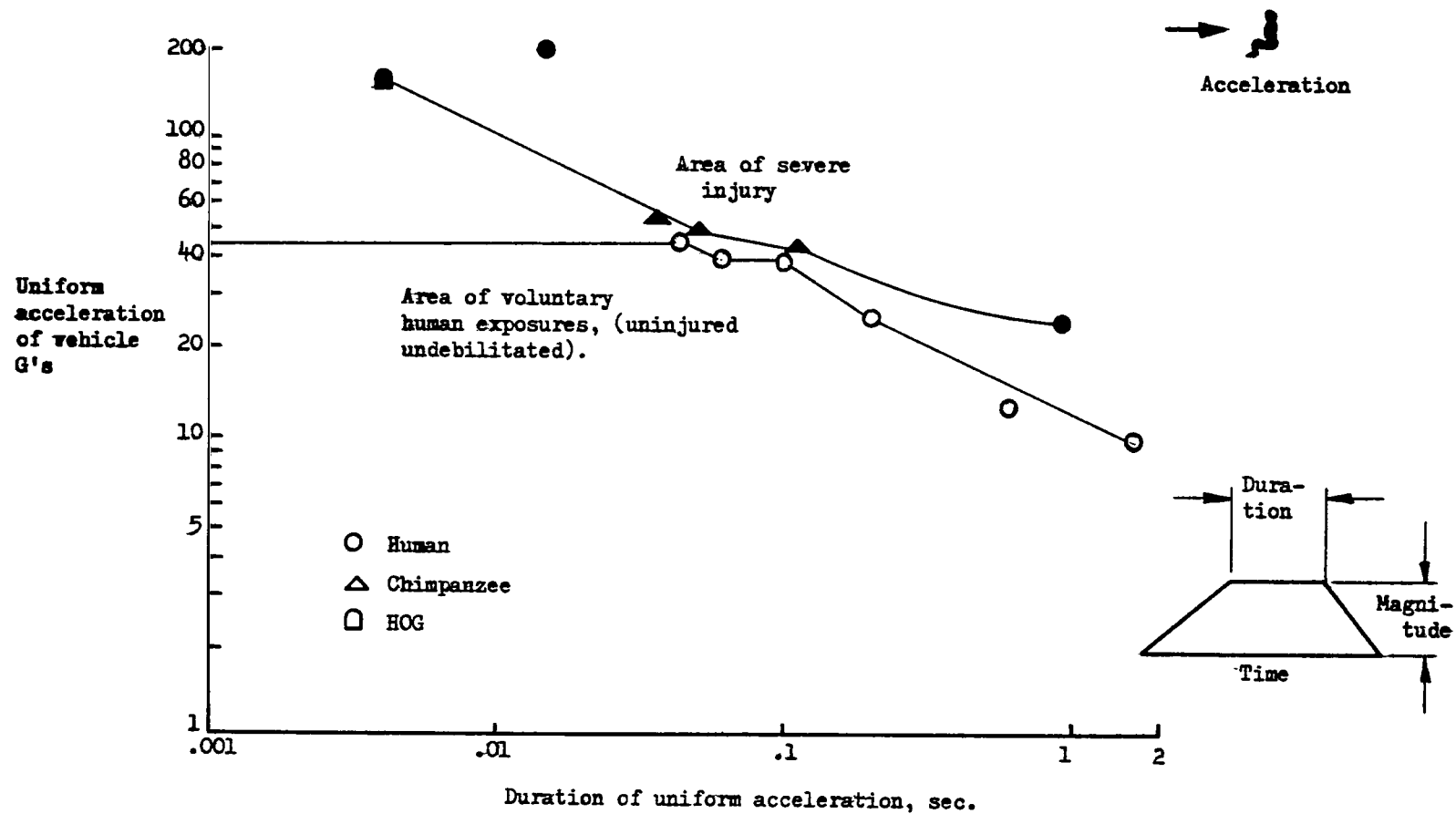


Fig. 3. Summary of Backward Acceleration Data (after Eiband, Ref. 2).

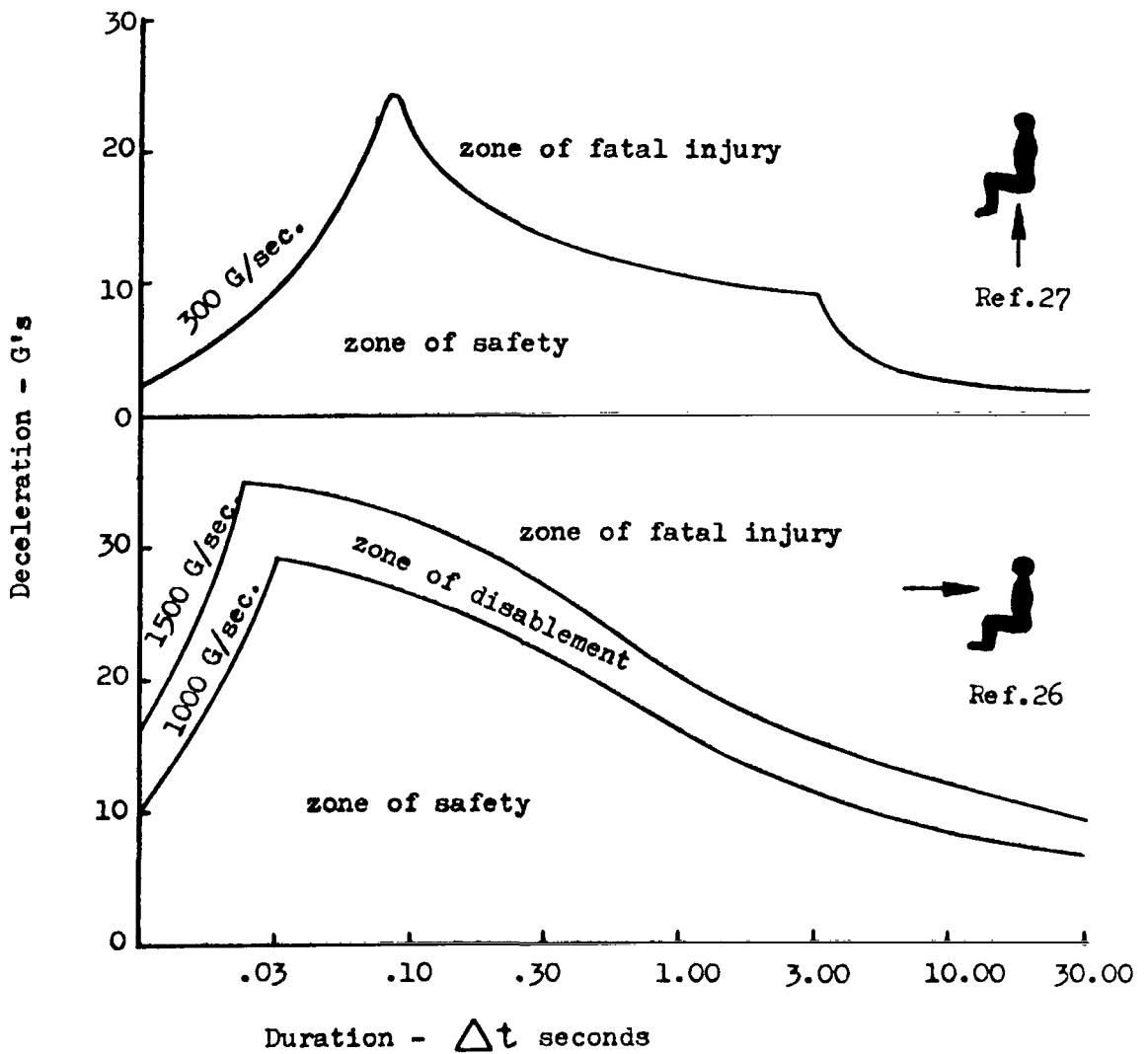
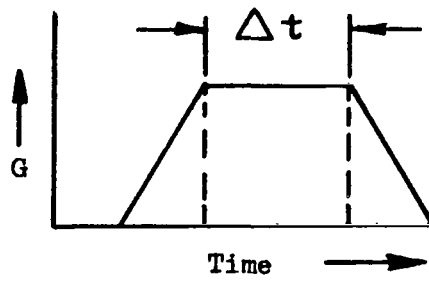
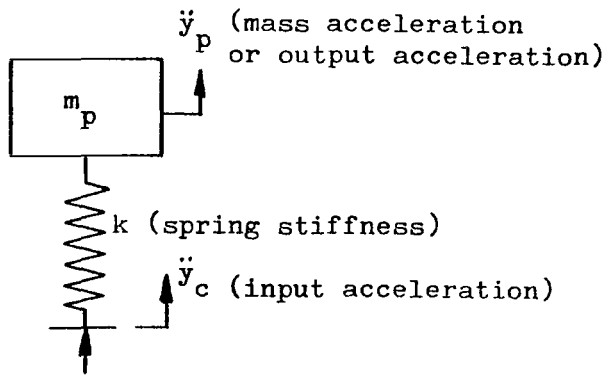
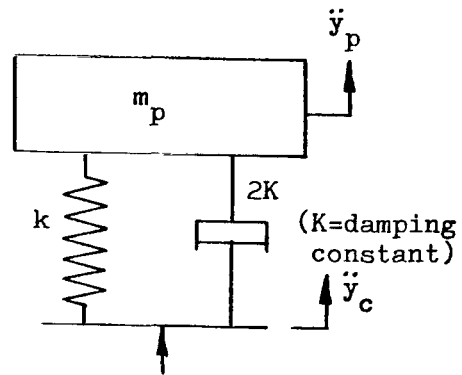


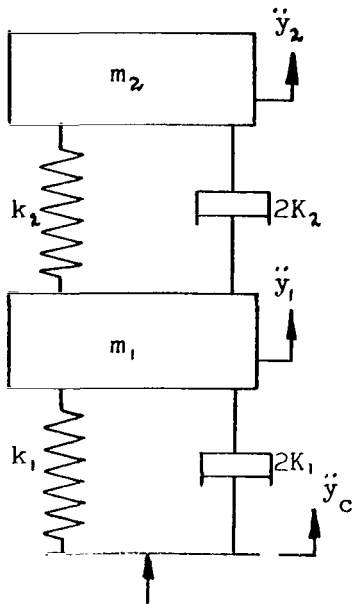
Fig.4 Allowable Short Duration Accelerations (HIAD)



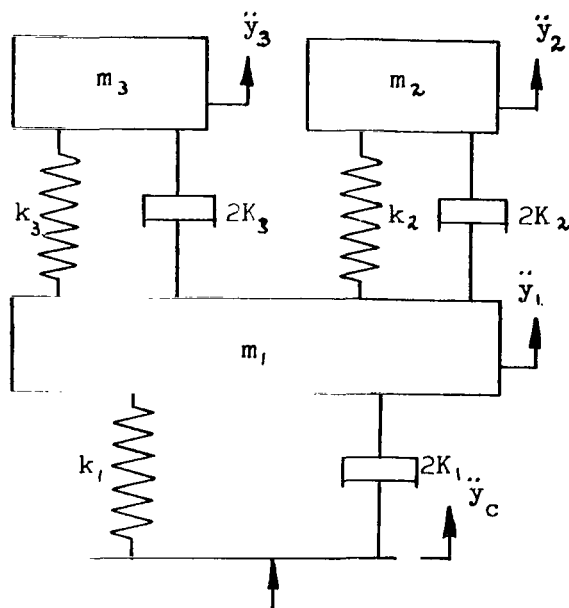
(a) single degree of freedom model



(b) single degree of freedom model with damping



(c) two degree of freedom model



(d) three degree of freedom model

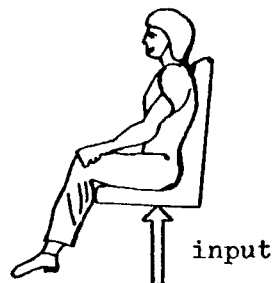


Fig. 5. Dynamic Models of a Human Subjected to Acceleration

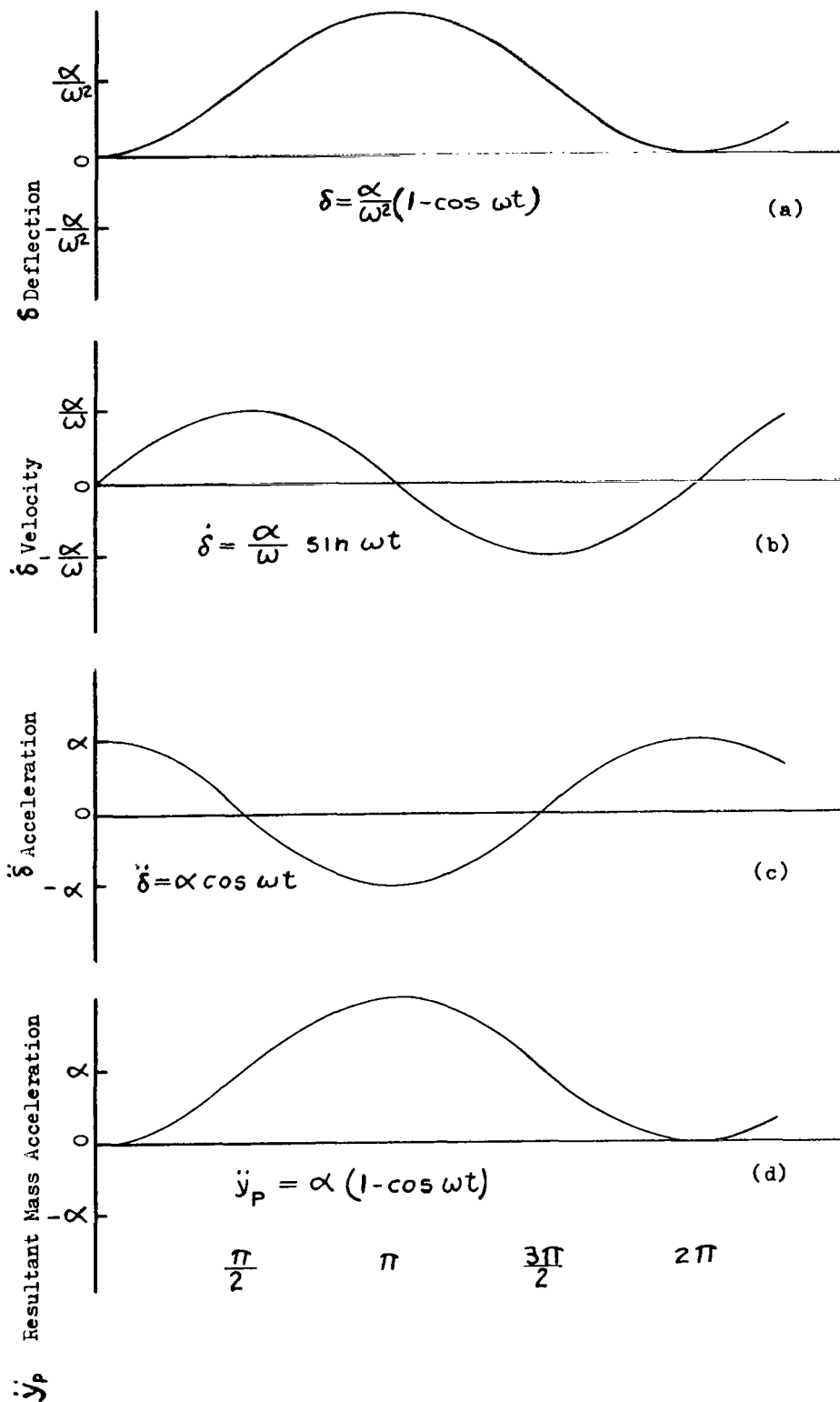


Fig. 6. Dynamic Response of a Single Spring-Mass System (Step Input)

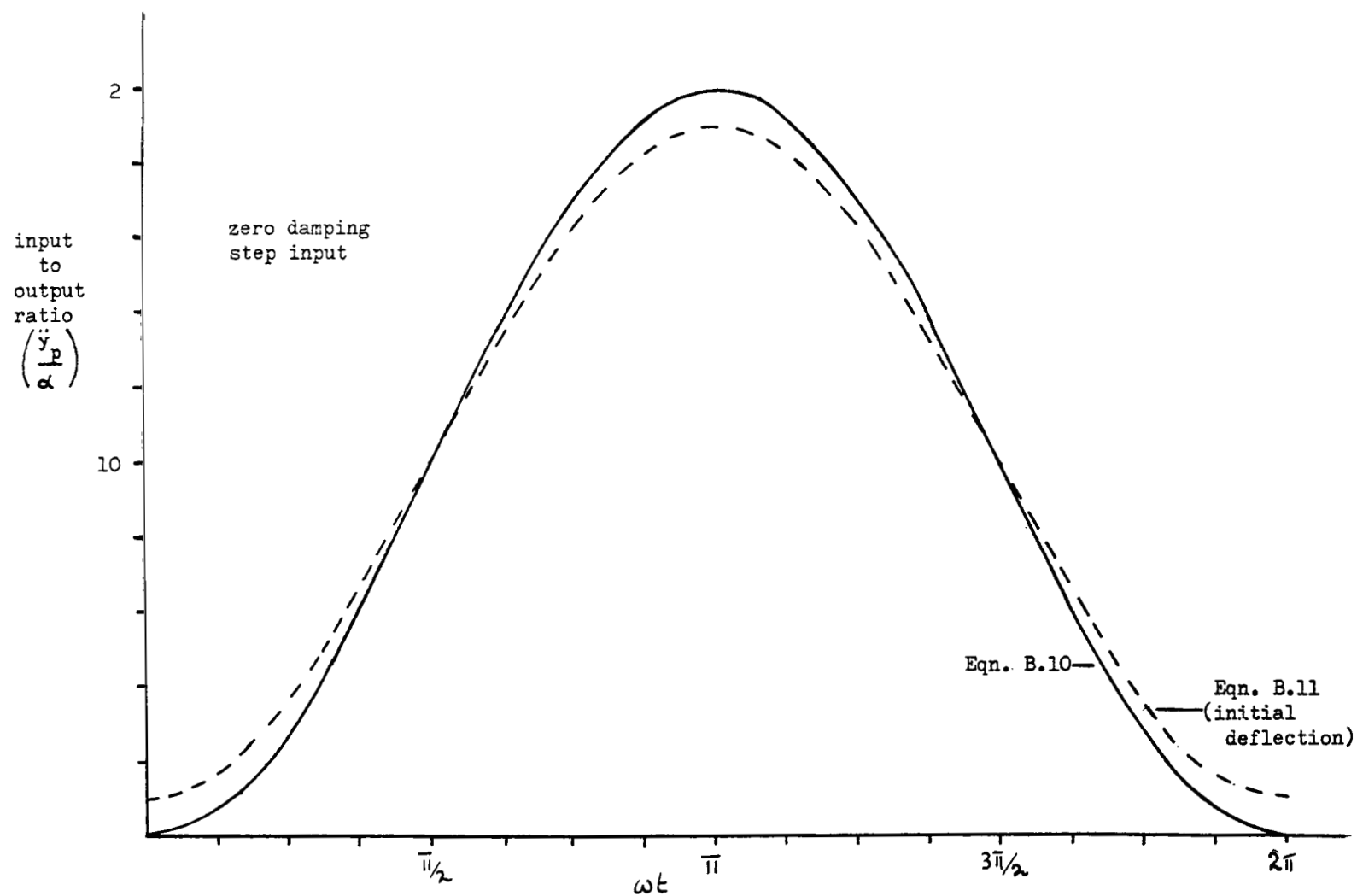


Fig. 7. Influence of Initial Deflection on Response of Single Degree of Freedom System

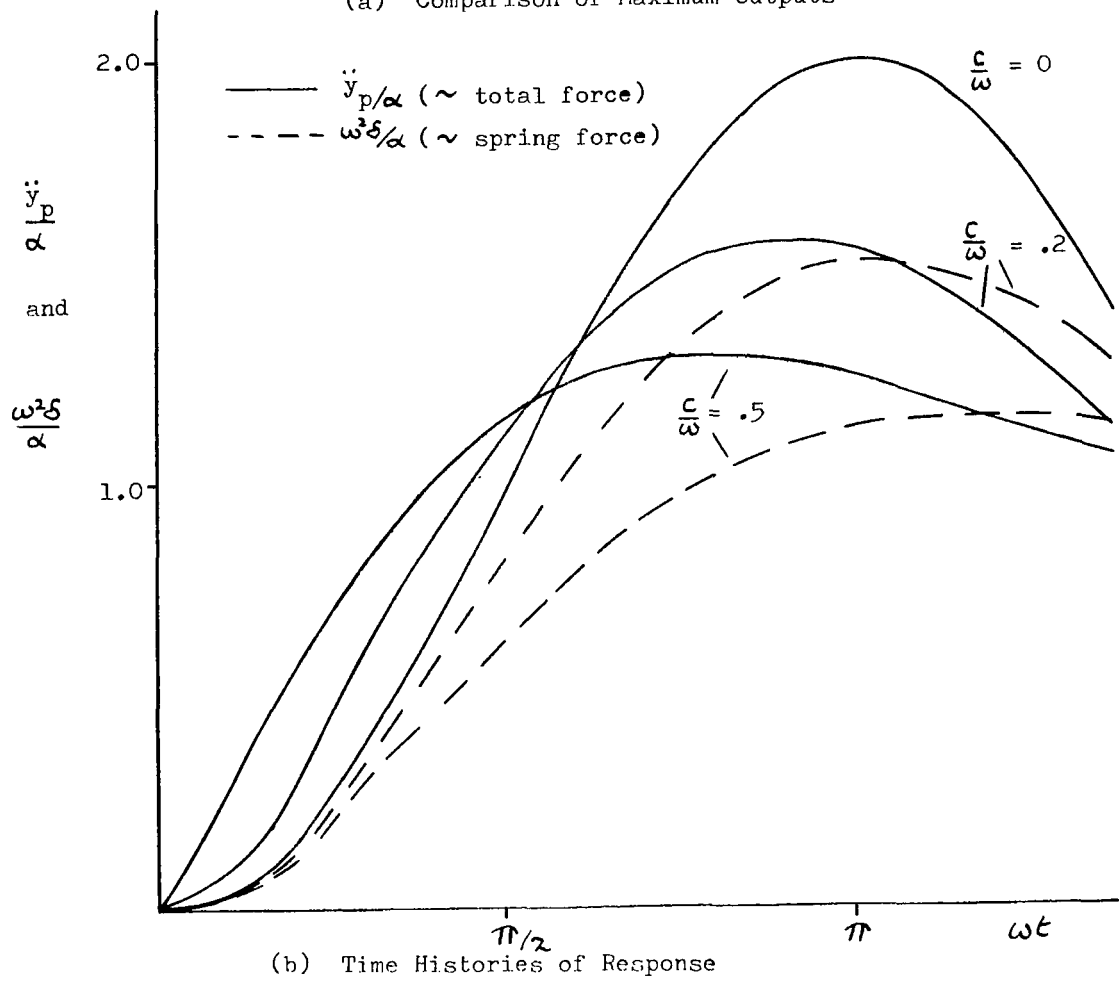
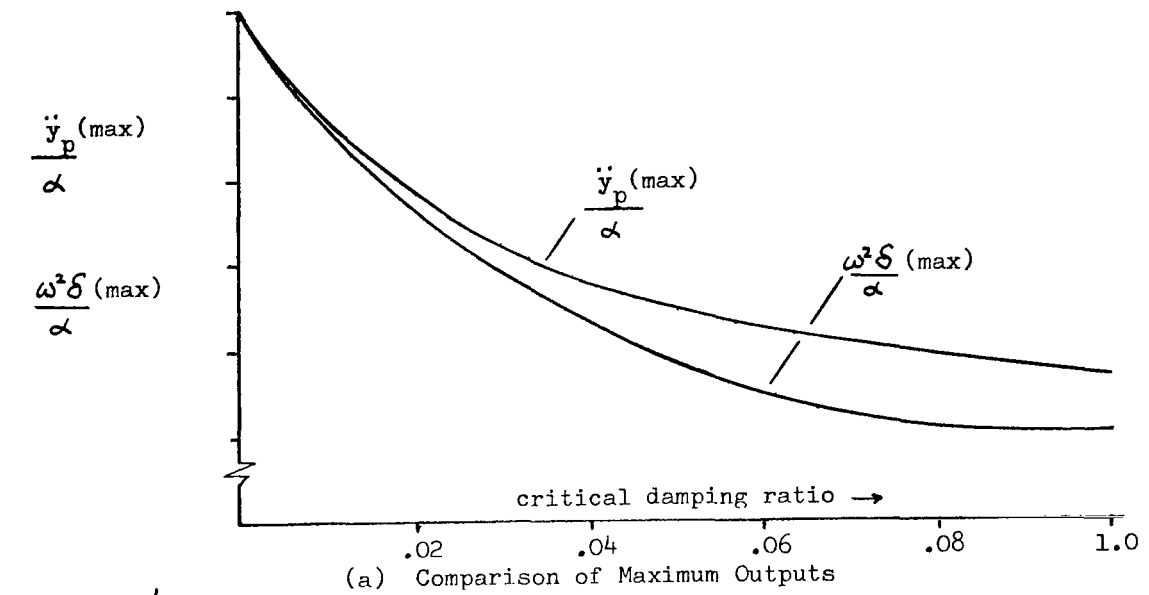


Fig. 8. Influence of Damping on Response of Single Degree of Freedom System for Step Input

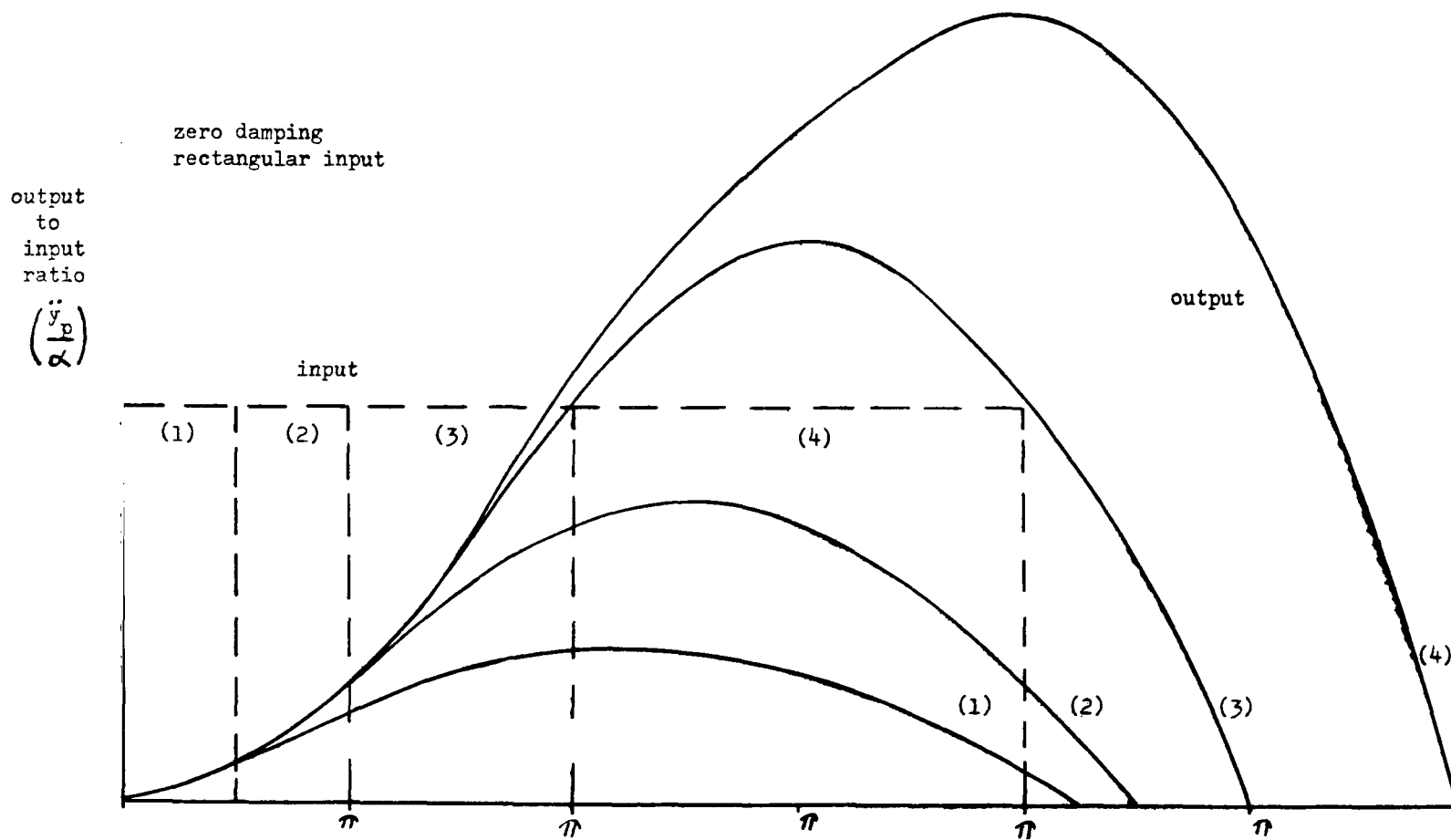


Fig. 9. Response of Single Degree of Freedom System for Various Input Durations

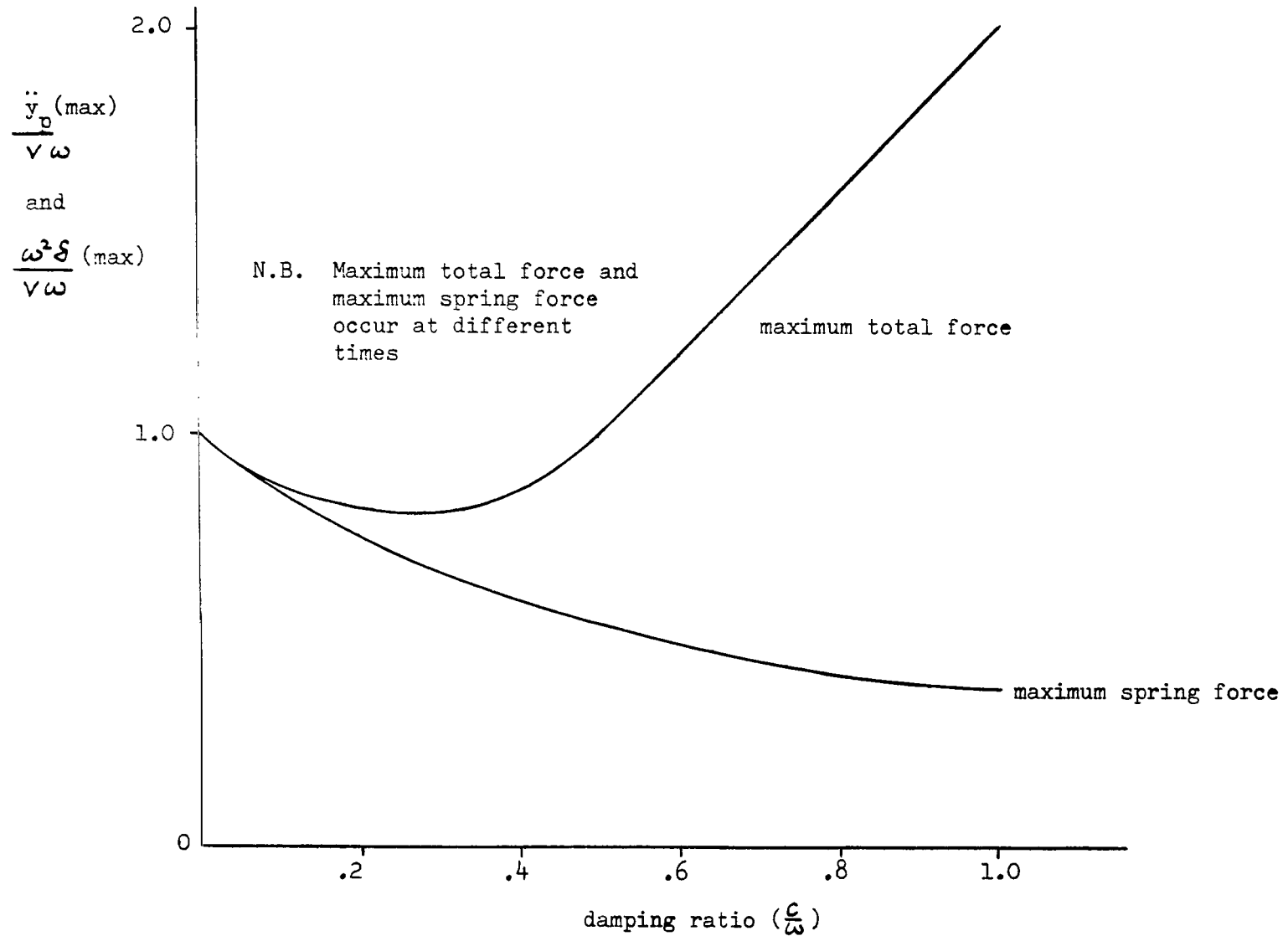


Fig. 10. Influence of Damping on Tolerance Criterion for Impulsive Inputs

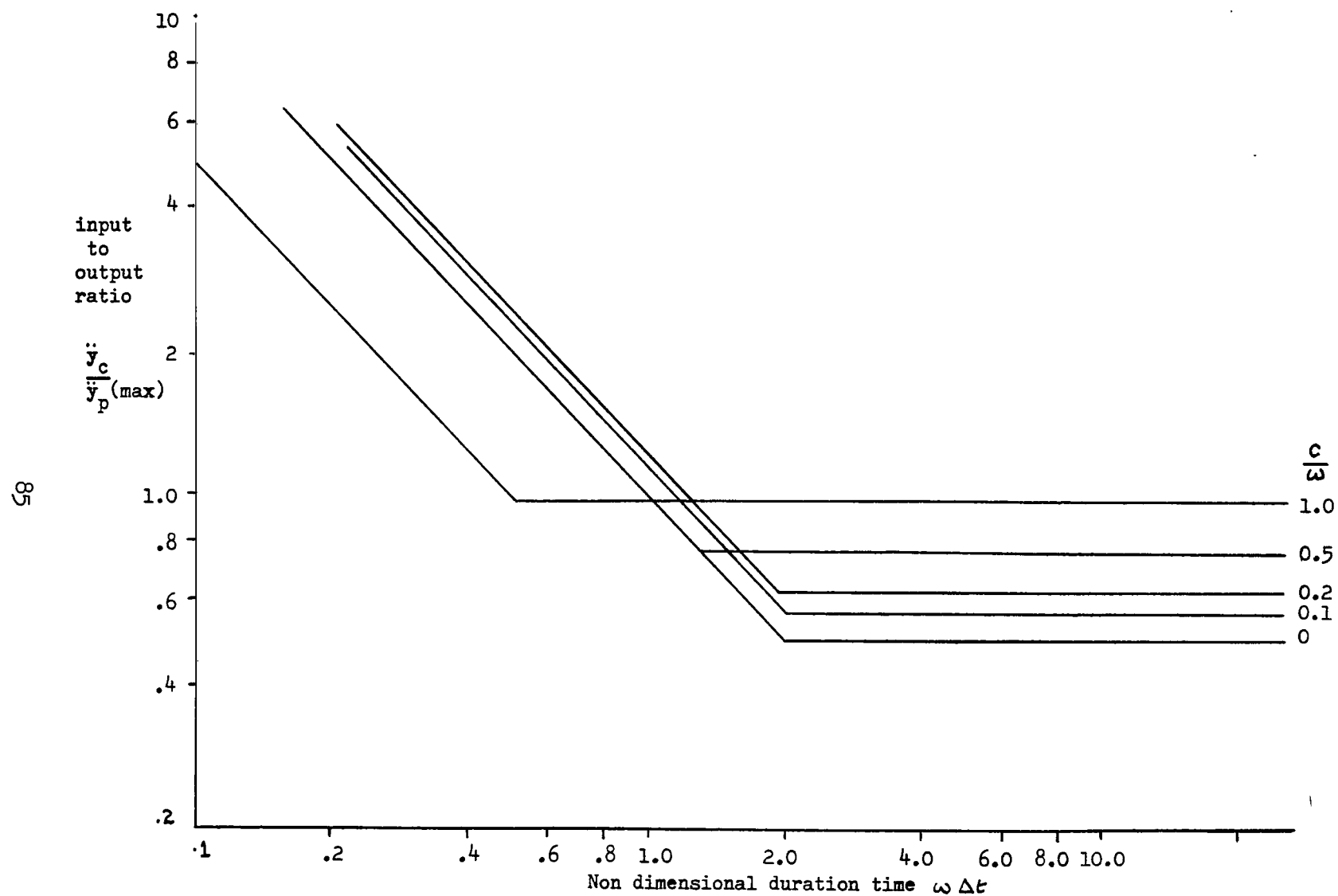


Fig. 11. Influence of Damping on Tolerance Curve

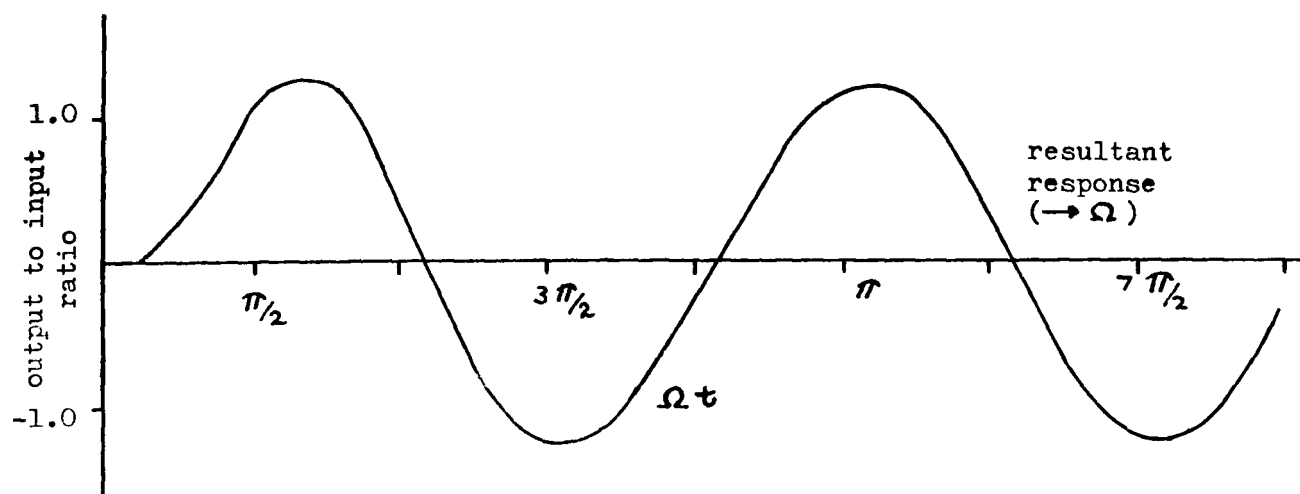
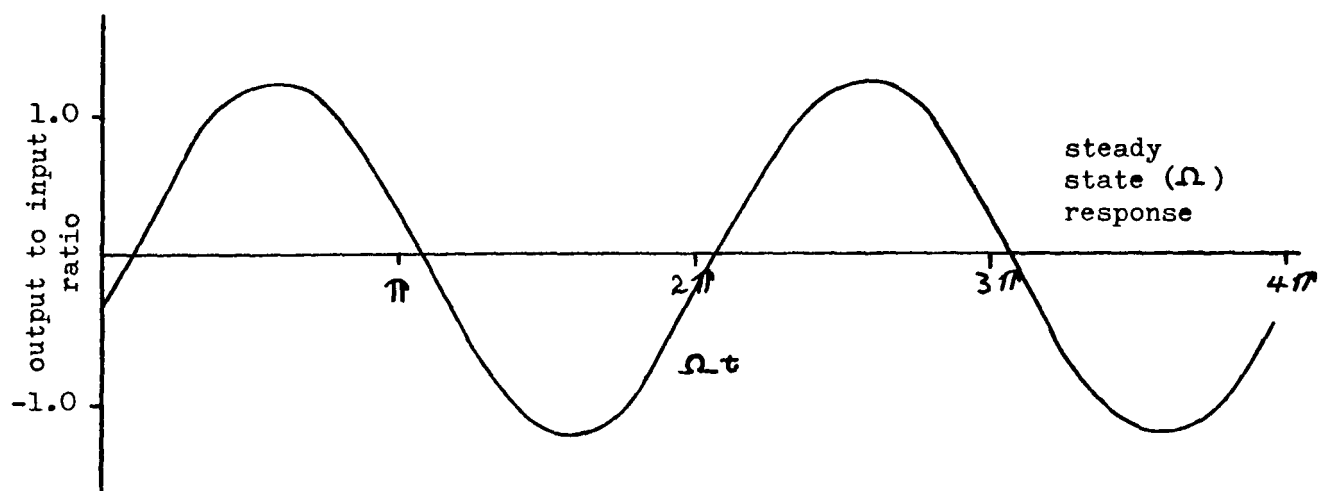
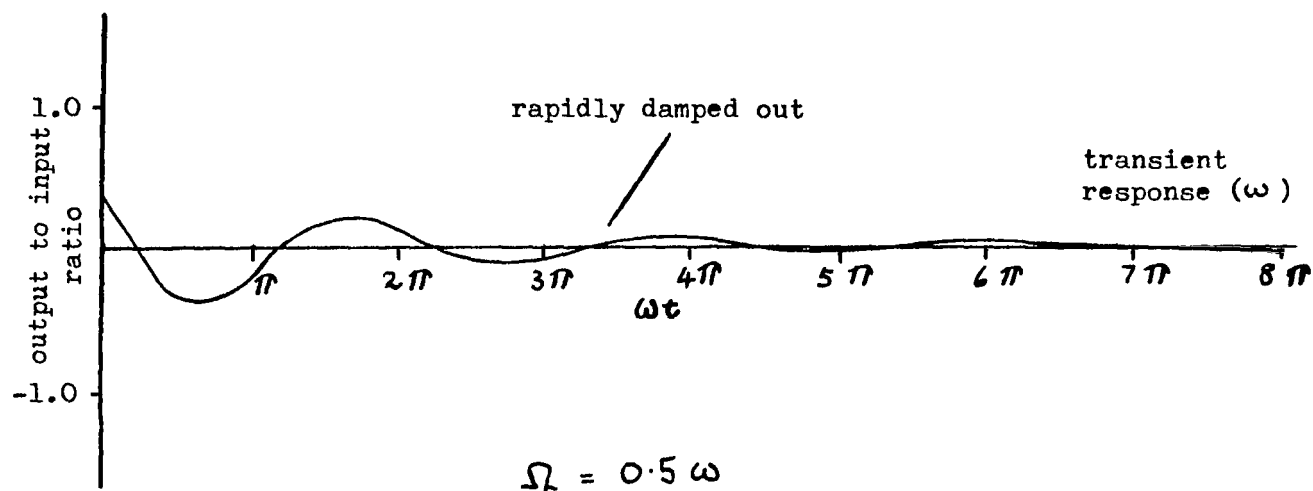


Fig. 12. Response of Single Degree of Freedom System to Sinusoidal Input

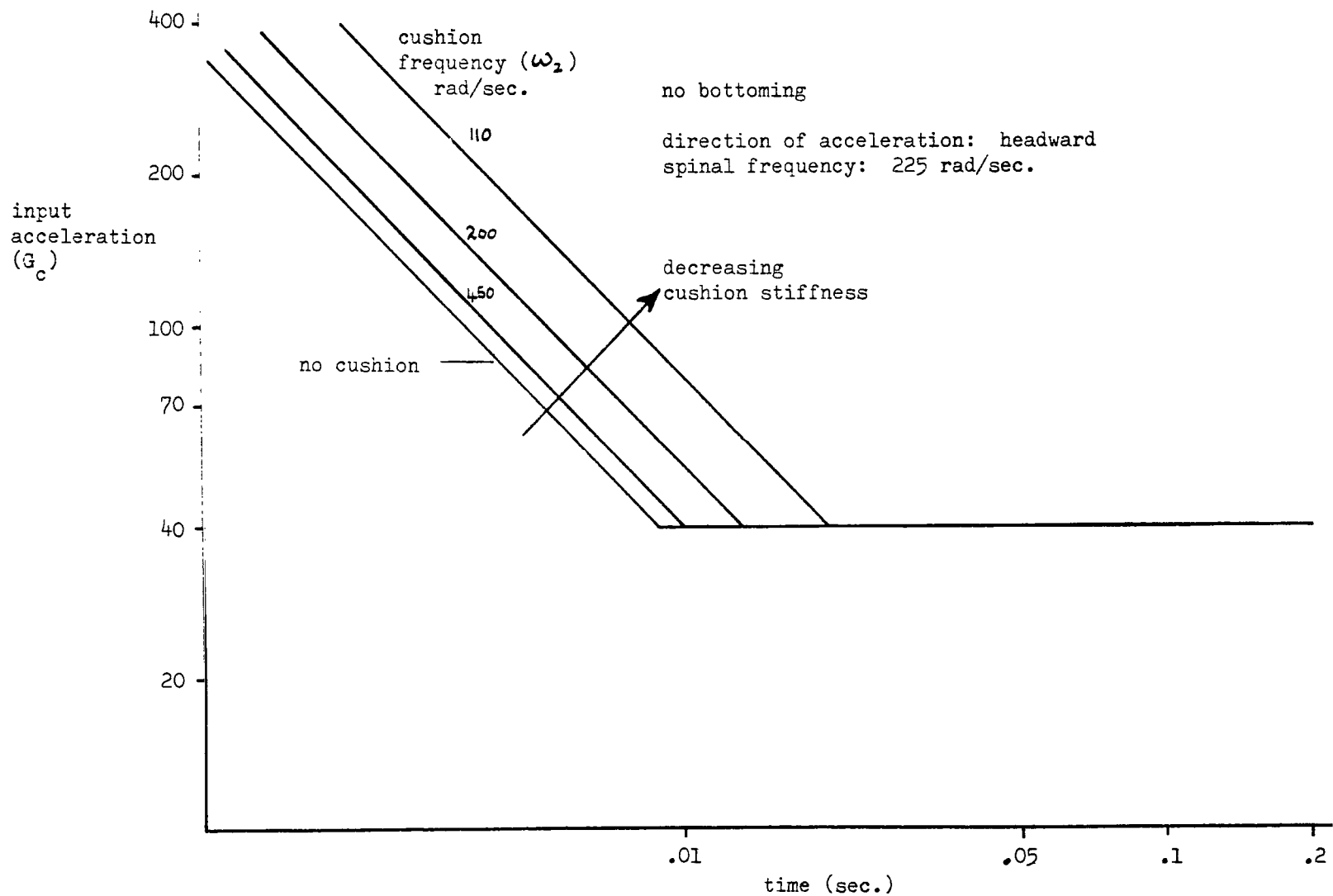


Fig. 13. Influence of Cushion on Tolerance Limits

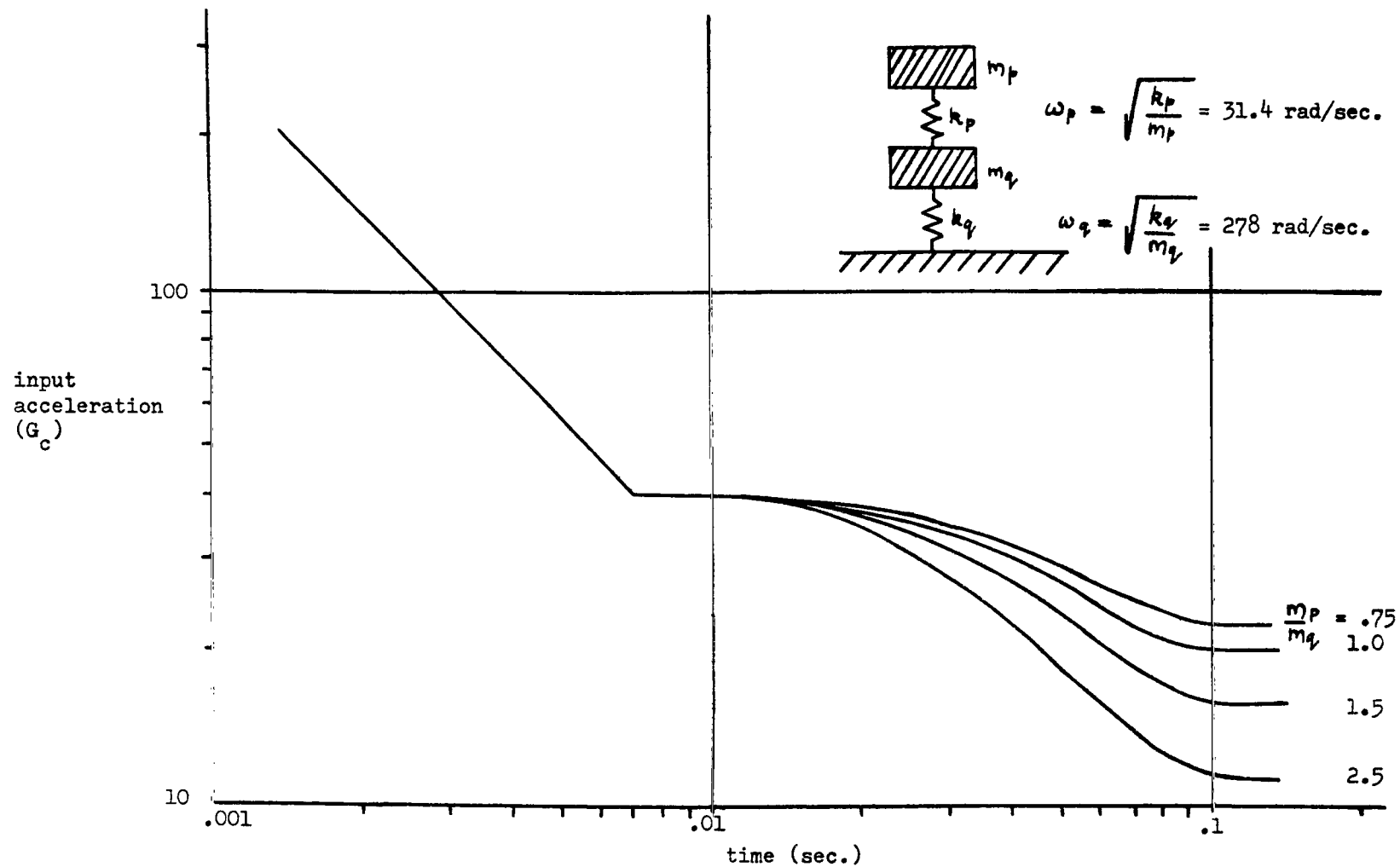


Fig. 14. Tolerance Curves Predicted by Two Degree of Freedom System

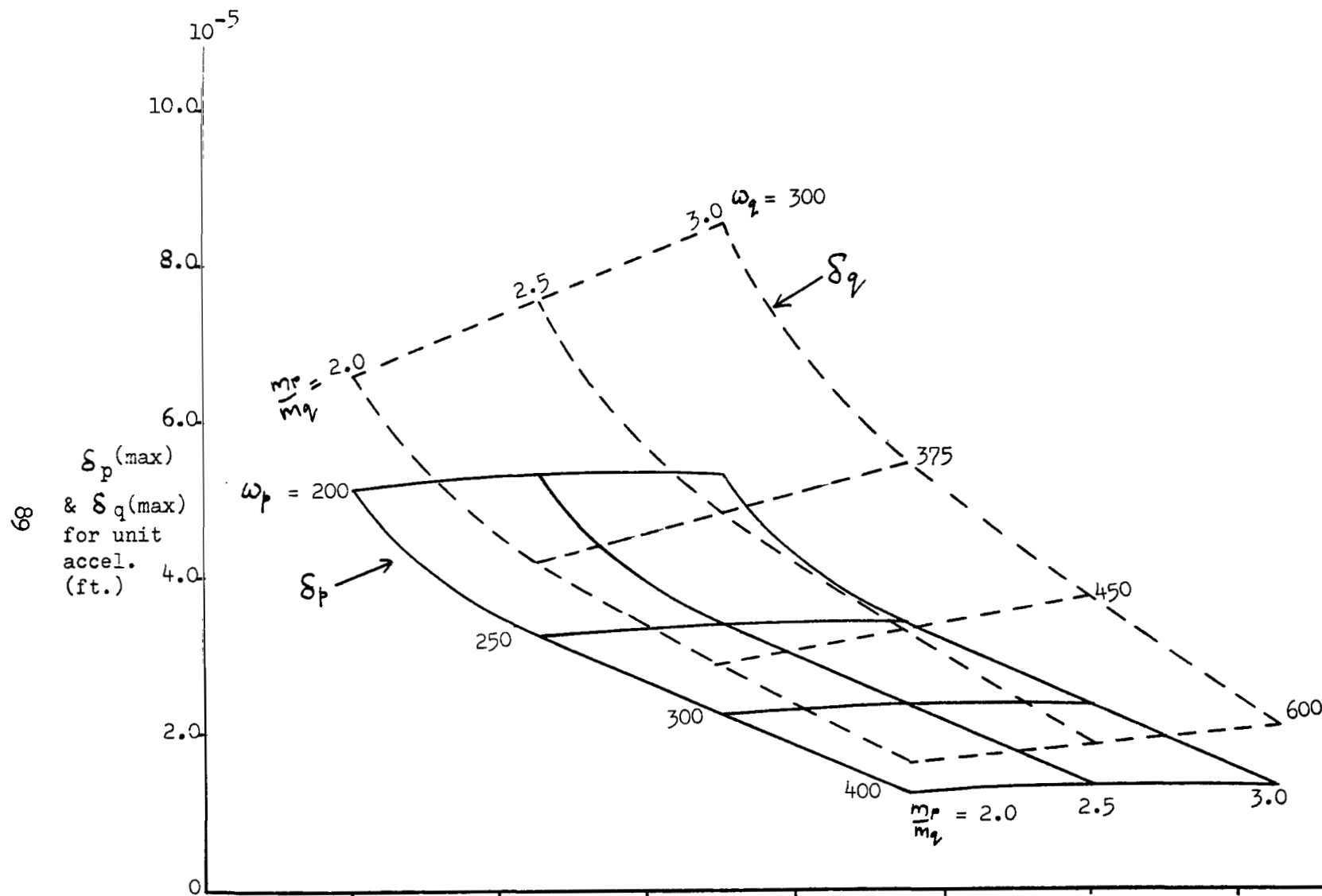


Fig. 15. Deflections and Frequencies for Various Mass Ratios Associated with the Two Degree of Freedom System

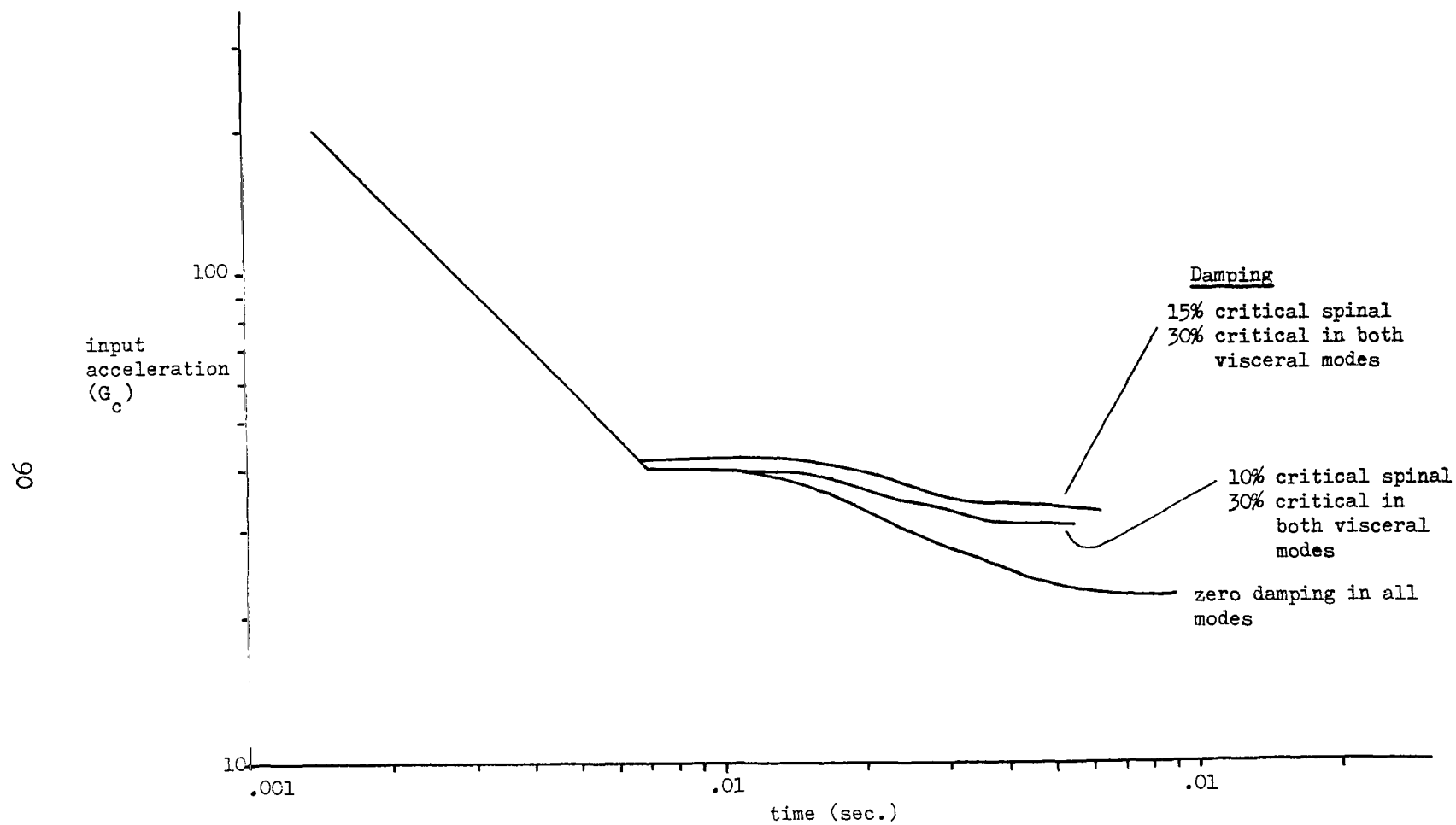
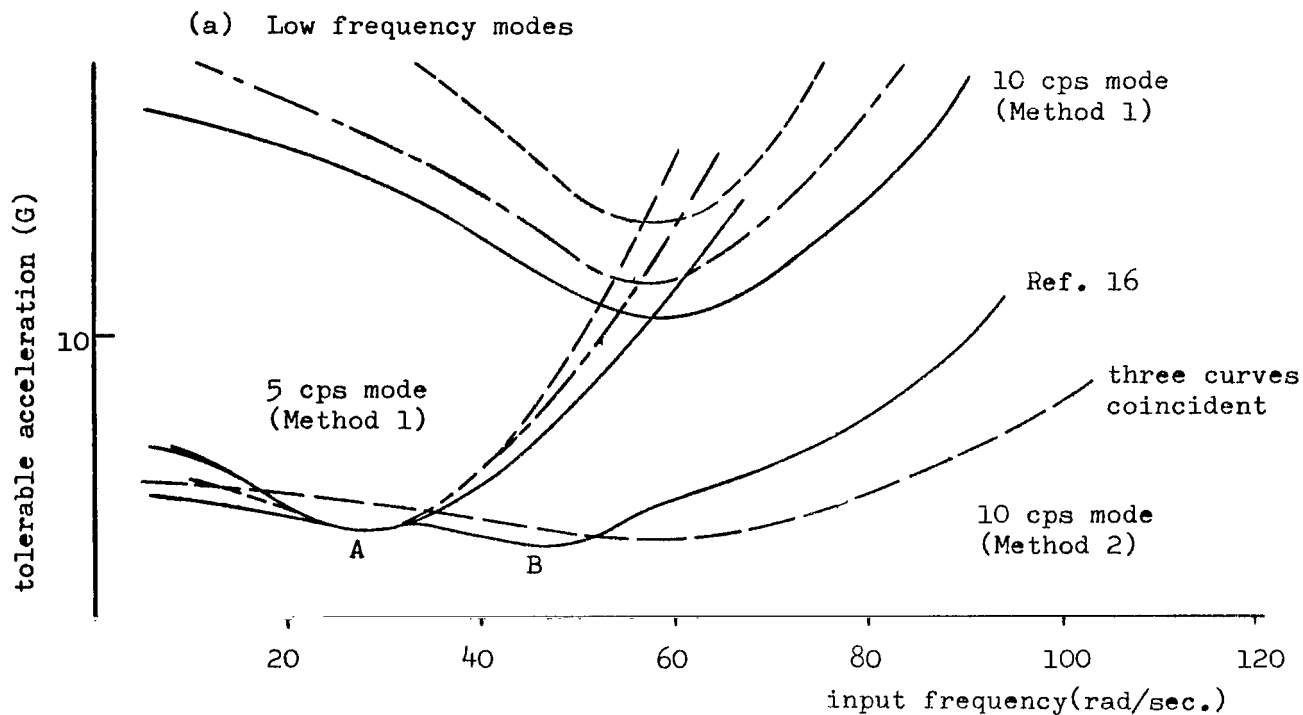
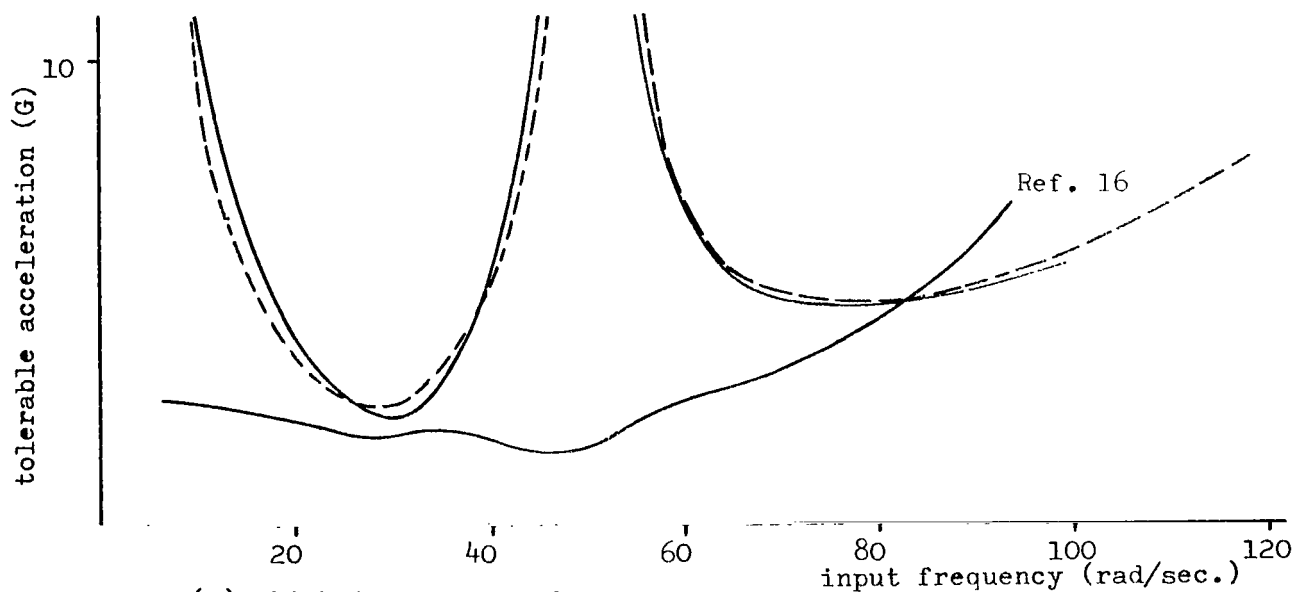


Fig. 16. Tolerance Curves Predicted by Three Degree of Freedom System



15% critical damping in spinal mode	}	all curves
30% critical damping in 10 cps visceral mode		
35% critical	}	damping in 5 cps visceral mode
30% critical		
25% critical		



(b) High frequency mode

Fig. 17. Tolerance to Sinusoidal Input Accelerations: Comparison of Three Degree of Freedom System Results with Experiment

Test Data

Source: Holloman A.F.B.
Run No: 390
Subject: Bear
Direction: Headward
Frequency: 278 rad/sec.
Injury: Spinal fracture
Analysis: IBM 1620

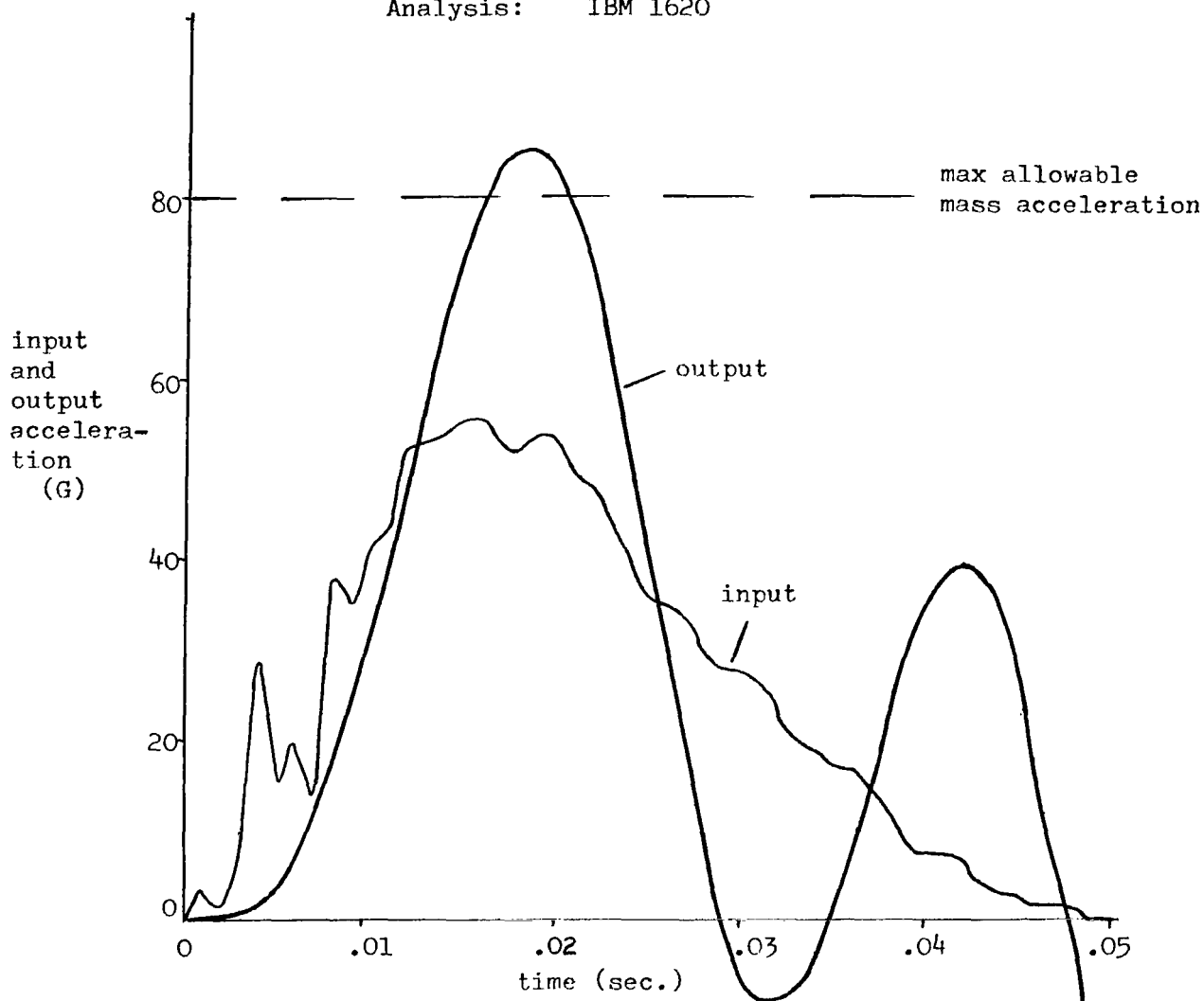


Fig. 18. Typical Digital Computer Analysis

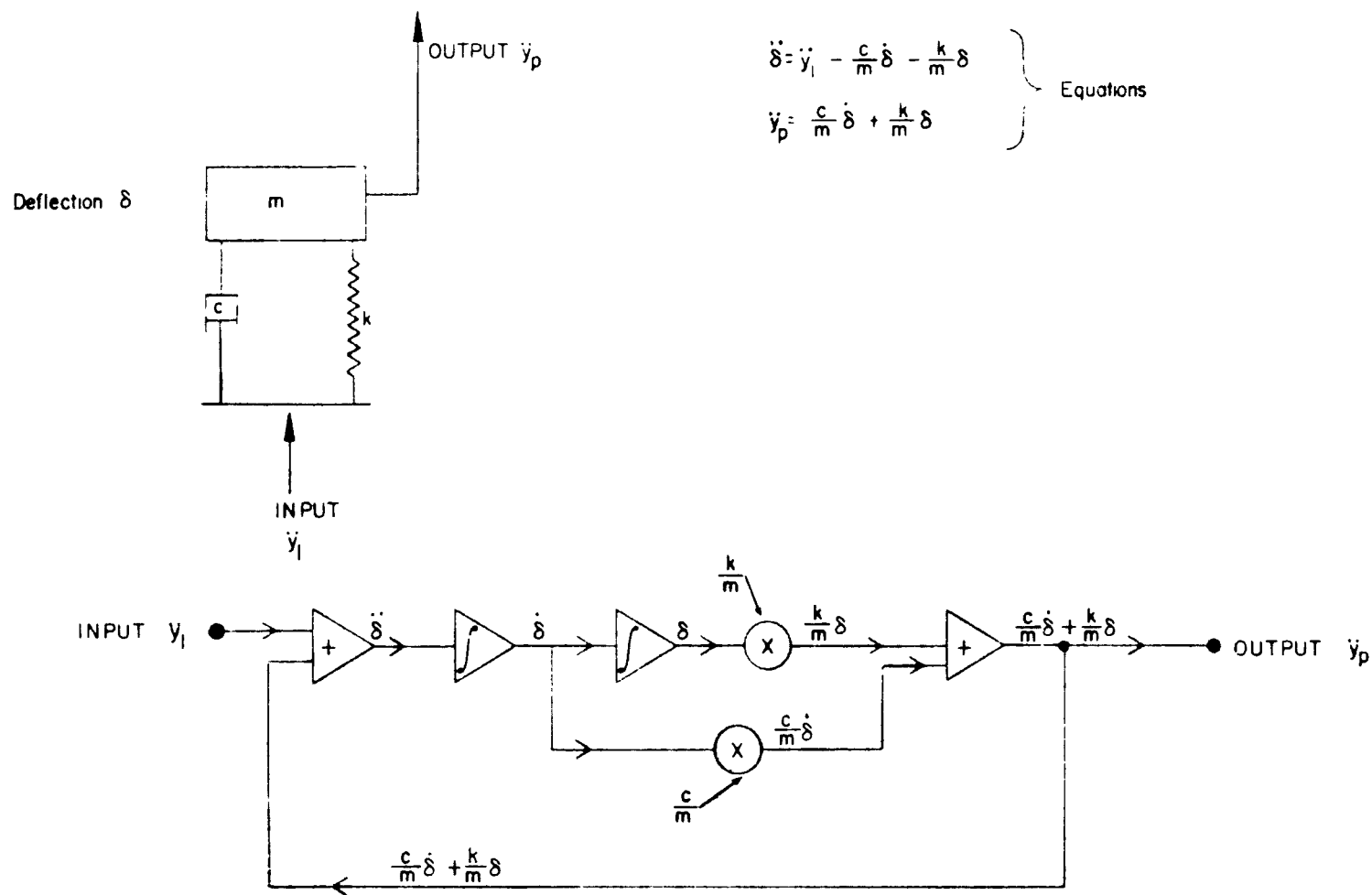


FIG 19 ANALOG COMPUTER - SIMPLIFIED FLOW DIAGRAM

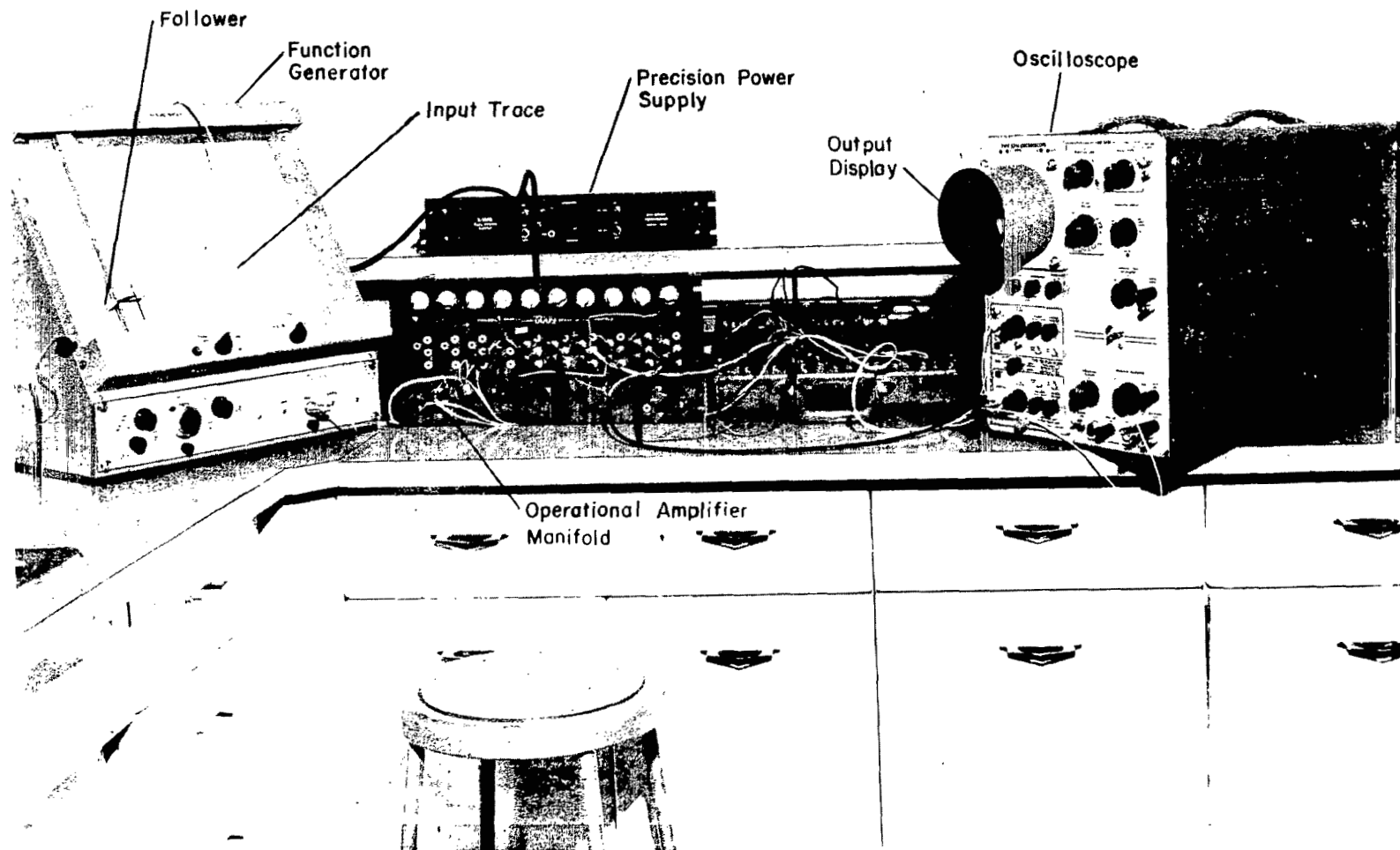
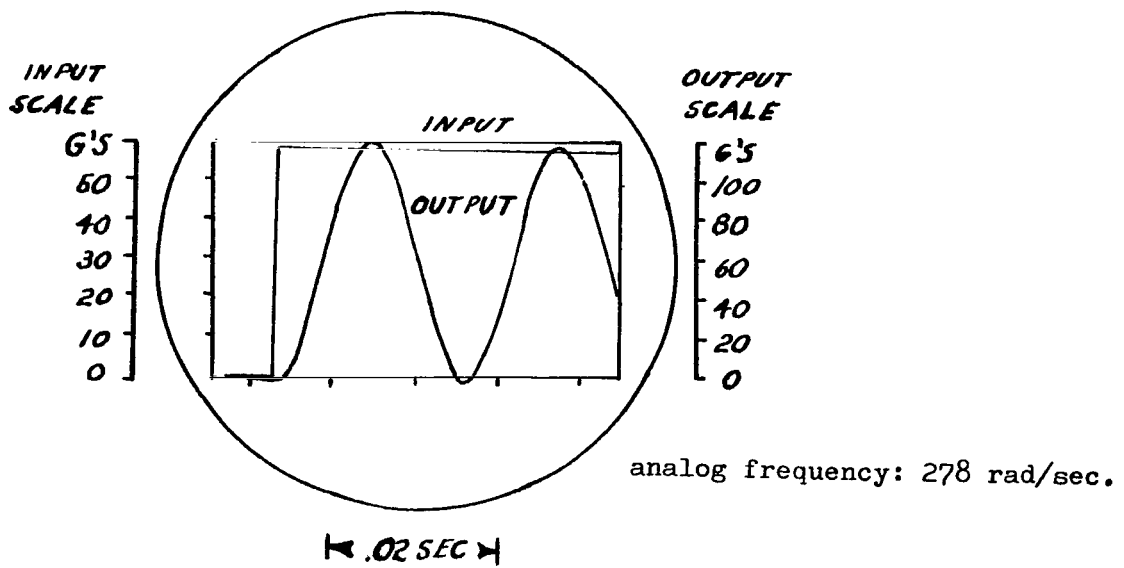
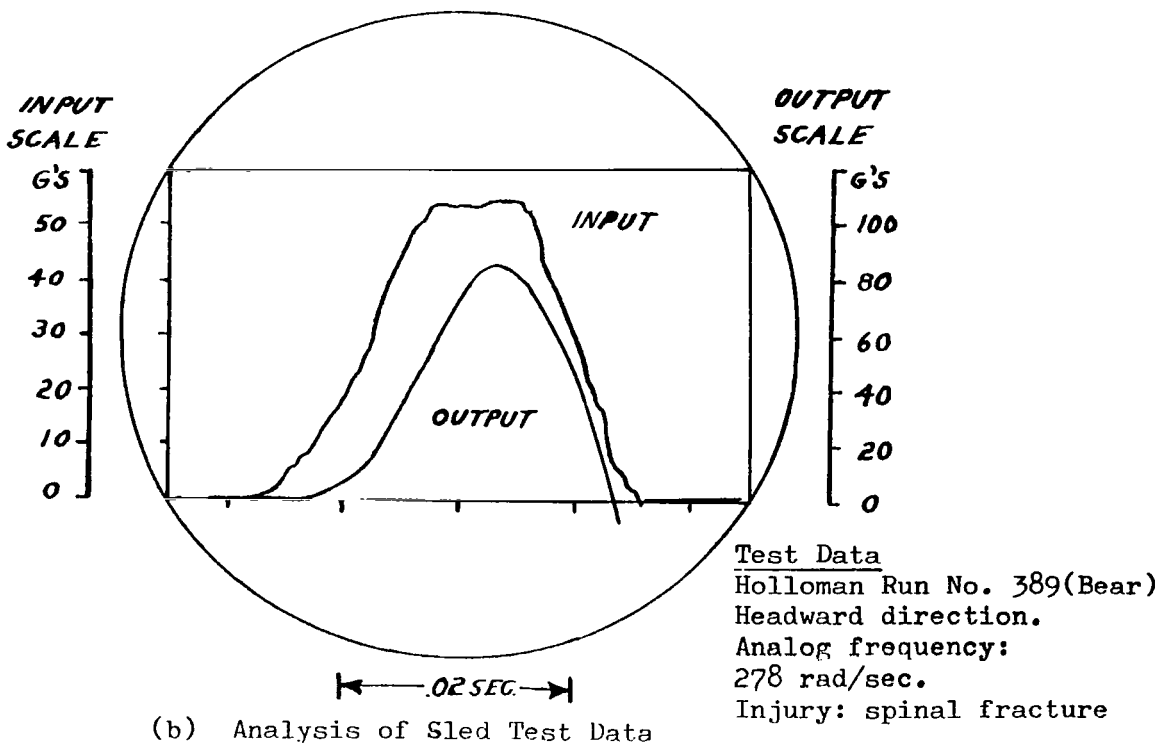


Fig. 20. Analog Computer - Experimental Arrangement

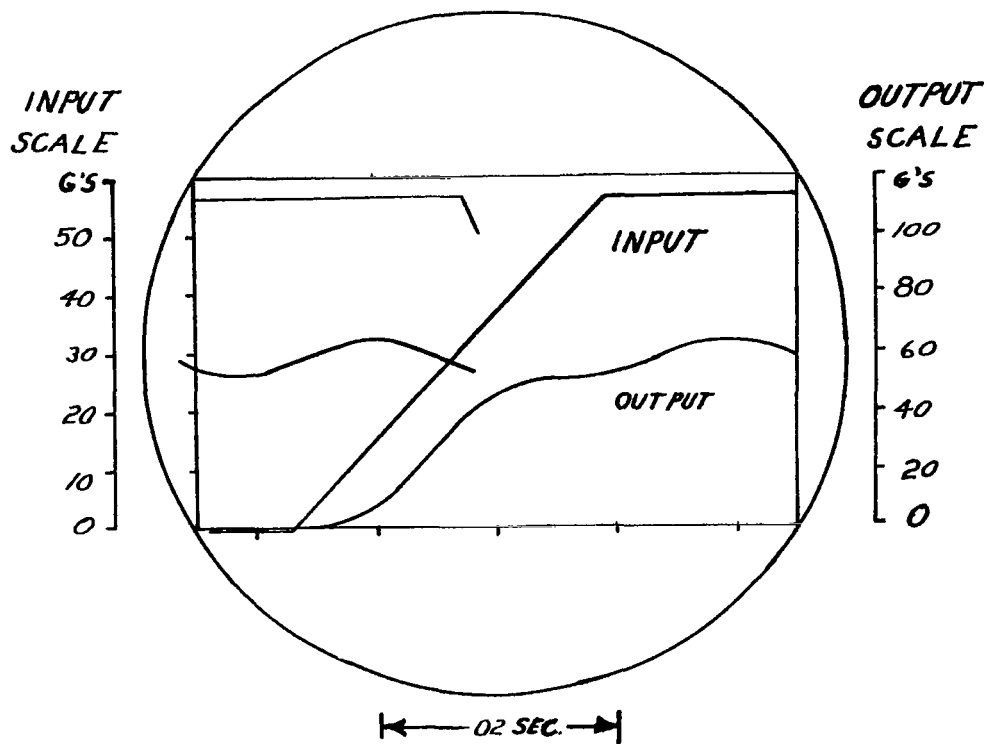


(a) Response to Step Input

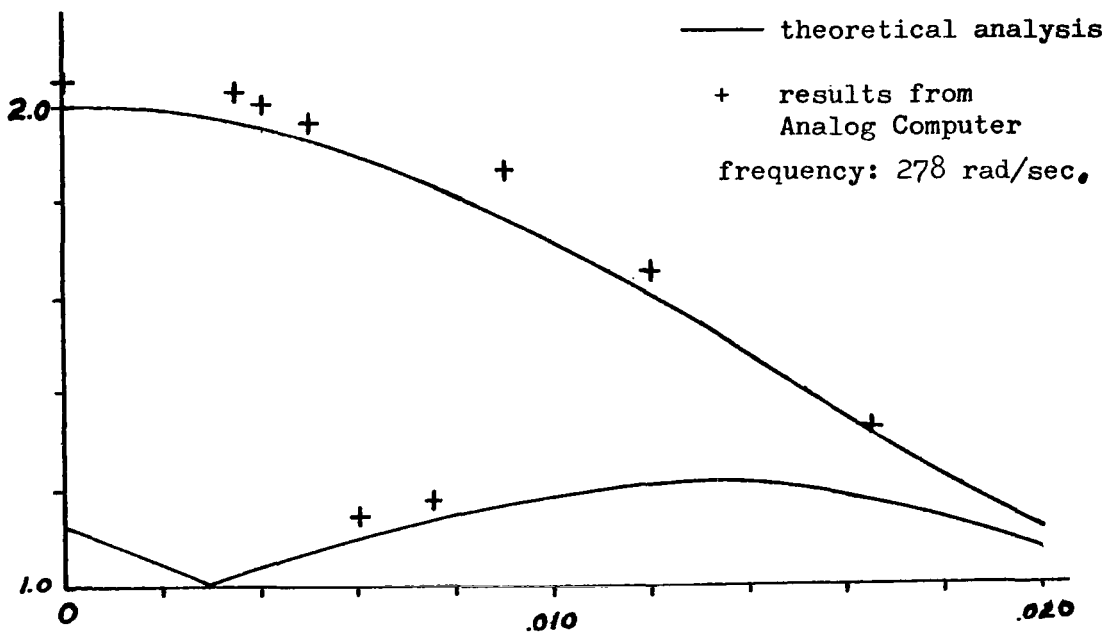


(b) Analysis of Sled Test Data

Fig. 21. Typical Analog Computer Analysis



(a) Analog Presentation for Rise Time 0.027 sec.



(b) Comparison of Theory and Analog Results

Fig. 22 Rise Time Effects (Analog Computer)

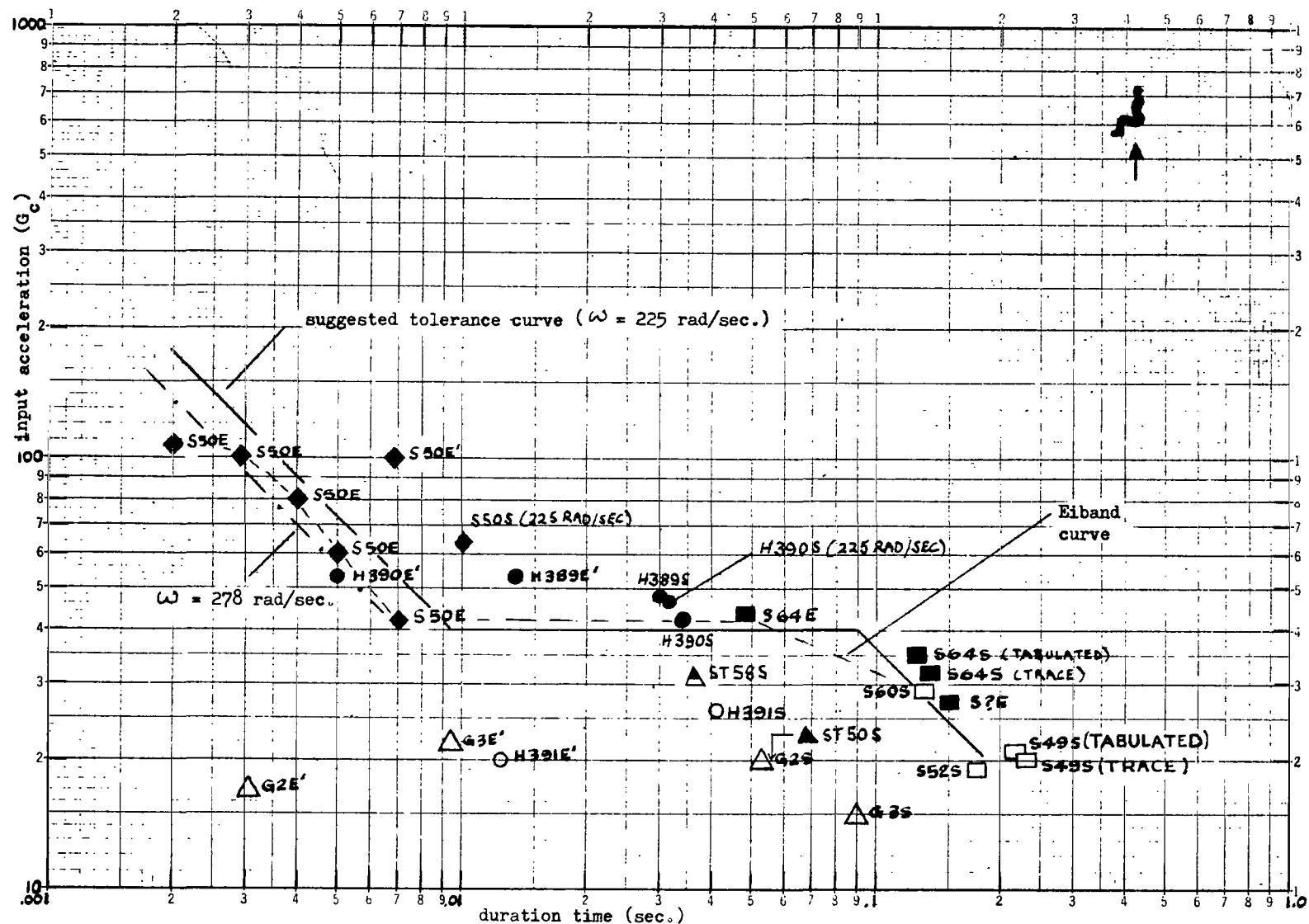
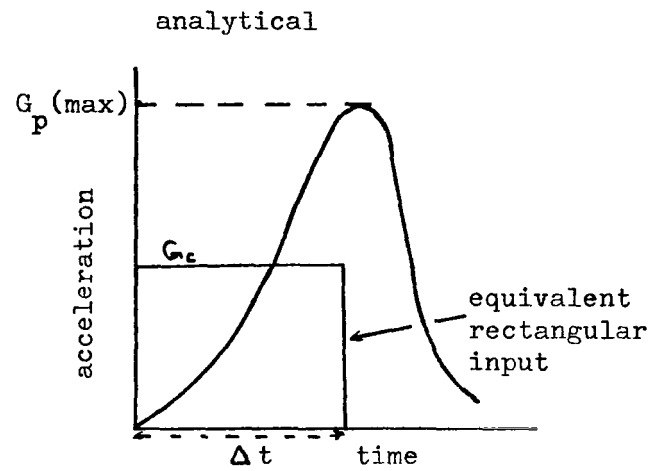
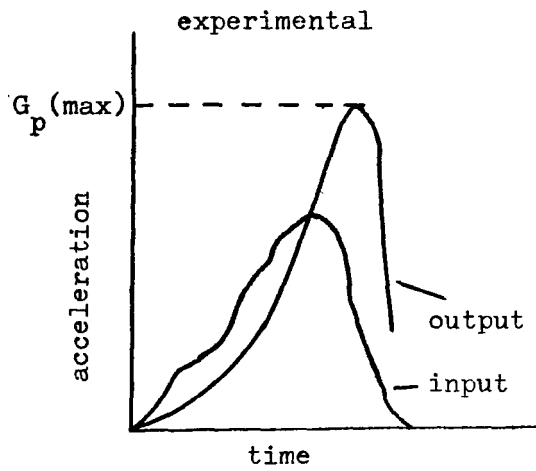


Fig. 23. Analysis of Experimental Headward Acceleration Data



$$\Delta v = \int_0^t G_c dt$$

$$\Delta v = G_c \Delta t$$

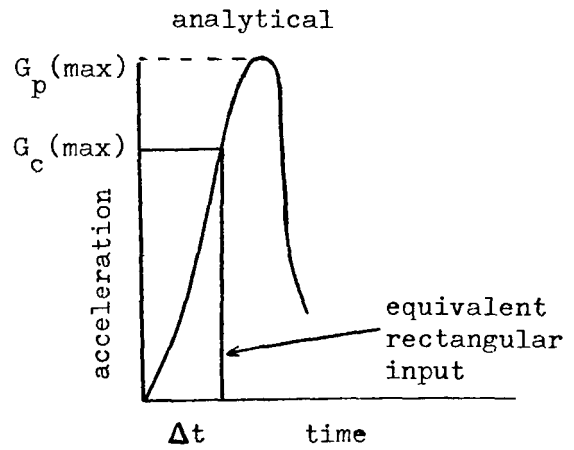
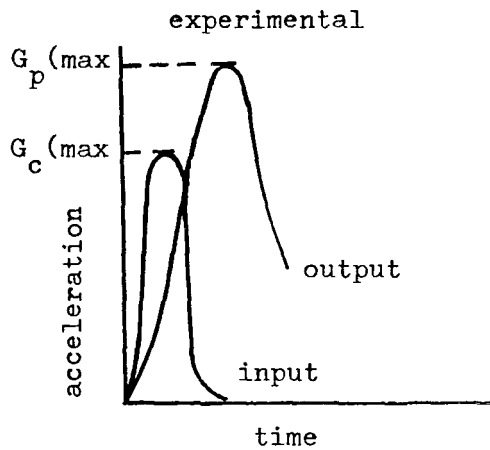


Fig. 24. Criteria Used in Analyzing Experimental Data

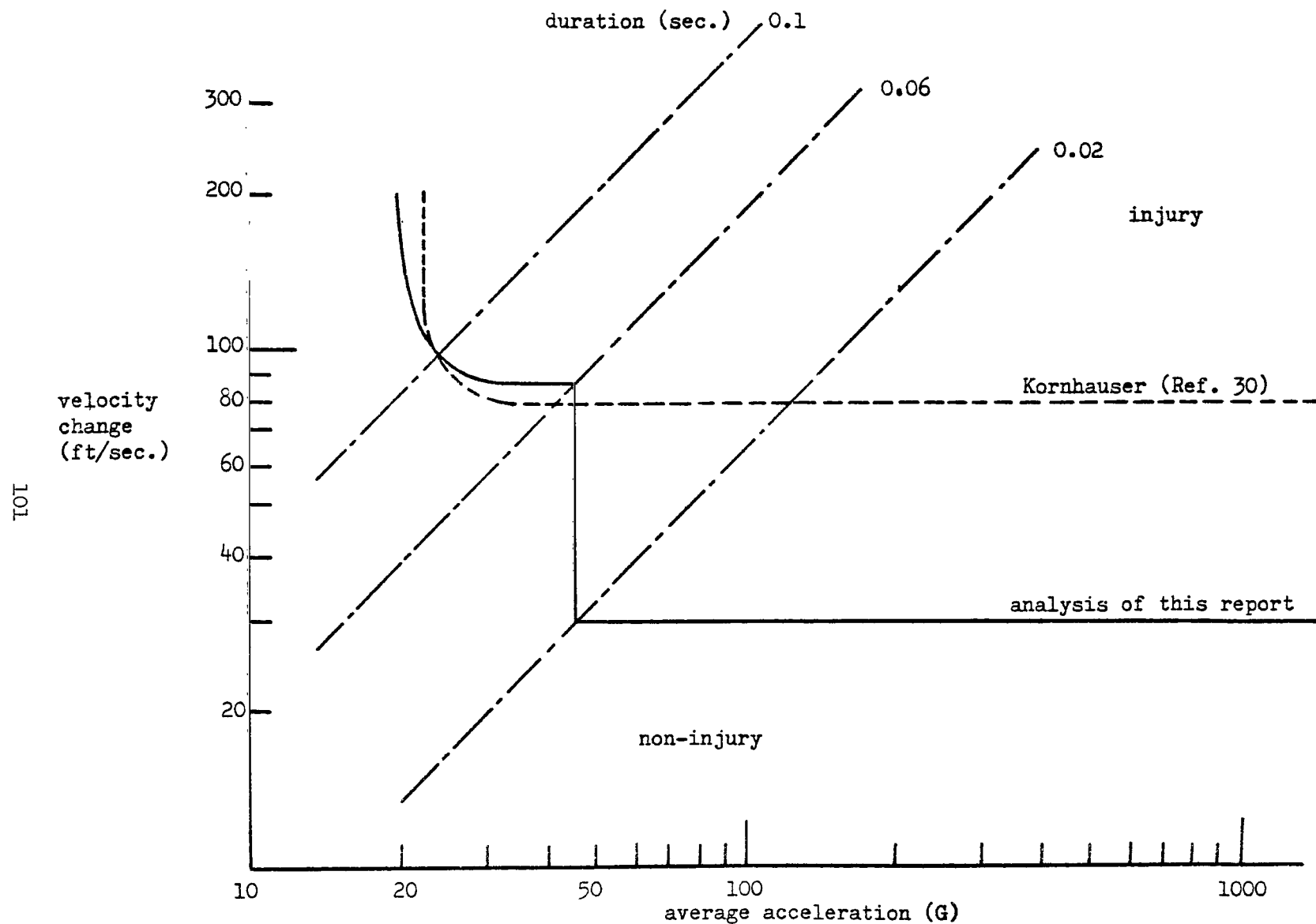


Fig. 27. Tolerance to Short Duration Accelerations as a Function of Velocity Change and Average Acceleration

APPENDIX A

NOTE ON MATHEMATICAL METHODS AND ANALYTICAL TECHNIQUES

SYMBOLS

h	arbitrary function of time
L	denotes "the Laplace transform of"
L^{-1}	denotes "the inverse Laplace transform of"
p	the independent variable in the transformed equation
t	time
x	function of p such that $Lh(t) = (p)$
x_0	value of δ at $t = 0$
\dot{x}_0	value of $\dot{\delta}$ at $t = 0$
\ddot{y}_c	input acceleration
$\delta, \dot{\delta}, \ddot{\delta}$	deflection, velocity (rate of change of deflection), acceleration (rate of change of velocity) of spring
ω	frequency of oscillation of the motion of the spring and mass

The object of the mathematical analysis of the dynamic response of a model represented by a spring-mass system when an acceleration input is applied to the system is to determine the motion with respect to time of a particular mass within the system, which is influenced by the input acceleration and the subsequent vibration of the springs themselves.

The first step is to evaluate the the forces developed in the system in terms of the characteristics of the system (spring stiffness, damping etc.) and to determine the algebraic sum of the forces acting on that part of the system which is of interest. If the part of the system under consideration is at rest, a condition of equilibrium exists where the sum of the forces is zero. If some resultant force acts on any mass however, motion results that can be described by Newton's second law of motion which gives

$$\text{force} = \text{mass} \times \text{acceleration}$$

The forces acting are usually determined in terms of the spring deflection or the spring velocity (rate of change of deflection), so an equation involving one or both of these quantities results. If the deflection is δ , the spring velocity is $\frac{d}{dt}(\delta)$ which is written $\dot{\delta}$ and the spring acceleration (rate of change of spring velocity) is $\frac{d^2}{dt^2}(\delta)$ or $\ddot{\delta}$. The input acceleration, usually denoted \ddot{y}_c is assumed known, and this is related to the spring acceleration and the resultant mass acceleration, so that the input can be introduced into the equation. Thus, for the single spring-mass system with no damping present, discussed in Appendix B, the equation governing the motion of the mass turns out to be

$$\ddot{y}_c = \omega^2 \delta + \ddot{\delta}$$

where ω is the frequency of the system.

This equation is referred to as the equation of motion of the system and it contains the ingredients necessary for evaluating the way that the mass moves with time. Written out fully, the above equation is

$$\frac{d^2 y_c}{dt^2} = \omega^2 \delta + \frac{d^2 \delta}{dt^2}$$

The equation of motion has to be solved to give the spring deflection at any time, which can in turn be related to the resultant mass acceleration. The equation of motion can be solved to give an analytical or closed form solution only for certain simple acceleration input forms, e.g. step function, ramp, impulsive inputs, but these cases are of considerable interest. When more complicated inputs have to be analyzed, the equation of motion must be solved either numerically in a step-by-step fashion, usually with the aid of a digital computer, or with the aid of an analog computer.

The method of analytical solution adopted in this report uses the Laplace transform or operational calculus technique, which is readily applicable to linear differential equations with constant coefficients. This method has the advantage that it is direct and does not need the evaluation of complex arbitrary constants. This convenient method of solving differential equations is easy to use as it is subject to strict rules. Mathematically a function, say $R(t)$ is transformed into another function $X(p)$ by the operation

$$X(p) = p \int_0^{\infty} e^{-pt} R(t) dt$$

This is usually written

$$X(p) = L R(t)$$

where L stands for "the Laplace transform of."

All functions appearing in the differential equation are transformed by the procedure specified above. The value of $X(p)$ for a variety of functions $R(t)$ are tabulated in standard texts so no integration labor is actually involved. In all cases an inverse transform exists denoted by

$$L^{-1} X(p) = R(t)$$

The procedure for solving a differential equation is to arrange the terms in such a way that known transforms exist, and after consulting the transforms and applicable theorems, to solve for the new variable. The inverse Laplace transform is then consulted, which gives the

solution in terms of the original variable directly. Thus the solution of differential equations is reduced to a matter of consulting particular transformations in a table of transforms.

As an example, take the equation cited above and let

$$x(p) = L \delta(t)$$

Then, consulting the tables of transforms

$$L \frac{d^2 \delta}{dt^2} = -p x_1 - p^2 x_0 + p^2 x$$

where x_0 and x_1 are the values of δ and $\dot{\delta}$ at $t = 0$, also

$$L \omega^2 \delta = \omega^2 x \text{ and if } \ddot{y}_c = \text{const}, L \ddot{y}_c = \ddot{y}_c$$

The transformed equation of motion, for the simple case where $\delta = \dot{\delta} = 0$ at $t = 0$, is

$$p^2 x + \omega^2 x = \ddot{y}_c$$

so that

$$x = \frac{\ddot{y}_c}{p^2 + \omega^2}$$

The inverse Laplace transform of the right hand side is $\frac{\ddot{y}_c}{\omega^2} (1 - \cos \omega t)$ hence

$$\delta = \frac{\ddot{y}_c}{\omega^2} (1 - \cos \omega t)$$

It should be noted that in some texts the Laplace transform is defined by

$$x(p) = \int_0^{\infty} e^{-pt} h(t) dt$$

which results in a different set of transforms but, of course, gives the same answer. The first definition is used throughout this report. Further information on Laplace transforms can be obtained by consulting the references given at the end of this appendix.

Having deduced the spring deflection, δ , from the equation of motion, it is usually required to investigate the conditions under which the deflection or related resultant mass acceleration attains a maximum value. This is done, where possible, by the standard procedure of examining $d\delta/dt = 0$ which gives the time at which turning points exist, and the conditions for $d^2\delta/dt^2$ to be negative indicates when δ is a maximum. In this way the peak deflection or peak mass acceleration can be determined and used as a criterion for determining human tolerance to acceleration, as described in the main text.

REFERENCES

<u>No.</u>	<u>Name</u>	<u>Title, etc.</u>
A.1	Pipes L. A.	"Applied Mathematics for Engineers and Physicists," New York, McGraw-Hill Book Co. Inc. 1946.
A.2	Churchill R. V.	"Operational Mathematics," New York, McGraw-Hill Book Co. Inc. 1948.
A.3		"Handbook of Chemistry and Physics," Cleveland, Chemical Rubber Publishing Co.
A.4	Hildebrand F. B.	"Advanced Calculus for Engineers," New York, Prentice-Hall, Inc. 1949.

APPENDIX B

GENERAL THEORY OF A LINEAR, UNDAMPED, SINGLE DEGREE OF FREEDOM MODEL

SYMBOLS

F	spring force
k	spring stiffness
ℓ	unloaded spring length
L	Laplace transform
m_p	mass
t	time
t_1	duration time of particular input acceleration
$y_p, \dot{y}_p, \ddot{y}_p$	coordinate, velocity, acceleration of mass m_p relative to fixed datum
$y_c, \dot{y}_c, \ddot{y}_c$	coordinate, velocity, acceleration of spring base relative to fixed datum
α, β, γ	constants appearing in input functions
$\delta, \dot{\delta}, \ddot{\delta}$	deflection, velocity (rate of change of deflection), acceleration (rate of change of velocity) of spring
δ_s	initial (static) spring deflection
ω	spring frequency

General Theory of a Linear, Undamped, Single Degree of Freedom Model

In this Appendix, the dynamic model in its simplest form (Figure B.1) will be treated; that is, a single degree of freedom spring-mass system with a linear response and no damping effects. The mathematics governing this basic model is fundamental to an understanding of the various modified dynamic models and should serve as a good introduction to the subject.

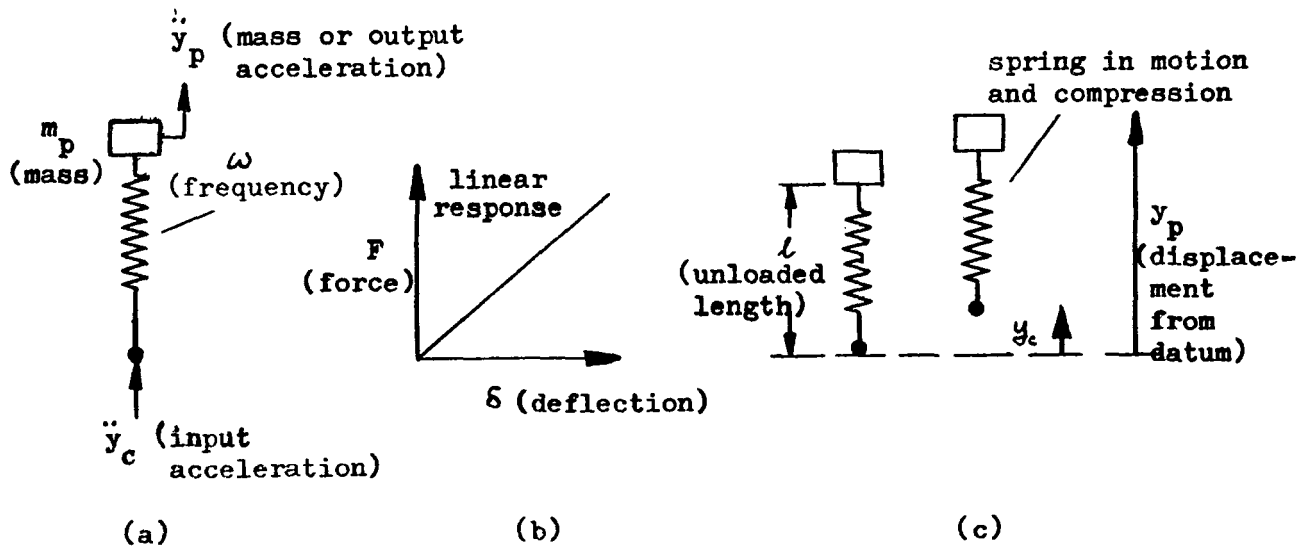


Figure B.1

A spring that has a linear response is one that has equal increments of deflection for equal increments of force, and a plot of force against deflection produces a straight-line. The force (F) is related to the deflection (δ) by the expression

$$F = k \delta$$

B.1

This force, developed in a spring, produces an acceleration of the mass, relative to the datum, and can be expressed by Newton's second law of motion (Force = mass x acceleration), as follows:

$$F = k \delta = m_p \ddot{y}_p \quad \text{B.2}$$

When a given acceleration (or force) is applied to the base of the spring, a force is developed in the spring in accordance with Equation B.1, which produces the mass acceleration given in B.2. It is desired to express B.2 in terms of the input, which is the known quantity in the problem, and the argument proceeds as follows: The deflection in the spring is equal to the unloaded length (\mathcal{L}), minus the loaded length ($y_p - y_c$). Adopting the coordinate system shown in Figure B.1 (c), this leads to

$$\delta = \mathcal{L} - (y_p - y_c) \quad \text{B.3}$$

The spring velocity (which can be interpreted as the rate of change of deflection, i.e. the velocity of the mass relative to the point of application) and acceleration (which is the rate of change of the spring velocity) are obtained by differentiating B.3 with respect to time, once and twice, respectively. Thus

$$\dot{\delta} = \dot{y}_c - \dot{y}_p$$

and

$$\ddot{\delta} = \ddot{y}_c - \ddot{y}_p \quad \text{B.4}$$

Substituting this value for \ddot{y}_p in B.2, gives

$$k \delta = m_p (\ddot{y}_c - \ddot{\delta})$$

or

$$\frac{k}{m_p} \delta = \ddot{y}_c - \ddot{\delta}$$

The natural frequency of the spring-mass system is related to the spring stiffness by the expression

$$\omega = \sqrt{\frac{k}{m_p}}$$

so the above equation can be written

$$\ddot{y}_c = \omega^2 \delta + \ddot{\delta} \quad \text{B.5}$$

This is the equation of motion of the system, and relates the input acceleration to the spring frequency, the deflection and the acceleration produced in the spring. Equation B.5 is a differential

equation of standard form that can be solved for simple inputs to give a solution representing the deflection (δ) at any time. The deflection can be used to obtain the spring acceleration ($\ddot{\delta}$) that can then be related to the mass acceleration (\ddot{y}_p), by B.4. The mass acceleration will be used to denote the acceleration of the mass relative to the fixed datum line and is the resultant of the applied input acceleration and the spring acceleration due to the spring deflecting.

Solution for a Step Input

For the initial analysis, a step input will be assumed, i.e., one which rises instantaneously to a given value and remains at that value for some time, which is considerably greater than the period of the system. The input function will be denoted as follows:

$$\ddot{y}_c = \alpha$$

and B.5, when written out fully, becomes

$$\frac{d^2\delta}{dt^2} + \omega^2\delta = \alpha$$

B.6

The Laplace transform method of operational calculus will be used to solve this equation, although any standard technique can be employed. The Laplace transform method reduces the solution of a differential equation to a matter of looking up a particular transformation in a table of transforms. Reference to standard texts (e.g. Refs. B.1, B.2, B.3, B.4) will clarify the procedure. If L denotes "the Laplace transform of," then

$$L \delta(t) = x(p)$$

In terms of x , B.6 becomes

$$p^2x + \omega^2x = \alpha$$

for the initial conditions $\delta = 0$, and $\dot{\delta} = 0$ at $t = 0$.

Hence,

$$x = \frac{\alpha}{p^2 + \omega^2}$$

B.4

The inverse Laplacian transform gives

$$\delta = \frac{\alpha}{\omega^2} (1 - \cos \omega t) \quad \text{B.7}$$

This is the solution of the equation of motion, and gives the value of the deflection at any time t for a step acceleration input of value α . Differentiating with respect to time gives the spring velocity (rate of change of spring deflection)

$$\dot{\delta} = \frac{\alpha}{\omega} \sin \omega t \quad \text{B.8}$$

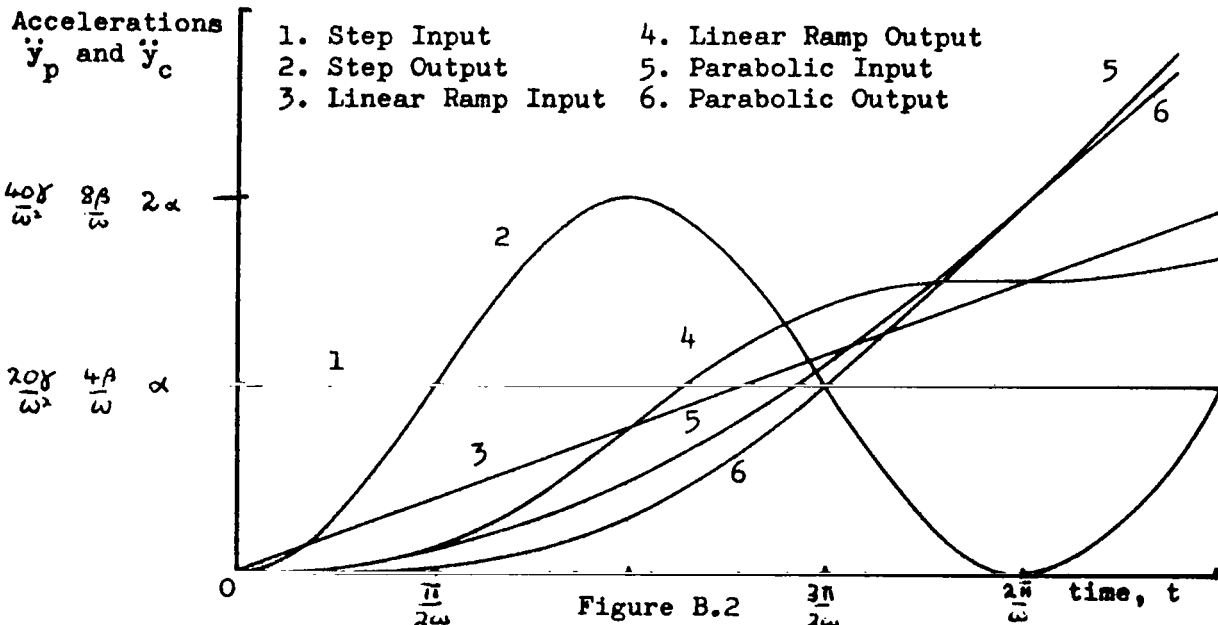
and a second differentiation gives the spring acceleration

$$\ddot{\delta} = \alpha \cos \omega t \quad \text{B.9}$$

Thus, from B.4, the expression for the mass acceleration becomes

$$\ddot{y}_p = \alpha (1 - \cos \omega t) \quad \text{B.10}$$

The output given by B.10 is sinusoidal in nature and has the form shown in Figure B.2



If there is some initial deflection in the spring given by δ_s , the Laplacian equation takes the form

$$-p^2 x_0 + p^2 x + \omega^2 x = \alpha$$

where $x_0 = \delta_3$ the value of δ at $t = 0$. Then,

$$x = \frac{\alpha + p^2 x_0}{p^2 + \omega^2}$$

The inverse Laplacian transform of this expression gives

$$\delta = \frac{\alpha}{\omega^2} (1 - \cos \omega t) + \delta_3 \cos \omega t$$

and

$$\ddot{\delta} = \alpha \cos \omega t - \omega^2 \delta_3 \cos \omega t$$

so that, in this case, the mass acceleration can be represented by

$$\ddot{y}_p = \alpha (1 - \cos \omega t) + \omega^2 \delta_3 \cos \omega t \quad \text{B.11}$$

Solution for a Linear Ramp Input

A linear ramp input is one that has a constant slope, i.e., its value rises linearly with time and may be represented by $\ddot{y}_c = \beta t$, where β is the slope.

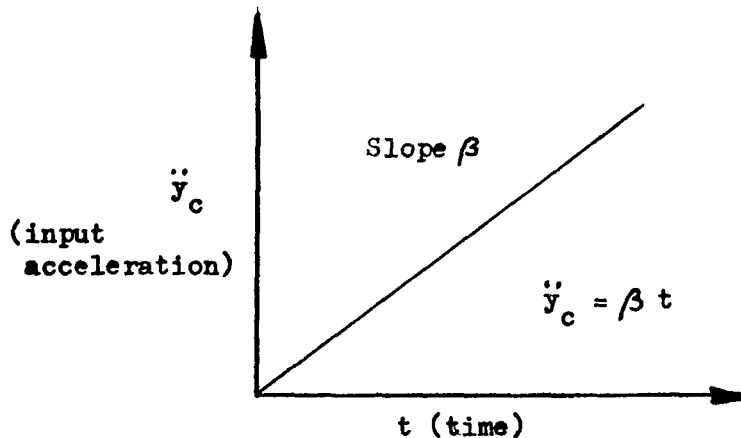


Figure B.3

The equation of motion can be written

$$\frac{d^2 \delta}{dt^2} + \omega^2 \delta = \beta t$$

The Laplace transform of this equation for $\delta = 0$, $\dot{\delta} = 0$ at $t = 0$ gives

$$p^2 x + \omega^2 x = \frac{\beta}{p}$$

and

$$x = \frac{\beta}{p(p^2 + \omega^2)}$$

The inverse Laplacian transform gives

$$\delta = \frac{\beta}{\omega^2} \left(t - \frac{\sin \omega t}{\omega} \right)$$

which represents the deflection at any time $t < t_1$, and the acceleration obtained by double differentiation is

$$\ddot{\delta} = \frac{\beta}{\omega} \sin \omega t$$

giving the mass acceleration by the expression

$$\ddot{y}_p = \beta \left(t - \frac{\sin \omega t}{\omega} \right)$$

B.13

The output corresponding to this expression is also plotted in Figure B.2.

If the input can be represented by a ramp function until time t_1 , and then assumes some other form, the mass acceleration may be represented by B.13 until $t = t_1$, thereafter the equation of motion must be solved using the conditions existing at $t = t_1$ as the new starting conditions.

Solution for a Parabolic Input

In this case, the input has the shape shown in Figure B.4, and can be represented by the equation $\ddot{y}_c = \gamma t^2$.

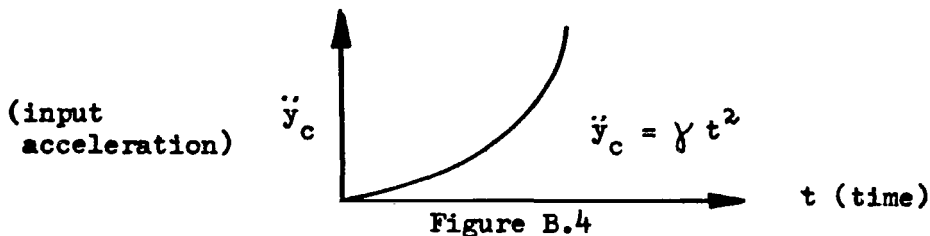


Figure B.4

The equation of motion is now

$$\frac{d^2 \delta}{dt^2} + \omega^2 \delta = \gamma t^2$$

B.14

The Laplace transform for $\delta = 0$, $\dot{\delta} = 0$ at $t = 0$ is

$$p^2 x + \omega^2 x = \frac{2\gamma}{p^2}$$

so that

$$x = \frac{2\gamma}{p^2(p^2 + \omega^2)} = \frac{2\gamma}{\omega^2 p^2} - \frac{2\gamma}{\omega^2(p^2 + \omega^2)}$$

The inverse Laplacian transform results in

$$\delta = \frac{\gamma}{\omega^2} \left\{ t^2 - \frac{2}{\omega^2} (1 - \cos \omega t) \right\}$$

and the acceleration is given by

$$\ddot{\delta} = \frac{2\gamma}{\omega^2} (1 - \cos \omega t)$$

and the mass acceleration from B.4, can be written

$$\ddot{y}_p = \gamma t^2 - \frac{2\gamma}{\omega^2} (1 - \cos \omega t) \quad \text{B.15}$$

The mass acceleration given by this expression is illustrated in Figure B.2.

Peak Accelerations

In applying tolerance criteria to the model, the quantity of main interest is the value of the maximum acceleration (or output) achieved by the mass. When a maximum occurs in the output due to the mass acceleration overshooting, it can be found analytically. The usual procedure is to differentiate with respect to time the equation representing the mass acceleration at any time, and equating to zero. For the step input from B.10,

$$\frac{d\ddot{y}_p}{dt} = \alpha \omega \sin \omega t = 0$$

The solution of this equation gives any turning point which might represent a maximum, minimum, or a point of inflection. In the above equation, $\alpha \omega$ is finite, and $\sin \omega t$ must be zero, which occurs

when $\omega t = 0, \pi, 2\pi$ etc. A second differentiation gives the condition for maximum or minimum.

$$\frac{d^2 \ddot{y}_p}{dt^2} = \alpha \omega^2 \cos \omega t$$

When $\omega t = \pi, 3\pi$ etc., the second differential is negative, indicating a maximum. Thus, the mass acceleration is a maximum for a step function input, when

$$t = \pi/\omega, 3\pi/\omega, 5\pi/\omega \text{ etc}$$

and has the value

$$\ddot{y}_p(\max) = \alpha (1 - \cos \omega t) = 2\alpha \quad \text{B.16}$$

Thus, if there is no damping present, the peak mass acceleration can be twice the input acceleration. This is the case of 100% overshoot.

The linear ramp and parabolic inputs show no maxima or minima, only points of inflection. These facts can be seen by consulting Figure B.2.

Square Wave Input

The square wave input case is of particular interest, since, in practice, the input is applied for a short finite time (t_1) only. The mass continues to move after the removal of the applied acceleration, so that the maximum acceleration experienced by the mass is usually obtained at some time greater than t_1 . Equations B.6 through B.10 hold up to time t_1 , but thereafter, since the input is removed, the equation of motion reduces to

$$\frac{d^2 \delta}{dt^2} + \omega^2 \delta = 0 \quad \text{B.17}$$

In this case, the initial conditions to be applied are those pertaining to $t = t_1$. The Laplace transform of B.17 is

$$-p^2 x_1 - p^2 x_0 + p^2 x + \omega^2 x = 0$$

where

$$x_0 = \delta \text{ at } t=0 \quad \text{i.e. } x_0 = \frac{\alpha}{\omega^2} (1 - \cos \omega t_1) \quad \text{from B.7}$$

and

$$x_1 = \dot{\delta} \text{ at } t=0 \quad \text{i.e. } x_1 = \frac{\alpha}{\omega} \sin \omega t_1 \quad \text{from B.8}$$

Hence,

$$x = \frac{p^2 x_0 + p x_1}{p^2 + \omega^2} = \frac{x_0 (p^2 + \frac{x_1}{x_0} p)}{p^2 + \omega^2}$$

The inverse Laplace transform of this expression gives

$$\delta = \frac{x_0}{\omega} \left\{ \left(\frac{x_1}{x_0} \right)^2 + \omega^2 \right\}^{1/2} \sin(\omega t + \phi)$$

$$\text{where } \tan \phi = \frac{\omega x_0}{x_1}$$

Substituting the values for x_1 and x_0 , leads to

$$\begin{aligned} \delta &= \left\{ \left(\frac{x_1}{\omega} \right)^2 + x_0^2 \right\}^{1/2} \sin(\omega t + \phi) \\ &= \left\{ \frac{\alpha^2}{\omega^4} \sin^2 \omega t_1 + \frac{\alpha^2}{\omega^4} (1 - \cos \omega t_1)^2 \right\}^{1/2} \sin(\omega t + \phi) \\ &= \frac{\alpha}{\omega^2} (\sin^2 \omega t_1 + 1 + \cos^2 \omega t_1 - 2 \cos \omega t_1)^{1/2} \sin(\omega t + \phi) \end{aligned}$$

and since $\sin^2 \omega t_1 + \cos^2 \omega t_1 = 1$

$$\delta = \frac{\alpha}{\omega^2} (2 - 2 \cos \omega t_1)^{1/2} \sin(\omega t + \phi)$$

From B.2,

$$\ddot{y}_p = \omega^2 \delta$$

so the mass acceleration for time greater than t_1 , is given by

$$\ddot{y}_p = \alpha (2 - 2 \cos \omega t_1)^{1/2} \sin(\omega t + \phi)$$

B.18

where time is now measured from $t = t_1$

B.18 is examined for maxima by differentiating with respect to time and equating to zero, i.e.,

$$\frac{d\ddot{y}_p}{dt} = \alpha \omega (2 - 2 \cos \omega t_1)^{1/2} \cos(\omega t + \phi) = 0$$

Turning points occur at $(\omega t + \phi) = \pi/2, 3\pi/2$ etc

Now,

$$\frac{d^2 \ddot{y}_p}{dt^2} = -\alpha \omega^2 (2 - 2 \cos \omega t_1)^{1/2} \sin(\omega t + \phi) \quad \text{B.19}$$

and this expression is negative when $(\omega t + \phi) = \pi/2, 5\pi/2$ etc so that maxima occur at these values. The peak mass acceleration is given by

$$\ddot{y}_p(\max) = \alpha (2 - 2 \cos \omega t_1)^{1/2}$$

Thus, for a given amplitude, the maximum output attained depends on the pulse duration and frequency, as shown in Figure B.5.

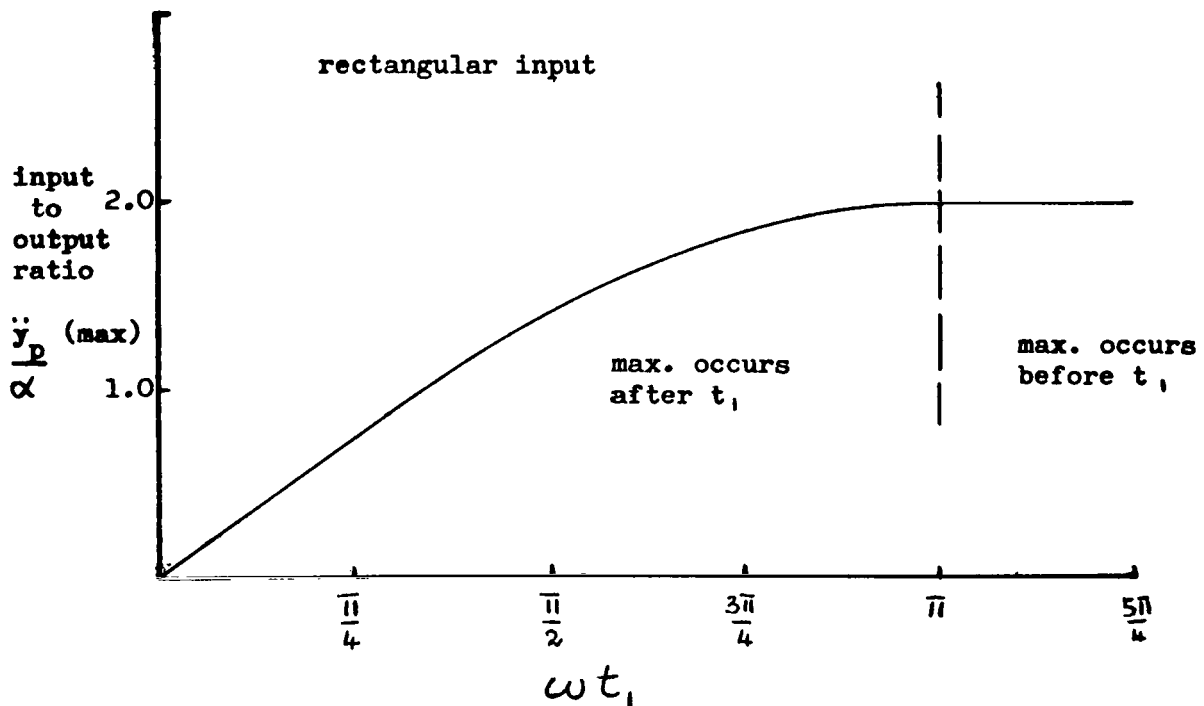


Figure B.5

REFERENCES

<u>No.</u>	<u>Name</u>	<u>Title, etc.</u>
B.1	Pipes, L. A.	"Applied Mathematics for Engineers and Physicists," New York, McGraw-Hill Book Co. Inc., 1946.
B.2	Churchill, R. V.	"Operational Mathematics," New York, McGraw-Hill Book Co. Inc., 1948.
B.3	—	"Handbook of Chemistry and Physics," Cleveland, Chemical Rubber Publishing Co.
B.4	Hildebrand F. B.	"Advanced Calculus for Engineers," New York, Prentice-Hall, Inc., 1949.

APPENDIX C

THEORY OF A NON-LINEAR, UNDAMPED, SINGLE DEGREE OF FREEDOM SYSTEM, SUBJECTED TO A STEP INPUT

SYMBOLS

F	spring force
g	acceleration due to gravity
k	spring stiffness
ℓ	unloaded spring length
m_p	mass
q	$= \frac{d\delta}{dt}$
t	time
t_1	time at which $\ddot{\delta} = 0$
t_2	time at which $\dot{\delta} = 0$
y_p, \ddot{y}_p	coordinate, acceleration of mass m_p relative to fixed datum
y_c, \ddot{y}_c	coordinate, acceleration of spring base relative to fixed datum
\ddot{y}_s	initial acceleration at $t = 0$
α	step function input acceleration
$\delta, \dot{\delta}, \ddot{\delta}$	deflection, velocity (rate of change of deflection), acceleration (rate of change of velocity) of spring
δ_s	initial (static) spring deflection
ζ_n	$= \omega_n^2 = \frac{k}{m_p}$
ω	spring frequency ($n=1$)

The basic model to be studied is shown in Figure C.1(a).

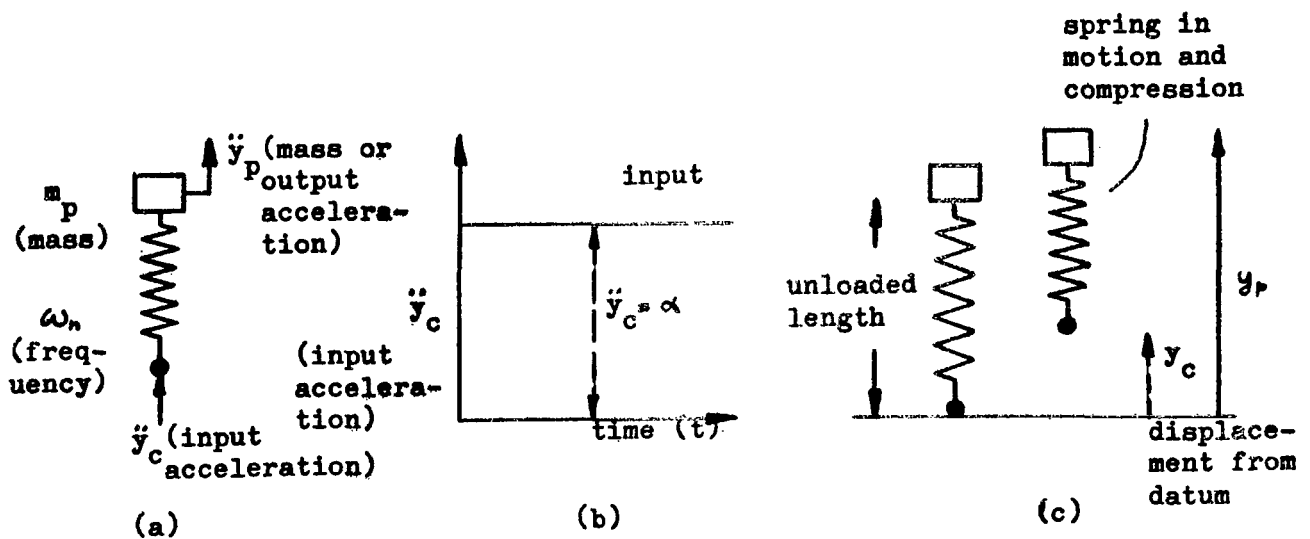


Figure C.1

The approach used is similar to that given in Appendix B, except that the force-deflection characteristics of the spring are assumed to be non-linear. Thus, the force developed in the spring during compression or extension must be represented by a relationship of the form.

$$F = k_n \delta^n \quad \text{C.1}$$

where δ^n denotes some power of δ and k_n is the corresponding value of spring stiffness.

The influence on the F versus δ curve of various values of n is shown in Figure C.2.

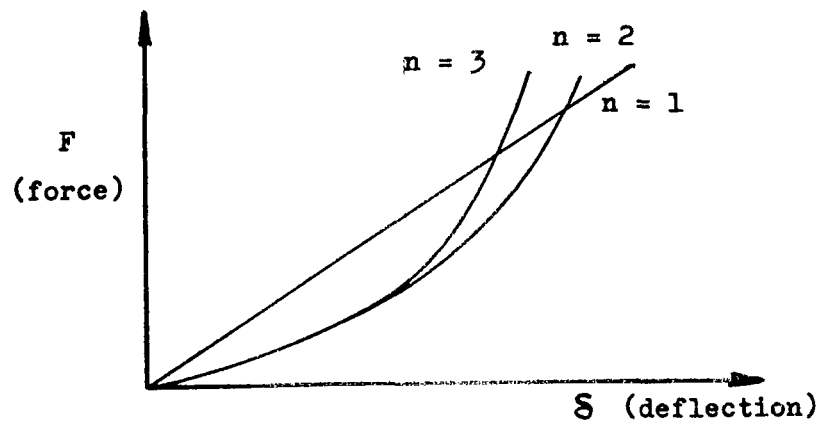


Figure C.2

Although this formula does not give a completely general representation of the system shown in Figure C.1, it enables a reasonable approximation to be made by selecting an appropriate value of the exponent n . This assumption allows us to prove a number of valuable theorems without complicating the mathematics too much.

Generally, from Newton's second law, the force developed in the spring causes an acceleration in the mass which is given by

$$F = m_P \ddot{y}_P = k_n \delta^n \quad \text{C.2}$$

Hence,

$$\delta^n = \frac{m_P \ddot{y}_P}{k_n}$$

and since $\frac{k_n}{m_P}$ can be written in terms of the frequency (ω), viz. $\omega_n^2 = \frac{k_n}{m_P} = \zeta_n$ (say), the deflection is given by

$$\delta = \left(\frac{\ddot{y}_P}{\zeta_n} \right)^{\frac{1}{n}} \quad \text{C.3}$$

The equation of motion of the system can now be written down for a given input since the resultant force on the mass is that developed in the spring, less the normal gravity force (its weight for the vertical direction). This force causes a mass acceleration \ddot{y}_P , so that

$$m_P \ddot{y}_P = k_n \delta^n - m_P g \quad \text{C.4}$$

The deflection δ is the distance through which the spring deflects when loaded, and is the unloaded spring length minus the loaded length. Using the coordinate system shown in Figure C.1(c)

$$\delta = \ell - (y_P - y_c)$$

Taking the second derivative with respect to time, the spring acceleration due to the deflecting of the spring is given by

$$\ddot{\delta} = \ddot{y}_c - \ddot{y}_P$$

which is the difference between the applied acceleration and the actual resultant acceleration experienced by the mass relative to the origin of the system (datum), and

$$\ddot{y}_p = \ddot{y}_c - \ddot{\delta} \quad \text{C.5}$$

Substituting C.5 in C.4, the equation of motion in terms of the input acceleration \ddot{y}_c is obtained

$$m_p(\ddot{y}_c - \ddot{\delta}) + m_p g = k_n \delta^n$$

or

$$\ddot{y}_c + g = \zeta_n \delta^n + \ddot{\delta} \quad \text{C.6}$$

where $\ddot{y}_c = f(t)$ is a function of time.

Effect of Constant Acceleration $\ddot{y}_c = \alpha$

If the input acceleration rises instantaneously to a value α and then remains constant (i.e., a step function), an expression for the maximum value of the resultant mass acceleration (\ddot{y}_p) can be derived. For convenience, the following substitution is made

$$\dot{\delta} = \frac{d\delta}{dt} = q, \quad \therefore \ddot{\delta} = \frac{dq}{dt} = q \frac{dq}{d\delta}$$

so that the equation of motion (C.6) becomes

$$q \frac{dq}{d\delta} + \zeta_n \delta^n = \alpha + g$$

and transposing terms and integrating, the following expression is obtained

$$\int_{q=0}^{q=0} q dq = \int_{\delta_s}^{\delta_{\max}} [(\alpha + g) - \zeta_n \delta^n] d\delta \quad \text{C.7}$$

The limits of the integration are as indicated, because at time $t = 0$ the velocity ($\dot{\delta} = q$) is zero when the deflection is δ_s (the static deflection, due to some steady state force, usually the weight of the mass), and when the deflection is a maximum (δ_{\max}), the velocity is again zero.

The left-hand side integrates to $\dot{q}^2/2$, which is the kinetic energy per unit mass, and for the limits given is zero, indicating that all the kinetic energy of the system appears as potential energy stored in the spring at maximum deflection. This is simply a statement of the conservation of energy (kinetic energy plus potential energy = 0). At maximum deflection, $\dot{\delta}$ is zero so that all the kinetic energy is converted to potential energy. These physical facts, described mathematically above, are illustrated graphically in Figure C.3.

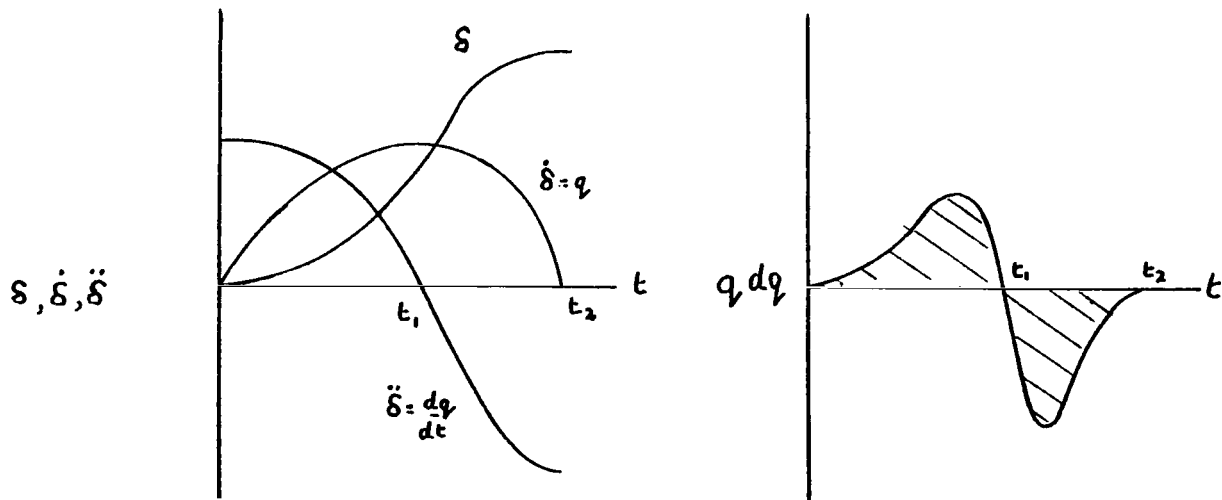


Figure C.3

The change in the sign of the $q dq$ curve at t_1 is due to the fact that the acceleration reverses its direction at that time. The two equal shaded areas show that the kinetic energy gained by the mass is gradually destroyed and stored as potential energy in the system.

Integrating the right-hand side of C.7 and equating to zero, gives

$$\frac{\zeta_n \delta_{\max}^{n+1}}{n+1} - (\alpha + g) \delta_{\max} = \frac{\zeta_n \delta_s^{n+1}}{n+1} - (\alpha + g) \delta_s \quad \text{C.8}$$

The initial acceleration \ddot{y}_s from C.3, can be represented by

$$\ddot{y}_s = \zeta_n \delta_s^n$$

so that C.8 becomes

$$\frac{\zeta_n \delta_{\max}^{n+1}}{n+1} - (\alpha + g) \delta_{\max} = \left(\frac{\ddot{y}_s}{\zeta_n} \right)^{1/n} \left\{ \frac{\ddot{y}_s}{n+1} - (\alpha + g) \right\} \quad \text{C.9}$$

If the initial deflection was zero, $\delta_s = 0$ and $\ddot{y}_s = 0$ and the weight is ignored, so the above equation reduces to

$$\zeta_n \delta_{\max}^n = \alpha (n+1)$$

Remembering that $\zeta_n \delta_{\max}^n = \ddot{y}_p(\max)$, from C.2 the following simple expression for the maximum resultant mass acceleration is obtained.

$$\ddot{y}_p(\max) = (n+1) \alpha \quad \text{C.10}$$

which, for a linear spring ($n = 1$), gives $\ddot{y}_p(\max) = 2\alpha$ in agreement with B.16.

General Solution for $n = 1$

If it is assumed that $n = 1$, equation C.9 can be written

$$\zeta_n^2 \delta_{\max}^2 - 2(\alpha + g) \delta_{\max} = \ddot{y}_s^2 - 2\ddot{y}_s(\alpha + g)$$

Adding $(\alpha + g)^2$ to each side and factorising gives

$$\left\{ \zeta_n \delta_{\max} - (\alpha + g) \right\}^2 = \left\{ \ddot{y}_s - (\alpha + g) \right\}^2$$

Thence,

$$\zeta_n \delta_{\max} = 2(\alpha + g) - \ddot{y}_s$$

Now when $n = 1$, $\zeta \delta_{\max} = \omega^2 \delta_{\max} = \ddot{y}_p(\max)$, therefore

$$\ddot{y}_p(\max) = 2(\alpha + g) - \ddot{y}_s \quad \text{C.11}$$

For zero static deflection, C.11 agrees with C.10 for the case $n = 1$.

Equation C.11 shows that if \ddot{y}_s is negative, as might occur in a negative "G" field, we have the worst physiological effects.

APPENDIX D

THE SINGLE DEGREE OF FREEDOM SYSTEM SUBJECTED TO AN IMPULSIVE INPUT

SYMBOLS

F	spring force
k_n	spring stiffness
ℓ	unloaded spring length
L	Laplace transform
m_p	mass of system
t	time
t_i	duration time of particular input acceleration
Δt_c	critical duration time for impulsive inputs
$y_p, \dot{y}_p, \ddot{y}_p$	coordinate, velocity, acceleration of mass m_p relative to a fixed datum
$y_o, \dot{y}_o, \ddot{y}_o$	coordinate, velocity, acceleration of spring base, relative to fixed datum
$\delta, \dot{\delta}, \ddot{\delta}$	deflection, velocity (rate of change of deflection), acceleration (rate of change of velocity) of spring
$\zeta_n \left(= \frac{k_n}{m_p} \right)$	referred to as the "frequency squared" of the system
ω_n	referred to as the "frequency" of the system
ω	frequency of system ($n=1$)
v	velocity
Δv	the velocity change, due to an impulse

In this Appendix it is intended to develop further the analysis of the response of the simple single degree of freedom system. Short-time duration accelerations will be considered, which, in the limit, reduce to impulsively applied accelerations. The model shown diagrammatically in Figure D.1 (a) will be studied

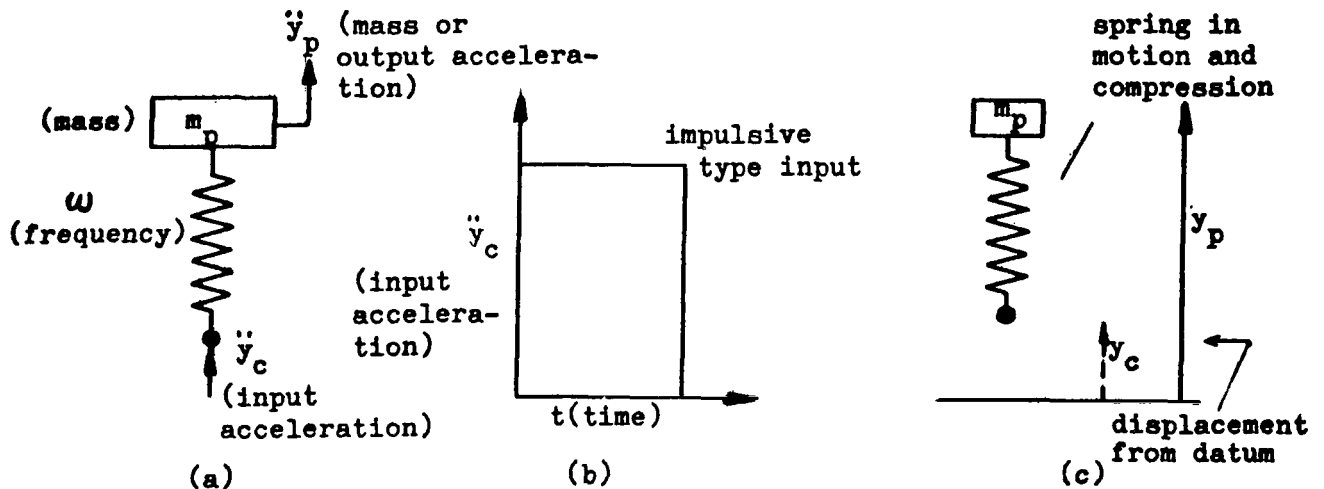


Figure D.1

The equations of motion of the non-linear system have been established in Appendix C. The equation of motion with no initial loading, from C.6, is

$$m_p (\ddot{y}_c - \ddot{s}) = k_n \delta^n \quad D.1$$

and with an initial load $m_p \ddot{y}_s$

$$m_p (\ddot{y}_c + \ddot{y}_s - \ddot{s}) = k_n \delta^n \quad D.2$$

Defining $\ddot{y}_c = \ddot{y}_c + \ddot{y}_s$, the equation can be condensed to the form of D.1

$$m_p (\ddot{y}_c - \ddot{s}) = k_n \delta^n \quad D.4$$

Rearranging terms and dividing throughout by m_p , yields the equation of motion in a more usable form

$$\ddot{s} + \zeta_n \delta^n = \ddot{y}_c \quad D.5$$

where $\zeta_n = \frac{k_n}{m_p} = \omega_n^2$ and ω_n is the "frequency" of the system.

Before proceeding, it is worthwhile discussing the spring force given by C.2

$$F = k_n \delta^n \quad \text{D.6}$$

If n is even, the force F does not change direction with change of sign of δ (that is, in changing from compression to extension). If our conclusions are limited to a compressed spring only, however, even values of n can be allowed. If n is odd, F changes sign with δ and no difficulty arises, since the force F is always directed towards the point of equilibrium.

In general, it is not possible to solve explicitly the differential equation given in D.5, but the energy equation can be derived from which several useful results may be obtained. From D.5

$$\ddot{\delta} + \zeta_n \delta^n = \ddot{y}_c$$

Now multiplying through by $\dot{\delta}$, the above equation becomes

$$\dot{\delta} \ddot{\delta} + \zeta_n \delta^n \dot{\delta} = \ddot{y}_c \dot{\delta}$$

which integrates with respect to time to give the energy equation

$$\frac{1}{2} \dot{\delta}^2 + \zeta_n \frac{\delta^{n+1}}{n+1} = \ddot{y}_c \delta + K \quad \text{D.7}$$

for a constant \ddot{y}_c . K is an arbitrary constant of integration (since the integration was not carried out between definite limits) which may be evaluated from the initial conditions.

Attention will now be confined to a motion started from rest by a constant acceleration \ddot{y}_c , applied from time $t = 0$ to time $t = t_1$, and solutions are required of the equation of motion or energy equation for times less, and greater than t_1 .

If $0 \leq t \leq t_1$, the energy equation is

$$\frac{1}{2} \dot{\delta}^2 + \frac{\zeta_n \delta^{n+1}}{n+1} = \ddot{y}_c \delta + K \quad \text{D.8}$$

and the initial conditions, expressed in mathematical form, are that at $t = 0$, $\delta = \dot{\delta} = 0$. On substituting these conditions in equation D.8, it follows that $K = 0$.

When $t > t_1$, the above conditions hold up to $t = t_1$, when the constant acceleration is removed; thereafter, the motion is considered using the initial conditions, $\delta = \delta_1$ and $\dot{\delta} = \dot{\delta}_1$, then

$$\frac{1}{2} \dot{\delta}_1^2 + \frac{\zeta_n \delta_1^{n+1}}{n+1} = \ddot{y}_c \delta + K \quad D.8(a)$$

Now for $t \geq t_1$, $\ddot{y}_c = 0$, i.e., $\ddot{y}_c = \ddot{y}_s$, so the general form of the energy equation is

$$\frac{1}{2} \dot{\delta}^2 + \frac{\zeta_n \delta^{n+1}}{n+1} = \ddot{y}_s \delta + K \quad D.9$$

Now at $t = t_1$, $\delta = \delta_1$ and $\dot{\delta} = \dot{\delta}_1$, so that from D.9, K is given by

$$\frac{1}{2} \dot{\delta}_1^2 + \frac{\zeta_n \delta_1^{n+1}}{n+1} = \ddot{y}_s \delta_1 + K \quad D.10$$

From D.8 and D.10

$$\ddot{y}_c \delta_1 = (\ddot{y}_c + \ddot{y}_s) \delta_1 = \ddot{y}_s \delta_1 + K$$

Hence,

$$K = \ddot{y}_c \delta_1$$

so that from D.9, the required form of the energy equation for $t \geq t_1$ is

$$\frac{1}{2} \dot{\delta}^2 + \frac{\zeta_n \delta^{n+1}}{n+1} = \ddot{y}_s \delta + \ddot{y}_c \delta_1$$

or

$$\frac{\zeta_n \delta^{n+1}}{n+1} - \ddot{y}_s \delta = \ddot{y}_c \delta_1 - \frac{1}{2} \dot{\delta}^2 \quad D.11$$

Since $\dot{\delta}^2$ is always positive, and δ_1 has some fixed value for a given \ddot{y}_c and \ddot{y}_s , the R.H.S. of D.11 is a maximum when $\dot{\delta}^2 = 0$; i.e., δ has its maximum value when $\dot{\delta}^2 = 0$, and

$$\frac{\zeta_n \delta_{\max}^{n+1}}{n+1} = \ddot{y}_s \delta_{\max} + \ddot{y}_c \delta_1 \quad D.12$$

Impulsively Started Motion (without initial loading)

Since $\ddot{y}_s = 0$, the equation yielding δ_{\max} , in this case is

$$\frac{\zeta_n \delta_{\max}^{n+1}}{n+1} = \ddot{y}_c \delta_1 \quad D.13$$

The basic motion equations state that (velocity)² = 2 (acceleration x distance), hence the velocity of the base of the spring is given by

$$\frac{1}{2} v^2 = \ddot{y}_c \delta, \quad \text{D.14}$$

Combining D.14 and D.13 gives

$$\delta_{\max} = \left(\frac{n+1}{2} \frac{v^2}{\zeta} \right)^{\frac{1}{n+1}} \quad \text{D.15}$$

Since $\ddot{y}_p(\max) = \zeta_n \delta_{\max}^n$ (see Equation C.2), the maximum acceleration of the mass is

$$\ddot{y}_p(\max) = \zeta_n \left(\frac{n+1}{2} \frac{v^2}{\zeta} \right)^{\frac{n}{n+1}} \quad \text{D.16}$$

It is of interest to establish the input duration time Δt_c below which the input can be regarded as an impulse. The impulse region is defined as pertaining to duration times that are short enough that full overshoot is not attained, and to determine the limiting duration, the relationships for $\ddot{y}_p(\max)$ relevant to the impulse duration region, as defined above, and to the full overshoot region (long duration times) can be equated.

It has been shown in Appendix C that for a long duration input, the peak mass acceleration is from C.10.

$$\ddot{y}_p(\max) = (n+1) \ddot{y}_c \quad \text{D.17}$$

The peak mass acceleration for an impulse type input is given by D.16, and putting $v = \ddot{y}_c \Delta t$ in Equation D.16, the following relationship is obtained

$$\ddot{y}_p(\max) = \zeta_n \left(\frac{n+1}{2} \frac{\ddot{y}_c^2 \Delta t^2}{\zeta} \right)^{\frac{n}{n+1}} \quad \text{D.18}$$

so that on equating D.17 to D.18 at the critical duration time Δt_c we have

$$(n+1) \ddot{y}_c = \zeta_n \left(\frac{n+1}{2} \frac{\ddot{y}_c^2 \Delta t_c^2}{\zeta} \right)^{\frac{n}{n+1}} \quad \text{D.19}$$

which yields

$$\Delta t_c = \sqrt{2} \left(\frac{n+1}{\zeta} \right)^{\frac{1}{2n}} \ddot{y}_c^{-\frac{(n-1)}{2n}} \quad \text{D.20}$$

Confining attention to the particular case of $n = 1$, (linear spring), the following expression for the peak mass acceleration is obtained from D.16.

$$\ddot{y}_p(\max) = \zeta^{1/2} v = \omega v \quad D.21$$

and the duration limit for an input to be regarded as an impulse or spike is from D.20

$$\Delta t_c = \frac{2}{\zeta^{1/2}} = \frac{2}{\omega} \quad D.22$$

D. 21 may be written in the form

$$\ddot{y}_p(\max) = \omega v = \omega \ddot{y}_c \Delta t$$

or if the accelerations are measured in G units

$$G_p(\max) = G_c \omega \Delta t \quad D.23$$

This equation holds for a linear spring in the impulse region where $\Delta t < \frac{2}{\omega}$

Spinal Headward Accelerations

It has been suggested that the maximum tolerable velocity change, Δv , produced by an impulse, is about 11 fps., and from Ruff (Ref. D.1), the maximum permissible deflection of the spine is approximately .05 ft. Thus, from Equation D.15

$$\zeta = \frac{n+1}{2} \frac{\Delta v^2}{\delta_{\max}^{n+1}}$$

from which the following values for ζ are obtained:

n	ζ (rad ² /sec ² /ft ^{$n-1$})	$\zeta^{1/2}$ (rad/sec/f ^{$\frac{n-1}{2}$})	$\delta_{\max}^{\frac{n-1}{2}} \zeta^{1/2}$ (rad/sec)
1	48,400	220	220
2	1.45×10^6	1.205×10^3	270
3	3.87×10^7	6.22×10^3	311
4	9.78×10^8	3.13×10^4	350

From Equation D.20

$$\Delta t_c = \sqrt{2} \left(\frac{n+1}{\zeta} \right)^{\frac{1}{2n}} \ddot{y}_c - \frac{n-1}{2n}$$

A reasonable value for \ddot{y}_c at the critical time can be taken at 40 G from the curves presented by Eiband (Ref. D.2), and using ζ as computed above, it is found that the value of Δt_c is approximately 0.009 sec. for all values of n .

REFERENCES

<u>No.</u>	<u>Name</u>	<u>Title, etc.</u>
D.1	Ruff S.	"Brief Acceleration - Less than One Second." German Aviation Medicine, World War II, Volume 1, P.584. Department of the Air Force, Washington. 1950.
D.2	Eiband A. M.	"Human Tolerance to Rapidly Applied Accelerations. A Summary of the Literature." NASA Memo 5-19-59E. June 1959.

APPENDIX E

THE INFLUENCE OF DAMPING ON A LINEAR SINGLE DEGREE OF FREEDOM SYSTEM

SYMBOLS

A	amplification factor (sinusoidal inputs)
C	damping coefficient
F	force
F_o	impulse (force x time)
F_s	force developed in spring
F_d	force developed in damper
k	spring stiffness
K	damping constant
t	time
t_c	critical duration time for impulsive input
v	velocity
\ddot{y}_p	mass acceleration relative to fixed datum
\ddot{y}_c	input acceleration
\ddot{y}_{co}	amplitude of sinusoidal input acceleration
α	steady (step) input acceleration
$\delta, \dot{\delta}, \ddot{\delta}$	deflection, velocity (rate of change of deflection), acceleration (rate of change of velocity) of spring
$\Delta(t)$	Dirac impulse function
ϕ	phase angle
ω	spring frequency
ω_o	damped frequency ($\omega_o^2 = \omega^2 - C^2$)
Ω	sinusoidal input frequency
α, α_1 β, β_1 }	constants used in reducing Equation E.23 to partial fractions

Damping is always present in a mechanical system, and the human body is no exception. Physically, this means that vibrations set up in the body will gradually die out, and the peak values obtained will be reduced. The basic model can be modified to include the influence of damping, as shown in Figure E.1, where the overall damping effect is represented by a "dash pot" mechanism, which may be regarded as a loose fitting piston moving in an oil-filled cylinder that introduces a viscous frictional resistance, proportional to the velocity.

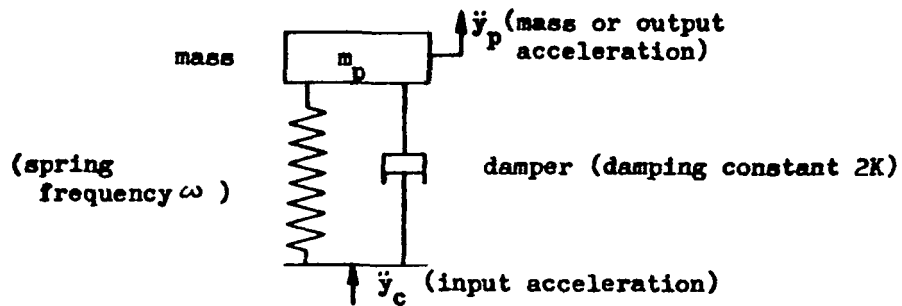


Figure E.1

When the mass moves relative to the datum, a force develops in the damper which is equal to the damping constant x spring velocity, i.e.,

$$F_d = 2K\dot{\delta} \quad \text{E.1}$$

The damping constant has been taken as $2K$ simply for convenience when handling the equations that govern the motion of the system.

The force developed in the spring due to compression, is that described in Appendix B, and is given by

$$F_s = k\delta \quad \text{E.2}$$

These two forces act on the mass, resulting in an acceleration given by

$$m\ddot{y}_p = k\delta + 2K\dot{\delta}$$

As shown in Appendix B, $\ddot{y}_p = \ddot{y}_c - \ddot{\delta}$, and the above equation becomes

$$\ddot{y}_c = \frac{k}{m_p}\delta + \frac{2K}{m_p}\dot{\delta} + \ddot{\delta}$$

Remembering that $\omega^2 = \frac{k}{m_p}$, and setting $\frac{k}{m_p} = C$, the equation of motion of the system can be written

$$\ddot{y}_c = \omega^2 \delta + 2c \dot{\delta} + \dot{\delta} \quad \text{E.3}$$

It should be noted that when damping is included in the system, the total force developed is not just that in the spring, but has an additional component, due to the damper. This means that a tolerance criterion could be based on the total force (or mass acceleration) or the spring force (or δ). In either case, E.3 has to be solved for δ , and to simplify the mathematics, a step input of the form

$$\ddot{y}_c = \alpha$$

will be assumed.

Again making use of the Laplace transform method in solving the equation of motion, $L \delta(t) = X(p)$, and E.3 can be transformed to

$$\omega^2 X + 2cpX + p^2 X = \alpha$$

for $\delta = 0$, $\dot{\delta} = 0$ at $t = 0$, which assumes the spring has no deflection or velocity at zero time. Then,

$$X = \frac{\alpha}{p^2 + 2cp + \omega^2}$$

A direct inverse Laplace transform exists for the denominator, and three solutions are obtained depending on whether ω^2 is greater than, less than, or equal to c^2 .

If $\omega^2 = c^2$, the effect of the damping is such that, when the forcing function is removed, the displacement (or deflection) of the mass approaches zero asymptotically, without oscillating about the $\delta = 0$ position.

Under these conditions, the system is said to be critically damped.

For this case, the solution of E.3 is

$$\delta = \frac{\alpha}{\omega^2} \{ 1 - e^{-ct} (1 + ct) \}$$

When $\omega^2 < c^2$, the damping is so great that, when the forcing

function is removed, the deflection returns to zero slowly with a dead beat motion. The solution is

$$\delta = \frac{\alpha}{\omega^2} \left\{ 1 - \frac{\omega^2}{n-m} \left(\frac{e^{-mt}}{m} - \frac{e^{-nt}}{n} \right) \right\}$$

where $(-m)$, $(-n)$ are the roots of the equation $p^2 + 2cp + \omega^2 = 0$

When $\omega^2 > c^2$, the case most applicable to the human body results since it represents a system where the damping is small, but not negligible. The deflections of the mass are periodic, but with the output amplitude less than the zero damping case. In this case, the oscillations would gradually damp to zero. When $\omega^2 > c^2$, the motion is described as sub-critically damped. The solution of the equation of motion in this case is

$$\delta = \frac{\alpha}{\omega^2} \left\{ 1 - \frac{\omega}{\omega_0} e^{-ct} \sin(\omega_0 t + \phi) \right\} \quad \text{E.4}$$

where $\omega_0^2 = \omega^2 - c^2$, and $\tan \phi = \frac{\omega_0}{c}$

Writing

$$\sin(\omega_0 t + \phi) = \sin \omega_0 t \cos \phi + \cos \omega_0 t \sin \phi$$

and using the fact that $\sin \phi = \frac{\omega_0}{\omega}$, and $\cos \phi = \frac{c}{\omega}$, E.4 can be written

$$\delta = \frac{\alpha}{\omega^2} \left\{ 1 - e^{-ct} \left(\frac{c}{\omega_0} \sin \omega_0 t + \cos \omega_0 t \right) \right\} \quad \text{E.5}$$

Differentiating with respect to time gives

$$\begin{aligned} \dot{\delta} = - \left\{ \frac{\alpha c}{\omega^2} e^{-ct} \cos \omega_0 t - \frac{\alpha c^2}{\omega^2 \omega_0} \sin \omega_0 t \right. \\ \left. - \frac{\alpha \omega_0}{\omega^2} e^{-ct} \sin \omega_0 t - \frac{\alpha c}{\omega^2} e^{-ct} \cos \omega_0 t \right\} \end{aligned}$$

so that

$$\dot{\delta} = \frac{\alpha}{\omega^2} e^{-ct} \sin \omega_0 t \left(\frac{c^2}{\omega_0} + \omega_0 \right)$$

and since $c^2 + \omega_0^2 = \omega^2$

$$\dot{\delta} = \frac{\alpha}{\omega_0} e^{-ct} \sin \omega_0 t$$

A further differentiation with respect to time gives the spring acceleration

$$\begin{aligned}\ddot{\delta} &= \frac{\alpha}{\omega_0} (\omega_0 e^{-ct} \cos \omega_0 t - c e^{-ct} \sin \omega_0 t) \\ &= \alpha e^{-ct} \left(\cos \omega_0 t - \frac{c}{\omega_0} \sin \omega_0 t \right)\end{aligned}$$

E.6

Making use of the ϕ relationships, E.6 can be written

$$\ddot{\delta} = -\alpha e^{-ct} \frac{\omega}{\omega_0} \sin(\omega_0 t - \phi)$$

E.7

Since $\ddot{y}_p = \ddot{y}_c - \ddot{\delta}$, the expression for the mass acceleration is

$$\ddot{y}_p = \alpha \left\{ 1 + \frac{\omega}{\omega_0} e^{-ct} \sin(\omega_0 t - \phi) \right\}$$

E.8

An alternative expression for the mass acceleration can be derived from E.6, viz.

$$\ddot{y}_p = \alpha \left\{ 1 - e^{-ct} \left(\cos \omega_0 t - \frac{c}{\omega_0} \sin \omega_0 t \right) \right\}$$

E.9

When the damping is removed, $c = 0$, and $\omega_0 = \omega$, and E.9 readily reduces to the undamped case discussed in Appendix B. (See equation B.10)

$$\ddot{y}_p = \alpha (1 - \cos \omega t)$$

The maximum value attained by \ddot{y}_p for a step input will now be determined. Differentiating E.9 yields

$$\begin{aligned}\frac{d\ddot{y}_p}{dt} &= -\alpha (-\omega_0 e^{-ct} \sin \omega_0 t - c e^{-ct} \cos \omega_0 t \\ &\quad - c e^{-ct} \cos \omega_0 t + \frac{c^2}{\omega_0} e^{-ct} \sin \omega_0 t) \\ &= \alpha e^{-ct} \left\{ 2c \cos \omega_0 t + \frac{(\omega_0^2 - c^2)}{\omega_0} \sin \omega_0 t \right\}\end{aligned}$$

The turning points are obtained by equating this expression to zero, and since e^{-ct} is positive for all values of t ,

$$2c \cos \omega_0 t = -\frac{(\omega_0^2 - c^2)}{\omega_0} \sin \omega_0 t$$

so that

$$\tan \omega_0 t = -\frac{2c\omega_0}{\omega_0^2 - c^2}$$

The expression $\frac{d^2 \ddot{y}_p}{dt^2}$ must now be investigated, and

$$\begin{aligned} \frac{d^2 \ddot{y}_p}{dt^2} &= \alpha \left\{ -2c^2 e^{-ct} \cos \omega_0 t - 2c \omega_0 e^{-ct} \sin \omega_0 t \right. \\ &\quad \left. - \frac{(\omega_0^2 - c^2)}{\omega_0} c e^{-ct} \sin \omega_0 t + (\omega_0^2 - c^2) e^{-ct} \cos \omega_0 t \right\} \\ &= \alpha e^{-ct} \left\{ (\omega_0^2 - 3c^2) \cos \omega_0 t - \frac{c(3\omega_0^2 - c^2)}{\omega_0} \sin \omega_0 t \right\} \end{aligned}$$

Now, if $\tan \omega_0 t = -\frac{2c\omega_0}{\omega_0^2 - c^2}$ then,

$$\sin \omega_0 t = \pm \frac{2c\omega_0}{\omega^2}, \quad \cos \omega_0 t = \mp \frac{\omega_0^2 - c^2}{\omega^2}$$

and the sine is negative when the cosine is positive, and vice versa.

Hence,

$$\frac{d^2 \ddot{y}_p}{dt^2} = \alpha e^{-ct} \left\{ \pm \frac{(\omega_0^2 - 3c^2)(\omega_0^2 - c^2)}{\omega^2} \pm \frac{2c^2(3\omega_0^2 - c^2)}{\omega^2} \right\}$$

\ddot{y}_p is a maximum when this expression is negative, and evaluating the terms inside the brackets gives

$$\pm \left(\frac{\omega_0^4 + c^4 + 2\omega_0 c^2}{\omega^2} \right)$$

The expression within the bracket is always positive, so $\frac{d^2 \ddot{y}_p}{dt^2}$ is negative when the sign outside is negative, and the peak mass acceleration occurs when

$$\sin \omega_0 t = + \frac{2\omega_0 c}{\omega^2} \quad \text{and} \quad \cos \omega_0 t = - \frac{(\omega_0^2 - c^2)}{\omega^2} \quad \text{E.10}$$

Substituting the values of E.10 in E.9 gives an expression for the peak mass acceleration

$$\ddot{y}_p(\max) = \alpha \left[1 - e^{-ct} \left\{ -\frac{(\omega_0^2 - c^2)}{\omega^2} - \frac{2c^2}{\omega^2} \right\} \right]$$

Therefore,

$$\ddot{y}_p(\max) = \alpha (1 + e^{-ct}) \quad \text{E.11}$$

where $t = \frac{\tan^{-1}}{\omega_0} \left(-\frac{2c\omega_0}{\omega_0^2 - c^2} \right)$

Note that if $c = 0$, $t = \infty$, and E.11 reduces to

$$\ddot{y}_p(\max) = 2\alpha$$

as predicted by Equation B.10. Figure E.2 shows how the output of a system is influenced by the choice of damping values

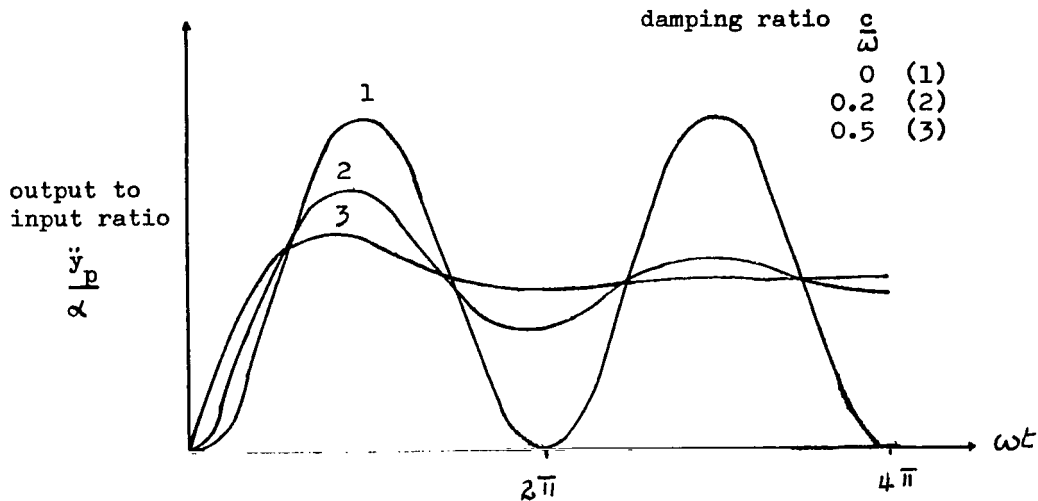


Figure E.2

Impulsive Input

The Dirac impulse function will be used in solving the equation of motion. Such a function is zero everywhere except at $t = 0$, when it is infinite, in such a way that

$$\int_{-\infty}^{+\infty} \Delta(t) dt = 1$$

where $\Delta(t)$ is the Dirac function. The equation of motion is

$$\omega^2 \delta + 2c \dot{\delta} + \ddot{\delta} = \ddot{y}_c = \frac{F_0}{m} \Delta(t) = v \Delta(t) \quad \text{E.12}$$

where F_0 is the impulse (force x time) applied at $t = 0$. The Laplace transform for $\delta = 0$, $\dot{\delta} = 0$ at $t = 0$ is as follows:

$$\omega^2 x + 2cp x + p^2 x = pv$$

where v is the velocity achieved by the system. Hence,

$$x = \frac{pv}{p^2 + 2cp + \omega^2}$$

The inverse Laplace transform gives

$$\delta = \frac{ve^{-ct}}{\omega_0} \sin \omega_0 t \quad \text{E.13}$$

where $\omega_o^2 = \omega^2 - c^2$, and E.13 holds for $\omega^2 > c^2$; i.e., the sub-critically damped case.

The maximum deflection is obtained by investigating the turning points of E.13.

$$\frac{d\delta}{dt} = \frac{v}{\omega_o} (e^{-ct} \omega_o \cos \omega_o t - c e^{-ct} \sin \omega_o t)$$

equating this expression to zero gives

$$\tan \omega_o t = \frac{\omega_o}{c} \quad \text{E.14}$$

This implies two conditions since the angle might be in the positive or negative quadrant. A second differentiation gives

$$\begin{aligned} \frac{d^2\delta}{dt^2} = \frac{v}{\omega_o} & (-e^{-ct} \omega_o^2 \sin \omega_o t - c e^{-ct} \omega_o \cos \omega_o t \\ & - c e^{-ct} \omega_o \cos \omega_o t + c^2 e^{-ct} \sin \omega_o t) \end{aligned} \quad \text{E.15}$$

For a maximum deflection, this expression is negative. From E.14,

$$\sin \omega_o t = \pm \frac{\omega_o}{(\omega_o^2 + c^2)^{1/2}}, \quad \cos \omega_o t = \pm \frac{c}{(\omega_o^2 + c^2)^{1/2}}$$

the sign depending upon the quadrant that contains $\omega_o t$. Substituting these values in E.15 gives

$$\begin{aligned} \frac{d^2\delta}{dt^2} &= -e^{-ct} \frac{v}{\omega_o} \left\{ (\omega_o^2 - c^2) \sin \omega_o t + 2 \omega_o c \cos \omega_o t \right\} \\ &= -e^{-ct} \frac{v}{\omega_o} \left\{ \pm \frac{(\omega_o^2 - c^2)}{(\omega_o^2 + c^2)^{1/2}} \pm \frac{2 c^2 \omega_o}{(\omega_o^2 + c^2)^{1/2}} \right\} \end{aligned}$$

which leads to

$$\begin{aligned} \frac{d^2\delta}{dt^2} &= -e^{-ct} v (\omega_o^2 + c^2)^{1/2} \quad \text{for } \sin \omega_o t, \cos \omega_o t +ve \\ &= -e^{-ct} v (\omega_o^2 + c^2)^{1/2} \quad \text{for } \sin \omega_o t, \cos \omega_o t -ve \end{aligned}$$

Since e^{-ct} is always positive, $\frac{d^2\delta}{dt^2}$ is negative when the angles are in the positive quadrant; i.e., a maximum occurs under these conditions.

From E.14, the maximum occurs when

$$t = \frac{1}{\omega_o} \tan^{-1} \frac{\omega_o}{c} \quad \text{E.14(a)}$$

Now, since $\ddot{y}_c = 0$, and $\ddot{y}_p = \ddot{y}_c - \ddot{\delta}$, $\ddot{y} = -\ddot{\delta}$, so that the mass acceleration for maximum deflection is

$$\ddot{y}_p = e^{-ct} v (\omega_o^2 + c^2)^{1/2}$$

but $\omega_o^2 = \omega^2 - c^2$, so

$$\ddot{y}_p (\max \delta) = v \omega e^{-\frac{c}{\omega_o} \tan^{-1}(\frac{\omega_o}{c})}$$

E.16

and the mass acceleration at any time is given by

$$\ddot{y}_p = e^{-ct} \frac{v}{\omega_o} \{ (\omega_o^2 - c^2) \sin \omega_o t + 2 \omega_o c \cos \omega_o t \}$$

Now the maximum mass acceleration does not occur when the deflection is a maximum (since damping is present). To investigate this condition, Equation E.13 is used

$$\delta = \frac{v e^{-ct}}{\omega_o} \sin \omega_o t$$

and

$$\dot{\delta} = \frac{v}{\omega_o} e^{-ct} (\omega_o \cos \omega_o t - c \sin \omega_o t)$$

which can be written in terms of a phase angle ϕ as

$$\dot{\delta} = \frac{v}{\omega_o} e^{-ct} \omega \{ \sin(\omega_o t + \phi) \}$$

where $\sin \phi = \frac{\omega_o}{(\omega_o^2 + c^2)^{1/2}}$, $\cos \phi = \frac{-c}{(\omega_o^2 + c^2)^{1/2}}$ and $\tan \phi = -\frac{\omega_o}{c}$

(This can be proved by expansion of the $\sin(\omega_o t + \phi)$ term, using the sine and cosine values given above).

Again, by similar reasoning

$$\begin{aligned} \ddot{\delta} &= \frac{v}{\omega_o} e^{-ct} \omega \{ \omega_o \cos(\omega_o t + \phi) - c \sin(\omega_o t + \phi) \} \\ &= \frac{v}{\omega_o} e^{-ct} \omega^2 \{ \sin(\omega_o t + 2\phi) \} \end{aligned}$$

Now $\ddot{y}_p = -\ddot{\delta}$ and therefore

$$\ddot{y}_p = -\frac{v}{\omega_o} e^{-ct} \omega^2 \sin(\omega_o t + 2\phi)$$

E.17

The turning points of E.17 are given by $\frac{d\ddot{y}_p}{dt} = 0$

i.e.,

$$\frac{d\ddot{y}_p}{dt} = -\frac{v}{\omega_0} e^{-ct} \omega^2 \{ \omega_0 \cos(\omega_0 t + 2\phi) - c \sin(\omega_0 t + 2\phi) \} = 0$$

i.e., when

$$\tan(\omega_0 t + 2\phi) = \frac{\omega_0}{c}$$

E.18

Evaluating $\frac{d^2\ddot{y}_p}{dt^2}$ gives

$$\frac{d^2\ddot{y}_p}{dt^2} = \frac{v}{\omega_0} e^{-ct} \omega^2 \{ (\omega_0^2 - c^2) \sin(\omega_0 t + 2\phi) + 2\omega_0 c \cos(\omega_0 t + 2\phi) \}$$

From E.18

$$\sin(\omega_0 t + 2\phi) = \pm \frac{\omega_0}{(\omega_0^2 + c^2)^{1/2}}, \quad \cos(\omega_0 t + 2\phi) = \frac{c}{(\omega_0^2 + c^2)^{1/2}}$$

The sign depending on the quadrant as before. The above expression is negative when the sine and cosine are negative. (This can be shown by evaluating $d^2\ddot{y}_p/dt^2$ as was done in deriving E.15).

Hence, the peak mass acceleration is given by

$$\ddot{y}_p(\max) = v \omega e^{-ct}$$

E.19

$$\text{where } t = \frac{1}{\omega_0} \left\{ \tan^{-1} \left(\frac{\omega_0}{c} \right) - 2\phi \right\}$$

When $c = 0$, E.19 reduces to

$$\ddot{y}_p(\max) = v \omega$$

which agrees with the non-damping case of Equation D.21.

It can be seen from E.18 that as the damping coefficient is increased, the time to reach maximum mass acceleration is reduced, and will occur at $t = 0$, for damping coefficients greater than a critical value C_c .

When $t = 0$

$$\tan 2\phi = \frac{\omega_0}{c}$$

and evaluating $\tan 2\phi$ in terms of $\tan \phi$ ($\tan \phi = -\frac{\omega_0}{c}$)

$$\frac{\omega}{C_c} = 2 \quad \text{or} \quad C_c = \frac{\omega}{2}$$

and for $\frac{\omega}{c} > 2$ the maximum occurs after $t = 0$.

It is of interest to show how the damping term influences the duration time for which the impulse theory is applicable. From E.19

$$\ddot{y}_p(\max) = \ddot{y}_c t_1 \omega e^{-c t_1}$$

where t_1 is the critical duration. The mass acceleration for a system subjected to a long-duration input is given by E.11 as

$$\ddot{y}_p(\max) = \ddot{y}_c (1 + e^{-c t})$$

The critical duration time occurs when these two expressions are equal as suggested in Appendix D. Hence,

$$t_1 e^{-c t_1} = \frac{1 + e^{-c t}}{\omega}$$

Expanding the exponentials gives

$$t_1 (1 - c t_1 + \frac{c^2 t_1^2}{2} - \dots) = \frac{1}{\omega} + \frac{1}{\omega} - \frac{c t}{\omega} + \frac{c^2 t^2}{2 \omega} - \dots$$

If terms in C are ignored the undamped condition $t_1 = \frac{2}{\omega}$ is obtained, and neglecting C^2 terms gives

$$t_1 - c t_1^2 = \frac{2 - c t}{\omega}$$

solving this equation gives

$$t_1 = \frac{1 \pm (1 - \frac{4c(2 - ct)}{\omega})^{1/2}}{2c}$$

Now from E.10

$$\omega_0 t = \tan^{-1} \left(-\frac{2\omega_0 c}{\omega_0^2 - c^2} \right)$$

and if the damping is small,

$$\omega_0 t = \tan^{-1} \left(-\frac{2c}{\omega_0} \right)$$

so that

$$t = \frac{\pi}{\omega_0} - \frac{2c}{\omega_0^2} \quad (\text{for small angles where } \tan \theta = \theta)$$

Using this value in the expression for t_1 , the following is obtained

$$t_1 = \frac{1 \pm \left(1 - \frac{4c \left\{2 - c \left(\frac{\pi}{\omega_0} - \frac{2c}{\omega_0^2}\right)\right\}}{\omega}\right)^{1/2}}{2c}$$

Now, $\omega_0^2 = \omega^2 - c^2 = \omega^2$ for small damping effects, and a solution for t_1 is obtained by expanding the expression under the root sign

$$\left(1 - \frac{4c \left\{2 - c \left(\frac{\pi}{\omega} - \frac{2c}{\omega^2}\right)\right\}}{\omega}\right)^{1/2} = 1 - \frac{2c \left\{2 - c \left(\frac{\pi}{\omega} - \frac{2c}{\omega^2}\right)\right\}}{\omega} + \dots$$

Since the negative part of the root is relevant in this case, (the smallest value of t_1 is required)

$$\begin{aligned} t_1 &= \frac{2c \left\{2 - c \left(\frac{\pi}{\omega} - \frac{2c}{\omega^2}\right)\right\}}{2c\omega} \\ &= \frac{2}{\omega} - \frac{c}{\omega} \left(\frac{\pi}{\omega} - \frac{2c}{\omega^2}\right) \end{aligned}$$

and again neglecting c^2 terms,

$$t_1 = \frac{2}{\omega} - \frac{c\pi}{\omega^2}$$

E.20

Sinusoidal Input Acceleration

In this section an acceleration of the form

$$\ddot{y}_c = \ddot{y}_{c0} \sin \Omega t$$

is considered, which represents a sine wave of amplitude \ddot{y}_{c0} and frequency Ω .

The equation of motion for a damped, single degree of freedom system is, from Equation E.3

$$\ddot{\delta} + 2c\dot{\delta} + \omega^2\delta = \ddot{y}_{c0} \sin \Omega t$$

E.21

The Laplace transform of $\sin \Omega t$ is

$$\frac{\Omega}{p^2 + \Omega^2}$$

E.12

and so, for the initial conditions $\delta = \dot{\delta} = 0$ the Laplace transform of Equation E.21 is

$$(p^2 + 2cp + \omega^2)x = \ddot{y}_{co} \frac{\Omega p}{p^2 + \Omega^2} \quad \text{E.22}$$

Therefore

$$x = \frac{\ddot{y}_{co} \Omega p}{(p^2 + 2cp + \omega^2)(p^2 + \Omega^2)} \quad \text{E.23}$$

To perform the inverse transformation, the right side of Equation E.23 must be expressed in partial fractions.

Let

$$x = \ddot{y}_{co} \Omega \left\{ \frac{\alpha_1 p + \beta_1}{p^2 + 2cp + \omega^2} + \frac{\alpha_2 p + \beta_2}{p^2 + \Omega^2} \right\} \quad \text{E.23(a)}$$

Combining the terms in this Equation gives

$$x = \ddot{y}_{co} \Omega \left\{ \frac{\alpha_1 p^3 + \beta_1 p^2 + \alpha_1 \Omega^2 p + \beta_1 \Omega^2 + \alpha_2 p^3 + (2c\alpha_2 + \beta_2)p^2 + (\omega^2\alpha_2 + 2c\beta_2)p + \beta_2\omega^2}{(p^2 + 2cp + \omega^2)(p^2 + \Omega^2)} \right\} \quad \text{E.24}$$

and equating coefficients of powers of p in E.23 and E.24 gives the following set of equations for α and β

$$\begin{aligned} \alpha_1 + \alpha_2 &= 0 & (a) \\ \beta_1 + 2c\alpha_2 + \beta_2 &= 0 & (b) \\ \alpha_1 \Omega^2 + \omega^2\alpha_2 + 2c\beta_2 &= 1 & (c) \\ \beta_1 \Omega^2 + \beta_2 \omega^2 &= 0 & (d) \end{aligned} \quad \text{E.25}$$

Substituting for α_1 from E.25 (a), E.25 (c) gives

$$(\omega^2 - \Omega^2)\alpha_2 + 2c\beta_2 = 1$$

and for β_1 of E.25 (d) into E.25 (b) leads to

$$2c\alpha_2 + \left(1 - \frac{\omega^2}{\Omega^2}\right)\beta_2 = 0$$

These two equations are rewritten

$$\begin{aligned} (\omega^2 - \Omega^2)\alpha_2 + 2c\beta_2 &= 1 \\ 2c\Omega^2\alpha_2 - (\omega^2 - \Omega^2)\beta_2 &= 0 \end{aligned}$$

Crout's formula is now used to solve this pair of simultaneous equations when the following values of α_2 and β_2 are obtained

$$\alpha_2 = \frac{-(\omega^2 - \Omega^2)}{-(\omega^2 - \Omega^2)^2 - 4c^2\Omega^2} = \frac{\omega^2 - \Omega^2}{(\omega^2 - \Omega^2)^2 + 4c^2\Omega^2} \quad \text{E.26(a)}$$

$$\beta_2 = -\frac{2c\Omega^2}{-(\omega^2 - \Omega^2)^2 - 4c^2\Omega^2} = \frac{2c\Omega^2}{(\omega^2 - \Omega^2)^2 + 4c^2\Omega^2} \quad \text{E.26(b)}$$

Values for α_1 and β_1 then follow from Equations E.25(a) and (d)

$$\alpha_1 = \frac{\Omega^2 - \omega^2}{(\omega^2 - \Omega^2)^2 + 4c^2\Omega^2} \quad \text{E.27(a)}$$

$$\beta_1 = -\frac{2c\omega^2}{(\omega^2 - \Omega^2)^2 + 4c^2\Omega^2} \quad \text{E.27(b)}$$

Substituting for the α 's and β 's in E.23(a) gives

$$x = \frac{\ddot{y}_{co}\Omega}{(\omega^2 - \Omega^2)^2 + 4c^2\Omega^2} \left\{ \frac{(\Omega^2 - \omega^2)p - 2c\omega^2}{p^2 + 2cp + \omega^2} + \frac{(\omega^2 - \Omega^2)p + 2c\Omega^2}{p^2 + \Omega^2} \right\}$$

The inverse Laplace transforms (Nos. 50, 51, 11 and 40 of Ref. E.1) are used to give

$$\begin{aligned} \delta &= \frac{\ddot{y}_{co}\Omega}{(\omega^2 - \Omega^2)^2 + 4c^2\Omega^2} \left[\frac{(\Omega^2 - \omega^2)e^{-ct}}{\omega_0} \sin \omega_0 t - 2c \left\{ 1 - \frac{\omega}{\omega_0} e^{-ct} \sin(\omega_0 t + \phi) \right\} \right. \\ &\quad \left. + \frac{\omega^2 - \Omega^2}{\Omega} \sin \Omega t + 2c \{ 1 - \cos \Omega t \} \right] \quad \text{E.28} \\ &= \frac{\ddot{y}_{co}\Omega}{(\omega^2 - \Omega^2)^2 + 4c^2\Omega^2} \left[e^{-ct} \left\{ \frac{(\Omega^2 - \omega^2)}{\omega_0} \sin \omega_0 t + \frac{2c\omega}{\omega_0} \sin(\omega_0 t + \phi) \right\} \right. \\ &\quad \left. + \frac{\omega^2 - \Omega^2}{\Omega} \sin \Omega t - 2c \cos \Omega t \right] \end{aligned}$$

where $\phi = \tan^{-1} \frac{\omega_0}{c}$ and $\omega_0 = (\omega^2 - c^2)^{1/2}$

The solution for δ has two distinct parts, one part

$$\left[\omega_0 \left\{ \frac{\ddot{y}_{co}\Omega}{(\omega^2 - \Omega^2)^2 + 4c^2\Omega^2} \right\} e^{-ct} \left\{ (\Omega^2 - \omega^2) \sin \omega_0 t + 2c\omega \sin(\omega_0 t + \phi) \right\} \right]$$

with a frequency (ω_0) dependent upon the parameters of the system, the second part

$$\frac{\ddot{y}_{co}\Omega}{(\omega^2 - \Omega^2)^2 + 4c^2\Omega^2} \left\{ \frac{(\omega^2 - \Omega^2)}{\Omega} \sin \Omega t - 2c \cos \Omega t \right\}$$

with the frequency (Ω) of the forcing function. The first and

second parts of the solution are known as the Transient Solution and the Steady State Solution respectively. The transient solution has a factor e^{-ct} , so that as t increases so the amplitude of this oscillation decreases and this motion is eventually damped out, leaving only the steady state solution.

Although the absolute maximum usually occurs while the transient solution is still significant, the steady state solution is of great importance for long duration inputs of an oscillatory nature, and this case only will be investigated.

The phenomenon of resonance is well known and will be demonstrated with the use of this model.

The steady state solution is

$$S = \frac{\ddot{y}_{co}}{(\omega^2 - \Omega^2)^2 + 4c^2\Omega^2} \{ (\omega^2 - \Omega^2) \sin \Omega t - 2c\Omega \cos \Omega t \} \quad E.29$$

which can be written

$$S = \frac{\ddot{y}_{co}}{\{(\omega^2 - \Omega^2)^2 + 4c^2\Omega^2\}^{1/2}} \sin(\Omega t - \psi)$$

$$\text{where } \psi = \tan^{-1} \frac{2c\Omega}{\omega^2 - \Omega^2}$$

This solution is a sine wave, out of phase with the input acceleration and of amplitude

$$\frac{\ddot{y}_{co}}{\{(\omega^2 - \Omega^2)^2 + 4c^2\Omega^2\}^{1/2}}$$

The ratio A of output to input amplitudes is the Amplification factor and can be written

$$A = \frac{1}{\{(\omega^2 - \Omega^2)^2 + 4c^2\Omega^2\}^{1/2}}$$

which must be maximized with respect to Ω to obtain the largest ratio of output to input accelerations.

A maximum or minimum occurs when

$$\frac{d}{d\omega} \frac{1}{\{(\omega^2 - \Omega^2)^2 + 4c^2\Omega^2\}^{1/2}} = 0$$

i.e. $-\frac{1}{2} \{(\omega^2 - \Omega^2)^2 + 4c^2\Omega^2\}^{-3/2} \{-4\Omega(\omega^2 - \Omega^2) + 8c^2\Omega\} = 0$

so that either

$$(\omega^2 - \Omega^2)^2 + 4c^2\Omega^2 = 0$$

or

$$-(\omega^2 - \Omega^2)^2 + 2c^2 = 0$$

or

$$\Omega = 0$$

The first expression is the sum of two squares and so for real ω_0 , ω and C cannot be zero except for the trivial case (no motion) $\omega_0 = \omega = C = 0$. The third expression is a statement that the forcing function is zero at all finite time, again trivial. The second expression gives

$$\Omega^2 = \omega^2 - 2c^2 \quad \text{E.30}$$

for which the following value of A is obtained

$$A = \frac{1}{\{(2c^2)^2 + 4c^2(\omega^2 - 2c^2)\}^{1/2}} = \frac{1}{\{4c^4 + 4c^2\omega^2 - 8c^4\}^{1/2}}$$

$$= \frac{1}{2c(\omega^2 - c^2)^{1/2}} = \frac{1}{2c\omega_0} \quad \text{E.31}$$

Now $\{(\omega^2 - \Omega^2)^2 + 4c^2\Omega^2\}^{-1/2}$ has a maximum when $(\omega^2 - \Omega^2)^2 + 4c^2\Omega^2$ has a minimum since the latter expression is positive for all real values of the variables, so the latter expression need only be investigated.

$$\frac{d}{d\Omega} \{(\omega^2 - \Omega^2)^2 + 4c^2\Omega^2\} = -4\Omega(\omega^2 - \Omega^2) + 8c^2\Omega$$

$$\frac{d^2}{d\Omega^2} \{(\omega^2 - \Omega^2)^2 + 4c^2\Omega^2\} = -4\omega^2 + 12\Omega^2 + 8c^2$$

The condition for a maximum or minimum from E.30 is $\Omega^2 = \omega^2 - 2c^2$ so that using this condition in the above expression gives

$$\begin{aligned} -4\omega^2 + 12(\omega^2 - 2c^2) + 8c^2 &= 8\omega^2 - 16c^2 \\ &= 8(\omega^2 - 2c^2) \end{aligned}$$

So if $\omega^2 - 2c^2$ is positive, a maximum occurs in the expression

$$\{(\omega^2 - \Omega^2)^2 + 4c^2\Omega^2\}^{-1/2}$$

and the amplification factor has a maximum value (for the steady state case) when $\Omega^2 = \omega^2 - 2c^2$ and has the value

$$A(\max) = \frac{1}{2c\omega_0}$$

where $\omega_0^2 = \omega^2 - c^2$

It can be seen that the zero damping case implies infinite magnification, but when any damping is present finite values result that are smaller for high frequency systems and high damping coefficients.

REFERENCES

<u>No.</u>	<u>Name</u>	<u>Title, etc.</u>
E.1	Pipes, L. A.	"Applied Mathematics for Engineers and Physicists," New York, McGraw-Hill Book Co., Inc. 1946.

APPENDIX F

EJECTION OF ESCAPE CAPSULE OR SEAT

SYMBOLS

A	amplification factor $\frac{\ddot{y}_p \max}{\ddot{y}_c \max}$
F	applied force
f	$= \frac{F}{m_c}$ for steady applied force
k	spring stiffness
m_p	mass of occupant
m_c	mass of capsule
M	$= (m_c + m_p)$
q	$= \frac{d\delta}{dt}$
t	time
v	velocity
v_R	velocity from rigid body theory
v_c	velocity from separate mass theory
\ddot{y}_c	acceleration of mass m_c relative to fixed datum
\ddot{y}_p	acceleration of mass m_p relative to fixed datum
\ddot{y}_s	initial acceleration at $t = 0$
$\delta, \dot{\delta}, \ddot{\delta}$	deflection, velocity (rate of change of deflection), acceleration (rate of change of velocity) of spring
δ_s	initial (static) spring deflection
ω	spring frequency ($n = 1$)
ζ_n	$= \omega_n^2$

During the ejection of an escape capsule or seat, the initial phase consists of an acceleration up the ejection rails, caused by a rocket supplying a force F . Large positive spinal accelerations are imposed on the occupant, and it is important to determine, at the design stage, whether the accelerations are physiologically tolerable.

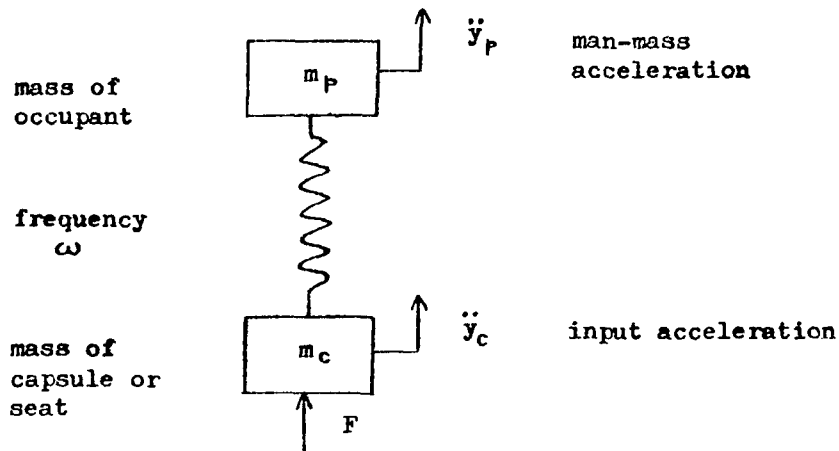


Figure F.1

Using the simple model of Figure F.1, where m_p and m_c are the occupant and capsule (or seat) mass respectively, the equations of motion can be obtained by applying Newton's second law. Considering the occupant, the accelerating force is that developed in the spring, hence

$$m_p \ddot{y}_p = k_n \delta^n$$

where a **non-linear** spring has been assumed.

Remembering (see Appendices B and C) that

$$\ddot{y}_p - \ddot{y}_c = -\ddot{\delta}$$

the above equation becomes

$$\ddot{y}_c = \frac{k_n}{m_p} \delta^n + \ddot{\delta}$$

and adopting the notation of Appendix C, that $\omega_n^2 = \frac{k_n}{m_p} = \zeta_n$ this equation can be written

$$\ddot{y}_c = \zeta_n \delta + \ddot{\delta} \quad \text{F.1}$$

Considering the mass m_c , the resultant force acting is the difference between the applied force and the "reaction" developed in the spring. Hence,

$$m_c \ddot{y}_c = F - k_n \delta^n$$

so that

$$\ddot{y}_c = \frac{F}{m_c} - \frac{k_n \delta^n}{m_c}$$

and since

$$\frac{k_n}{m_c} = \frac{k_n}{m_c} \frac{m_P}{m_P} = \zeta_n \frac{m_P}{m_c}$$

it follows that

$$y_c = \frac{F}{m_c} - \zeta_n \frac{m_P}{m_c} \delta^n \quad \text{F.2}$$

Equating F.1 and F.2 gives the equation of motion

$$\ddot{\delta} + \zeta_n \delta^n (1 + \frac{m_P}{m_c}) = \frac{F}{m_c} \quad \text{F.3}$$

Constant Force Application

As in Appendix C the substitution $q = \dot{\delta}$ is made; therefore, $\ddot{\delta} = q \frac{dq}{d\delta}$, and F.3 can be written

$$q \frac{dq}{d\delta} + \zeta_n \delta^n (1+M) = \frac{F}{m_c} = f \text{ (say)}$$

where $\frac{m_P}{m_c}$ has been replaced by M for convenience. Transposing and

integrating yields

$$\int_0^0 q dq = \int_{\delta_s}^{\delta_{max}} \{ f - \zeta_n \delta^n (1+M) \} d\delta$$

The integration limits have been taken from δ_s , the static deflection, to δ_{max} , the maximum deflection, which corresponds to a range of q from zero to zero, as explained in Appendix C. The static deflection could be due to some initial g field at time $t = 0$ which can be included in the quantity f. The left hand side is zero for the limits shown, so

$$\int_{\delta_s}^{\delta_{max}} \{ f - \zeta_n \delta^n (1+M) \} d\delta = 0$$

Integration gives

$$f(\delta_{\max} - \delta_s) - \zeta_n \frac{(1+M)}{n+1} \left\{ \delta_{\max}^{n+1} - \delta_s^{n+1} \right\} = 0 \quad \text{F.4}$$

Since the initial acceleration can be written

$$\ddot{y}_s = \zeta_n \delta_s^n$$

F.4 becomes

$$f \delta_{\max} - \zeta_n \frac{(1+M)}{1+n} \delta_{\max}^{n+1} = f \left(\frac{\ddot{y}_s}{\zeta_n} \right)^{\frac{1}{n}} - \frac{1+M}{1+n} \left(\ddot{y}_s \right)^{\frac{n+1}{n}} \frac{1}{\zeta_n^{1/n}} \quad \text{F.5}$$

Again, the peak mass acceleration $\ddot{y}_p(\max)$ is given by

$$\ddot{y}_p(\max) = \zeta_n \delta_{\max}^n$$

so that

$$\delta_{\max} = \left(\frac{\ddot{y}_p(\max)}{\zeta_n} \right)^{\frac{1}{n}}$$

and F.5 becomes

$$f \left[\frac{\ddot{y}_p(\max)}{\zeta_n} \right]^{\frac{1}{n}} - \frac{1+M}{1+n} \left(\ddot{y}_s \right)^{\frac{n+1}{n}} \cdot \frac{1}{\zeta_n^{1/n}} \quad \text{F.6}$$

If $\delta_s = 0$, equation F.6 reduces to

$$f = \frac{F}{m_c} = \frac{1 + \frac{m_p}{m_c}}{1+n} \ddot{y}_p(\max)$$

or

$$\ddot{y}_p(\max) = \frac{F}{m_c} \left(\frac{1+n}{1 + \frac{m_p}{m_c}} \right) = \frac{F(n+1)}{(m_c + m_p)} \quad \text{F.7}$$

If $n = 1$, (linear spring), the peak (max) mass acceleration is given by

$$\ddot{y}_p(\max) = \frac{2F}{m_c + m_p} \quad \text{F.8}$$

Note that $\frac{F}{m_p + m_c}$ is the acceleration obtained when regarding the two masses as a "rigid body," and the result is identical to that given in Equation B.16. The conclusion is, that for a long duration step input, the acceleration history obtained by taking the occupant and capsule as a rigid mass, can be used to assess tolerability.

It is possible to define an amplification factor given by

$$A = \frac{\text{peak acceleration on occupant}}{\text{peak acceleration on capsule}}$$

The peak acceleration of the equivalent occupant's mass is given by F.8, and the peak capsule acceleration is attained when the force developed in the spring, in opposition to the applied force, is zero. Hence

$$\ddot{y}_c(\max) = \frac{F}{m_c}$$

and

$$A = \frac{2F}{m_c + m_p} \frac{m_c}{F} = \frac{2m_c}{m_c + m_p} = 2\left(1 - \frac{m_p}{m_p + m_c}\right)$$

Thus, the lighter the capsule in relation to its occupant, the lower is the relative acceleration amplification. However, the peak occupant acceleration is always twice the value which would be calculated if the capsule and occupant were regarded as a combined rigid mass.

Impulsive Input

In the present context, an impulsive input would be a force F which lasts only for a short period, Δt , so that the spring does not deflect significantly (the force developed is small). Newton's law gives

$$F = m_c \ddot{y}_c$$

giving a velocity change

$$\Delta v_c = \Delta t \ddot{y}_c = \Delta t \frac{F}{m_c}$$

which is greater than that calculated from rigid body theory. After the spike input has been removed, the motion of the spring continues and the velocity change given above constitutes an initial condition for the subsequent motion. The equation of motion is now

$$\ddot{\delta} + \zeta_n \delta^n (1 + M) = 0$$

F.9

F.9 has to be integrated between certain limits which must be ascertained. The velocity change due to the spike input gives a velocity $v_c = \dot{\delta}$ to the spring at $t = 0$, when it can be assumed the deflection δ is zero, and when the maximum deflection δ_{max} is reached, the velocity is again zero. Thus, substituting $q = \dot{\delta}$, as before, $\ddot{\delta} = q \frac{dq}{d\delta}$ and

$$\int_{q=v_c}^{q=0} q dq = - \int_{\delta=0}^{\delta_{max}} \zeta_n \delta^{n(1+M)} d\delta$$

which gives

$$\left[\frac{q^2}{2} \right]_{v_c}^0 = \left[- \zeta_n \left(\frac{1+M}{1+n} \right) \delta^{n+1} \right]_0^{\delta_{max}}$$

i.e.

$$\frac{v_c^2}{2} = - \zeta_n \left(\frac{1+M}{1+n} \right) \delta_{max}^{n+1}$$

giving

$$\delta_{max} = \left\{ \frac{n+1}{2} \frac{v_c^2}{\zeta_n(1+M)} \right\}^{\frac{1}{n+1}}$$

and since $\ddot{y}_p(max) = \zeta_n \delta_{max}^n$

$$\ddot{y}_p(max) = \left\{ \left(\frac{n+1}{M+1} \right) \frac{v_c^2}{2} \zeta_n^{\frac{1}{n}} \right\}^{\frac{n}{n+1}}$$

F.10

Now, using rigid body theory, the initial velocity change is given by

$$\Delta v_R = \frac{F \Delta t}{m_c + m_p}$$

whereas

$$\Delta v_c = \frac{F \Delta t}{m_c}$$

Therefore,

$$\Delta v_c = \frac{\Delta v_R (m_c + m_p)}{m_c} = \Delta v_R (1+M)$$

so that F.10 becomes

$$\ddot{y}_p(max) = \left(\frac{n+1}{2} \zeta_n^{\frac{1}{n}} v_R^2 \right)^{\frac{n}{n+1}}$$

F.11

If F.11 is compared with D.16 of Appendix D, it can be seen that the two equations are identical (initial deflections have been ignored in deriving F.11, but could easily have been included). Hence, it can be concluded that, employing the spring-mass analogy of the human body, a man-capsule system subjected to an impulsive input can be analyzed by the rigid body theory.

The results of the analyses described in this Appendix might appear somewhat negative, but it has been possible to demonstrate mathematically that the dynamic model of a two mass system can be treated as a rigid body in calculating the peak acceleration output of the equivalent man mass.

APPENDIX G

THE EFFECT OF A LINEAR CUSHION ON TOLERANCE LIMITS - EQUIVALENT SYSTEMS

SYMBOLS

c	damping coefficient
E_c	energy absorption capacity of cushion
F	spring force
k	spring stiffness
K	damping constant
m	mass
t	time
Δt	duration of input acceleration
Δt_c	duration limit for impulsive theory
v	velocity
\ddot{y}_p	mass acceleration relative to fixed datum
\ddot{y}_c	input acceleration
α	steady input acceleration
$\delta, \dot{\delta}, \ddot{\delta}$	deflection, velocity (rate of change of deflection), acceleration (rate of change of velocity) of spring
ω	spring frequency
Ω	$= \frac{k_1}{k_2} = \frac{\omega_1^2}{\omega_2^2}$

SUFFICIES

1	man
2	cushion
B	conditions at bottoming of cushion
S	initial (static) conditions

When a cushion or other form of elastic restraint is placed in series with the human body, the system can be represented as in Figure G.1. The presence of the dampers complicates the problem considerably, since the proportion of the resultant force transmitted by damper or spring depends on the mechanical characteristics of each.

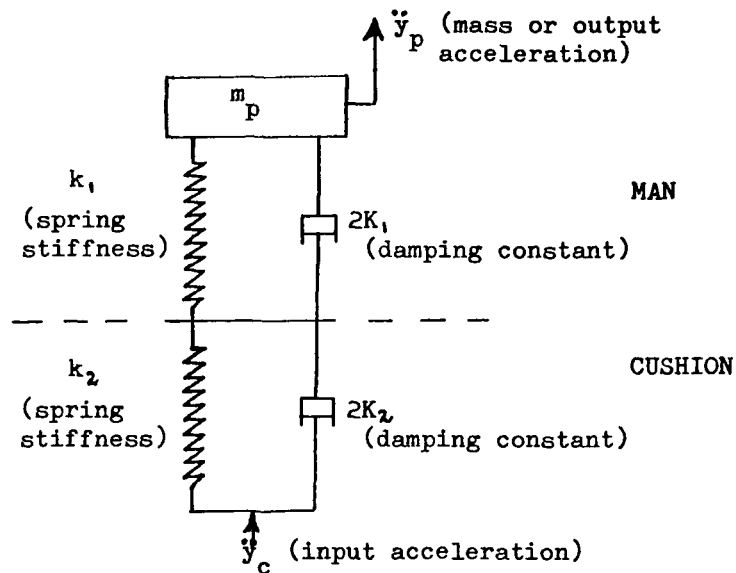


Figure G.1

If either the dampers or the springs are removed, each system can be reduced to a simple equivalent spring or damper. This simplifies the mathematics and, although not a complete representation of what actually happens, will give some insight into the influence of the various components on the occupant.

Equivalent Spring System

In the static case, a force F would produce deflections δ_1 and δ_2 in the man and cushion springs, respectively, so that

G.1

$$F = k_1 \delta_1 = k_2 \delta_2$$

If the two springs are replaced by a single equivalent spring, the deflection would be δ and the force-deflection relationship is

$$F = k \delta = k (\delta_1 + \delta_2) \quad \text{G.2}$$

Hence, the equivalent stiffness is given by

$$k = \frac{F}{\delta_1 + \delta_2} = \frac{F}{\frac{F}{k_1} + \frac{F}{k_2}} = \frac{k_1 k_2}{k_1 + k_2} \quad \text{G.3}$$

The equivalent natural frequency $\omega = \sqrt{\frac{k}{m_p}}$ follows from G.3, and can be represented by

$$\omega^2 = \frac{\omega_1^2 \omega_2^2}{\omega_1^2 + \omega_2^2} = \frac{\omega_1^2}{1 + \Omega} \quad \text{G.4}$$

where $\Omega = \frac{\omega_1^2}{\omega_2^2} = \frac{k_1}{k_2}$

Equivalent Damper System

For two dampers alone in series, it can be argued similarly that

$$F = 2K_1 V_1 + 2K_2 V_2$$

and

$$F = 2KV = 2K(V_1 + V_2)$$

Hence, the equivalent damping constant is given by

$$K = \frac{F}{2(V_1 + V_2)} = \frac{K_1 K_2}{K_1 + K_2} \quad \text{G.5}$$

and the equivalent damping coefficient $C = \frac{K}{m_p}$ becomes

$$C = \frac{C_1 C_2}{C_1 + C_2} \quad \text{G.6}$$

Model with Zero Damping

If the cushion-man system is now represented by a single equivalent spring of frequency ω , the solutions already deduced apply. Thus, for an impulsive input, the peak mass acceleration is given by D.16, and for a linear system ($n = 1$), this becomes

$$\ddot{y}_p(\max) = \left(\frac{\omega_1^2 V}{1 + \Omega} \right)^{1/2} \quad \text{G.7}$$

The duration Δt_c which limits the impulse theory is from D.22

$$\Delta t_c = \frac{2}{\omega} = \frac{2}{\omega_1} (1 + \Omega)^{1/2}$$

Now, since $V = \ddot{y}_c \Delta t$, employing G.7, the following ratio can be formed

$$\frac{\ddot{y}_p(\max)}{\ddot{y}_c} = \frac{\omega_1 \Delta t}{(1 + \Omega)^{1/2}} \quad \text{for } \Delta t < \Delta t_c \quad \text{G.8}$$

For times greater than Δt_c , the ratio given in G.8 becomes 2, since for an undamped system the overshoot of the output is 100%. Hence,

$$\frac{\ddot{y}_p(\max)}{\ddot{y}_c} = 2 \quad \text{for } \Delta t \geq \Delta t_c$$

It follows that although a cushion does not reduce the severity of a long period acceleration, it can be beneficial in the impulse region. This conclusion is based on the fact that the cushion does not bottom. The influence of the cushion can be seen from the relationship

$$\frac{\ddot{y}_{p \max} \text{ (with cushion)}}{\ddot{y}_{p \max} \text{ (no cushion)}} = \left(\frac{\omega_1 V^2}{1 + \Omega} \right)^{1/2} \frac{1}{(\omega_1^2 V^2)^{1/2}} = \frac{1}{(1 + \Omega)^{1/2}} \quad \text{G.9}$$

This ratio is plotted in Figure G.2, which illustrates the fact that for a non-bottoming cushion, the attenuation of the input is greater for large values of $\Omega = k_1/k_2$, i.e., for low cushion frequencies.

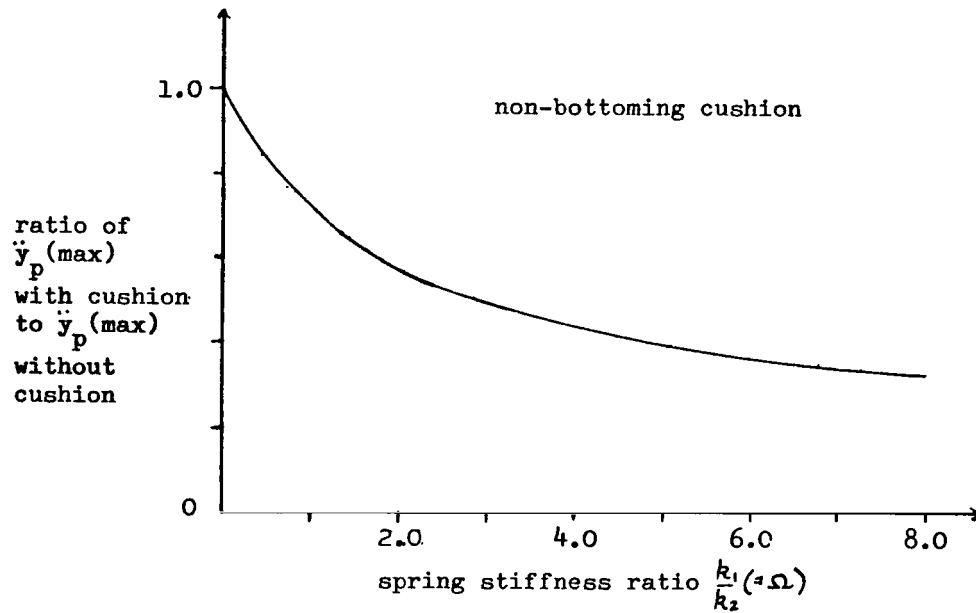


Figure G.2

Cushion Bottoming

Bottoming of the cushion occurs when the deflection of the cushion spring has a value δ_{2B} (say). At this instant, the force in the spring is

$$F_B = k_2 \delta_{2B} = k_1 \delta_{1B}$$

so that

$$\delta_{1B} = \delta_{2B} \frac{k_2}{k_1}$$

Just before bottoming, the kinetic energy of the system $\frac{1}{2} m_p \Delta v^2$ where Δv is the velocity change of the application point due to the impulse, is distributed as potential energy and kinetic energy of the various parts of the system. When bottoming occurs, the lower spring retains its potential energy only. Since an impulsive input is under consideration, the mass does not move its position initially, although the spring (k_1) may have velocity $\dot{\delta}_1$, due to compression. As shown previously, the maximum deflection of k_1 will be attained when the spring velocity $\dot{\delta}_1$ is zero, so that the surplus energy is given by

$$\frac{1}{2} m_p \Delta v^2 - \frac{1}{2} k_1 \delta_{2B}^2$$

i.e., total kinetic energy of the system minus the potential energy retained by spring k_1 will appear as potential energy stored in spring k_1 . Hence,

$$\frac{1}{2} k_1 \delta_{1max}^2 = \frac{1}{2} m_p \Delta v^2 - \frac{1}{2} k_2 \delta_{2B}^2$$

and

$$\Delta v^2 = \omega_1^2 \delta_{1max}^2 + \omega_2^2 \delta_{2B}^2$$

G.10

Now, $\omega_1^2 \delta_{1max}^2 \ddot{y}_p(\max)$ and $\frac{1}{2} k_2 \delta_{2B}^2$ is the total energy absorption capability of the cushion (E_c). Hence, G.10 can be rewritten

$$\Delta v^2 = \frac{2 E_c}{m_p} + \frac{\ddot{y}_p(\max)}{\omega_1^2}$$

so that the peak mass acceleration is

$$\ddot{y}_p(\max) = \omega_1 \left(\Delta v^2 - \frac{2 E_c}{m_p} \right)^{1/2}$$

G.11

If allowance is made for some initial deflection δ_s in the springs, G.10 becomes

$$\Delta v^2 = \omega_1^2 (\delta_{1max}^2 - \delta_{1s}^2) + \omega_2^2 (\delta_{2B}^2 - \delta_{2s}^2)$$

and G.11 takes the form

$$\ddot{y}_p(\max) = \left\{ (1 + \Omega) \ddot{y}_s^2 + \omega_1^2 \left(\Delta v^2 - \frac{2 E_c}{m_p} \right) \right\}^{1/2}$$

G.12

where $\ddot{y}_s = \omega_1^2 \delta_{1s} = \omega_2^2 \delta_{2s}$

The condition for bottoming is that the available kinetic energy must be equal to, or greater than the potential energy storing capacity of the system, i.e.

$$\frac{1}{2} m_p \Delta v^2 \geq \frac{1}{2} k_1 (\delta_{1B}^2 - \delta_{1s}^2) + \frac{1}{2} k_2 (\delta_{2B}^2 - \delta_{2s}^2)$$

where the suffix B implies conditions prevailing when spring k_2 bottoms. When the two sides of the above expression are equal, the velocity change that will just cause bottoming of the cushion can be deduced, viz.

$$\Delta v_B^2 = \frac{2 E_c}{m_p} - \frac{\ddot{y}_s^2}{\omega_2^2} + \frac{k_1 \delta_{1B}^2}{m_p} - \frac{\ddot{y}_s^2}{\omega_1^2}$$

and since $S_{1B} = S_{2B} \frac{k_2}{k_1}$

$$\Delta V_B^2 = \frac{2E_c}{m_p} - \frac{\ddot{y}_s^2}{\omega_1^2} + \frac{k_1 S_{1B}^2}{m_p} - \frac{\ddot{y}_s^2}{\omega_1^2}$$

or

$$\Delta V_B = \left\{ \frac{2E_c}{m_p} \left(1 + \frac{1}{\Omega}\right) - \ddot{y}_s \frac{(1+\Omega)}{\omega_1^2} \right\}^{1/2} \quad G.13$$

When $\ddot{y}_s = 0$, G.13 simplifies to

$$\Delta V_B = \left\{ \frac{2E_c}{m_p} \frac{(1+\Omega)}{\Omega} \right\}^{1/2} \quad G.14$$

G.14 is plotted in Figure G.3 to show the influence of cushion stiffness on the bottoming velocity ratio.

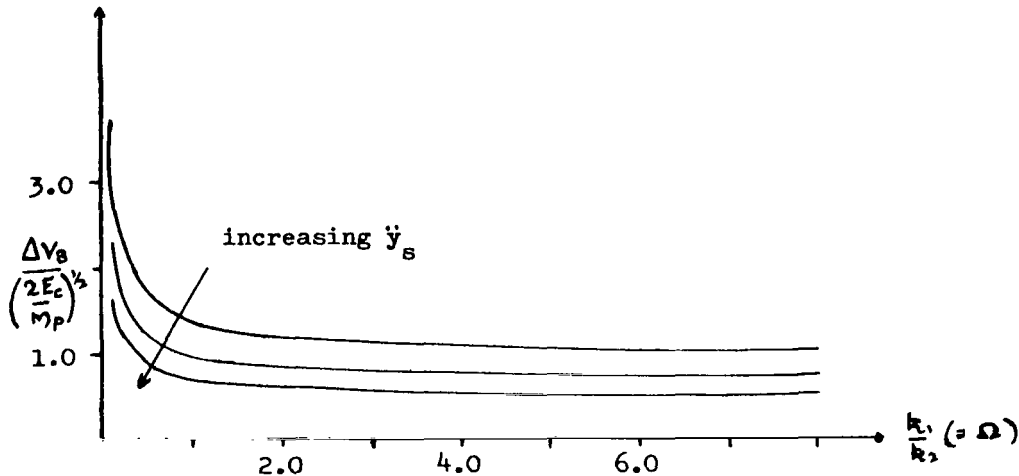


Figure G.3

Thus, for a low value of k_1 , (i.e., a weak spring), the bottoming velocity is small, whereas a large k_1 , also implies a low bottoming velocity since the spring deflects only a small amount and cannot store large amounts of energy. This latter point has **important implications** when considering the direction of application of the impulse, since the natural frequency of the body ($\sim k_1$) is different for each direction.

The attenuation of the input acceleration for non-bottoming velocity changes is given by G.9. For values of $\Delta V > \Delta V_B$ from G.11

$$\ddot{y}_p(\max) = \omega_1 \Delta V \left(1 - \frac{2E_c}{m_p \Delta V^2}\right)^{1/2}$$

so that

$$\frac{\ddot{y}_p \text{ max (with cushion)}}{\ddot{y}_p \text{ max (no cushion)}} = \left(1 - \frac{2E_c}{m_p \Delta v^2}\right)^{1/2} \quad \text{G.15}$$

In this case, the energy absorption capacity of the cushion is important, but the stiffness ratio (Ω) does not enter the expression.

Equations G.9 and G.11 show that, in impact cases, the presence of a cushion is always beneficial.

Long Duration Input

If the cushion does not bottom, the usual 100% overshoot will occur (no damping). The general solution of the equation of motion has been deduced in Appendix B. From B.7

$$\delta = \frac{\alpha}{\omega^2} (1 - \cos \omega t) \quad \text{G.16}$$

which refers to the equivalent spring. Now, the equivalent spring deflection must be the sum of the individual deflections, so

$$\delta = \delta_1 + \delta_2$$

and since from G.1, $k_1 \delta_1 = k_2 \delta_2$

$$\delta = \delta_1 + \delta_2 = \delta_2 \left(1 + \frac{k_2}{k_1}\right) = \delta_2 \left(1 + \frac{1}{\Omega}\right) \quad \text{G.17}$$

Now bottoming occurs when $\delta_2 = \delta_{2B}$ at $t = t_B$ and from G.16

$$\delta = \delta_{2B} \left(1 + \frac{1}{\Omega}\right) = \frac{\alpha}{\omega^2} (1 - \cos \omega t_B) \quad \text{G.18}$$

Using the value of ω given by G.4 gives

$$\omega_1^2 \delta_{2B} = \alpha (1 - \cos \omega t_B)$$

If the acceleration needed to bottom the cushion is defined by

$$\ddot{y}_B = \omega_1^2 \delta_{2B} \quad \text{G.19}$$

and from G.18

$$\cos \frac{\omega_1 t_B}{(1+\Omega)^{1/2}} = \frac{\alpha - \ddot{y}_B}{\alpha} \quad \text{G.20}$$

Differentiating G.16 gives the spring velocity at bottoming

$$\dot{S}_B = \frac{\alpha}{\omega} \sin \omega t_B$$

so that

$$\dot{S}_B = \frac{\alpha(1+\Omega)^{1/2}}{\omega_1} \sin \frac{\omega_1 t_B}{(1+\Omega)^{1/2}}$$

Remembering that $\sin^2 \theta + \cos^2 \theta = 1$ and using G.20, the above equation becomes

$$\dot{S}_B = \frac{(1+\Omega)^{1/2}}{\omega_1} (2\alpha \ddot{y}_B - \ddot{y}_B^2)^{1/2} \quad \text{G.21}$$

Equations G.18 and G.21 give the values of the equivalent spring deflection, and velocity at bottoming. Subsequent motion will affect only the spring k_1 , and the equation of motion can be solved using G.18 and G.21 to provide the initial conditions, i.e., taking t_B as the new $t = 0$.

The equation of motion is

$$\frac{d^2 S}{dt^2} + \omega^2 S = \alpha$$

and the Laplace transform of this equation is

$$-p x_1 - p^2 x_0 + p^2 x + \omega^2 x = \alpha$$

where $x_0 = S$ at $t=0(t_B)$ and $x_1 = \dot{S}$ at $t=0(t_B)$

Hence,

$$x = \frac{\alpha + p x_1 + p^2 x_0}{p^2 + \omega^2} = \frac{\alpha}{p^2 + \omega^2} + \frac{p x_1 \omega}{\omega(p^2 + \omega^2)} + \frac{p^2 x_0}{p^2 + \omega^2}$$

the inverse Laplace transform gives

$$S = \frac{\alpha}{\omega^2} (1 - \cos \omega t) + \frac{x_1}{\omega} \sin \omega t + x_0 \cos \omega t$$

Substituting $x_0 = S_{2B}$ and $x_1 = \dot{S}_{2B}$ gives

$$S = \frac{\alpha}{\omega^2} - \left(\frac{\alpha}{\omega^2} - S_{2B} \right) \cos \omega t + \frac{\dot{S}_{2B}}{\omega} \sin \omega t \quad \text{G.22}$$

Where ω is now ω_1 , since spring k_1 is fully compressed.

Using the values of S_{2B} and \dot{S}_{2B} of G.19 and G.21, the above expression becomes

$$\omega_1^2 S = \alpha - (\alpha - \ddot{y}_B \Omega) \cos \omega_1 t + (1+\Omega)^{1/2} (2\alpha \ddot{y}_B - \ddot{y}_B^2)^{1/2} \sin \omega_1 t$$

and $\omega_1 \delta = \ddot{y}_p$. The above equation can be rewritten, including a phase angle ϕ viz.

$$\ddot{y}_p = \alpha - \left\{ (\alpha - \ddot{y}_B \Omega)^2 + (1 + \Omega)(2\alpha\ddot{y}_B - \ddot{y}_B^2) \right\}^{1/2} \sin(\omega_1 t + \phi) \quad G.23$$

$$\text{where } \sin \phi = \frac{\alpha - \ddot{y}_B \Omega}{\left\{ (\alpha - \ddot{y}_B \Omega)^2 + (1 + \Omega)(2\alpha\ddot{y}_B - \ddot{y}_B^2) \right\}^{1/2}}, \quad \cos \phi = \frac{(1 + \Omega)^{1/2} (2\alpha\ddot{y}_B - \ddot{y}_B^2)^{1/2}}{\left\{ (\alpha - \ddot{y}_B \Omega)^2 + (1 + \Omega)(2\alpha\ddot{y}_B - \ddot{y}_B^2) \right\}^{1/2}}$$

(This step can be shown by expanding $\sin(\omega_1 t + \phi)$ in Equation G.23).

The turning points of \ddot{y}_p occur when $d\ddot{y}_p/dt = 0$, i.e., when $(\omega_1 t + \phi)$ has values of $\pi/2, 3\pi/2$ etc. For maxima, $d^2\ddot{y}_p/dt^2$ is negative, i.e., when $(\omega_1 t + \phi)$ has values $3\pi/2, 7\pi/2$ etc.

Hence, the maximum mass acceleration after bottoming has occurred is given by

$$\ddot{y}_p(\max) = \alpha + \left\{ \alpha^2 + 2\alpha\ddot{y}_B - \ddot{y}_B^2(1 + \Omega - \Omega^2) \right\}^{1/2} \quad G.24$$

Note that if $\ddot{y}_B = 0$, i.e., the cushion is already bottomed, G.24 reduces to the usual expression

$$\ddot{y}_p(\max) = 2\alpha$$

For the condition

$$2\alpha\ddot{y}_B - \ddot{y}_B^2(1 + \Omega - \Omega^2) > 0$$

or

$$\frac{2\alpha}{\ddot{y}_B} > 1 + \Omega - \Omega^2$$

the overshoot is greater than 100%, which means that, under these conditions, bottoming during a long duration input can have serious consequences.

A plot of the ratio peak mass acceleration to input acceleration ($\ddot{y}_p(\max)/\alpha$) against Ω is given in Figure G.4, for various values of \ddot{y}_B . The graph illustrates the fact that decreasing the cushion stiffness is advantageous when bottoming can occur. All the curves are above $\ddot{y}_p(\max)/\alpha = 2$, since no damping is present, and the pulse duration is long enough for full overshoot to have been obtained.

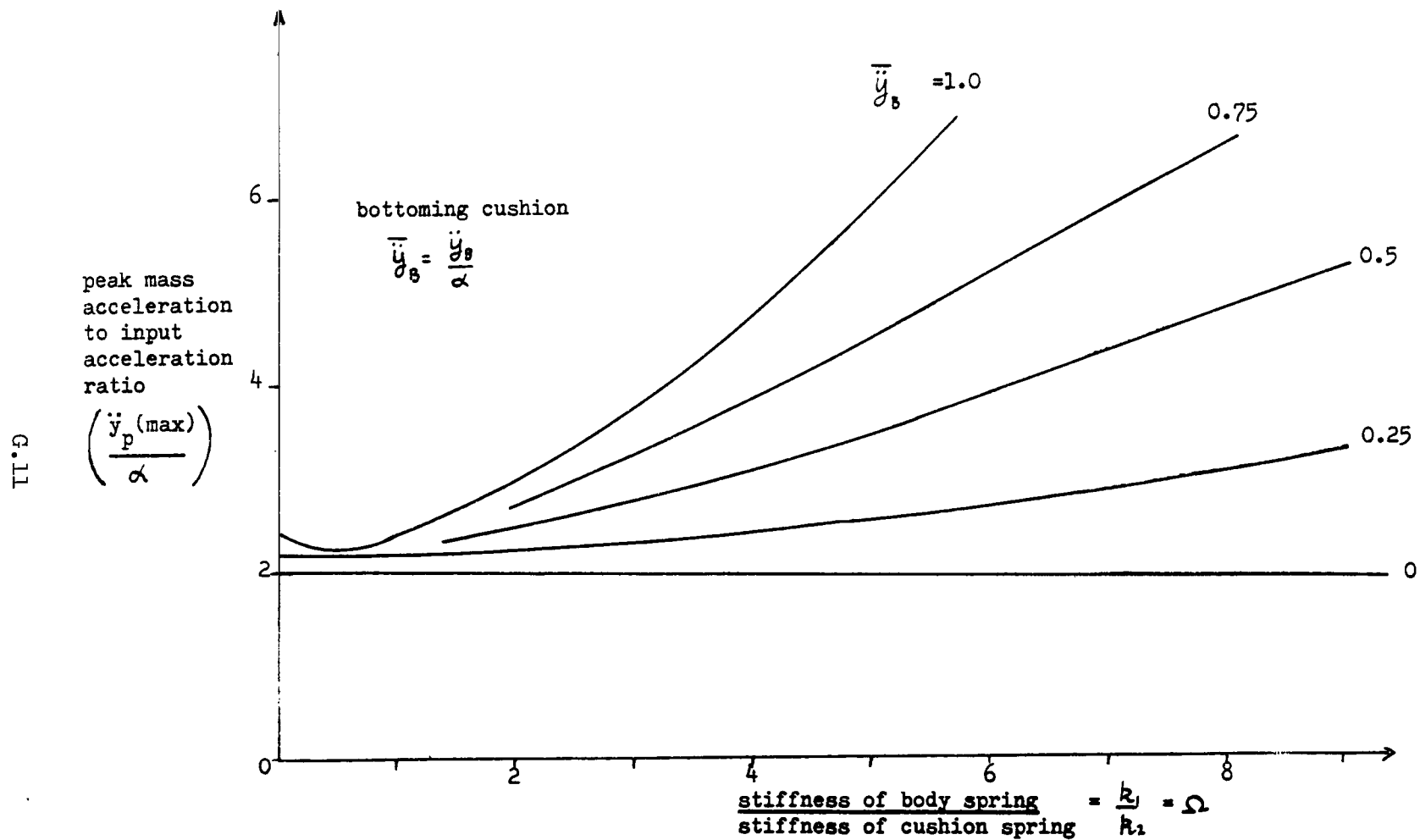


Figure G.4 Effect on Man-Cushion Frequency Ratio on Peak Body Response

APPENDIX H

REBOUND IN A LINEAR SYSTEM

SYMBOLS

k	spring stiffness
m_p	mass
\ddot{y}_p	mass acceleration relative to fixed datum
\ddot{y}_c	input acceleration
t	time
t_1	duration of input acceleration
t_2	time when restraint becomes active
α	step function input
$\delta, \dot{\delta}, \ddot{\delta}$	deflection, velocity (rate of change of deflection), acceleration (rate of change of velocity) of spring
ϕ	phase angle
ω	spring frequency

SUFFICES

1	man
2	restraint

A linear single degree of freedom system (Figure H.1) will be used to investigate the magnitude of the acceleration imposed on a human during a rebound process.

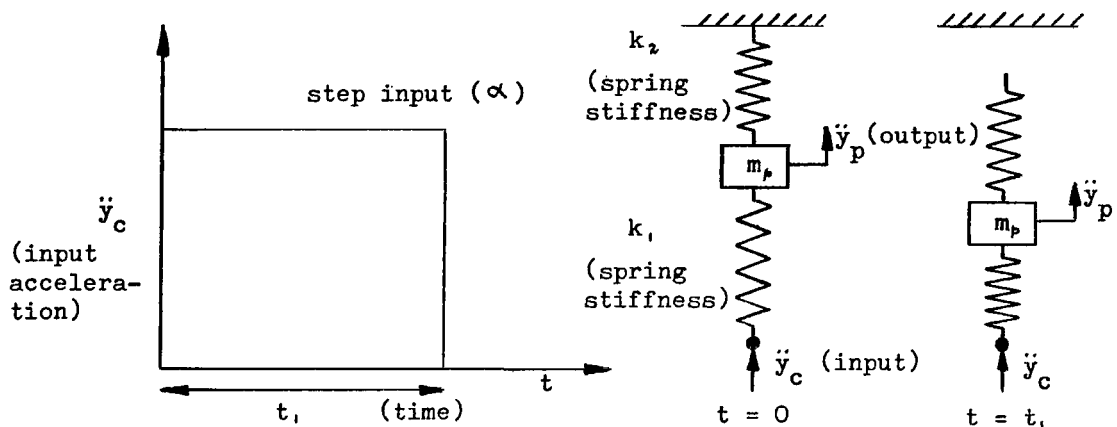


Figure H.1

The occupant of a seat or capsule is represented by the spring k_1 , and k_2 is analogous to some restraint device which might be a harness (in extension) or a shock absorber (in compression). A step function input (α) of duration t_1 is applied to the base of the spring k_1 , which causes the spring to compress. At t_1 the input is removed and the spring returns to its original position ($\delta_1 = 0$), but with a velocity $\dot{\delta}_1$. Up to this point in time (t_2 , say), the spring k_2 has been inactive since the restraint only acts when the occupant leaves his seat. For $t > t_1$, k_1 is inoperative and k_2 deflects.

Up to $t = t_1$ the equation of motion of the mass takes the form derived in previous appendices, viz.

$$\ddot{y}_c = \alpha = \omega_1^2 \delta + \ddot{\delta} \quad \text{H.1}$$

The solution of this equation is developed in Appendix B (Equation B.7).

When $\underline{t_2} > t > t_1$, the equation of motion is

$$\omega_1^2 \delta + \ddot{\delta} = 0 \quad \text{H.2}$$

which also has been solved in Appendix B, using $\dot{\delta}$ and δ (from H.1)

at $t = t_1$, as the initial conditions. (See B.17 and B.18). One form of the solution given is

$$\delta_1 = \left\{ \left(\frac{x_1}{\omega_1} \right)^2 + x_0^2 \right\}^{1/2} \sin(\omega_1 t + \phi) \quad \text{H.3}$$

where x_0 and x_1 are the initial values of δ and $\dot{\delta}$, respectively.

$\tan \phi = \frac{\omega_1 x_0}{x_1}$, so that $\sin \phi = \frac{\omega_1 x_0}{(\omega_1^2 x_0^2 + x_1^2)^{1/2}}$ and $\cos \phi = \frac{x_1}{(\omega_1^2 x_0^2 + x_1^2)^{1/2}}$

so that expanding the $\sin(\omega_1 t + \phi)$ term of H.3, and substituting these values, leads to

$$\delta_1 = \frac{x_1}{\omega_1^2} \left\{ \cos \omega_1 t - \cos(t - t_1) \omega_1 \right\} \quad \text{H.4}$$

where time is now measured from $t = t_1$.

During the rebound phase, starting at t_2 , the equation of motion is

$$\omega_2^2 \delta + \ddot{\delta} = 0 \quad \text{H.5}$$

since there is no applied input. Now, at $t = t_2$, $\delta_1 = \delta_2 = 0$

and the solution of H.5 is similar to that given in H.3, but with $x_0 = 0$ i.e. $\phi = 0$, hence

$$\delta_2 = \frac{x_1}{x_2} \sin \omega_2 t \quad \text{H.6}$$

and the acceleration is obtained by two differentiations with respect to time, viz.

$$\ddot{\delta}_2 = -x_1 \omega_2 \sin \omega_2 t \quad \text{H.7}$$

where time is measured from $t = t_2$

To insure that t in these equations is always measured from true zero,

H.7 is rewritten as

$$\ddot{\delta}_2 = -x_1 \omega_2 \sin \omega_2 (t - t_2) \quad \text{H.8}$$

and similarly H.4 as

$$\delta_1 = \frac{x_1}{\omega_1^2} \left\{ \cos \omega_1 (t - t_1) - \cos \omega_1 t \right\} \quad \text{H.9}$$

so that the value of x_1 in H.8 is, from H.9

$$x_1 = \dot{\delta}_1 = \frac{x_1}{\omega_1} \left\{ \sin \omega_1 t_2 - \sin \omega_1 (t_2 - t_1) \right\}$$

Using this value, H.8 becomes

$$\ddot{\delta}_2 = -\alpha \frac{\omega_2}{\omega_1} \left\{ \sin \omega_1 t_2 - \sin \omega_1 (t_2 - t_1) \right\} \sin \omega_2 (t - t_2)$$

This expression will have its maximum value when $\sin \omega_2 (t - t_2) = 1$ so that

$$\ddot{\delta}_2(\max) = -\alpha \frac{\omega_2}{\omega_1} \left\{ \sin \omega_1 t_2 - \sin \omega_1 (t_2 - t_1) \right\} \quad \text{H.10}$$

For a very short pulse, use is made of the fact that the sine of a small angle approaches the value of the angle (in radians).

Hence, H.10 becomes

$$\ddot{\delta}_2(\max) = -\alpha \frac{\omega_2}{\omega_1} \omega_1 t_1 = -\alpha \omega_2 t_1 \quad \text{for small } t$$

and

$$\ddot{y}_p(\max) = \ddot{\delta}_2(\max) = -\alpha \omega_2 t_1 \quad \text{H.11}$$

This expression is similar to that derived in Appendix D (cf., D.23) except that ω_1 replaces ω .

Note that H.10 itself has a maximum value for a certain $\omega_1 t_1$ (\sim input duration). Writing H.10 in the form

$$\ddot{\delta}_2(\max) = -\alpha \frac{\omega_2}{\omega_1} \left\{ \sin \omega_1 t_2 (1 - \cos \omega_1 t_1) + \sin \omega_1 t_1 \cos \omega_1 t_2 \right\}$$

this expression is a maximum when $\cos \omega_1 t_1 = 0$ or $\omega_1 t_1 = \pi/2, 3\pi/2$ etc., and when $\sin \omega_1 t_1 = -1$ or $\omega_1 t_1 = 3\pi/2, \dots$ etc., so that

$$\ddot{y}_p(\max) = -\alpha \frac{\omega_2}{\omega_1} 2 \sin \omega_1 t_2$$

which has an ultimate maximum when $\omega_1 t_2$ (\sim start of rebound) has the value $\pi/2$ etc.

Hence

$$\ddot{y}_p(\max) = -2\alpha \frac{\omega_2}{\omega_1} \quad \text{H.12}$$

The result resembles the standard box 100% overshoot case, except that the expression H.12 contains a frequency ratio. The application is quite general in that ω_1 and ω_2 can be regarded as equivalent frequencies. Thus, the effective contribution of the spine can be included in ω_2 and a seat cushion spring in ω_1 . The equations show that considerable amplification is possible if the restraint system is stiffer than the system receiving the initial impulse.

APPENDIX I

THE INFLUENCE OF RISE TIME

SYMBOLS

g	acceleration due to gravity
L	denotes "Laplace transform of"
L^{-1}	denotes "inverse Laplace transform of"
m_p	mass of the system
n	an integer, takes the values 0, 1, 2, 3 etc.
t	time
t_r	rise time of the input acceleration
\ddot{y}_c	input acceleration
\ddot{y}_p	acceleration of the mass m_p
β	rate of onset of the input acceleration
δ	deflection of the spring
ω	frequency of the mass-spring system

The fact that rate of onset influences human tolerance to rapidly applied accelerations has been recognized by early workers in the human factors field. As explained in the main text, a more useful parameter to consider is the rise time (t_r) which is the time elapsed before the peak or plateau acceleration is obtained, as illustrated in Figure I.1.

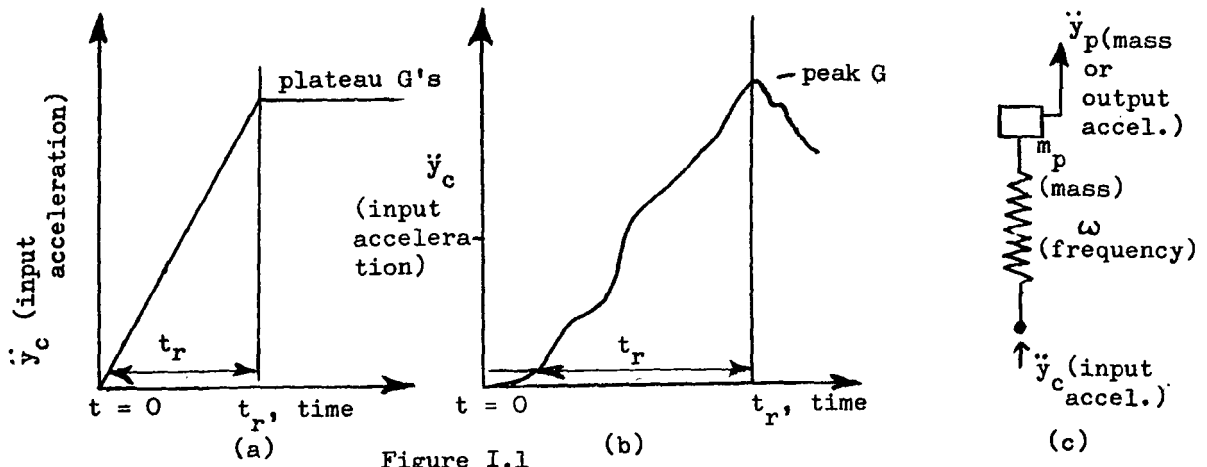


Figure I.1

A linear ramp type of acceleration, followed by a continuous constant acceleration (Fig. I.1 (a)) is more amenable to mathematical analysis and will be used to illustrate the influence of rise time on the resultant mass acceleration.

The equation of motion of the spring-mass system (Fig. 1 (c)) is derived in the usual way (see Appendix B) and can be written

$$\frac{d^2\delta}{dt^2} + \omega^2\delta = \ddot{y}_c \quad \text{I.1}$$

where the input acceleration \ddot{y}_c has the values

$$\ddot{y}_c = \beta t \quad \text{for} \quad 0 \leq t \leq t_r \quad \text{I.2(a)}$$

and

$$\ddot{y}_c = \beta t_r \quad \text{constant for} \quad t \geq t_r \quad \text{I.2(b)}$$

I.2 (a) describes a ramp function and I.2(b) a constant input function, both of which have direct Laplace transforms (e.g. transform numbers 78 and 79 of Ref. I.1) which are

$$\frac{\beta}{p}(1 - e^{-t_r p}) - \beta t_r e^{-t_r p} \quad \text{for the ramp function}$$

and

$$\beta t_r e^{-t_r p} \text{ for the continuous function}$$

These two can be added so the Laplace transform of Equation I.1 can be written

$$p^2 x + \omega^2 x = \frac{\beta}{p} (1 - e^{-t_r p})$$

so that

$$x = \frac{\beta(1 - e^{-t_r p})}{p(p^2 + \omega^2)} = \frac{\beta}{p(p^2 + \omega^2)} - \frac{\beta e^{-t_r p}}{p(p^2 + \omega^2)} \quad \text{I.3}$$

where the initial conditions $\delta = \dot{\delta} = 0$ at $t = 0$ to apply.

The inverse Laplace transform of the first term is

$$L^{-1} \frac{\beta}{p(p^2 + \omega^2)} = \beta \left(\frac{t}{\omega^2} - \frac{1}{\omega^3} \sin \omega t \right)$$

and for the second term

$$L^{-1} - \frac{\beta e^{-t_r p}}{p(p^2 + \omega^2)} = \beta \left\{ -\frac{(t - t_r)}{\omega^2} + \frac{1}{\omega^3} \sin(\omega t - \omega t_r) \right\}$$

(Theorem VII applied to transform 47 - Ref. I.1)

Hence the spring deflection is given by

$$\delta = \frac{\beta t_r}{\omega^2} - \frac{\beta}{\omega^3} \left\{ \sin \omega t - \sin \omega(t - t_r) \right\}$$

Applying the basic addition theorem of trigonometry to this expression gives

$$\delta = \frac{\beta t_r}{\omega^2} - \frac{\beta}{\omega^3} \left\{ 2 \cos \omega \left(t - \frac{t_r}{2} \right) \sin \frac{\omega t_r}{2} \right\} \quad \text{I.4}$$

Since $\ddot{y}_p = \omega^2 \delta$, the mass acceleration is represented by

$$\ddot{y}_p = \beta t_r - \frac{2\beta}{\omega} \left\{ \cos \omega \left(t - \frac{t_r}{2} \right) \sin \frac{\omega t_r}{2} \right\} \quad \text{I.5}$$

Turning points exist when

$$\frac{d\ddot{y}_p}{dt} = 2\beta \left\{ \sin \omega \left(t - \frac{t_r}{2} \right) \sin \frac{\omega t_r}{2} \right\} = 0$$

i.e. when

$$\sin \omega \left(t - \frac{t_r}{2} \right) = 0 \quad \text{or} \quad \omega \left(t - \frac{t_r}{2} \right) = n\pi$$

where n is an integer.

The maximum value of \ddot{y}_p exists when $\frac{d^2\ddot{y}_p}{dt^2}$ is negative, and

$$\frac{d^2\ddot{y}_p}{dt^2} = 2\beta\omega \left\{ \cos\omega\left(t - \frac{t_r}{2}\right) \sin\frac{\omega t_r}{2} \right\}$$

Substituting the turning point condition obtained above yields

$$\frac{d^2\ddot{y}_p}{dt^2} = \pm 2\beta\omega \sin\frac{\omega t_r}{2} \quad \text{I.6}$$

depending on the quadrant of ωt (+ve for $n = 0, 2, 4$ etc. -ve for $n = 1, 3, 5$ etc.) Thus the sign of I.6 depends on the sign of $\sin\omega t$, and the value of n . The condition $n = 0$ is of no interest and when $n = 1$, equation I.6 is negative when $\sin\frac{\omega t_r}{2}$ is positive, i.e. when

$$0 \leq \frac{\omega t_r}{2} \leq \pi$$

so that

$$t_r \text{ must be } \leq \frac{2\pi}{\omega}$$

If $n = 2$, I.6 is negative when $\sin\frac{\omega t_r}{2}$ is negative, i.e. when

$$\pi \leq \frac{\omega t_r}{2} \leq 2\pi$$

so that t_r lies between $2\pi/\omega$ and $4\pi/\omega$

Summarizing these conditions, the mass acceleration is a maximum if $t_r \leq \frac{2\pi}{\omega}$ for $n = 1$, and if $\frac{2\pi}{\omega} \leq t_r \leq \frac{4\pi}{\omega}$ for $n = 2$ etc.

The peak mass acceleration can then be written

$$\ddot{y}_p(\max) = \beta t_r - (-)^n \frac{2\beta}{\omega} \sin\frac{\omega t_r}{2} \quad \text{I.7}$$

which satisfies the conditions deduced above.

Now βt_r is the plateau acceleration input, and the following ratio can be formed

$$\frac{\ddot{y}_p(\max)}{\beta t_r} = 1 - (-)^n \frac{\sin\frac{\omega t_r}{2}}{\frac{\omega t_r}{2}} \quad \text{I.8}$$

which for $n = 1$ and $t_r = 0$ reduces to

$$\frac{\ddot{y}_p(\max)}{\beta t_r} = 2$$

since in the limit, as t_r approaches zero, $\frac{\sin \frac{\omega t_r}{2}}{\frac{\omega t_r}{2}}$ approaches unity. This agrees with the case of a step function input (Equation B.16) which corresponds to a zero rise time.

Equation I.8 is plotted in Figure I.2 and since the location is in non-dimensional form, the result is applicable for any value of the variable parameters.

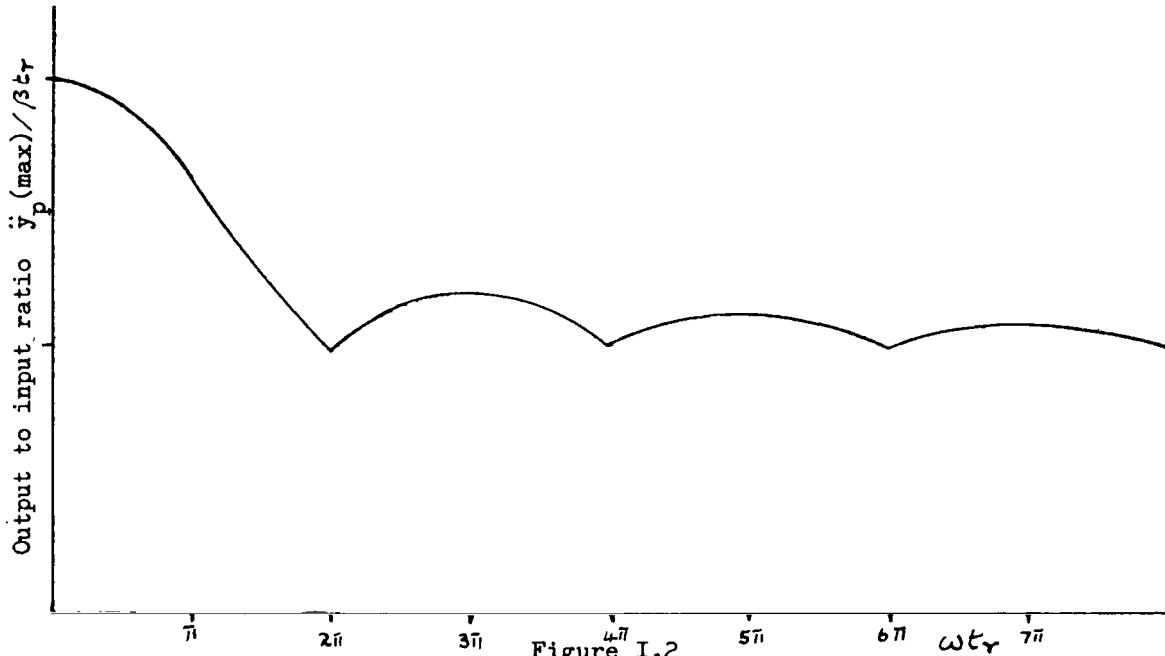


Figure I.2

These results indicate that for very short rise times full 100% overshoot can be attained, but as the rise time increases the overshoot is reduced and higher input acceleration can be applied before the level becomes intolerable. Rise time should not be confused with duration time. Both parameters influence the peak mas acceleration attained, but in the present study the influence of duration time has been eliminated by assuming a continuous (long duration) input.

REFERENCES

<u>No.</u>	<u>Name</u>	<u>Title, etc.</u>
I.1	Pipes L. A.	"Applied Mathematics for Engineers and Physicists," New York, McGraw-Hill Book Co. Inc., 1946.

APPENDIX J

THE TWO DEGREE OF FREEDOM SYSTEM

SYMBOLS

A, B, C, D	constants used in solving the problem, see Equations J.31 and J.32
$\bar{A}, \bar{B}, \bar{C}, \bar{D}$	
c	$= \frac{k}{m}$ the damping coefficient
F	force
K	damping constant
k	spring constant
L	denotes "the Laplace transform of"
m	mass
p	Laplace variable corresponding to time (t)
t	time
Δt	duration of input acceleration
v	velocity arising from an impulsive input acceleration
y, \dot{y}, \ddot{y}	displacement, velocity and acceleration of some point of the model
$\delta, \dot{\delta}, \ddot{\delta}$	deflection, velocity (rate of change of deflection), acceleration (rate of change of velocity) of spring
Ω	resonant frequency of the coupled system
ω	frequency of an uncoupled spring-mass system

SUFFICES

c	relates variable or parameter to the point C in Figure J.1 (c)
p	relates variable or parameter to the upper mass-spring damper system
q	relates variable or parameter to the lower mass-spring damper system
T	denotes sum of components of quantity
max	denotes maximum value of variable
1, 2	used to distinguish between the resonant frequencies of the coupled system

The next step towards a better mathematical representation of the human body subjected to acceleration stress is to extend the spring-mass concept to include two spring-mass systems in series, with associated damping elements. Such a system is shown in Figure J.1 and represents a two degree of freedom model. The mathematics involved in the investigation of this model is much more complex than that associated with the single degree of freedom system, but the basic principles are similar.

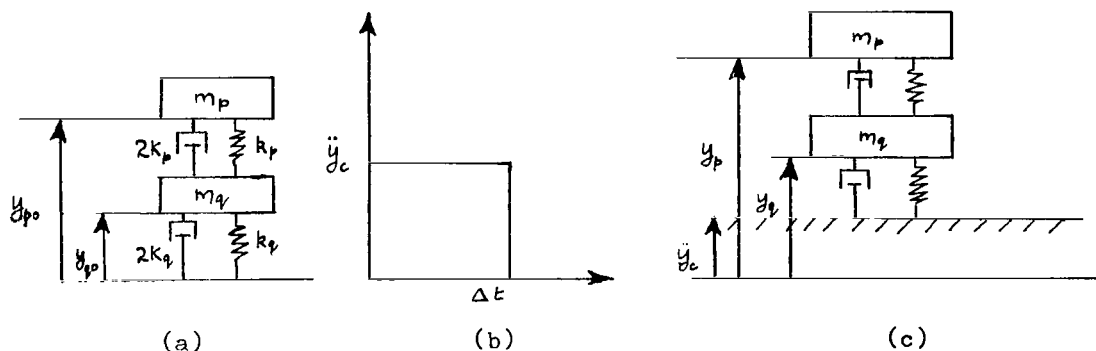


Figure J.1

The forces acting on each mass are evaluated and the equations of motion determined in terms of spring deflection, spring acceleration and the particular input acceleration. The equations of motion are then solved to yield the spring deflection which is used to determine the resultant mass acceleration. The peak mass acceleration is then investigated by maximizing the relevant equations. This latter process involves complex algebraic terms and a digital computer has been used to facilitate the analysis.

Derivation of the Equations of Motion

The forces developed in the springs (assumed linear) can be represented as follows:

$$\begin{aligned} \text{Spring } p & \quad F_p = k_p \delta_p \\ \text{Spring } q & \quad F_q = k_q \delta_q \end{aligned}$$

J.1

where k_p and k_q are the spring stiffness values associated with the springs. The forces developed in the dampers (of constants $2k_p$ and $2k_q$) are

$$\begin{array}{ll} \text{Damper } p & \bar{F}_p = 2k_p \dot{\delta}_p \\ \text{Damper } q & \bar{F}_q = 2k_q \dot{\delta}_q \end{array}$$

J.2

The Equation of Motion of the Mass m_p

Only the spring and damper of constants k_p and $2k_p$ are attached directly to the mass m_p so that any force transmitted to the mass m_p due to an acceleration applied at C must be transmitted through the spring k_p and damper $2k_p$. Hence, for some given deflection and rate of change of deflection $\dot{\delta}_p$, the force on m_p is given by

$$\begin{aligned} F_{pT} &= F_p + \bar{F}_p \\ &= k_p \delta_p + 2k_p \dot{\delta}_p \end{aligned}$$

J.3

on using the values for F_p and \bar{F}_p given in Equations J.1 and J.2 respectively. Newton's second law of motion states that this force, F_{pT} , is equal to the product of the mass m_p and its acceleration. So, in symbols this statement is written

$$m_p \ddot{y}_p = k_p \delta_p + 2k_p \dot{\delta}_p$$

which is the equation of motion for the mass m_p .

The Equation of Motion for the Mass m_q

It will be demonstrated now that the equation of motion for the mass m_q is

$$m_q \ddot{y}_q = 2k_q \dot{\delta}_q + k_q \delta_q - (2k_p \dot{\delta}_p + k_p \delta_p)$$

The R.H.S. of this equation states that the force F_{qT} acting on the mass m_q is the force produced in the spring and damper, k_q and $2k_q$ respectively, less the force F_{pT} transmitted to the mass m_p .

Consider the spring k_p and damper $2K_p$. These are attached directly to the mass m_q so that any force generated in them is transferred directly to the mass m_q . The force generated in the spring k_p and damper $2K_p$ is given by Equation J.3

$$F_{pT} = k_p \delta_p + 2K_p \dot{\delta}_p$$

This force F_{pT} is trying, for positive δ_p (compression), to push the masses further apart so that the force on m_q is equal and opposite to that on m_p .

The forces in the spring k_q and damper $2K_q$ are given in Equations J.1 and J.2. The total force due to this spring-damper system is

$$F = 2K_q \dot{\delta}_q + k_q \delta_q \quad J.5$$

and its direction, for positive δ_q , is such that it tries to force m_q closer to m_p , that is, in the opposite direction to the force on m_q due to the spring k_p and damper $2K_p$. The total force acting on the mass m_q is then

$$F_{qT} = F - F_{pT}$$

and applying Newton's second law to mass m_q gives

$$m_q \ddot{y}_q = 2K_q \dot{\delta}_q + k_q \delta_q - (k_p \delta_p + 2K_p \dot{\delta}_p) \quad J.6$$

after substituting for F_{pT} and F from J.3 and J.5 respectively.

In order to introduce the given input acceleration into the equation of motion it is necessary now to express \ddot{y}_p and \ddot{y}_q in terms of $\ddot{\delta}_p$, $\ddot{\delta}_q$ and \ddot{y}_c the input acceleration.

The original (uncompressed) length of the spring k_q is y_{q0} (Fig. J.1(a)) and from Fig. J.1(b) its length at some time during the motion is

$$\bar{y}_q = y_{q0} - y_c \quad J.7$$

The difference in these two lengths $y_{q0} - \bar{y}_q$ is the compression in the spring δ_q so

$$y_{q0} - \bar{y}_q = \delta_q$$

but

$$\bar{y}_q = y_1 - y_c$$

so

$$\delta_q = y_{q0} - y_1 + y_c$$

or

$$y_q = y_c - \delta_q + y_{q0}$$

Equation J.8 is now differentiated with respect to time to yield the velocities

$$\dot{y}_q = \dot{y}_c - \dot{\delta}_q \quad \text{J.9}$$

because y_{q0} is a constant for a given spring so that it does not change with time, i.e. $dy_{q0}/dt = 0$. Differentiating J.9 with respect to time gives the acceleration of m_q in terms of the input acceleration and spring acceleration (rate of change of rate of change of deflection)

$$\ddot{y}_q = \ddot{y}_c - \ddot{\delta}_q$$

An expression relating $\ddot{\delta}_p$, \ddot{y}_p and \ddot{y}_c is obtained similarly. The unextended length of spring k_p is seen to be from Fig. J.1(a)

$$\bar{y}_{p0} = y_{p0} - y_{q0} \quad \text{J.11}$$

From inspection of Fig. J.1(b) it is seen that the compressed length of the spring k_p is

$$\bar{y}_p = y_p - y_q \quad \text{J.12}$$

Again, the difference between undeflected length and the deflected length is, by definition, δ_p hence,

$$\begin{aligned} \delta_p &= \bar{y}_{p0} - \bar{y}_p \\ &= y_{p0} - y_{q0} - y_p + y_q \end{aligned}$$

or

$$y_p = y_q - \delta_p + y_{p0} - y_{q0} \quad \text{J.13}$$

Now both y_{p0} and y_{q0} are constants, so that on differentiation with respect to time, both quantities yield zero. Differentiating J.13 twice with respect to time gives

$$\ddot{y}_p = \ddot{y}_q - \ddot{\delta}_p \quad \text{J.14}$$

But, from Equation J.10

$$\ddot{y}_q = \ddot{y}_c - \ddot{\delta}_q$$

Substituting this value in J.14 gives an expression for the acceleration of m_p

$$\ddot{y}_p = \ddot{y}_c - \ddot{\delta}_q - \ddot{\delta}_p \quad \text{J.15}$$

Now, using the results of J.10 and J.15 by substituting for \ddot{y}_p and \ddot{y}_q , the equations of motion of the mass m_p and m_q can be rewritten as follows

For the mass m_p

$$m_p (\ddot{y}_c - \ddot{\delta}_q - \ddot{\delta}_p) = k_p \delta_p + 2k_p \dot{\delta}_p \quad \text{J.16}$$

For the mass m_q

$$m_q (\ddot{y}_c - \ddot{\delta}_q) = 2k_q \dot{\delta}_q + k_q \delta_q - (2k_p \dot{\delta}_p + k_p \delta_p) \quad \text{J.17}$$

Dividing J.16 and J.17 throughout by m_p and m_q respectively gives

$$\ddot{y}_c - \ddot{\delta}_q - \ddot{\delta}_p = \frac{k_p}{m_p} \delta_p + \frac{2k_p}{m_p} \dot{\delta}_p \quad \text{J.18}$$

and

$$\ddot{y}_c - \ddot{\delta}_q = \frac{2k_q}{m_q} \dot{\delta}_q + \frac{k_q}{m_q} \delta_q - \left(\frac{2k_p}{m_q} \dot{\delta}_p + \frac{k_p}{m_q} \delta_p \right) \quad \text{J.19}$$

Adopting the definitions used in previous appendices some of the above quantities can be written in terms of frequency (ω), which each spring-mass system would have if vibrating alone, viz.

$$\frac{k_p}{m_p} = \omega_p^2, \quad \frac{k_q}{m_q} = \omega_q^2, \quad \frac{k_p}{m_q} = \omega_{pq}^2$$

and associated damping coefficient (c)

$$\frac{K_p}{m_p} = c_p, \quad \frac{K_q}{m_q} = c_q, \quad \frac{K_p}{m_q} = c_{pq}$$

so that J.18 and J.19 become

$$\ddot{y}_c - \ddot{\delta}_q - \ddot{\delta}_p = \omega_p^2 \delta_p + 2c_p \dot{\delta}_p$$

and

$$\ddot{y}_c - \ddot{\delta}_q = \omega_q^2 \delta_q + 2c_q \dot{\delta}_q - (2c_{pq} \dot{\delta}_p + \omega_{pq}^2 \delta_p)$$

The terms are now rearranged to give the equations of motion in the desired form

$$\ddot{y}_c = \ddot{\delta}_p + \ddot{\delta}_q + \omega_p^2 \delta_p + 2c_p \dot{\delta}_p \quad \text{J.20}$$

and

$$\ddot{y}_c = \ddot{\delta}_q + \omega_q^2 \delta_q + 2c_q \dot{\delta}_q - (2c_{pq} \dot{\delta}_p + \omega_{pq}^2 \delta_p) \quad \text{J.21}$$

Analytical Solution of Equations of Motion for the Special Case of Zero Damping

Analytical solutions of the equations of motion, including the damping terms are possible, but it is considered, at this stage, that it is acceptable to avoid too much mathematical complexity in an attempt to preserve physical significance. Also, the errors introduced by ignoring damping effects in the human body are not excessive..

When the zero damping case is considered the equations of motion become

$$\ddot{\delta}_p + \omega_p^2 \delta_p + \ddot{\delta}_q = \ddot{y}_c \quad \text{J.22}$$

and

$$-\omega_{pq}^2 \delta_p + \ddot{\delta}_q + \omega_q^2 \delta_q = \ddot{y}_c \quad \text{J.23}$$

General Case of a Rectangular Input

If x_p and x_q are the Laplace Transforms of δ_p and δ_q respectively and \ddot{y}_c has some constant value from $t = 0$ to $t = \Delta t$, Equations J.22 and J.23 transform into

$$\ddot{y}_c (1 - e^{-p\Delta t}) = (p^2 + \omega_p^2)x_p + p^2 x_q \quad \text{J.24}$$

and

$$\ddot{y}_c (1 - e^{-p\Delta t}) = -\omega_{pq}^2 x_p + (p^2 + \omega_q^2)x_q \quad \text{J.25}$$

for the conditions $\delta_p, \dot{\delta}_p, \delta_q$ and $\dot{\delta}_q = 0$ at $t = 0$

Equations J.24 and J.25 are simultaneous equations in δ_p and δ_q and can be solved by use of a standard technique. (Crout's Method e.g. see page 69 of Ref. J.1).

$$x_p = \frac{\ddot{y}_c (1 - e^{-p\Delta t}) (p^2 + \omega_q^2) - p^2 \ddot{y}_c (1 - e^{-p\Delta t})}{(p^2 + \omega_p^2)(p^2 + \omega_q^2) + p^2 \omega_{pq}^2}$$

$$x_q = \frac{\ddot{y}_c (1 - e^{-p\Delta t}) (p^2 + \omega_p^2) + \omega_{pq}^2 \ddot{y}_c (1 - e^{-p\Delta t})}{(p^2 + \omega_p^2)(p^2 + \omega_q^2) + p^2 \omega_{pq}^2}$$

These expressions may be simplified by evaluating the terms inside the brackets and regrouping

$$x_p = \frac{\ddot{y}_c (1 - e^{-p\Delta t}) \omega_q^2}{p^4 + p^2(\omega_p^2 + \omega_q^2 + \omega_{pq}^2) + \omega_p^2 \omega_q^2} \quad \text{J.26}$$

$$x_q = \frac{\ddot{y}_c (1 - e^{-p\Delta t}) (p^2 + \omega_p^2 + \omega_{pq}^2)}{p^4 + p^2(\omega_p^2 + \omega_q^2 + \omega_{pq}^2) + \omega_p^2 \omega_q^2} \quad \text{J.27}$$

The denominator of Equation J.26 and J.27 can be factored and written as

$$(p^2 + \Omega_1^2)(p^2 + \Omega_2^2) \quad \text{J.28}$$

where

$$\Omega_1^2 = \frac{1}{2} (\omega_p^2 + \omega_q^2 + \omega_{pq}^2 - \{(\omega_p^2 + \omega_q^2 + \omega_{pq}^2)^2 - 4\omega_p^2 \omega_q^2\}^{1/2}) \quad \text{J.29}$$

$$\Omega_2^2 = \frac{1}{2} (\omega_p^2 + \omega_q^2 + \omega_{pq}^2 + \{(\omega_p^2 + \omega_q^2 + \omega_{pq}^2)^2 - 4\omega_p^2 \omega_q^2\}^{1/2}) \quad \text{J.30}$$

Ω_1 , , and Ω_2 are, in fact, the resonant frequencies of the system and are termed coupled frequencies. They may be regarded as the frequencies of two equivalent spring-mass systems that may be combined to describe the motion of the two degree of freedom model.

Now since ω_p^2 , ω_q^2 and ω_{pq}^2 are always positive quantities

$$\{(\omega_p^2 + \omega_q^2 + \omega_{pq}^2)^2 - 4\omega_p^2 \omega_q^2\}^{1/2} < \{(\omega_p^2 + \omega_q^2 + \omega_{pq}^2)^2\}^{1/2}$$

i.e.

$$(\omega_p^2 + \omega_q^2 + \omega_{pq}^2)^2 - 4\omega_p^2 \omega_q^2 < \omega_p^2 + \omega_q^2 + \omega_{pq}^2$$

But, the term

$$\{(\omega_p^2 + \omega_q^2 + \omega_{pq}^2)^2 - 4\omega_p^2 \omega_q^2\}$$

can be expanded to give

$$\begin{aligned} & \{ \omega_p^4 + \omega_q^4 + \omega_{pq}^4 + 2\omega_p^2\omega_q^2 + 2\omega_q^2\omega_{pq}^2 + \omega_p^2\omega_{pq}^2 - 4\omega_p^2\omega_q^2 \} \\ &= \{ \omega_p^4 + \omega_q^4 + \omega_{pq}^4 - 2\omega_p^2\omega_q^2 + 2\omega_q^2\omega_{pq}^2 - 2\omega_p^2\omega_{pq}^2 + 4\omega_p^2\omega_q^2 \} \\ &= \{ (\omega_p^2 - \omega_q^2 - \omega_{pq}^2)^2 + 4\omega_p^2\omega_{pq}^2 \} \end{aligned}$$

which is a positive, real quantity since ω_p^2 , $\omega_q^2 + \omega_{pq}^2$ are real and positive. It follows that the original expression $\{(\omega_p^2 + \omega_q^2 + \omega_{pq}^2)^2 - 4\omega_p^2\omega_q^2\}^{1/2}$ must also be real. Now $\omega_p^2 + \omega_q^2 + \omega_{pq}^2$ is real since each term is real and has been shown to be greater than $\{(\omega_p^2 + \omega_q^2 + \omega_{pq}^2)^2 - 4\omega_p^2\omega_q^2\}^{1/2}$. Therefore, the difference $\omega_p^2 + \omega_q^2 + \omega_{pq}^2 - \{(\omega_p^2 + \omega_q^2 + \omega_{pq}^2)^2 - 4\omega_p^2\omega_q^2\}^{1/2}$ of the two quantities and their sum, which appear in Equations J.29 and J.30 respectively, are real and positive, hence Ω_1 and Ω_2 must be positive, real quantities. Reverting now to Equations J.26 and J.27, these may be expressed in partial fraction form by letting

$$x_p = \ddot{y}_c (1 - e^{-p\Delta t}) \left\{ \frac{Ap+B}{p^2+\Omega_1^2} + \frac{Cp+D}{p^2+\Omega_2^2} \right\} \quad J.31$$

and

$$x_q = \ddot{y}_c (1 - e^{-p\Delta t}) \left\{ \frac{\bar{A}p+\bar{B}}{p^2+\Omega_1^2} + \frac{\bar{C}p+\bar{D}}{p^2+\Omega_2^2} \right\} \quad J.32$$

i.e.

$$x_p = \ddot{y}_c (1 - e^{-p\Delta t}) \left\{ \frac{(Ap+B)(p^2+\Omega_2^2) + (Cp+D)(p^2-\Omega_1^2)}{(p^2+\Omega_1^2)(p^2+\Omega_2^2)} \right\} \quad J.31(a)$$

$$x_q = \ddot{y}_c (1 - e^{-p\Delta t}) \left\{ \frac{(\bar{A}p+\bar{B})(p^2+\Omega_2^2) + (\bar{C}p+\bar{D})(p^2-\Omega_1^2)}{(p^2+\Omega_1^2)(p^2+\Omega_2^2)} \right\} \quad J.32(a)$$

Now, the expression for x_p and x_q in Equation J.31(a) and J.32(a) must be identical to Equations J.26 and J.27 so that the coefficients of powers of p may be equated. From Equations J.31(a) and J.26, the following set of equations for A, B, C , and D are obtained.

$$A + C = 0$$

$$B + D = 0$$

$$A\Omega_2^2 + C\Omega_1^2 = 0$$

$$B\Omega_2^2 + D\Omega_1^2 = \omega_q^2$$

Hence

$$A = C = 0$$

and

$$D = \frac{\omega_q^2}{\Omega_1^2 - \Omega_2^2}$$

$$B = - \frac{\omega_q^2}{\Omega_1^2 - \Omega_2^2}$$

Similarly, the following equations are obtained for \bar{A} , \bar{B} , \bar{C} , \bar{D} , by equating the coefficients of powers of p in J.32(a) and J.27.

$$\begin{aligned}\bar{A} + \bar{C} &= 0 \\ \bar{B} + \bar{D} &= 1 \\ \bar{A}\Omega_1^2 + \bar{C}\Omega_1^2 &= 0 \\ \bar{B}\Omega_2^2 + \bar{D}\Omega_1^2 &= \omega_p^2 + \omega_{pq}^2\end{aligned}$$

Hence

$$\begin{aligned}\bar{A} = \bar{C} &= 0 \\ \bar{B} &= \frac{\Omega_1^2 - (\omega_p^2 + \omega_{pq}^2)}{\Omega_1^2 - \Omega_2^2} = \frac{\omega_q^2 - \Omega_2^2}{\Omega_1^2 - \Omega_2^2} \\ \bar{D} &= \frac{\omega_{pq}^2 + \omega_p^2 - \Omega_2^2}{\Omega_1^2 - \Omega_2^2} = \frac{\Omega_1^2 - \omega_q^2}{\Omega_1^2 - \Omega_2^2}\end{aligned}$$

since from Equations J.29 and J.30

$$\Omega_1^2 + \Omega_2^2 = \omega_p^2 + \omega_q^2 + \omega_{pq}^2$$

Now these quantities are substituted into Equations J.31 and J.32 to yield

$$x_p = \ddot{y}_c (1 - e^{-p\Delta t}) \left\{ - \frac{\omega_q^2}{\Omega_1^2 - \Omega_2^2} \left(\frac{1}{p^2 + \Omega_1^2} \right) + \frac{\omega_q^2}{\Omega_1^2 - \Omega_2^2} \left(\frac{1}{p^2 + \Omega_2^2} \right) \right\}$$

and

$$x_q = \ddot{y}_c (1 - e^{-p\Delta t}) \left\{ \frac{\omega_q^2 - \Omega_2^2}{\Omega_1^2 - \Omega_2^2} \left(\frac{1}{p^2 + \Omega_1^2} \right) + \frac{\Omega_1^2 - \omega_q^2}{\Omega_1^2 - \Omega_2^2} \left(\frac{1}{p^2 + \Omega_2^2} \right) \right\}$$

These equations are now in a form for which direct Laplace transforms exist and using No. 40, and applying Theorem VII of Reference J.1, the inverse Laplace transforms obtained are for $t > \Delta t$

$$\delta_p = \frac{-2\omega_q^2 \ddot{y}_c}{\Omega_1^2 - \Omega_2^2} \left\{ \frac{\sin \Omega_1 \frac{\Delta t}{2}}{\Omega_1^2} \sin \Omega_1 (t - \frac{\Delta t}{2}) - \frac{\sin \Omega_2 \frac{\Delta t}{2}}{\Omega_2^2} \sin \Omega_2 (t - \frac{\Delta t}{2}) \right\} \quad J.33$$

$$\delta_q = \frac{2\ddot{y}_c}{\Omega_1^2 - \Omega_2^2} \left\{ \frac{\omega_q^2 - \Omega_2^2}{\Omega_1^2} \sin \Omega_1 \frac{\Delta t}{2} \sin \Omega_1 (t - \frac{\Delta t}{2}) - \frac{\Omega_1^2 - \omega_q^2}{\Omega_2^2} \sin \Omega_2 \frac{\Delta t}{2} \sin \Omega_2 (t + \frac{\Delta t}{2}) \right\} \quad J.34$$

and for $t < \Delta t$

$$\delta_p = -\frac{\omega_q^2 \ddot{y}_c}{\Omega_1^2 - \Omega_2^2} \left\{ \frac{1 - \cos \Omega_1 t}{\Omega_1^2} - \frac{1 - \cos \Omega_2 t}{\Omega_2^2} \right\} \quad J.35$$

$$\delta_q = \frac{\ddot{y}_c}{\Omega_1^2 - \Omega_2^2} \left\{ \frac{\omega_q^2 - \Omega_2^2}{\Omega_1^2} (1 - \cos \Omega_1 t) + \frac{\Omega_1^2 - \omega_q^2}{\Omega_2^2} (1 - \cos \Omega_2 t) \right\} \quad J.36$$

Equations J.35 and J.36 also represent solutions of the equations of motion for a continuous step function input acceleration, since this is the limiting case when Δt approaches infinity.

Thus by solving the equations of motion describing the two degree of freedom model, expressions for the deflection of each spring has been obtained in terms of the coupled and uncoupled frequencies, input acceleration and time.

Impulsive Acceleration Input

As in Appendix E, use is made of the Dirac Impulse Function in solving the equations of motion when an impulsive input is applied to the system. Equations J.22 and J.23 are then transformed into

$$v_p = (p^2 + \omega_p^2) x_p + p^2 x_q$$

and

$$v_q = -\omega_{pq}^2 x_p + (p^2 + \omega_q^2) x_q$$

where v is the velocity achieved by the system.

Equating the right hand sides of these equations gives x_p in terms of x_q so that the equations can be solved to give

$$x_p = \frac{v p \omega_q^2}{(p^2 + \omega_p^2)(p^2 + \omega_q^2) + p^2 \omega_{pq}^2} \quad J.37$$

$$x_q = \frac{v p (p^2 + \omega_p^2 + \omega_{pq}^2)}{(p^2 + \omega_p^2)(p^2 + \omega_q^2) + p^2 \omega_{pq}^2} \quad J.39$$

It can be seen that these equations are similar to J.26 and J.27, except that $v p$ replaces $\ddot{y}_c (1 - e^{-p \Delta t})$ in the numerator. Remembering this

fact, equations similar to J.26 through J.32(b) can be used, and J.31(b) take the form

$$x_p = \frac{v \omega_q^2}{\Omega_1^2 - \Omega_2^2} \left\{ -\frac{p}{p^2 + \Omega_1^2} + \frac{p}{p^2 + \Omega_2^2} \right\} \quad J.39$$

$$x_q = \frac{v}{\Omega_1^2 - \Omega_2^2} \left\{ (\omega_q^2 - \Omega_2^2) \frac{p}{p^2 + \Omega_1^2} + (\Omega_1^2 - \omega_q^2) \frac{p}{p^2 + \Omega_2^2} \right\} \quad J.40$$

The inverse Laplace transforms of these equations can be written down (Transform No. 11, Ref. J.1), allowing δ_p and δ_q to be expressed as follows

$$\delta_p = \frac{v \omega_q^2}{\Omega_1^2 - \Omega_2^2} \left\{ \frac{1}{\Omega_1} \sin \Omega_1 t + \frac{1}{\Omega_2} \sin \Omega_2 t \right\}$$

$$\delta_q = \frac{v}{\Omega_1^2 - \Omega_2^2} \left\{ \frac{\omega_q^2 - \Omega_2^2}{\Omega_1} \sin \Omega_1 t + \frac{\Omega_1^2 - \omega_q^2}{\Omega_2} \sin \Omega_2 t \right\}$$

Application of the Two Degree of Freedom Model

There are two possible criteria for determining the permissible input acceleration. One, a limit on \ddot{y}_p (and \ddot{y}_q) has been used previously, the other, based on the strain developed in the spring puts a limit on $\delta_p^{(max)}$ and $\delta_q^{(max)}$. Since a linear system without damping is being used, it is permissible to use the results of Ruff's work, Ref. J.2 to determine $\delta_p^{(max)}$ and $\delta_q^{(max)}$ if applicable, since, in both cases, all the forces within the system are generated by the deflection of springs. Instead of maximizing δ_p and δ_q as has been done in previous appendices for \ddot{y}_p , a digital computer program has been written to evaluate and plot δ_p and δ_q against time. If a sufficiently small interval of time is used the maximum values of δ_p and δ_q may be obtained from inspection of the plots of these deflections. The results obtained from application of this model is discussed in the main text.

REFERENCES

<u>No.</u>	<u>Name</u>	<u>Title, etc.</u>
J.1	Pipes, L.A.	"Applied Mathematics for Engineers and Physicists," McGraw-Hill Book Co., Inc., New York, 1946
J.2	Geertz, A.	"Limits and Special Problems in the Use of Seat Catapults," translated 30 Aug. 1946, at AAF Aeromedical Center, Armed Services Technical Information Agency, No. ATI-56946

APPENDIX K

THE THREE DEGREE OF FREEDOM SYSTEM

SYMBOLS

A	constant introduced to assist in obtaining the steady state solution of Equation K.43
B	constant, see Equation K.27
C	damping coefficient in uncoupled mode
\bar{C}	damping coefficient in coupled mode
F	force
i	defined by $i^2 = -1$
K	damping constant of damper
L	denotes "Laplace transform of"
\bar{L}	denotes "Inverse Laplace transform of"
ℓ	length of the spring
m	mass
p	independent Laplace variable
R	amplification factor
t	time
Δt	duration of a rectangular input
v	velocity due to an impulsive input acceleration
x	dependent Laplace variable
y, \dot{y} , \ddot{y}	displacement coordinate, velocity, acceleration relative to a fixed datum
α, β	constants used in Equation K.28
$\delta, \dot{\delta}, \ddot{\delta}$	deflection, velocity (rate of change of deflection), acceleration (rate of change of velocity) of spring
μ, ν }	constants defined by $\mu + i\nu = A$

ϕ	phase angle = $\tan^{-1} \frac{\bar{\Omega}}{\zeta}$
ψ	phase angle = $\tan^{-1} \frac{\mu}{\nu}$
Ω	coupled frequency of undamped system
$\bar{\Omega}$	coupled frequency of damped system
ω	uncoupled frequency
$\Delta(t)$	Dirac impulse function

SUFFICES

0	relates symbol to conditions at time $t = 0$ or independent of time
1,2,3	relates symbol to appropriate sub-system of Figure K.1(a)
C	relates symbol to point C of Figure K.1(a) and (b)

As explained in the main text, the three degree of freedom model was introduced in an attempt to establish a model that would include the main structural (as opposed to hydraulic) effects of accelerations on the human body. The three degree of freedom model allows the dynamic response of at least three parts of the body to be determined simultaneously, and modes of widely different frequency responses may be studied, e.g. low frequency body effects together with the high frequency spinal mode. The model consists of three sets of spring-mass systems with damping, as illustrated in Figure K.1(a) and (b).

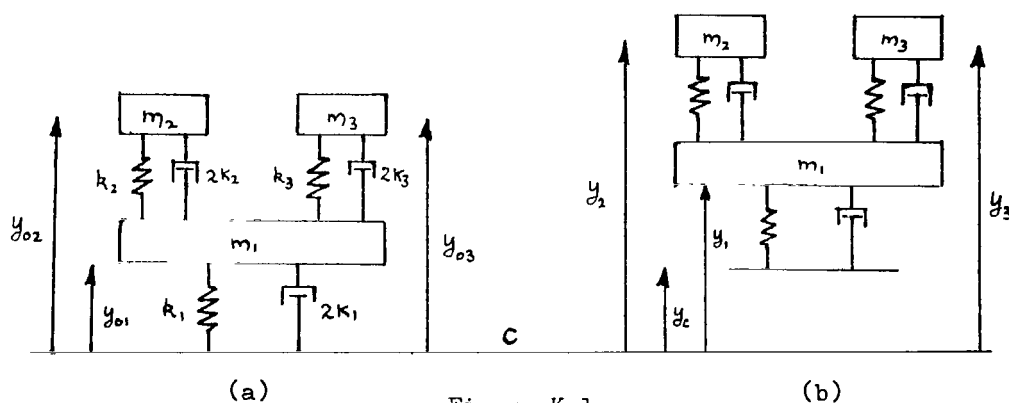


Figure K.1

Evaluation of the Forces Acting on Each Mass

The analysis of the forces acting on the three masses of the system is similar to that described in Appendix J for the two degree of freedom model, and will not be discussed in detail here.

The forces F_2 and F_3 , due to the associated springs and dampers, acting on the masses m_2 and m_3 are

$$F_2 = k_2 \delta_2 + 2K_2 \dot{\delta}_2 \quad \text{K.1}$$

and

$$F_3 = k_3 \delta_3 + 2K_3 \dot{\delta}_3 \quad \text{K.2}$$

for given spring deflections δ_2 and δ_3 . Forces F_2 and F_3 act on mass m_1 in addition to the force developed in its own spring-damper combination, but in the opposite direction. So

$$F_1 = k_1 \delta_1 + 2\kappa_1 \dot{\delta}_1 - k_2 \delta_2 - 2\kappa_2 \dot{\delta}_2 - k_3 \delta_3 - 2\kappa_3 \dot{\delta}_3$$

Newton's second law of motion is used to give the equations of motion for the three masses m_1, m_2, m_3 . These are

$$m_1 y_1 = k_1 \delta_1 + 2\kappa_1 \dot{\delta}_1 - k_2 \delta_2 - 2\kappa_2 \dot{\delta}_2 - k_3 \delta_3 - 2\kappa_3 \dot{\delta}_3$$

$$m_2 y_2 = k_2 \delta_2 + 2\kappa_2 \dot{\delta}_2$$

K.3

$$m_3 y_3 = k_3 \delta_3 + 2\kappa_3 \dot{\delta}_3$$

The output accelerations $\ddot{y}_1, \ddot{y}_2, \ddot{y}_3$ must be expressed in terms of $\ddot{\delta}_1, \ddot{\delta}_2, \ddot{\delta}_3$ and \ddot{y}_c the input acceleration in order to solve the equations of motion. Now, from Figure K.1(a), the undeflected length \mathcal{L}_{20} of the spring k_2 is

$$\mathcal{L}_{20} = y_{02} - y_{01}$$

K.4

and the deflected length \mathcal{L}_2 is

$$\mathcal{L}_2 = y_2 - y_1$$

K.5

The deflection, δ_2 , in the spring k_2 is, by definition

$$\begin{aligned} \delta_2 &= \mathcal{L}_{20} - \mathcal{L}_2 \\ &= y_{02} - y_{01} - y_2 + y_1 \end{aligned}$$

K.6

Equation K.6 is differentiated twice with respect to time to give

$$\ddot{\delta}_2 = \ddot{y}_1 - \ddot{y}_2$$

K.7

since y_{02} and y_{01} are constants and hence

$$\dot{y}_{02} = \dot{y}_{01} = 0$$

Similarly, (since the masses m_2 and m_3 and their spring-damper systems may be interchanged without loss of generality)

$$\ddot{\delta}_3 = \ddot{y}_1 - \ddot{y}_3$$

K.8

The undeflected length of spring k_1 is (see Fig. K.1(a)) y_{01} and the deflected length $y_1 - y_c$

So, by definition

$$\delta_1 = y_{o1} - y_1 + y_c \quad K.9$$

which, after differentiating twice with respect to time, yields

$$\ddot{\delta}_1 = \ddot{y}_c - \ddot{y}_1 \quad K.10$$

since y_{o1} is a constant and so $\dot{y}_{o1} = 0$.

The three equations K.7, K.8 and K.10 may now be solved to give

$$\ddot{y}_1, \ddot{y}_2 \text{ and } \ddot{y}_3 \text{ in terms of } \ddot{\delta}_1, \ddot{\delta}_2, \ddot{\delta}_3 \text{ and } \ddot{y}_c$$

Equation K.10 is rearranged and so giving

$$\ddot{y}_1 = \ddot{y}_c - \ddot{\delta}_1 \quad K.11$$

Equations K.7 and K.11 are now used to give an expression for \ddot{y}_2

$$\ddot{y}_2 = \ddot{y}_1 - \ddot{\delta}_2 \quad (\text{from Equation K.7})$$

But, $\ddot{y}_1 = \ddot{y}_c - \ddot{\delta}_1$ so that on substituting for \ddot{y}_1 above, the required form for \ddot{y}_2 is obtained.

$$\ddot{y}_2 = \ddot{y}_c - \ddot{\delta}_1 - \ddot{\delta}_2 \quad K.12$$

Similarly, the expression for \ddot{y}_3 is obtained by using Equations K.8 and K.11 to give

$$\ddot{y}_3 = \ddot{y}_c - \ddot{\delta}_1 - \ddot{\delta}_3 \quad K.13$$

The expressions for \ddot{y}_1 , \ddot{y}_2 and \ddot{y}_3 are now used in the set of Equations K.3 to give the equations of motion in a form consistent with that used throughout the appendices. The equations of motion become

$$\begin{aligned} m_1(\ddot{y}_c - \ddot{\delta}_1) &= k_1 \delta_1 + 2k_1 \dot{\delta}_1 - k_2 \delta_2 - 2k_2 \dot{\delta}_2 - k_3 \delta_3 - 2k_3 \dot{\delta}_3 \\ m_2(\ddot{y}_c - \ddot{\delta}_1 - \ddot{\delta}_2) &= k_2 \delta_1 + 2k_2 \dot{\delta}_2 \\ m_3(\ddot{y}_c - \ddot{\delta}_1 - \ddot{\delta}_3) &= k_3 \delta_3 + 2k_3 \dot{\delta}_3 \end{aligned} \quad K.14$$

These equations are now rearranged and divided through by the appropriate mass to give

$$\begin{aligned} \ddot{\delta}_1 + \frac{2k_1}{m_1} \dot{\delta}_1 + \frac{k_1}{m_1} \delta_1 - 2\frac{k_2}{m_1} \dot{\delta}_2 - \frac{k_2}{m_1} \delta_2 - \frac{2k_3}{m_1} \dot{\delta}_3 - \frac{k_3}{m_1} \delta_3 &= \ddot{y}_c \\ \ddot{\delta}_1 + \ddot{\delta}_2 + 2\frac{k_2}{m_2} \dot{\delta}_2 + \frac{k_2}{m_2} \delta_2 &= \ddot{y}_c \\ \ddot{\delta}_1 + \ddot{\delta}_3 + 2\frac{k_3}{m_3} \dot{\delta}_3 + \frac{k_3}{m_3} \delta_3 &= \ddot{y}_c \end{aligned} \quad K.15$$

Certain parameters of the system can now be defined as follows

$$\frac{k_i}{m_i} = \omega_i^2, \quad \frac{K_i}{m_i} = c_i, \quad i = 1, 2, 3 \quad \text{K.16}$$

where ω_i is the uncoupled frequency of the appropriate spring-mass system and C is the damping coefficient.

Note that

$$\frac{k_i}{m_j} = \frac{m_i}{m_j} \cdot \frac{k_i}{m_i} = \frac{m_i}{m_j} \omega_i^2 \quad j = 1, 2, 3$$

and

$$\frac{K_i}{m_j} = \frac{m_i}{m_j} \frac{K_i}{m_i} = \frac{m_i}{m_j} c_i$$

so that using these parameters (K.16) in the equations of motion gives

$$\begin{aligned} \ddot{\delta}_1 + 2c_1\dot{\delta}_1 + \omega_1^2\delta_1 - 2\frac{m_2}{m_1}c_2\dot{\delta}_2 - \frac{m_2}{m_1}\omega_2^2\delta_2 - 2\frac{m_3}{m_1}c_3\dot{\delta}_3 - \frac{m_3}{m_1}\omega_3^2\delta_3 &= \ddot{y}_c \\ \ddot{\delta}_1 + \ddot{\delta}_2 + 2c_2\dot{\delta}_2 + \omega_2^2\delta_2 &= \ddot{y}_c \\ \ddot{\delta}_1 + \ddot{\delta}_3 + 2c_3\dot{\delta}_3 + \omega_3^2\delta_3 &= \ddot{y}_c \end{aligned} \quad \text{K.17}$$

These are the equations of motion of the system for which a solution is required using the Laplace transform method.

Solution of the Equations of Motion

There are two distinct input accelerations of interest and for which experimental results exist. These are:

- (a) short duration input with duration times, less than one second (Ref. K.2)
- (b) long (seconds or minutes) duration sinusoidal inputs as reported in Ref. K.1

The solution for case (a) will be obtained by the use of the Laplace transformation, as in previous appendices. The method used for case (b) will be explained during the solution.

(a) The General Case of the Rectangular Input

In this case the solution follows along lines similar to that of previous appendices. It will be remembered that the Laplace transform for a rectangular input acceleration, of the form $\ddot{y} = \text{constant}$ from $t = 0$ to $t = \Delta t$ is (see Appendix J or Transform 78, page 136, Ref. K.3).

$$\ddot{y}_c (1 - e^{-\Delta t p})$$

Then, for $\delta_i = \dot{\delta}_i = 0$ at $t = 0$, Equations K.17 transform readily into

$$\ddot{y}_c (1 - e^{-p\Delta t}) = (p^2 + 2c_1 p + \omega_1^2)x_1 - \frac{m_2}{m_1}(2c_2 p + \omega_2^2)x_2 - \frac{m_3}{m_1}(2c_3 p + \omega_3^2)x_3 \quad K.18(a)$$

$$\ddot{y}_c (1 - e^{-p\Delta t}) = p^2 x_1 + (p^2 + 2c_2 p + \omega_2^2)x_2 \quad K.18(b)$$

$$\ddot{y}_c (1 - e^{-p\Delta t}) = p^2 x_1 + (p^2 + 2c_3 p + \omega_3^2)x_3 \quad K.18(c)$$

The second and third Equations K.18 may be rewritten to give x_2 and x_3 in terms of x_1 and p as follows

$$x_2 = \frac{\ddot{y}_c (1 - e^{-p\Delta t}) - p^2 x_1}{p^2 + 2c_2 p + \omega_2^2} \quad K.19(a)$$

$$x_3 = \frac{\ddot{y}_c (1 - e^{-p\Delta t}) - p^2 x_1}{p^2 + 2c_3 p + \omega_3^2} \quad K.19(b)$$

The expressions for x_2 and x_3 from Equation K.19 are now substituted in Equation K.18(a) to give the following equation for x_1 ,

$$\begin{aligned} \ddot{y}_c (1 - e^{-p\Delta t}) = & (p^2 + 2c_1 p + \omega_1^2)x_1 - \frac{m_2}{m_1}(2c_2 p + \omega_2^2) \left(\frac{\ddot{y}_c (1 - e^{-p\Delta t}) - p^2 x_1}{p^2 + 2c_2 p + \omega_2^2} \right) \\ & - \frac{m_3}{m_1}(2c_3 p + \omega_3^2) \left(\frac{\ddot{y}_c (1 - e^{-p\Delta t}) - p^2 x_1}{p^2 + 2c_3 p + \omega_3^2} \right) \end{aligned} \quad K.20$$

This expression is now multiplied throughout by

$$(p^2 + 2c_2 p + \omega_2^2)(p^2 + 2c_3 p + \omega_3^2)$$

to clear the denominators, and the terms inside the brackets are expanded and regrouped.

In the first instance, only the terms independent of x_1 will be collected and transferred to the right side of K.20, so

$$\begin{aligned} \text{Right side} = & \ddot{y}_c (1 - e^{-p\Delta t}) \{ (p^2 + 2c_1 p + \omega_1^2)(p^2 + 2c_3 p + \omega_3^2) \\ & + \frac{m_2}{m_1}(2c_2 p + \omega_2^2)(p^2 + 2c_3 p + \omega_3^2) + \frac{m_3}{m_1}(2c_3 p + \omega_3^2)(p^2 + 2c_2 p + \omega_2^2) \} \end{aligned}$$

$$\begin{aligned}
= & \ddot{y}_c (1 - e^{-p\Delta t}) \left\{ p^4 + p^3 (2c_2 + 2c_3 + \frac{m_2}{m_1} 2c_2 + \frac{m_3}{m_1} 2c_3) \right. \\
& + p^2 (\omega_1^2 + \omega_3^2 + 4c_2c_3 + \frac{m_2}{m_1} \omega_1^2 + \frac{m_3}{m_1} \omega_3^2 + \frac{m_2}{m_1} 4c_2c_3 + \frac{m_3}{m_1} 4c_2c_3) \\
& + p (2c_2\omega_3^2 + 2c_3\omega_1^2 + \frac{m_2}{m_1} 2c_2\omega_3^2 + \frac{m_3}{m_1} 2c_3\omega_1^2 + \frac{m_2}{m_1} 2c_3\omega_1^2 + \frac{m_3}{m_1} 2c_2\omega_3^2) \\
& \left. + \omega_1^2\omega_3^2 + \frac{m_2}{m_1} \omega_1^2\omega_3^2 + \frac{m_3}{m_1} \omega_1^2\omega_3^2 \right\} \quad K.21
\end{aligned}$$

$$\begin{aligned}
= & \ddot{y}_c (1 - e^{-p\Delta t}) \left\{ p^4 + 2 \left[\left(1 + \frac{m_2}{m_1}\right) c_2 + \left(1 + \frac{m_3}{m_1}\right) c_3 \right] p^3 \right. \\
& + \left[\left(1 + \frac{m_2}{m_1}\right) \omega_1^2 + \left(1 + \frac{m_3}{m_1}\right) \omega_3^2 + 4 \left(1 + \frac{m_2}{m_1} + \frac{m_3}{m_1}\right) c_2c_3 \right] p^2 \\
& \left. + 2 \left(1 + \frac{m_2}{m_1} + \frac{m_3}{m_1}\right) (c_2\omega_3^2 + c_3\omega_1^2) p + \left(1 + \frac{m_2}{m_1} + \frac{m_3}{m_1}\right) \omega_1^2\omega_3^2 \right\}
\end{aligned}$$

The terms containing \mathcal{X}_1 are now collected on the left side

$$\begin{aligned}
\mathcal{X}_1 \left\{ (p^2 + 2c_1p + \omega_1^2)(p^2 + 2c_2p + \omega_2^2)(p^2 + 2c_3p + \omega_3^2) + \frac{m_2}{m_1} (2c_2p + \omega_2^2) p^2 (p^2 + 2c_3p + \omega_3^2) \right. \\
\left. + \frac{m_3}{m_1} (2c_3p + \omega_3^2) p^2 (p^2 + 2c_2p + \omega_2^2) \right\} \\
= \mathcal{X}_1 \left\{ p^6 + (2c_1 + 2c_2 + 2c_3) p^5 + (\omega_1^2 + \omega_2^2 + \omega_3^2 + 4c_1c_2 + 4c_2c_3 + 4c_3c_1) p^4 \right. \\
+ (2c_2\omega_3^2 + 2c_3\omega_1^2 + 2c_1\omega_2^2 + 2c_3\omega_1^2 + 2c_2\omega_1^2 + 2c_1\omega_2^2 + 8c_1c_2c_3) p^3 \\
+ (\omega_1^2\omega_2^2 + \omega_2^2\omega_3^2 + \omega_3^2\omega_1^2 + 4c_1c_2\omega_3^2 + 4c_2c_3\omega_1^2 + 4c_3c_1\omega_2^2) p^2 \\
+ (2c_1\omega_2^2\omega_3^2 + 2c_2\omega_3^2\omega_1^2 + 2c_3\omega_1^2\omega_2^2) p + \omega_1^2\omega_2^2\omega_3^2 \\
+ \frac{m_2}{m_1} [2c_2p^5 + (\omega_2^2 + 4c_2c_3) p^4 + 2(c_2\omega_3^2 + c_3\omega_1^2) p^3 + \omega_2^2\omega_3^2 p^2 \\
+ \frac{m_3}{m_1} [2c_3p^5 + (\omega_3^2 + 4c_2c_3) p^4 + 2(c_3\omega_1^2 + c_2\omega_2^2) p^3 + \omega_2^2\omega_3^2 p^2] \left. \right\} \quad K.22 \\
= \mathcal{X}_1 \left\{ p^6 + 2 \left[c_1 + \left(1 + \frac{m_2}{m_1}\right) c_2 + \left(1 + \frac{m_3}{m_1}\right) c_3 \right] p^5 \right. \\
+ \left[\omega_1^2 + \left(1 + \frac{m_2}{m_1}\right) \omega_2^2 + \left(1 + \frac{m_3}{m_1}\right) \omega_3^2 + 4c_1c_2 + 4 \left(1 + \frac{m_2}{m_1} + \frac{m_3}{m_1}\right) c_2c_3 + 4c_3c_1 \right] p^4 \\
+ 2 \left[\left(1 + \frac{m_2}{m_1} + \frac{m_3}{m_1}\right) (c_2\omega_3^2 + c_3\omega_1^2) + c_1\omega_2^2 + c_3\omega_1^2 + c_2\omega_1^2 + c_1\omega_2^2 + 4c_1c_2c_3 \right] p^3 \\
+ \left[\omega_1^2\omega_2^2 + \omega_2^2\omega_3^2 + \left(1 + \frac{m_2}{m_1} + \frac{m_3}{m_1}\right) \omega_1^2\omega_3^2 + 4c_1c_2\omega_3^2 + 4c_2c_3\omega_1^2 + 4c_3c_1\omega_2^2 \right] p^2 \\
\left. + 2 \left[c_1\omega_2^2\omega_3^2 + c_2\omega_3^2\omega_1^2 + c_3\omega_1^2\omega_2^2 \right] p + \omega_1^2\omega_2^2\omega_3^2 \right\} \quad K.23
\end{aligned}$$

When K.21 and K.22 are combined, an equation results that gives \mathcal{X} in terms of p , c and ω . Remembering that \mathcal{X} is the Laplace transform of δ , such an expression must contain information on the three natural modes of the system and by standard practice must factor to give the frequencies and damping in the modes. The system has three degrees of freedom and there are three ways (modes) in which

it can vibrate when considered as a combined system. Let Ω_i be the undamped frequency and \bar{C}_i the associated damping of each mode. The damped frequency of vibration is therefore given by

$$\bar{\Omega}_i^2 = \Omega_i^2 - \bar{C}_i^2$$

which represents the sub-critically damped case of $\bar{C}_i < \Omega_i$ (compare Appendix E). K.23 may now be expressed as

$$x_1 (p^2 + 2\bar{C}_1 p + \Omega_1^2) (p^2 + 2\bar{C}_2 p + \Omega_2^2) (p^2 + 2\bar{C}_3 p + \Omega_3^2) \quad K.24$$

which follows from similar reasoning to that used in Appendix J in obtaining Equation J.31(b) from J.26. This expression may be expanded and written in descending powers of p as follows

$$\begin{aligned} x_1 \{ & p^6 + 2(\bar{C}_1 + \bar{C}_2 + \bar{C}_3)p^5 + (\Omega_1^2 + \Omega_2^2 + \Omega_3^2 + 4\bar{C}_1\bar{C}_2 + 4\bar{C}_1\bar{C}_3 + 4\bar{C}_2\bar{C}_3)p^4 \\ & + 2(\bar{C}_2\Omega_3^2 + \bar{C}_3\Omega_2^2 + \bar{C}_1\Omega_3^2 + \bar{C}_3\Omega_1^2 + \bar{C}_2\Omega_1^2 + \bar{C}_1\Omega_2^2 + 4\bar{C}_1\bar{C}_2\bar{C}_3)p^3 \\ & + (\Omega_1^2\Omega_2^2 + \Omega_1^2\Omega_3^2 + \Omega_2^2\Omega_3^2 + 4\bar{C}_1\bar{C}_2\Omega_3^2 + 4\bar{C}_2\bar{C}_3\Omega_1^2 + 4\bar{C}_3\bar{C}_1\Omega_2^2)p^2 \\ & + 2(\bar{C}_1\Omega_2^2\Omega_3^2 + \bar{C}_2\Omega_3^2\Omega_1^2 + \bar{C}_3\Omega_1^2\Omega_2^2)p + \Omega_1^2\Omega_2^2\Omega_3^2 \} \quad K.25 \end{aligned}$$

Now, if K.24 is expression K.23 factored, then K.23 and K.25 must be identical and so the coefficients of powers of p may be equated to give the following equations for ω_i and C_i in terms of Ω_i and \bar{C}_i .

$$C_1 + (1 + \frac{m_2}{m_1})C_2 + (1 + \frac{m_3}{m_1})C_3 = \bar{C}_1 + \bar{C}_2 + \bar{C}_3 \quad K.26(a)$$

$$\omega_1^2 + (1 + \frac{m_2}{m_1})\omega_2^2 + (1 + \frac{m_3}{m_1})\omega_3^2 + 4C_1C_2 + 4(1 + \frac{m_2}{m_1} + \frac{m_3}{m_1})C_1C_3 + 4C_2C_3 = \Omega_1^2 + \Omega_2^2 + \Omega_3^2 + 4\bar{C}_1\bar{C}_2 + 4\bar{C}_1\bar{C}_3 + 4\bar{C}_2\bar{C}_3 \quad (b)$$

$$(1 + \frac{m_2}{m_1} + \frac{m_3}{m_1})(C_2\omega_3^2 + C_3\omega_2^2) + C_1\omega_3^2 + C_3\omega_1^2 + C_2\omega_1^2 + C_1\omega_2^2 + 4C_1C_2C_3 = \bar{C}_2\Omega_3^2 + \bar{C}_3\Omega_2^2 + \bar{C}_1\Omega_3^2 + \bar{C}_3\Omega_1^2 + \bar{C}_2\Omega_1^2 + \bar{C}_1\Omega_2^2 + 4\bar{C}_1\bar{C}_2\bar{C}_3 \quad (c)$$

$$\omega_1^2\omega_2^2 + \omega_3^2\omega_1^2 + (1 + \frac{m_2}{m_1} + \frac{m_3}{m_1})\omega_2^2\omega_3^2 + 4C_1C_2\omega_3^2 + 4C_2C_3\omega_1^2 + 4C_3C_1\omega_2^2 = \Omega_1^2\Omega_2^2 + \Omega_2^2\Omega_3^2 + \Omega_3^2\Omega_1^2 + 4\bar{C}_1\bar{C}_2\Omega_3^2 + 4\bar{C}_2\bar{C}_3\Omega_1^2 + 4\bar{C}_3\bar{C}_1\Omega_2^2 \quad (d)$$

$$C_1\omega_2^2\omega_3^2 + C_2\omega_3^2\omega_1^2 + C_3\omega_1^2\omega_2^2 = \bar{C}_1\Omega_2^2\Omega_3^2 + \bar{C}_2\Omega_3^2\Omega_1^2 + \bar{C}_3\Omega_1^2\Omega_2^2 \quad (e)$$

$$\omega_1^2\omega_2^2\omega_3^2 = \Omega_1^2\Omega_2^2\Omega_3^2 \quad (f)$$

Ω_i and \bar{C}_i may be obtained from test data e.g. from Ref. 1 and Ref. 2, and an iterative solution of Equations K.26 can be obtained. To avoid tedious calculations, an IBM 1620 digital computer has been programmed to obtain a solution to Equation K.26 for assumed mass ratios. The solution gives values of ω_i and C_i which refer to the individual characteristics of the component mass-spring systems.

x_1 may now be expressed in terms of known quantities and p from Expression K.21 and K.24 as follows, since the right and left hand sides of Equation K.20 regrouped

$$x_1 = \ddot{y}_c (1 - e^{-p\Delta t}) \frac{p^4 + B_3 p^3 + B_2 p^2 + B_1 p + B_0}{(p^2 + 2\bar{c}_1 p + \Omega_1^2)(p^2 + 2\bar{c}_2 p + \Omega_2^2)(p^2 + 2\bar{c}_3 p + \Omega_3^2)} \quad K.27$$

where $B_3 = 2 \left\{ \left(1 + \frac{m_2}{m_1}\right) c_2 + \left(1 + \frac{m_3}{m_1}\right) c_3 \right\}$

$$B_2 = \left(1 + \frac{m_2}{m_1}\right) \omega_2^2 + \left(1 + \frac{m_3}{m_1}\right) \omega_3^2 + 4 \left(1 + \frac{m_2}{m_1} + \frac{m_3}{m_1}\right) c_2 c_3$$

$$B_1 = 2 \left(1 + \frac{m_2}{m_1} + \frac{m_3}{m_1}\right) (c_2 \omega_3^2 + c_3 \omega_2^2)$$

$$B_0 = \left(1 + \frac{m_2}{m_1} + \frac{m_3}{m_1}\right) \omega_2^2 \omega_3^2$$

from K.21 and the C_i and ω_i are known from K.26. In order to proceed with the solution, the right side of Equation K.27 must be expressed in the form of partial fractions, so let

$$x_1 = \ddot{y}_c (1 - e^{-p\Delta t}) \left\{ \frac{\alpha_1 p + \beta_1}{p^2 + 2\bar{c}_1 p + \Omega_1^2} + \frac{\alpha_2 p + \beta_2}{p^2 + 2\bar{c}_2 p + \Omega_2^2} + \frac{\alpha_3 p + \beta_3}{p^2 + 2\bar{c}_3 p + \Omega_3^2} \right\} \quad K.28$$

The α_i and β_i are evaluated by combining the terms inside the curly bracket of Equation K.28 and equating the coefficients of the powers of p so obtained, to those of Equation K.27, since this is the condition for the two expressions to be identical. Thus, K.28

becomes

$$x_1 = \ddot{y}_c \frac{(1 - e^{-p\Delta t})}{(p^2 + 2\bar{c}_1 p + \Omega_1^2)(p^2 + 2\bar{c}_2 p + \Omega_2^2)(p^2 + 2\bar{c}_3 p + \Omega_3^2)} \left\{ (\alpha_1 p + \beta_1)(p^2 + 2\bar{c}_2 p + \Omega_2^2)(p^2 + 2\bar{c}_3 p + \Omega_3^2) \right. \\ \left. + (\alpha_2 p + \beta_2)(p^2 + 2\bar{c}_3 p + \Omega_3^2)(p^2 + 2\bar{c}_1 p + \Omega_1^2) + (\alpha_3 p + \beta_3)(p^2 + 2\bar{c}_1 p + \Omega_1^2)(p^2 + 2\bar{c}_2 p + \Omega_2^2) \right\} \quad K.29$$

$$x_1 = \ddot{y}_c \frac{(1 - e^{-p\Delta t})}{D} \left\{ (\alpha_1 + \alpha_2 + \alpha_3) p^5 + [\beta_1 + \beta_2 + \beta_3 + 2\alpha_1(\bar{c}_2 + \bar{c}_3) + 2\alpha_2(\bar{c}_3 + \bar{c}_1) + 2\alpha_3(\bar{c}_1 + \bar{c}_2)] p^4 \right. \\ + [\alpha_1(\Omega_2^2 + \Omega_3^2 + 4\bar{c}_2\bar{c}_3) + \alpha_2(\Omega_3^2 + \Omega_1^2 + 4\bar{c}_3\bar{c}_1) + \alpha_3(\Omega_1^2 + \Omega_2^2 + 4\bar{c}_1\bar{c}_2) + 2\beta_1(\bar{c}_2 + \bar{c}_3) + 2\beta_2(\bar{c}_3 + \bar{c}_1) \\ + 2\beta_3(\bar{c}_1 + \bar{c}_2)] p^3 + [\beta_1(\Omega_2^2 + \Omega_3^2 + 4\bar{c}_2\bar{c}_3) + \beta_2(\Omega_3^2 + \Omega_1^2 + 4\bar{c}_3\bar{c}_1) + \beta_3(\Omega_1^2 + \Omega_2^2 + 4\bar{c}_1\bar{c}_2) \\ + \alpha_1(2\bar{c}_2\Omega_3^2 + 2\bar{c}_3\Omega_2^2) + \alpha_2(2\bar{c}_3\Omega_1^2 + 2\bar{c}_1\Omega_3^2) + \alpha_3(2\bar{c}_1\Omega_2^2 + 2\bar{c}_2\Omega_1^2)] p^2 \\ + [\alpha_1\Omega_2^2\Omega_3^2 + \alpha_2\Omega_3^2\Omega_1^2 + \alpha_3\Omega_1^2\Omega_2^2 + 2\beta_1(\bar{c}_2\Omega_3^2 + \bar{c}_3\Omega_2^2) + 2\beta_2(\bar{c}_3\Omega_1^2 + \bar{c}_1\Omega_3^2) + 2\beta_3(\bar{c}_1\Omega_2^2 + \bar{c}_2\Omega_1^2)] p \\ \left. + \beta_1\Omega_2^2\Omega_3^2 + \beta_2\Omega_3^2\Omega_1^2 + \beta_3\Omega_1^2\Omega_2^2 \right\} \quad K.30$$

where $D = (p^2 + 2\bar{c}_1 p + \Omega_1^2)(p^2 + 2\bar{c}_2 p + \Omega_2^2)(p^2 + 2\bar{c}_3 p + \Omega_3^2)$

Equating coefficients of powers of p in Equation K.27 and K.30 gives the following equations

$$\alpha_1 + \alpha_2 + \alpha_3 = 0 \quad K.31(a)$$

$$\beta_1 + \beta_2 + \beta_3 + 2\alpha_1(\bar{c}_2 + \bar{c}_3) + 2\alpha_2(\bar{c}_3 + \bar{c}_1) + 2\alpha_3(\bar{c}_1 + \bar{c}_2) = 1 \quad (b)$$

$$\alpha_1(-\Omega_2^2 + \Omega_3^2 + 4\bar{c}_1\bar{c}_3) + \alpha_2(-\Omega_3^2 + \Omega_1^2 + 4\bar{c}_3\bar{c}_1) + \alpha_3(-\Omega_1^2 + \Omega_2^2 + 4\bar{c}_1\bar{c}_2) \quad K.31(c)$$

$$+ 2\beta_1(\bar{c}_2 + \bar{c}_3) + 2\beta_2(\bar{c}_3 + \bar{c}_1) + 2\beta_3(\bar{c}_1 + \bar{c}_2) = B_3$$

$$\beta_1(\Omega_1^2 + \Omega_3^2 + 4\bar{c}_2\bar{c}_3) + \beta_2(-\Omega_3^2 + \Omega_1^2 + 4\bar{c}_3\bar{c}_1) + \beta_3(-\Omega_1^2 + \Omega_2^2 + 4\bar{c}_1\bar{c}_2) \\ + \alpha_1(2\bar{c}_2\Omega_3^2 + 2\bar{c}_3\Omega_2^2) + \alpha_2(2\bar{c}_3\Omega_1^2 + 2\bar{c}_1\Omega_3^2) + \alpha_3(2\bar{c}_1\Omega_2^2 + 2\bar{c}_2\Omega_1^2) = B_2 \quad (d)$$

$$\alpha_1\Omega_2^2\Omega_3^2 + \alpha_2\Omega_3^2\Omega_1^2 + \alpha_3\Omega_1^2\Omega_2^2 + 2\beta_1(\bar{c}_2\Omega_3^2 + \bar{c}_3\Omega_2^2) \\ + 2\beta_2(\bar{c}_3\Omega_1^2 + \bar{c}_1\Omega_3^2) + 2\beta_3(\bar{c}_1\Omega_2^2 + \bar{c}_2\Omega_1^2) = B_1 \quad (e)$$

$$\beta_1\Omega_2^2\Omega_3^2 + \beta_2\Omega_3^2\Omega_1^2 + \beta_3\Omega_1^2\Omega_2^2 = B_0 \quad (f)$$

These equations can also be solved with the aid of a digital computer to yield values for the α 's and β 's.

Returning to Equation K.28 and applying transforms 50 and 51, pages 133 and 134 of Ref. 3, the solution of the problem may be written in terms of α_i , β_i , Ω_i and \bar{c}_i . For convenience, the transforms are written here and combined, the case of $\Omega_i^2 > \bar{c}_i^2$ is considered.

$$L^{-1} \frac{p}{p^2 + 2\bar{c}p + \Omega^2} = \frac{e^{-\bar{c}t}}{\bar{\Omega}} \sin \bar{\Omega} t$$

$$L^{-1} \frac{1}{p^2 + 2\bar{c}p + \Omega^2} = \frac{1}{\Omega^2} \left\{ 1 - \frac{\Omega}{\bar{\Omega}} e^{-\bar{c}t} \sin(\bar{\Omega} t + \phi) \right\}$$

$$L^{-1} \frac{\alpha p + \beta}{p^2 + 2\bar{c}p + \Omega^2} = \frac{\alpha}{\bar{\Omega}} e^{-\bar{c}t} \sin \bar{\Omega} t + \frac{\beta}{\Omega^2} \left\{ 1 + \frac{\Omega}{\bar{\Omega}} e^{-\bar{c}t} \sin(\bar{\Omega} t + \phi) \right\}$$

where $\bar{\Omega}^2 = \Omega^2 - \bar{c}^2$, $\tan \phi = \frac{\bar{\Omega}}{\bar{c}}$

Combining this result with Theorem VII gives for $t > \Delta t$

$$L^{-1} \frac{\alpha p + \beta}{p^2 + 2\bar{c}p + \Omega^2} (1 - e^{-p\Delta t}) = \frac{\alpha}{\bar{\Omega}} e^{-\bar{c}t} \sin \bar{\Omega} t + \frac{\beta}{\Omega^2} \left\{ 1 - \frac{\Omega}{\bar{\Omega}} e^{-\bar{c}t} \sin(\bar{\Omega} t + \phi) \right\} \\ - \frac{\alpha}{\bar{\Omega}} e^{-\bar{c}(t-\Delta t)} \sin \bar{\Omega}(t-\Delta t) - \frac{\beta}{\Omega^2} \left\{ 1 - \frac{\Omega}{\bar{\Omega}} e^{-\bar{c}(t-\Delta t)} \sin[\bar{\Omega}(t-\Delta t) + \phi] \right\}$$

and for $t < \Delta t$

$$L^{-1} \frac{\alpha p + \beta}{p^2 + 2\bar{c}p + \Omega^2} (1 - e^{-p\Delta t}) = \frac{\alpha}{\bar{\Omega}} e^{-\bar{c}t} \sin \bar{\Omega} t + \frac{\beta}{\Omega^2} \left\{ 1 - \frac{\Omega}{\bar{\Omega}} e^{-\bar{c}t} \sin(\bar{\Omega} t + \phi) \right\}$$

The \sum notation is now introduced in order to abbreviate the equations. On inspection of Equation K.28 it is seen that the right side of the equation consists of three terms of the form

$$\ddot{y}_c (1 - e^{-\bar{c}t}) \frac{\alpha t + \beta}{p^2 + 2\bar{c}p + \Omega^2}$$

for which the inverse Laplace transform has been obtained above.

The solution now follows

$$\begin{aligned} t > \Delta t \\ \delta_1 = \ddot{y}_c \sum_{i=1}^{i=3} \left[\frac{\alpha_i}{\bar{\Omega}_i} e^{-\bar{c}t} \left\{ \sin \bar{\Omega}_i t - e^{\Delta t} \sin \bar{\Omega}_i (t - \Delta t) \right\} \right. \\ \left. + \frac{\beta_i}{\bar{\Omega}_i \bar{\Omega}_i} e^{-\bar{c}t} \left\{ e^{\Delta t} \sin (\bar{\Omega}_i (t - \Delta t) + \phi_i) - \sin (\bar{\Omega}_i t + \phi_i) \right\} \right] \end{aligned} \quad \text{K.32(a)}$$

and for $t < \Delta t$

$$\delta_1 = \ddot{y}_c \sum_{i=1}^{i=3} \left[\frac{\alpha_i}{\bar{\Omega}_i} e^{-\bar{c}t} \sin \bar{\Omega}_i t + \frac{\beta_i}{\bar{\Omega}_i^2} \left\{ 1 - \frac{\bar{\Omega}_i}{\bar{\Omega}_i} e^{-\bar{c}t} \sin (\bar{\Omega}_i t + \phi_i) \right\} \right] \quad \text{(b)}$$

where

$$\phi_i = \tan^{-1} \frac{\bar{\Omega}_i}{\bar{c}}$$

and

$$\bar{\Omega}_i^2 = \Omega_i^2 - \bar{c}_i^2$$

Since the terms involving damping have been retained, the spring is no longer the sole means of transmitting force and the limitation on δ cannot necessarily be used to determine limiting g's.

Total force exerted on the mass by its associated spring-damper system, will be used as a tolerance criterion in the spinal mode, considered here. This force is given by

$$F = m_1 (\omega_1^2 \delta_1 + 2c_1 \dot{\delta}_1)$$

or written as an acceleration

$$\ddot{y}_1 = \omega_1^2 \delta_1 + 2c_1 \dot{\delta}_1 \quad \text{K.33}$$

the acceleration that the mass m_1 would experience if masses m_2 and m_3 were detached. An expression for $\dot{\delta}_1$ must be obtained from Equation K.32 in order that \ddot{y}_1 may be evaluated.

Differentiating Equation K.32 involves differentiating expressions

such as

$$e^{-\bar{c}(t-\Delta t)} \sin \{ \bar{\Omega}(t-\Delta t) + \phi \} \quad K.34$$

where \bar{c} , $\bar{\Omega}$, Δt and ϕ are independent of time.

The well known formula

$$\frac{d}{dt}(uv) = u \frac{du}{dt} + u \frac{dv}{dt} \quad K.35$$

is used to differentiate Expression K.34. Replacing u by $e^{-\bar{c}(t-\Delta t)}$ and v by $\sin \{ \bar{\Omega}(t-\Delta t) + \phi \}$ in K.35 yields

$$\begin{aligned} \frac{d}{dt} \{ e^{-\bar{c}(t-\Delta t)} \sin [\bar{\Omega}(t-\Delta t) + \phi] \} \\ = \sin [\bar{\Omega}(t-\Delta t) + \phi] [-\bar{c} e^{-\bar{c}(t-\Delta t)}] + e^{-\bar{c}(t-\Delta t)} \bar{\Omega} \cos [\bar{\Omega}(t-\Delta t) + \phi] \\ = e^{-\bar{c}(t-\Delta t)} [-\bar{c} \sin \{ \bar{\Omega}(t-\Delta t) + \phi \} + \bar{\Omega} \cos \{ \bar{\Omega}(t-\Delta t) + \phi \}] \end{aligned}$$

But $\phi = \tan^{-1} \frac{\bar{\Omega}}{\bar{c}}$, therefore

$$\sin \phi = \left\{ \frac{\bar{\Omega}^2}{\bar{\Omega}^2 + \bar{c}^2} \right\}^{1/2} = \frac{\bar{\Omega}}{\bar{\Omega}^2 + \bar{c}^2}^{1/2}$$

$$\cos \phi = \left\{ \frac{\bar{c}^2}{\bar{\Omega}^2 + \bar{c}^2} \right\}^{1/2} = \frac{\bar{c}}{\bar{\Omega}^2 + \bar{c}^2}^{1/2}$$

since $\bar{\Omega}^2 = \bar{\Omega}^2 - \bar{c}^2$

therefore

$$\begin{aligned} \frac{d}{dt} (e^{-\bar{c}(t-\Delta t)} \sin \{ \bar{\Omega}(t-\Delta t) + \phi \}) \\ = \bar{\Omega} e^{-\bar{c}(t-\Delta t)} [-\cos \phi \sin \{ \bar{\Omega}(t-\Delta t) + \phi \} + \sin \phi \cos \{ \bar{\Omega}(t-\Delta t) + \phi \}] \\ = -\bar{\Omega} e^{-\bar{c}(t-\Delta t)} \sin \bar{\Omega}(t-\Delta t) \end{aligned} \quad K.36$$

on application of the identity

$$\sin(A+B) = \sin A \cos B + \cos A \sin B$$

Using this result in differentiating K.32 gives

for $t > \Delta t_{i=3}$

$$\begin{aligned} \dot{s}_i = \ddot{y}_c \sum_{i=1} \left[\frac{\alpha_i \bar{\Omega}_i}{\bar{\Omega}} e^{-\bar{c}_i t} \{ e^{\Delta t} \sin(\bar{\Omega}_i(t-\Delta t) - \phi) - \sin(\bar{\Omega}_i t - \phi) \} \right. \\ \left. + \frac{\beta_i}{\bar{\Omega}_i} e^{-\bar{c}_i t} \{ \sin \bar{\Omega}_i t - e^{\Delta t} \sin(\bar{\Omega}_i(t-\Delta t)) \} \right] \end{aligned}$$

and for $t < \Delta t$

$$\dot{\delta}_i = -\ddot{y}_c \sum \left\{ \frac{\alpha_i \Omega_i}{\bar{\Omega}_i} e^{-\bar{c}_i t} \sin(\bar{\Omega}_i t - \phi_i) - \frac{\beta_i}{\bar{\Omega}_i} e^{-\bar{c}_i t} \sin \bar{\Omega}_i t \right\} \quad K.37$$

A program for the IBM 1620 digital computer has been written for the evaluation of the quantity \ddot{y}_p so that its maximum value may be obtained by inspection of a plot of \ddot{y}_p against time.

Since the step input acceleration (continuous) case is the limit of the rectangular input case as $\Delta t \rightarrow \infty$ the above solution of δ_i for $t < \Delta t$ is also the solution for the step input.

Impulsive Input Acceleration

The Dirac impulse function (see Appendix E) is used again to obtain a solution for the impulsive input case. If v is the velocity change within the system due to the applied acceleration, then the Laplace transform of the input acceleration is

$$vp$$

The transformed equations of motion (Equation K.17) for $\ddot{y}_c = v \Delta(t)$ ($\Delta(t)$ is the Dirac impulse function) is then

$$vp = (p^2 + 2c_1 p + \omega_1^2)x_1 + \frac{m_2}{m_1}(2c_2 p + \omega_2^2)x_2 - \frac{m_3}{m_1}(2c_3 p + \omega_3^2)x_3 \quad K.38(a)$$

$$vp = p^2 x_1 + (p^2 + 2c_2 p + \omega_2^2)x_2 \quad (b)$$

$$vp = p^2 x_1 + (p^2 + 2c_3 p + \omega_3^2)x_3 \quad (c)$$

The set of Equations K.38 is the same as the set K.18 with vp replacing $\ddot{y}_c(1 - e^{-p\Delta t})$ and the solution of x_i from the set of Equations K.38 may be obtained from K.27 by replacing $\ddot{y}_c(1 - e^{-p\Delta t})$ by vp . Hence

$$x_1 = v \frac{p^5 + B_3 p^4 + B_2 p^3 + B_1 p^2 + B_0 p}{(p^2 + 2\bar{c}_1 p + \bar{\Omega}_1^2)(p^2 + 2\bar{c}_2 p + \bar{\Omega}_2^2)(p^2 + 2\bar{c}_3 p + \bar{\Omega}_3^2)} \quad K.39$$

K.39 is expressed in partial fractions (c.f. Equation K.28)

$$x_1 = \left\{ \frac{\alpha_1 p + \beta_1}{p^2 + 2\bar{c}_1 p + \bar{\Omega}_1^2} + \frac{\alpha_2 p + \beta_2}{p^2 + 2\bar{c}_2 p + \bar{\Omega}_2^2} + \frac{\alpha_3 + \beta_3}{p^2 + 2\bar{c}_3 p + \bar{\Omega}_3^2} \right\} \quad K.40$$

The results of Equation K.30 are used, with $\ddot{y}_c (1 - e^{-p\Delta t})$ replaced by v since only v is taken outside the brackets, so that the coefficients of powers of p may be equated. The following set of equations is obtained (c.f. Equation K.31)

$$\alpha_1 + \alpha_2 + \alpha_3 = 1 \quad \text{K.41(a)}$$

$$\beta_1 + \beta_2 + \beta_3 + 2\alpha_1(\bar{c}_2 + \bar{c}_3) + 2\alpha_2(\bar{c}_3 + \bar{c}_1) + 2\alpha_3(\bar{c}_1 + \bar{c}_2) = B_3 \quad \text{(b)}$$

$$\alpha_1(\Omega_2^2 + \Omega_3^2 + 4\bar{c}_1\bar{c}_3) + \alpha_2(\Omega_3^2 + \Omega_1^2 + 4\bar{c}_3\bar{c}_1) + \alpha_3(\Omega_1^2 + \Omega_2^2 + 4\bar{c}_1\bar{c}_2) + 2\beta_1(\bar{c}_2 + \bar{c}_3) + 2\beta_2(\bar{c}_3 + \bar{c}_1) + 2\beta_3(\bar{c}_1 + \bar{c}_2) = B_2 \quad \text{(c)}$$

$$\beta_1(\Omega_2^2 + \Omega_3^2 + 4\bar{c}_2\bar{c}_3) + \beta_2(\Omega_3^2 + \Omega_1^2 + 4\bar{c}_3\bar{c}_1) + \beta_3(\Omega_1^2 + \Omega_2^2 + 4\bar{c}_1\bar{c}_2) + \alpha_1(2\bar{c}_2\Omega_3^2 + 2\bar{c}_3\Omega_2^2) + \alpha_2(2\bar{c}_3\Omega_1^2 + 2\bar{c}_1\Omega_3^2) + \alpha_3(2\bar{c}_1\Omega_2^2 + 2\bar{c}_2\Omega_1^2) = B_1 \quad \text{(d)}$$

$$\alpha_1\Omega_2^2\Omega_3^2 + \alpha_2\Omega_3^2\Omega_1^2 + \alpha_3\Omega_1^2\Omega_2^2 + 2\beta_1(\bar{c}_2\Omega_3^2 + \bar{c}_3\Omega_2^2) + 2\beta_2(\bar{c}_3\Omega_1^2 + \bar{c}_1\Omega_3^2) + 2\beta_3(\bar{c}_1\Omega_2^2 + \bar{c}_2\Omega_1^2) = B_0 \quad \text{(e)}$$

$$\beta_1\Omega_2^2\Omega_3^2 + \beta_2\Omega_3^2\Omega_1^2 + \beta_3\Omega_1^2\Omega_2^2 = 0 \quad \text{(f)}$$

where B_0 through B_3 are obtained from Equation K.27.

The inverse Laplace transforms used for the previous case are applicable, so the solution may be obtained from K.32(b) by replacing \ddot{y}_c by v

Thence $i=3$

$$\delta_i = v \sum_{i=1}^3 \left[\frac{\alpha_i}{\bar{\Omega}_i} e^{-\bar{c}_i t} \sin \bar{\Omega}_i t + \frac{\beta_i}{\Omega_i^2} \left\{ 1 - \frac{\Omega_i}{\bar{\Omega}_i} e^{-\bar{c}_i t} \sin(\bar{\Omega}_i t + \phi_i) \right\} \right] \quad \text{K.42}$$

where

$$\phi_i = \tan^{-1} \frac{\bar{\Omega}_i}{\bar{c}_i}$$

and

$$\bar{\Omega}_i^2 = \Omega_i^2 - \bar{c}_i^2$$

Differentiating K.42 once with respect to time gives

$$\dot{\delta}_i = -v \sum_{i=1}^3 \left\{ \frac{\alpha_i \Omega_i}{\bar{\Omega}_i} e^{-\bar{c}_i t} \sin(\bar{\Omega}_i t - \phi_i) + \frac{\beta_i}{\bar{\Omega}_i} e^{-\bar{c}_i t} \sin \bar{\Omega}_i t \right\}$$

The technique and computer programs developed for the general rectangular input are used to maximize \ddot{y}_1 , the acceleration that the mass m_1 would experience if uncoupled from the system.

(b) Sinusoidal Input Acceleration

The equations of motion for this case are obtained from Equation K.17 on putting

$$\ddot{y}_c = \ddot{y}_{c0} \sin \omega t$$

where \ddot{y}_{c0} is the amplitude and ω the frequency of the input acceleration. The following equations are then obtained

$$\ddot{s}_1 + 2c_1 \dot{s}_1 + \omega_1^2 s_1 - 2 \frac{m_2}{m_1} c_2 \dot{s}_2 - \frac{m_2}{m_1} \omega_2^2 s_2 - 2 \frac{m_3}{m_1} c_3 \dot{s}_3 - \frac{m_3}{m_1} \omega_3^2 s_3 = \ddot{y}_{c0} \sin \omega t$$

$$\ddot{s}_1 + \ddot{s}_2 + 2c_2 \dot{s}_2 + \omega_2^2 s_2 = \ddot{y}_{c0} \sin \omega t$$

K.43

$$\ddot{s}_1 + \ddot{s}_3 + 2c_3 \dot{s}_3 + \omega_3^2 s_3 = \ddot{y}_{c0} \sin \omega t$$

The input acceleration is now written as the "Imaginary Part of"

$$\ddot{y}_{c0} e^{i\omega t}, \text{ where } i^2 = -1, \text{ since } e^{i\omega t} = \cos \omega t + i \sin \omega t.$$

The damping in the system will, after a sufficiently long time, attenuate all motion except that with a frequency ω (see Appendix E).

This part of the solution is known as the "steady state" solution.

If the solution represents an oscillation of frequency ω then it can be represented by $A_j e^{i\omega t}$ where A_j is some complex constant to be determined and $j = 1, 2, 3$.

$A_j e^{i\omega t}$ and $\ddot{y}_{c0} e^{i\omega t}$ are substituted for s_j and $\ddot{y}_{c0} \sin \omega t$ respectively. \dot{s}_j and \ddot{s}_j can be obtained by differentiation and since $\frac{d}{dt} e^{i\omega t} = i\omega e^{i\omega t}$, $e^{i\omega t}$ will be a factor of each term of each equation. Making these substitutions in K.43 and dividing throughout by $e^{i\omega t}$ gives

$$(-\omega^2 + i2c_1\omega + \omega_1^2) A_1 - \frac{m_2}{m_1} (i2c_2\omega + \omega_2^2) A_2 - \frac{m_3}{m_1} (i2c_3\omega + \omega_3^2) A_3 = \ddot{y}_{c0}$$

$$-\omega^2 A_1 + (-\omega^2 + i2c_2\omega + \omega_2^2) A_2 = \ddot{y}_{c0}$$

K.44

$$-\omega^2 A_1 + (-\omega^2 + i2c_3\omega + \omega_3^2) A_3 = \ddot{y}_{c0}$$

Since complex numbers have been introduced, the constant A_j is complex and, in order to continue with the solution, the real

constants μ and ν are defined as follows

$$\mu_j + i\nu_j = A_j$$

The above substitution for A_j is made and real and imaginary parts separated and equated on each side of each equation of the set K.44

$$\begin{aligned} (-\omega^2 + i2c_1\omega + \omega_1^2)(\mu_1 + i\nu_1) - \frac{m_2}{m_1}(i2c_2\omega + \omega_2^2)(\mu_2 + i\nu_2) \\ - \frac{m_3}{m_1}(i2c_3\omega + \omega_3^2)(\mu_3 + i\nu_3) = \ddot{y}_{co} \\ -\omega^2(\mu_1 + i\nu_1) + (-\omega^2 + i2c_2\omega + \omega_2^2)(\mu_2 + i\nu_2) = \ddot{y}_{co} \\ -\omega^2(\mu_1 + i\nu_1) + (-\omega^2 + i2c_3\omega + \omega_3^2)(\mu_3 + i\nu_3) = \ddot{y}_{co} \end{aligned}$$

On equating real and imaginary parts of each equation, the following set is obtained.

$$\begin{aligned} (\omega_1^2 - \omega^2)\mu_1 - \frac{m_2}{m_1}\omega_2^2\mu_2 - \frac{m_3}{m_1}\omega_3^2\mu_3 - 2c_1\omega\nu_1 + \frac{m_2}{m_1}2c_2\omega\nu_2 + \frac{m_3}{m_1}2c_3\omega\nu_3 &= \ddot{y}_{co} \\ 2c_1\omega\mu_1 - \frac{m_2}{m_1}2c_2\omega\mu_2 - \frac{m_3}{m_1}2c_3\omega\mu_3 + (\omega_1^2 - \omega^2)\nu_1 - \frac{m_2}{m_1}\omega_2^2\nu_2 - \frac{m_3}{m_1}\omega_3^2\nu_3 &= 0 \\ -\omega^2\mu_1 + (\omega_2^2 - \omega^2)\mu_2 - 2c_2\omega\nu_2 &= \ddot{y}_{co} \\ 2c_2\omega\mu_2 - \omega^2\nu_1 + (\omega_2^2 - \omega^2)\nu_2 &= 0 \\ -\omega^2\mu_1 + (\omega_3^2 - \omega^2)\mu_3 - 2c_3\omega\nu_3 &= \ddot{y}_{co} \\ 2c_3\omega\mu_3 - \omega^2\nu_1 + (\omega_3^2 - \omega^2)\nu_3 &= 0 \end{aligned}$$

K.45

The solution of these equations can be obtained numerically using a digital computer to give μ_j and ν_j , since ω_j, c_j are known from K.26.

The ratio R of the output or response amplitude to the input amplitude is now obtained

$$R_j = \frac{|A_j|}{\ddot{y}_{co}} = \frac{(\mu_j^2 + \nu_j^2)^{1/2}}{\ddot{y}_{co}}$$

K.46

and the phase angle

$$\psi_j = \frac{\nu_j}{\mu_j}$$

REFERENCES

<u>No.</u>	<u>Name</u>	<u>Title, etc.</u>
K.1	Coermann, R.R.	"The Mechanical Impedance of the Human Body in Sitting and Standing Position at Low Frequencies," ASD Technical Report, 61-492
K.2	Eiband, A.M.	"Human Tolerance to Rapidly Applied Accelerations: A Summary of the Literature," NASA Memo 5-19-59E
K.3	Pipes, L.A.	"Applied Mathematics for Engineers and Physicists," McGraw-Hill Book Co. Inc., New York, 1946

APPENDIX L

SUMMARY OF RELEVANT HOLLOMAN A.F.B. AND STANLEY AVIATION TEST RESULTS

This appendix summarizes the experimental data, used in connection with the dynamic model analysis, that have not previously received wide publication. Most of this data concerns experiments performed on the Daisy Track sled at Holloman A.F.B. during a program to investigate the effect of short duration accelerations of up to 80 G on human and animal subjects (Task 78503). This test program is still being carried on. Four experiments are also reported that were carried out at Stanley Aviation using a monorail facility, as part of a comprehensive series of tests to evaluate the landing characteristics of the Stanley B-58 escape capsule.

The Holloman data are given in the following table (see also Refs. L.1, L.2 and L.3). The angle quoted indicates the position of the body relative to the direction of the accelerating force, which is assumed acting from 0°.

TABLE L.1

Run No.	Subject	Peak G	Rate of Onset G/sec	Total Duration (sec)	Velocity Change (ft/sec)	Dirn. of Accel	Medical Report
335	Human	41.8	2140	.05	48.1	80 fwd.	Shock, lost consciousness. Severe paid L.2 to coccyx.
344	Bear	43.2	1660	.09	47.3	100 backward	Check out, no autopsy. No injuries(?)
389	Bear	55	3980	.03	47.2	0 headward	Compression fractures of thoracic vertebrae. Fracture of rib and pelvis. Internal and external hemorrhage.
390	Bear	55.3	4200	.05	46.1	0 headward	Fracture of vertebrae T.5 & T.6, 4th rib and pelvis. Multiple hemorrhage.

Run No.	Subject	Peak G	Rate of Onset G/sec	Total Duration (sec)	Velocity Change (ft/sec)	Dirn. of Accel	Medical Report
661	Human	34.0	942	.08	46.4	100 back-ward	Cervical spine pain. Partial loss of vision. Beginning syncope.
665	Human	27.0	775	.08	41.9	100 back-ward	No injury
667	Human	30.5	942	.08	45.9	100 back-ward	No injury
674	Human	33.5	1036	.08	45.3	100 back-ward	Cervical spine pain
675	Human	34.0	1080	.08	46.0	100 back-ward	Slight shock. Compression fracture T.5. Fracture of L.5
677	Human	29.0	1100	.09	43.5	100 back-ward	No injury

In the experiments carried out at Stanley Aviation, the subjects were seated in an escape capsule with full restraint, and dropped from a monorail with forward and vertical velocity. Impact forces were alleviated by a yielding metal attenuator and accelerations in the three major directions were measured by accelerometers mounted on the rigid seat back. The seat cushion of General Tire 1205 polyurethane was about 90% bottomed by the occupant's normal weight. In all, 34 tests with bears and humans were performed and the results reported in Table L.2 are of particular interest in that some form of injury occurred.

TABLE L.2

Run No.	Subject	Spinal	Peak G		Transverse Velocity Change	Medical Report
			Forward Transverse	Lateral		
49	Human	19.5 foot-ward	45.3	7.8	35 ft/sec.	Slight discomfort, T.3 and T.4, gone in 24 hours.
50	Human	37.4 head-ward	37.4	11.7	36 ft/sec.	Compression fracture T.3
51	Human	28.8 foot-ward	86.6	17.7	33.5 ft/sec	Severe shock (pallor and trembling).
58	Human	20 head-ward	63.3	27.5	37.6 ft/sec	Occipital headache, pain in T.4.

Other drop tests carried out at Stanley Aviation have included 62 static tests (i.e. no forward velocity) and 49 drops from a moving truck. These experiments covered a range of heights up to 12 ft. (transverse position) and no injuries were reported.

REFERENCES

<u>No.</u>	<u>Name</u>	<u>Title, etc.</u>
L.1	Beeding E. L.. and Mosely J. D.	"Human Deceleration Tests," Holloman A.F.B., AFMDC-TN-60-2, Jan. 1960.
L.2	Beeding E. L.	Daisy Track Test Report (Nos. 338-519), Holloman A.F.B., Dec. 1959.
L.3	Beeding E. L.	Daisy Decelerator Tests (Nos. 520-707), Holloman A.F.B., July 1960.

2/11/58
02

"The aeronautical and space activities of the United States shall be conducted so as to contribute . . . to the expansion of human knowledge of phenomena in the atmosphere and space. The Administration shall provide for the widest practicable and appropriate dissemination of information concerning its activities and the results thereof."

—NATIONAL AERONAUTICS AND SPACE ACT OF 1958

NASA SCIENTIFIC AND TECHNICAL PUBLICATIONS

TECHNICAL REPORTS: Scientific and technical information considered important, complete, and a lasting contribution to existing knowledge.

TECHNICAL NOTES: Information less broad in scope but nevertheless of importance as a contribution to existing knowledge.

TECHNICAL MEMORANDUMS: Information receiving limited distribution because of preliminary data, security classification, or other reasons.

CONTRACTOR REPORTS: Technical information generated in connection with a NASA contract or grant and released under NASA auspices.

TECHNICAL TRANSLATIONS: Information published in a foreign language considered to merit NASA distribution in English.

TECHNICAL REPRINTS: Information derived from NASA activities and initially published in the form of journal articles.

SPECIAL PUBLICATIONS: Information derived from or of value to NASA activities but not necessarily reporting the results of individual NASA-programmed scientific efforts. Publications include conference proceedings, monographs, data compilations, handbooks, sourcebooks, and special bibliographies.

Details on the availability of these publications may be obtained from:

SCIENTIFIC AND TECHNICAL INFORMATION DIVISION
NATIONAL AERONAUTICS AND SPACE ADMINISTRATION

Washington, D.C. 20546